UNIVERSITY OF NATAL

DURBAN, SOUTH AFRICA

DESIGN AND OPERATION OF A MULTISTAGE PRESSURIZED FLUIDIZED BED COMBUSTOR

by

CHRISTOS MIMI ELEFTHERIADES (B.Sc(Eng.), A.C.G.I.)

Submitted in partial fulfilment of the requirements for the degree of Doctor of Philosophy in the Department of Chemical Engineering, University of Natal.

Durban

Aug. 1981

I wish to declare that this whole thesis, unless specifically indicated to the contrary in the text, is my own work.

C. M. ELEFTHERIADES

ABSTRACT

A three-stage Pressurized Fluidized Bed Combustor (PFBC) of principal dimensions, 0,45m internal diameter by 4 m high was designed and fabricated to burn South African coals, with particular reference to coals unsuitable for burning in conventional boilers.

The combustor which is the first of its kind and probably one of very few operational PFBCs in the world, was made of three jacketed sections positioned vertically one above the other and bolted together at the flanges. Distributor plates were located at the flanges which gave the combustor a multistage capability. A three, two, or one deep Fluidized Bed (FB) configurations were possible by removing the interstage distributors. Interstage solids circulation was made possible by the use of downcomers transporting solids downwards between the FBs. The solids were returned to the top FB using a pneumatic conveyor.

The design of the PFBC was a sequence to a series of experimental and theoretical investigations which were carried out in order to provide us with the necessary PFBC design parameters. These investigations dealt with the following areas of research: (a) the development of a new type of cyclonic tuyere capable of transmitting through it high quantities of solids with the fluidizing gas, without choking, (b) the transfer and control of the downward flow of solids through downcomer pipes, (c) the control of the circulation of solids in a circulatory system using a non-mechanical solids flow control valve, (d) the development of a new type of start up burner which could operate immersed under the solids, and (e) the combustion of coal in a small FB under batch conditions and the study of reaction kinetics of South African coals. On the basis of the results of the investigation in these research areas and the findings of research of individuals and of organizations working in the field of fluidization technology the PFBC

was designed, built, and successfully commissioned. A series of 12 runs, with each run lasting between 2 and 8 days, totalling more than 1500 hours, were carried out on the PFBC. Char and coal with ash content between 30 and 70 per cent were burnt in the combustor using various combinations of feeding ports and number of FBs. System pressures ranged between atmospheric and 6 bar(abs). For some of the runs the reactor was operated in a counter-current mode with solids and combustibles descending against the upflowing fluidizing air in order to study the effect that counter-current flow had on the efficiency of combustion.

The combustion trials showed that the two-FB combustor, operated preferably without solids circulation, with the bottom FB acting as the main combustion cell and the top FB as a smuts burn-out cell, proved to be the most practical and most suitable combustor for burning South African high ash coals and fines or, in general, any low-grade carbonaceous materials of any size. With this configuration combustion efficiencies of up to 99 per cent, based on the combustibles in the feed and the ash, were achieved.

The department computer (CDC1700) was successfully linked with the PFBC for real time data logging and data processing.

A mathematical model which was based on our research findings and the work of T.P. Chen and S.C. Saxena, C. Fryer and O.E. Potter, and D. Levenspiel was successfully developed and applied to the two-FB PFBC. The model describes the devolatilization and combustion of coal particles in the FB in accordance with a shrinking core type model and uses a population balance over all particles for the overall mass balance. The results from this model, which was put onto the computer, compared favourably with the experimental results and the model can be confidently used to predict the behaviour of the PFBC.

It can also be easily adapted for use on any other single or multi-fluidized bed reactors provided that the assumptions made for the derivation of this mathematical model still hold .

A mathematical model based on the work of H.C. Hottel and A.F. Sarofim, and L. Wender and G.T. Copper was also developed. This model describes the transfer of heat from the FB to the cooling coils using a stepwise heat and mass balance along the length of the cooling coil. Although this mathematical model was developed specifically for the cooling coils of our combustor it is strongly believed that it can also form the basis of a general purpose model.

To my Wife

ACKNOWLEDGEMENTS

There are a number of people and organizations who have been of valuable assistance to me both during the period of research and during the preparation of this thesis and I would like to express my sincere appreciation to:

The National Institute for Metallurgy who provided financial support in the form of a bursary and the purchase of equipment.

The Council for Scientific and Industrial Research for financial support and General Mining for the supply of coal.

Professor M.R. Judd, M.F. Dawson, C. Brouckaert and other colleagues who have provided constant encouragement and many helpful suggestions.

The staff of the Chemical Engineering workshop and in particular to D. Penn and J. Visser for their continuous interest and assistance with the combustor pilot plant.

My family for their invaluable encouragement and support.

Mrs E.M. Beard, J.H. Johnson and A.H. Reay for their encouragement and help.

Mrs E.B. Schravesande and Mrs M. Arinto for preparing the transcript of this thesis.

CONTENTS

LIST OF FIGURES

LIST OF TABLES

NOTATION

Symbol	Significance	Units of measurement
A	cross sectional area of FB	m^2
AFBC	atmospheric fluidized bed combustor	
B_1	constant (E.3.11)	
C_1	constant taken as unity (E.3.1)	
c_1	constant in elutriation equation (E.7.2)	
c_2	parameter defined in E.7.3	
c_3	fraction of fixed carbon in coal	
c_d	gas discharge coefficient	
C	concentration of oxygen in gas stream	kg mol/m^3
D	diameter, diameter of FB	m
D_1	constant (E.3.11)	
D_G	gas diffusivity	m^2/s
d_p	particle diameter	m
d_t	downcomer diameter	m
f_s	solids friction factor	
f_w	volume ratio of cloud wake and bubble phase	
F_o	coal feedrate	kg/s
F_o'	upper limit of F_o necessary to cause solids circulation	kg/s
F_1	coal entrainment rate	kg/s
F_c	fraction of fixed carbon in coal	
FB	fluidized bed	
g	gravitational acceleration	m/s^2
H	total FB height	m
k_e	coal elutriation constant	1/s

k_{CE}	volumetric rate of gas exchanged between cloud and emulsion phase per unit bubble volume	1/s
k_{BC}	volumetric rate of gas exchanged between bubble and cloud phase per unit bubble volume	1/s
L_B	solids height in FB	m
L_T	solids height in downcomer	m
l_t	downcomer length	m
m	mass of a coal	kg
M_c	molecular weight of carbon	
M_R	total mass change rate of coal in FB	kg/s
N_A	kg mol of component A	kg mol
N	number of reacting coal particles	
p_o to p_6	pressure (gauge)	Pa or bar
P_o	coal size distribution in feed	1/m
P_1	coal size distribution in entrained stream	1/m
P_B	coal size distribution in FB	1/m
PFBC	pressurized fluidized bed combustor	
q	fraction of coal feed remaining in emulsion phase	
Q	gas volumetric flow (STP)	m^3/s
R, r	coal particle radius	m
r_c	radius of unreacted coal particle	m
R'_{O_2}	rate of combustion expressed as kg mol oxygen consumed per sec per m^2 bed area	kg mol/m^2s
R_{O_2}	normalised rate of combustion (E.8.1)	kg mol/m^2s
R_0	initial coal particle radius	m
Sh	Sherwood number	
t	time	s

T	temperature	^{o}C
U	superficial velocity	m/s
u	interstitial velocity	m/s
W	weight of sand and coal in a FB	kg
W_s	mass flux of solids (through λ valve)	$kg/m^2.s$
W_{tb}	weight of coal in top FB	kg
W_{Pb}	weight of coal in bottom FB	kg
z	height	m

Greek symbols

δp	difference in pressure	Pa
$\delta\sigma$	difference in interparticle normal stresses between two levels	Pa
Δu	slip velocity	m/s
δ	internal angle of friction	
ε	voidage	
$\bar{\varepsilon}$	voidage of FB	
ε_B	ratio of the bubble phase volume to the total FB volume	
$\varepsilon\varepsilon_s$	effective emissivity of silica sand (E.A.10.7)	
$\varepsilon\varepsilon_t$	effective emissivity of cooling coils (E.A.10.8)	
μ_g	gas viscosity	kg/m.s
ρ	density, coal density	kg/m^3
$\bar{\rho}$	mean particle density in FB	kg/m^3
σ	interparticle normal stress	Pa
τ	shear stress	Pa
ϕ	angle of wall friction	
ϕ_s	shape factor	
ϕ_l	mass change rate of a single coal particle	kg/s

Φ_2	rate of shrinkage of a single particle	m/s
Φ_3	average rate of shrinkage of coal particles in an FB	m/s
Φ_4	gas consumption due to the reaction with a single particle	kg mol/s

Subscripts

o	inlet conditions
a	region (a) of λ valve
b	region (b) of λ valve, bottom FB
B	bubble phase, bubble
C	cloud phase
d	distributor
E	emulsion phase
F	FB
g	gas
H	total height of FB
L	conveyor, lift line
M	maximum value
mf	incipient fluidization
or	orifice
p	coal particle, vicinity of coal particle
r	radius
s	solids
W	cloud wake
w	condition at wall
z	in z direction
λ	λ valve

Definitions

$$\varepsilon_B f_w = \frac{\text{volume of cloud wake phase}}{\text{volume of FB}}$$

$$1 - \varepsilon_B(1+f_w) = \frac{\text{volume of emulsion phase}}{\text{volume of FB}}$$

CHAPTER ONE

INTRODUCTION

The world in general and the western world in particular is heavily dependent on oil as a source of energy and petrochemicals. It is only recently and after the realization that oil and gas reserves will shortly become exhausted that a number of countries have turned to coal as a long-term source of energy and carbon.

Large coal reserves in South Africa have prompted the early use of coal in an economy that is now almost independent of imported oil. However, the selective use of high-grade coal for local demand and export and the upgrading of coals for use in the pyrometallurgical industry, has left this country with vast amounts of discard coals and coal fines. If the low-grade coal reserves (greater than 35 per cent ash) are added to the discard coals and coal fines the usable coal reserves can be increased by more than 80 per cent.

The advantages of FBCs and the possibility of using such a combustor for burning discard coals and fines to raise steam were realized more than 7 years ago and preliminary investigations on FBCs were carried out in this country using South African coals[1].

The advantages of FBCs compared with conventional coal-fired boilers can be summarized as follows.

(1) FBCs can combust low-grade coals of any size whereas conventional boilers are designed to burn a specific type and size range of coal.

(2) Combustion efficiency in FBCs is higher because of the uniform temperature of the bed of inert material and the continuous removal of the ash formed around the burning coal particles. This secures a more complete combustion and high combustion rates.

(3) Heat transfer in FBCs is much better because the heat transfer surfaces can be placed inside the hot turbulent bed of solids.

(4) When high ash coals are used in conventional boilers ash fusion and deposition of alkali metals on the heat exchanger surfaces causes blockages, corrosion, and reduces the efficiency of the boiler. The FBCs operate at much lower temperatures and are therefore free of this kind of problem. The low combustion temperature also facilitates the possibility of removing valuable minerals from the ash.

(5) FBCs emit less pollutants. NO_x emissions are low because of the low combustion temperatures (800 to 900°C compared with 1200 to 1400°C in conventional boilers). It is also very easy to add limestone or dolomite in the FBC to reduce the volume of SO_2 leaving the combustor by the formation of sulphates. This is much cheaper than using a gas purification apparatus to remove the SO_2 from the flue gas as happens in conventional boilers.

Although the combustion process in an FBC has received a considerable amount of research world-wide during the last two decades and most of the advantages of FBCs have now been conclusively verified, little is known about the scaling-up of FBCs. This is because the scaling-up using as a basis results from bench-scale units is a complex problem. There is also the reluctance, which characterizes industry, to utilize the findings of a new technology. From a recent survey on the status of FBCs in the U.K. and U.S.A.[2] the authors report that they found only 'half a dozen' large installations operational with a few others in advanced stages of development. In addition most of these installations were designed for atmospheric pressure operations (AFBCs).

For power generation the choice is directed rather towards pressurized combustion (PFBC) because of the higher thermal efficiencies and better combustion characteristics. The physical size of the combustor is also greatly reduced. Combustion of coal at high pressures adds a

few more unknown parameters to the already long list of problem areas regarding the operation of an FBC. To these problems, adding our limited knowledge on the behaviour of South African coals in FBCs, the questions that need to be answered in order to successfully operate an FBC in this country are the following.

(a) What is the best method for feeding coal in a pressurized system?

(b) Does ash fusion and sintering occur during the combustion of our coals in an FBC?

(c) Can the FBC burn any size of coal from duff (-6mm) to industrial nuts (18mm to 30mm) bypassing the use of double screened coal[2]?

(d) How can the elutriation of fines which seems particularly high in pressurized combustors be reduced?

(e) What is the highest ash content in the coal that can be tolerated for continuous operation of the FBC?

(f) Can the turndown of the FBC be improved from a value of 2,5 to a value of 4 which is the value currently achieved by other types of utility boilers?

(g) How well does the performance of an FBC boiler compare with that of conventional utility boilers?

(h) How can the generated heat best be removed from the combustor?

(i) How severe is the erosion and corrosion of the immersed or freeboard heat exchanger surfaces?

(j) What is the optimum operation pressure for FBCs? From existing experimental combustors[2] the Americans show a preference towards a combustor pressure of approximately 8 bar while the British converge to an operating pressure greater than 14 bar.

(k) How can the FBC be instrumented to ensure an uninterrupted and efficient operation?

(l) How to start up the FBC.

(m) Can the FBC meet the stringent requirements regarding atmospheric emmisions?

To answer these questions and enable South Africa, which is one of the world's major coal producers, to contribute to the field of FBC technology, we undertook to design and build a 1 MW(t) multistage PFBC. The reasons for choosing a multistage combustor will be explained in detail in the following chapters.

The PFBC is made up of three vertically staged FBs lined with firebricks, each contained in a water jacketted pressure vessel. The height of each stage is 0,7m and each stage has an internal diameter of 0,46m. Each FB has an operating height of 0,4m determined by the height of the overflow downcomers which are used for connecting the three FBs. Distributor plates are located at the flanged joints of each stage and they can be removed to reduce the PFBC from a three to a two or to one deep FB. In the three-FB configuration coal can be fed in the top bed where it gets devolatilized and traverses down one or two stages with the solids, before reaching the critical fineness at which it gets elutriated upwards during its final burnout in the upper stages. As a two-FB system, depending on which distributor plate has been removed, the combustor can operate with the deeper FB positioned above or below the shallow one and coal can be fed into either of the beds. When the PFBC is reduced to a single FB system coal can be fed into the deep FB or above it.

Circulation of solids outside the PFBC is achieved by the use of a pneumatic lift line and a non-mechanical solids flow control valve. Circulation can be started or stopped depending on the required concentration of coal and intensity of combustion in each FB.

To study the behaviour of the PFBC theoretically a mathematical

model was developed for the combustion of coal in an FB and was applied to the multistage system. A series of experiments were carried out on the PFBC to establish the most suitable PFBC configuration and best operating conditions for combustion of South African coals. The versatility and high possible efficiency offered by the multistage combustor were investigated and the PFBC was assessed bearing in mind its complexity in hardware and control.

To enable the continuous recording of all experimental parameters, which include chemical analyses of gas streams, flowrates, temperatures, and pressures all sensor instruments were linked with the departmental computer (CDC 1700). The computer was run on a real-time basis and all experimental data were recorded.

CHAPTER TWO

THE SOUTH AFRICAN COAL SITUATION AND THE CURRENT STATUS OF DEVELOPMENT IN FLUIDIZED COMBUSTION

2.1. COAL SITUATION IN SOUTH AFRICA

South Africa is in the fortunate position of deriving most of its energy from coal and having an economy which is almost independent of imported oil.

From a recent Government survey the coal reserves and extractable coal determined on the basis of coal with ash content less than 35 per cent is as follows:

coal *in situ* : $81{,}3 \times 10^9$ tons

extractable coal : $25{,}0 \times 10^9$ tons

The low tonnage of extractable coal (31 per cent) is estimated on the basis of current mining methods which could improve in the future. Looking at the current and future developments, our coal is sufficient to last us probably until the end of the next century. However, there is a growing feeling that many of our coal utilization methods should be reconsidered in an effort to relieve the strain on the good quality coals and at the same time utilize the continuously increasing quantities of discard and coal fines.

The major South African coal consumers and their contribution to the accumulation of discard and coal fines are the following:

(1) The Electricity Supply Commission (ESCOM), which currently uses 40×10^6 tons per year, which is 55 per cent of the annual coal production. ESCOM has been using the industrial-type boiler in its earlier power stations, However, these boilers have now been replaced by Pulverized Fuel (PF) boilers. In spite of the initial capital outlay on plants for processing and pulverizing of the coal and the problems

of handling and storing the coal in its fine form, ESCOM power stations are economical because of their large size (2000 to 3500MWe). It is fortunate that the PF boilers do not contribute towards the accumulation of coal fines. However, they are using good quality coals (less than 35 per cent ash).

(2) The local industry which currently uses 15 per cent of the annual coal production. Although,it is possible for ESCOM to resort to large PF utility boilers, for economical reasons and efficiency, the industrial sector has to use the chain grate or stoker type of boiler which requires little handling or processing of the fuel. Lately, in an effort to reduce the oversupply of duff coal, a new type of coal, 'mixed smalls' with a size of minus 25mm was introduced to replace the conventional 'pea size' coal (6,3 to 25mm). Unfortunately, due to coal segregation either in the feeding hoppers or after coal is fed onto the grate, the fines in the 'smalls' tend to get elutriated or become the cause of localized overheating due to air channeling. This causes considerable operating problems in the industrial boiler and increases the preference of the industrial sector to burn 'pea size' coal.

(3) The third major coal consumer are SASOL I and SASOL II, which will be using over 17 per cent of the annual coal production by mid 1981. The coal consumption of these projects, with a SASOL III plant to be completed within five years, is significant. The SASOL plants with their main objective to produce liquid fuel from coal use our good quality coals.

(4) The fourth major consumer is the metallurgical industry, using 10 per cent of the annual coal production. A large portion of this coal production is taken by the iron and steel industry which uses high quality coking coal as a reductant in the Blast Furnace (BF). These furnaces are very sensitive to the quality of coke used and as in the

case of power stations, they are only economical if they treat high quantities of ore (at least 2×10^6 ton of ore per annum).

It is therefore clear that in this country there is a growing demand for good quality coals and indications show that the current trends will continue in the future. There is also not a single process available which uses the discard coals and the high ash (greater than 35 per cent ash) coal reserves. This is clearly the area where the use of an FBC could ease the current imbalance in the use of coal and save the good quality coals for chemicals and use in the food industry rather than burning them in boilers for raising steam.

The advantages offered by fluidized combustors and their ability to burn low quality coals and fine material have been proven in a number of small-scale combustors. However, the only way that industry and ESCOM will consider the adoption of the FBC is by building such a boiler. The FBC must be tested on a variety of South African coals and tried under similar experimental and environmental conditions. The use of South African coals is essential because of their unique features, as given below.

(1) South African coals are characterized by a high fixed ash, if they are compared with American and British coals. The ash is spread throughout the coal so homogeneously that it makes the washability and upgrading of our coals extremely difficult[3].

(2) Most of the high-ash coals are also high in sulphur content.

(3) Some of our coal deposits contain valuable minerals in the ash (e.g. uranium). Recovery of these minerals is favoured by a low coal combustion temperature (less than $680^{\circ}C$).

2.2. CURRENT STATUS OF DEVELOPMENT

Combustion of coal in an FB has been known since the late 1920s

when it was used along with coal gasification in the Winkler process. Experiments in the use of FBCs for steam generation began only after the end of World War II when the advantages of FB combustion over existing boilers were realized[4].

Most of the current development work is carried out in UK and U.S.A. In the UK the emphasis is on using FBCs for generating power, whereas in the U.S.A., the emphasis is more orientated towards the pollution-free utilization of high-sulphur coal in utility boilers.

In the UK the development of commercial FBC systems is carried out mainly by the British Coal Utilization Research Association (BCURA), and the National Coal Board (NCB) and subsidiaries. In the U.S.A. the work in this field is funded by the Department of Energy (DOE) and is concentrated on industrial and utility boilers. A great portion of the government allocated funds for fossil energy research is invested annually in companies involved in research and development of FB boilers. Table 2.1. shows the developments, till the end of 1979, in the UK and U.S.A. and gives a description of the main FBCs in these countries and some of their problems which are of relevance to our work.

Looking closer at the FBCs included in Table 2.1 it may be concluded that in spite of the fact that most of these combustors have been scaled up to industrial sizes, many of them still suffer from high carbon losses and erosion problems. Further, some of them use coal in a pulverized form or after being double screened which is clearly uneconomical.

A further description of mainly AFBCs which are still under construction, and which will be used for experimental work and industrial applications may be found in References 2, 5, and 6. The indications are that AFBCs will reach industry by 1983 after sufficient demonstration units have been built and adequately tried. The PFBC

TABLE 2.1.

Atmospheric and pressurized FBC systems currently operating or near commissioning

Atmospheric FBC systems actually operating or in commissioning stage

	Plant	Capacity	Miscellaneous	Operational date
RIVESVILLE (USA) Pope Evans & Robbins Foster Wheeler	AFBC for steam turbine 4 modular cells Demonstration	136 000 kg/hr 30 MW(e)	2" needles into bed, 12x5mm double screened coal, 12-18% ash, drilled bolt distributor, 2,5m/s, limestone modular 4 cells C, burn-up cell, 0,9m bed depth	From 1977 for several thousands of hours
GEORGETOWN UNIVERSITY	AFBC for utility steam Demonstration	46 000 kg/hr 20 bar steam	Overbed fuel feed, flyash re-injection 25x5 mm double screened coal, 8% ash, limestone, 2 cell bed.	Being commissioned
RENFREW (UK) Combustion Systems Babcock & Wilcox	AFBC for utility steam Demonstration retrofit	20 000 kg/hr 13 MW(thermal)	Coal or oil to NCB type underbed feeders, 18-60% ash, NCB distributor, compartment windbox, 1,2-2,5 m/s, limestone, 0,9m bed depth, 20% excess air, C losses 4-14%, load control by slumping.	From 1975
STATE OF OHIO, PSYCHIATRIC HOSPITAL (USA) Babcock & Wilcox	AFBC for utility steam	27 000 kg/hr	6x1,5mm, 4%S, 10% ash, 2 m/s, limestone, 0,9m bed, load control by slumping.	Commissioning end 1979
ALLIANCE RESEARCH CENTRE, OHIO (USA) Babcock & Wilcox	AFBC retrofit PDU scale	4 500 kg/hr	2mm x 0, woven wire, perforate plate, bubble cap, 2 m/s, limestone.	From 1977 several '000 hrs
BCURA, LEATHERHEAD (UK) National Coal Board	AFBC boiler test facility	3 600 kg/hr 3,5MW(thermal)	NCB type underbed, NCB distributor	

Atmospheric FBC systems due to be operational soon

	Plant	Scale	Due for commissioning
CADBURY'S (UK) Energy Equipment Co.	AFBC for utility steam Retrofit of a John Thompson boiler	90 000 kg/hr (hailed as the biggest production AFBC in existence)	Dec 1979
STATE OF OHIO, OERDA PROJECT (USA) Coal Process Consultants Babcock & Wilcox	AFBC for utility steam	(a) 45 000 kg/hr (b)161 000 kg/hr	-Design complete -conceptual design
HOWARD TYLER, YORKSHIRE (UK) Stone-Platt	AFBC for utility steam Shallow bed design	4 500 kg/hr	Nov. 1979
GENERAL MOTORS (USA) Stone-Platt	?	?	Being supplied
Y-ARD MARINE FOR 'PANAMA' BULK CARRIER	AFBC marine unit for steam turbine	27 000 kg/hr	Designed
RIVER DON WORKS, BRITISH STEEL Babcock & Wilcox ?	?	36 000 kg/hr	Ordered?
DEPT OF NATIONAL DEFENSA, CANADA Coal Process Consultants		18 000 kg/hr	Start up 1980?
HUNGARY Coal Process Consultants	AFBC for district heating	20-220 t/hr	?
NEW BRUNSWICK POWER Coal Process Consultants	AFBC	18 000 kg/hr	?
MORGANTOWN Morgantown Energy Tech. Centre	Stacked AFB's	About 8'x8'	In construction
WILKES BARRE PENNSYLVANIA	AFBC for district heating	46 000 kg/hr	? Operating
IBM, MICHIGAN Johnson Boilers	AFBC for utility steam	40 000 kg/hr	?
SWEDEN Babcock & Wilcox	AFBC for electricity generation and district heating	(a)50 MW(e) (b)80 MW(th)	Study being assessed

Pressurized FBC systems actually operating or in commissioning stage

	Plant	Capacity	Miscellaneous	Operational date
GRIMETHORPE (UK) International Energy Agency National Coal Board	PFBC for gas turbine	80 MW (thermal)	2,5 m/s; 10 bar Stal Laval test blades?	Near commissioning
BCURA LEATHERHEAD (UK) National Coal Board	PFBC test facility	12" square ± 4 MW (th)	6x10 mm feed and 3x10 mm feed 3 m/s; 8 bar? Stal Laval test blades	
EXXON MINIPLANT (USA) Exxon Research	PFBC test facility	1 MW(e)	3 m/s; 10 bar	Since 1974 > 1500 hours
UNIVERSITY OF NATAL (SA)	PFBC multi-tier	1-2 MW (th)	Up to 8 bar	1979
WOODRIDGE FACILITY (USA) Curtiss Wright Dorr Olivier	PFBC for combined cycle		3x0 mm, 0,8 m/s, 7 bar, test turbine by Lucas-Rover	> 1000 hrs total > 100 hrs uninterrupted

Atmospheric FBC systems due to be operational soon

	Plant	Scale	Due for commissioning
CADBURY'S (UK) Energy Equipment Co.	AFBC for utility steam Retrofit of a John Thompson boiler	90 000 kg/hr (hailed as the biggest production AFBC in existence)	Dec 1979
STATE OF OHIO, OERDA PROJECT (USA) Coal Process Consultants Babcock & Wilcox	AFBC for utility steam	(a) 45 000 kg/hr (b)161 000 kg/hr	- Design complete - conceptual design
HOWARD TYLER, YORKSHIRE (UK) Stone-Platt	AFBC for utility steam Shallow bed design	4 500 kg/hr	Nov. 1979
GENERAL MOTORS (USA) Stone-Platt	?	?	Being supplied
Y-ARD MARINE FOR 'PANAMA' BULK CARRIER	AFBC marine unit for steam turbine	27 000 kg/hr	Designed
RIVER DON WORKS, BRITISH STEEL Babcock & Wilcox ?	?	36 000 kg/hr	Ordered?
DEPT OF NATIONAL DEFENSA, CANADA Coal Process Consultants		18 000 kg/hr	Start up 1980?
HUNGARY Coal Process Consultants	AFBC for district heating	20-220 t/hr	?
NEW BRUNSWICK POWER Coal Process Consultants	AFBC	18 000 kg/hr	?
MORGANTOWN Morgantown Energy Tech. Centre	Stacked AFB's	About 8'x8'	In construction
WILKES BARRE PENNSYLVANIA	AFBC for district heating	46 000 kg/hr	? Operating
IBM, MICHIGAN Johnson Boilers	AFBC for utility steam	40 000 kg/hr	?
SWEDEN Babcock & Wilcox	AFBC for electricity generation and district heating	(a)50 MW(e) (b)80 MW(th)	Study being assessed

Pressurized FBC systems of the near future

	Plant	Scale	Due for commissioning
BRITISH COLUMBIA HYDRO & POWER AUTHORITY Intercontinental Engineering, Vancouver Combustion Systems Ltd	PFBC for combined cycle?	(a) 2000 MW (b) 70 MW?	Conceptual design
AMERICAN ELECTRIC POWER CO. (USA) (Ohio Power Co., Brilliant Ohio River) Babcock & Wilcox National Coal Board	PFBC for combined cycle	170 MW (15 bar)	Being designed
WOODRIDGE PILOT PLANT (USA) Curtiss Wright	PFBC for combined cycle	3x160 MW modules	Under construction Start up 1981
BRITISH PFBC DEMONSTRATION Babcock & Wilcox	PFBC combined cycle	200 MW	Proposals being studied by Government
UNIVERSITY OF NATAL (SA)	PFBC	45 cm 6 m	Late 1980

is also receiving an increasing portion of the FBC research effort because of its compactness high thermal efficiencies and combined cycle applications. PFBCs are lined up for use in utility boilers and a conceptual design for a 2000 MW PFBC unit has been investigated by Combustion Systems Ltd. Industrial scale PFBCs are expected to reach industry in the 1990s.

2.3. ASPECTS OF RESEARCH AND DEVELOPMENT IN FLUIDIZED COMBUSTION THAT FORMED THE BASIS OF OUR INVESTIGATION

An enormous amount of work has been carried out in this field[7-28]. A short review and discussion of relevant research findings and operating experiences which formed the foundation of our own contribution to research and the development of our PFBC is given below.

2.3.1. Heat transfer

The main parameters influencing the rate of heat transfer in an FB are:

(a) The particle physical properties and size distribution.

(b) The temperature of the FB and uniformity of fluidization.

(c) The properties and shape of the heat transfer surfaces and their disposition in the FB.

The research work in this field is enormous. However, to enable one to choose the correct fluidizing material, the operating temperature of the FB and the orientation, shape and disposition of the cooling coils in the FB,the following research findings have to be considered: The heat transfer rate in an FBC increases with a decrease in the mean particle size. Attainable rate values for particle sizes less than 1,8mm, are 460 to 550 W/m^2 ^oC[10,11] whereas on coarser sizes the transfer rate drops to 200 to 300 W/m^2 ^oC[12]. The physical properties of the fluidizing particles are of lesser importance unless segregation exists

due to differences in particle densities[13]. Higher gas velocities are then required to induce backmixing especially in high pressure combustors where coal particles tend to segregate to the top. Variation in the oversize fraction of a given particle size distribution has little effect on the heat transfer while similar increases of the undersize fraction increase transfer rates due to the effective reduction of the minimum fluidizing velocity (U_{mf}). It has also been reported[14] that heat transfer rates continue increasing with up to gas velocities of 6 x U_{mf}. Further increase of the superficial gas velocity effectively causes dilution and a levelling off of the heat transfer rates.

The heat is transferred to the heat exchanger surfaces by radiation and convection. The radiactive term contributes between 25 and 35 per cent of the total heat transfer rate for FB temperatures of 750^{o}C to 950^{o}C[14]. For a given combustor temperature, radiation increases with increase in particle size while convective heat decreases sharply. The heat transfer coefficient between fluidized solids and immersed steam coils was found[14] to increase linearly with increasing FB temperatures.

The heat removal from an FB is directly dependent on the immersed heat transfer area, though the actual temperature of the bed is determined by the coal feedrate rather than the amount of heat removed. This is mainly due to the fact that the heat transfer rate which depends on the temperature difference between the fluidized solids and coolant cannot be varied significantly unless different coolants are sequentially used. Heat transfer surfaces can also be placed in the freeboard region to extract heat from the flue gas. However, this minimizes the freeboard combustion of elutriated carbon particles which would have normally burned because of radiation from the walls of the combustor. Therefore unless the carbon particles are recycled this would represent a significant carbon loss.

The cooling coils can be arranged either in a vertical or horizontal orientation. The use of horizontal coils is not recommended due to the erosion caused by the vertical movement of the fluidizing solids in the bubble and emulsion phase. Movement of solids occurs predominantly in deep FBs which are used to provide both adequate residence time for small particles and room for sufficient heat transfer tubes. Investigations on the tube spacing using two different tubes of D=36mm and 60mm and pitch-to-diameter ratios of 2 to 8 showed that,by decreasing the pitch-to-diameter ratio,the heat transfer coefficient decreases by 15 to 20 per cent. In addition the 60mm diameter tube gave 15 per cent higher coefficients for the same pitch-to-diameter ratio.

In conclusion the heat transfer in the FB increases with a decrease in the particle size distribution while changes in the physical properties of the particles are of lesser importance. The heat transfer improves with increase in the FB temperature and superficial air velocity. Better transfer rates are attained, if vertical coils are used immersed under the solids. The cooling coils must also be well spaced and preferably of a relatively large tube diameter.

To get an understanding on the expected heat transfer properties of the cooling coils after a long stay in an FBC the following must be considered: In an FBC the temperature of operation is relatively low and sintering of the ash does not occur. Furthermore alkali salts cannot form on the metal surfaces. The erosion problem in an FBC is less severe mainly because of the lower gas and solids circulation velocities within the bed of solids. Hall *et al.*[15] measured particle velocities within an FB using a cinecamera and identified a small fraction of particles with velocities up to 10 m/s which was five times the bed superficial gas velocity. They also observed erosion on their 316 s/s water cooled tubes with metal temperatures of

less than 130°C. However, at higher metal temperatures an oxide film formed which appeared to reduce erosion.

2.3.2. Principles of operation

The research work into the dynamic behaviour and efficient operation of an FBC is of great value because it provides an initial understanding of the contribution and importance of all the parameters which characterize the FBC. The research work into the operation of an FBC is concentrated into the following areas:

(a) fluidizing velocity of gas,

(b) coal feeding,

(c) distributor plates, and

(d) preheating of the combustor.

Looking closer at these areas of research, the effect of the fluidizing gas velocity on the performance of the FBC may be summarized as follows: The fluidizing gas velocity contributes towards the solids mixing and determines the extent of fluidization. Its lowest value is fixed by the velocity required for incipient fluidization, while the highest is set by the highest permissible amount of carbon loss by elutriation for the case of a non-circulating bed. The highest gas velocity in this type of FBC depends very little on the properties of the fluidizing material. To achieve higher gas velocities deep FBs with solids recirculation may be used which provide a higher residence time of coal particles and reduce elutriation. This was confirmed by Wright *et al.*[18] who found that at 800°C using coal feed of 2mm and gas velocities of 0,6 m/s the carbon loss was 6,5 per cent of the feed but recycling fines reduced elutriation to 0,2 per cent.

The methods of coal feeding in an FBC may be summarized as follows: Coal feeding systems differ between them depending on the feeding mechanism and the position of the feeding device relative to the bed of solids. Fine coal particles are commonly fed pneumatically using

the main air supply as the carrier. For this feeding system a more elaborate recycling system is required to reduce the carbon loss. In addition the air stream and coal particles must be both dry. A much simpler and less expensive method is overbed feeding using chutes or screw feeders. However, coarser particles must be used because fine particles, in general, get elutriated before they even reach the bed of solids. A compromise between the two methods of feeding is the submerge coal feeder. Coarse particles with a low fraction of fines can be screwfed and combusted with minimum carbon losses. In PFBCs feeding into the bed of solids may be achieved by using a screw feeder connected to a set of lock hoppers of the Petrocarb type design.

The contribution of the distributor plate to the performance of an FBC may be summarized as follows. A high pressure drop across the distributor ensures good mixing and eliminates hot spots and gas chanelling. However, for an AFBC high pressure drop distributors are undesirable because of the cost of pumping the fluidizing air. Zenz[19] provided a compromise when he recommended that the distributor pressure drop (Δp_d) should be at least 30 per cent of the pressure drop across the bed of solids.

$$\Delta p_d = 0{,}3g\, L_B \bar{\rho} \qquad \text{E.2.1}$$

where L_B and $\bar{\rho}$ are the bed height and density respectively.

Porous distributors are extensively used in bench-scale FBC units but for large-scale pilot plants, distributors with tuyeres like in distillation columns are used. For design purposes the distributor plate is treated as a multiorifice distributor. Assuming an incompressible gas and a square edge orifice the distributor pressure

drop can be expressed as:

$$\Delta p_d = \frac{U_{or}^2 \rho_g}{2c_d^2} \qquad \text{E.2.2.}$$

where U_{or}, ρ_g, and c_d are the orifice gas velocity, the gas density, and gas discharge coefficient respectively. The orifice discharge coefficient is a function of the Reynolds number and the orifice shape. Behie *et al.*[20] showed that for orifice velocities U_{or} = 15,2 m/s the discharge coefficient for an empty column was 22 per cent higher than the value of 0,63 used when fluidized solids were present, while at U_{or} = 61 m/s the difference was only 3 per cent. This indicates that the solids interfere with the gas jet boundary layer and this is more effective at lower gas velocities. Whitehead *et al.*[21] and Whitehead and Dent[22] studied the pressure and flow maldistribution at the distributor level of a number of FBs with cross sectional areas, between 0,09 and 5,9m^2, and determined the minimum superficial gas velocity U_{min} (ft/sec) for continuous operation of all tuyeres. Their equation is listed below:

$$\frac{U_{min}}{U_{mf}} = 0,7 + [0,49 + \frac{3,23 \times 10^{-7} N_T^{0,22} K_D^2 \rho_s H_T}{U_{mf}^2}]^{\frac{1}{2}} \qquad \text{E.2.3.}$$

where N_T : total number of tuyeres

K_D : the distributor flow factor, $60\, U(\Delta p_d)^{-\frac{1}{2}}$

H_T : is the fluidized bed height (ft)

ρ_s : is the solids particle density (lb/ft^3)

E.2.3 shows the dependance of U_{min} on the distributor resistance to gas flow rather than the orifice velocity, this suggests that E.2.3 can be used for multituyere distributors of different design to the ones used by the investigators. Fakhimi and Harrison[23] did similar work and presented an equation relating the number of operating orifices, to the properties of the distributor and the gas superficial velocity.

In a situation where there is a need to transfer particulates through the distributor like in a case of a multistage FBC,a calciner, the use of an FB for prereducing iron ore,where gases from the smelter are used as a reductant[24], a bubble cap type tuyere may be used. Johnson and Davidson[25] have used metal and ceramic bubble caps in experiments to determine the maximum allowable solids gas load. All their attempts using a solids loading of $\sim$ 17 g/m^3 at 1000^{o}C caused blocking of the bubble cap orifices after operating for no more than 10 hours.

The research work on the start up burners for FBs may be summarized as follows. The start up of FB reactors has never been an area of major investigation mainly because it is relatively easy to convert existing burners to preheat FBs. A number of methods for starting up the reactor are currently used. The most common is the use of a conventional oil or gas burner positioned on the side of the reactor in the freeboard area. The entire FB or just a section of it is heated by the burner to a desired temperature and combustion is then spread to the entire bulk of solids. The heat losses from this type of system are high especially if this burner is used for preheating a deep FB. In addition the burner flame creates an undesirably hot zone, in the vicinity of the burner, which is higher than the normal operating temperatures of the FB.

Another method for preheating an FBC is by the use of the combustion gases from a separate preheater unit positioned close to the FB.

A ducting able to withstand temperatures of over 1000°C is used to carry the hot gases from the burner to the FBC plenum. In a system like this the heat losses are high and the capital expenditure for the housing of a separate start-up burner considerable.

When dealing with a pressurized system the burners described above can not be used to supply heat to this system if it is needed when operating at high pressures.

Premixing of combustible gases within the FB is also being used for preheating the reactor. Baskakov and Makhorin[26] have studied the combustion of air and natural gas in an FB. They observed that during start up and up to solids temperatures of 800°C a stoichiometric mixture could only burn above the bed. At solids temperatures of between 800°C to 1000°C, depending on the stoichiometry, combustion took place both in the fluidized bed and freeboard area with temperatures in the proximity of the bed reaching 2000°C. At solids temperatures exceeding the above values and air gas mixtures near stoichiometric, combustion of the gases occurred in a zone near the grid with combustion zone temperatures of 300°C above the FB temperature. Similar high temperature regions within the fluidized solids were also observed by Broughton[27] who, in addition, studied the effect that the premixed gas velocity had on combustion in an FB and set criteria for preventing sintering and overheating of the distributor plate. From experiments at 830°C Broughton found that by decreasing the solids mean particle diameter, more fuel bypassed the bed without being burnt, resulting finally to an unstable situation. Fuel bypassing also increased by up to 15 per cent by increasing the gas velocity from 2 to 10 x U_{mf}. Pillai[28] confirmed Broughton's work and improved his model on fuel bypassing, by introducing the effect of combustion within the bubbles.

2.4. CONCLUSION

The combination of a number of factors such as (a) the characteristic properties of our coals, (b) the necessity to burn our discard coals and fines, (c) the results of research work in fluidized combustion, and (d) the experience obtained from the operation of FBCs in various research centres, pointed clearly to the research areas where our research had to be directed, in order to develop an FBC capable of operating satisfactorily using our low-grade coals, discards and fines. These research areas included the development of equipment, which were used during the operation of our combustor, as it is shown in Chapter 3, and the combustion tests under batch conditions which provided the necessary kinetic data for the theoretical model and the design of the combustor (Chapter 4). A combination of the results which were obtained from our research (Chapters 3 and 4), and the published research findings in the fluidization field provided the basis for the design of our combustor which had to conform with the requirement for a satisfactory combustion of our low quality coals. This design of our PFBC is presented in Chapter 5.

CHAPTER THREE

DEVELOPMENT OF EQUIPMENT USED DURING THE OPERATION OF OUR PFBC

The development of the equipment used during the operation of our our PFBC and the experimental and theoretical work, which was carried out for this purpose,was the result of our decision to use a pressurized multistage combustor,for the combustion of our low-grade discard coals and fines. The reasons given for the choice of this type of combustor are listed below.

(1) A pressurized combustor is compact and is characterized by high thermal efficiencies and very good combustion characteristics.

(2) It is believed that if research into gas turbines produces satisfactory results then pressurized combustors will be the most probable successors of the conventional boilers. It would then be possible at a later stage to convert our PFBC into a combined cycle system and investigate the efficiency of such a system.

(3) Mainly coarse coal particles fed into the top stage can transverse down one or two stages before reaching a critical size when they can be elutriated upwards for the final burnout.

(4) Fine coal particles can be fed into an intermediate stage and extra air may be fed to the upper stages to achieve complete combustion of the elutriated particles.

(5) Using a multistage system it would no longer be necessary to double screen the coal feed as in the case of conventional industrial boilers.

(6) The problem of pollutants and in particular the emissions of NO_x can be expected to be less serious due to the controlled temperature profile that can be achieved in a multistage combustor.

(7) The control of the temperature of the combustor should also aid the recovery of precious metals from the ash as discussed in Section 2.1.

The research work which dealt with the development of equipment and the supply of the necessary data for the design of our PFBC included the following areas(a) the interstage downcomers transferring solids downwards, (b) the external conveying line used for returning the solids to the top stage, (c) the distributor plate which had to let through it, with the fluidizing gas, high quantities of elutriated fines, and (d) the immersed start-up burner.

3.1 DESIGN OF DOWNCOMERS TRANSPORTING SOLIDS BETWEEN FBs

The behaviour of downcomers used in ambient temperature operations has been studied by a number of authors[29-35]. In these systems the control of solids is achieved by the use of a slide valve or side aeration, introduced at the lower end of the downcomer. However, in FBCs, solids flow cannot be mechanically controlled due to the high operating temperatures and abrasive nature of solids. An investigation into the use of a downcomer which had the form of a plain pipe was thus undertaken. It was our intention to study this downcomer and, if suitable, to use it to transport solids in our multistage PFBC.

3.1.1. Theoretical analysis

Solids can flow down a downcomer acting as an overflow in four different ways:

(a) In the slip-stick flow regime which is characteristic of completely non-aerated flow of large particles. In this regime the solids move downwards in a jerky fashion.

(b) In the moving bed flow regime where the solids flow smoothly downwards with a small relative motion between particles and in the absence of significant discontinuities such as cracks or bubbles. The voidage is generally a little smaller than the incipient voidage.

(c) In the FB flow regime where the flow pattern resembles a FB of solids travelling down the standpipe. Bubbles are present, and the overall voidage in the downcomer is greater than the minimum fluidization voidage.

(d) In the dilute phase regime where the particles are streaming down either singly or in small clusters and the overall voidage is almost unity.

Leung[33,34] describes these regimes as well and advances an analysis for types (a,b,c),for the case of a standpipe which is bottom restrained with a slide valve or orifice. The present analysis is confined to the moving bed flow regime in a downcomer with no bottom restriction.

For the theoretical analysis the following assumptions are made:

(1) The entry and discharge losses for the moving bed flow regime are neglected because of the low solids velocity and the similarity between the solids bulk density in the downcomer and in the FB in the vicinity of the discharge end of the downcomer.

(2) For a fixed set of conditions the voidage (ε) is taken as constant (incompressible flow). For the moving bed flow regime the value of ε_{mf} is used for all conditions.

(3) The flow is assumed to be axisymmetric with no interparticle forces in the vertical direction. Frictional forces are considered between the solids and the walls of the standpipe.

(4) The solids passing through the standpipe have zero initial velocity and no gas is entrained with the particles.

Representing the system mathematically apart from continuity considerations only two equations are needed to describe the solids downflow. They are a force momentum balance equation and a gas drag equation. These equations have been derived in Appendix 1.

The final form of the force momentum equation is thus:

$$\Delta p - C_1 \frac{W_s^2}{\rho_s(1-\varepsilon mf)} - 2f_s \frac{L_T W_s^2}{d_t \rho_s(1-\varepsilon mf)} + \rho_s(1-\varepsilon mf)gL_T = 0 \qquad \text{E.3.1.}$$

The gas drag equation is:

$$-\frac{\Delta p}{L_T} = 150\left(\frac{1-\varepsilon mf}{\varepsilon mf}\right)^2 \frac{\mu_g \Delta u}{\phi_s^2 d_p^2} + 1{,}75\left(\frac{1-\varepsilon mf}{\varepsilon mf}\right) \frac{\rho_g}{\phi_s d_p}(\Delta u)^2 \qquad \text{E.3.2.}$$

where the slip velocity Δu is expressed as:

$$\Delta u = \frac{U_g}{\varepsilon mf} + \frac{W_s}{\rho_s(1-\varepsilon mf)} \qquad \text{E.3.3.}$$

The pressure gradient for the fluidized solids is given by the following equation:

$$-\frac{\Delta p_B}{L_B} = \rho_s(1-\bar{\varepsilon})g \qquad \text{E.3.4.}$$

where $\bar{\varepsilon}$ is the average bed voidage calculated experimentally (Figure 3.1)

3.1.2. Apparatus and procedure

Two FBs (D = 0,14m) placed vertically above one another were joined with a downcomer acting as an overflow of the top bed (Figure 3.2)

Sand with a mean diameter $d_p = 5 \times 10^{-4}$m used as the fluidizing material (see Appendix 1, Table A.1.1), was fed through a hopper to the top FB and descended through the downcomer to the bottom bed. The solids leaving the bottom FB overflowed into an airtight solids collector.

Fluidizing gas (air) supplied to the system passed through a flowmeter before entering the bottom FB. A fraction of the inlet

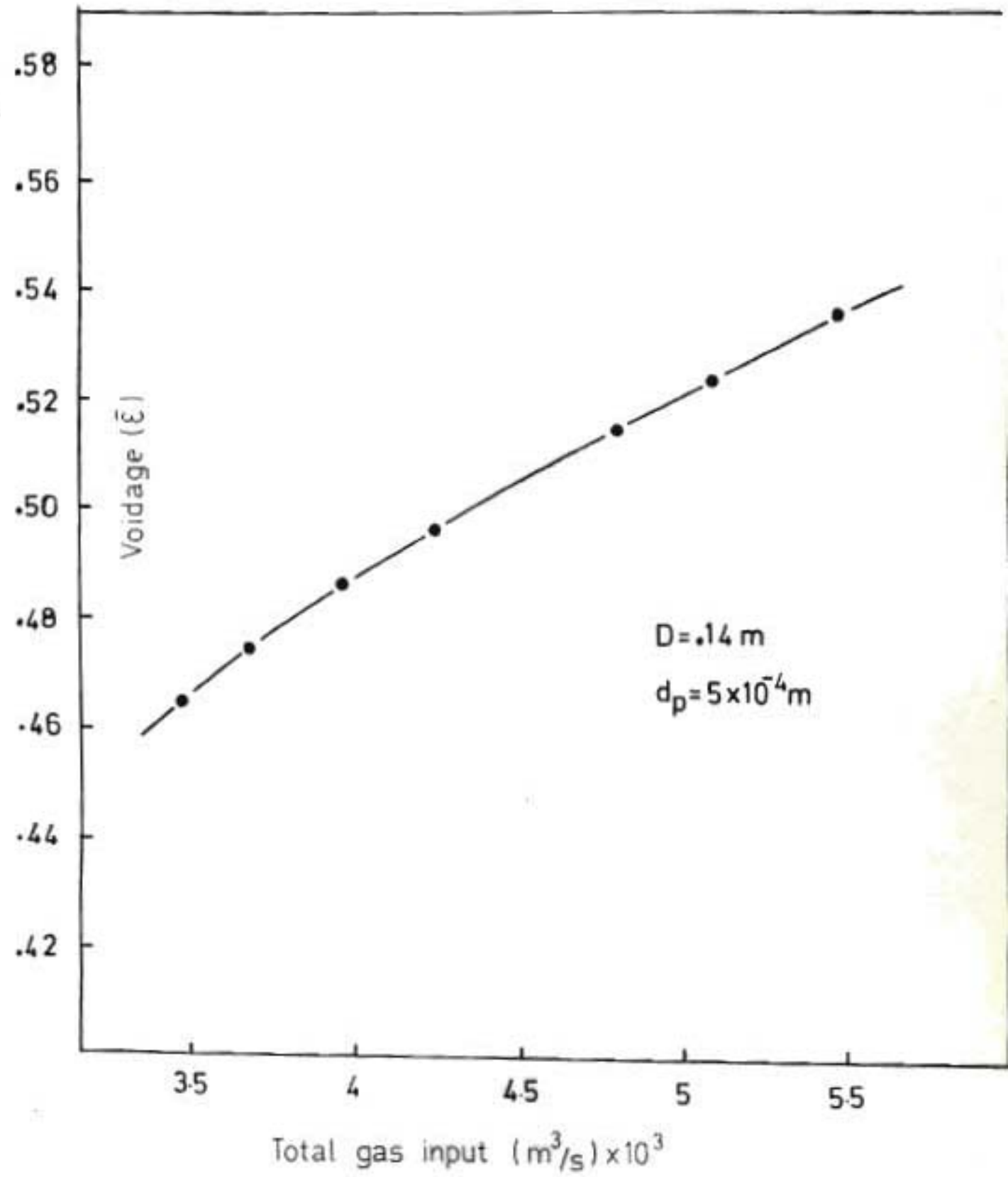

Figure 3.1 : Relation of the solids voidage in the FB system and the total gas throughput

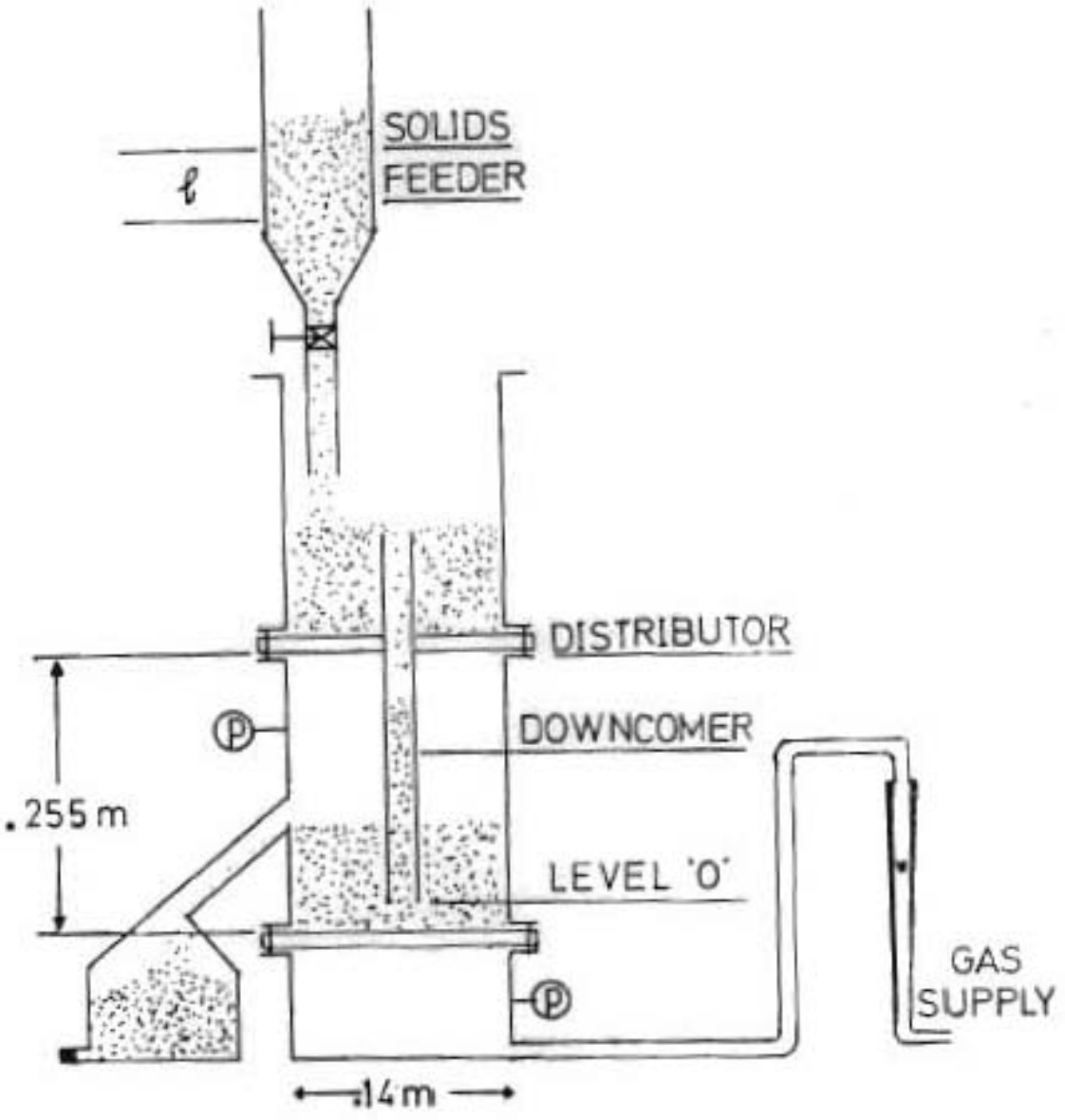

Figure 3.2. Apparatus used to investigate the solids downflow in a downcomer and its relation to the total gas supply

gas travelled up through the downcomer while the rest passed through the interstage distributor.

In a set of experiments the solids level in the downcomer was fixed at an arbitrary level and kept at this level by regulating the solids supply from the feed hopper. Different values of total gas flowrate to the system were used for each selected solids level.

The solids mass rate was measured by the time taken for the level of solids to descend a measured distance (ℓ) in the hopper (Figure 3.2)

To determine the amount of gas travelling through the FB only, (excluding the downcomer) a separate set of experiments were carried out on the apparatus shown in Figure 3.3. In these experiments the same solids and gas rates were chosen but the level in the downcomer was held artificially as shown in the figure rather than by overflow from the top bed. The gas travelling through the downcomer was obtained by difference.

Experiments at selected solids levels in the downcomer were performed using four different downcomers of internal diameters 0,070m, 0,054m, 0,036m and 0,025m.

The apparatus used was made out of plexiglass for easy observation. Fine stainless steel mesh was used for the distributor plates. This incurred only a very small pressure drop.

3.1.3. Results and discussion

The experiments on the downcomers were focused on the moving bed regime of solids. Downcomers can operate under FB conditions as well, though this regime often causes problems because of high gas velocities, slug formation and an unsteady solids downflow. In the

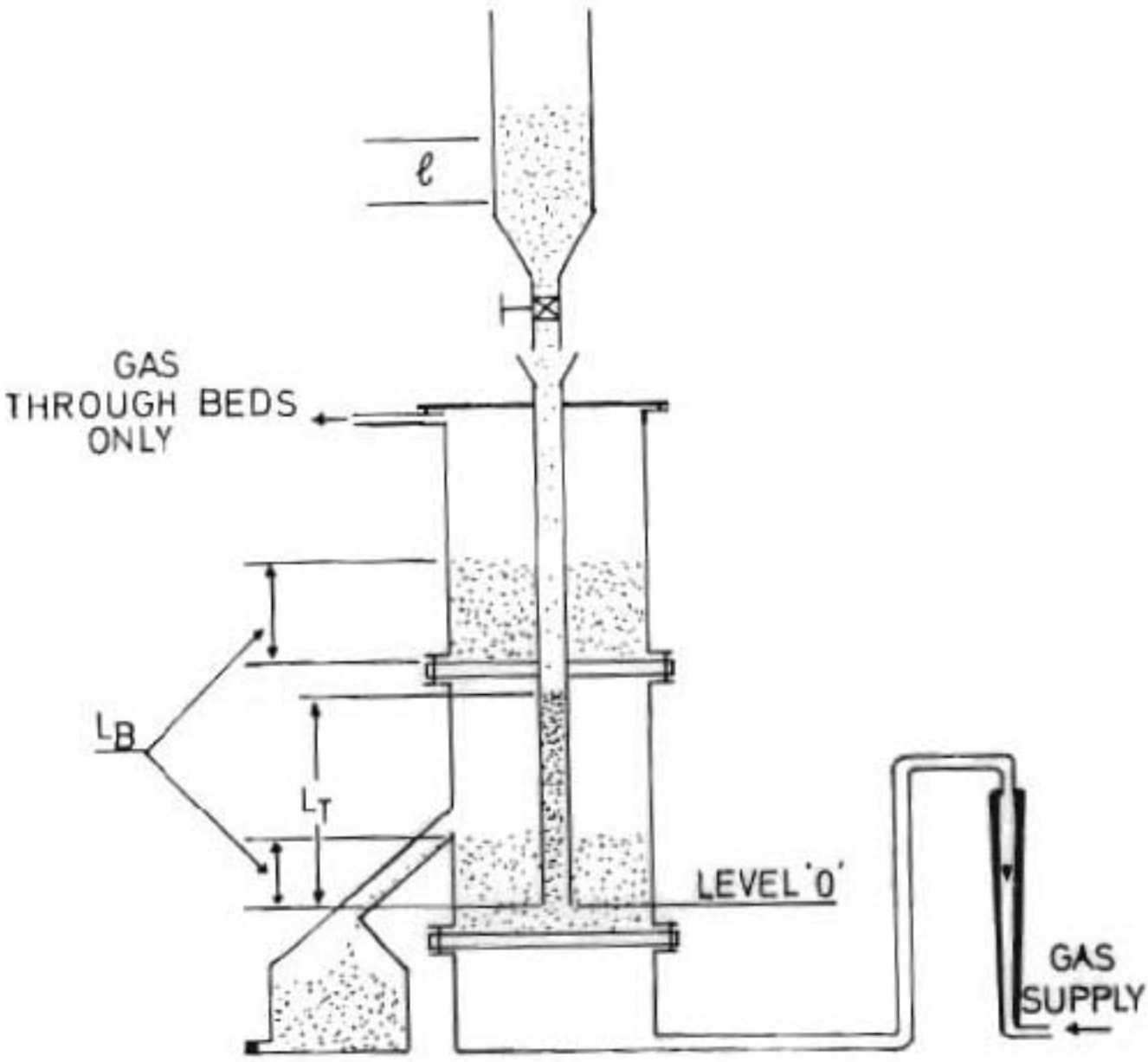

Figure 3.3. A variation of apparatus shown in Figure 3.2 used for the determination of the fraction of gas passing through the FBs only

moving bed flow regime the solids downflow in the downcomer was found to increase linearly with total gas supply until it reached a maximum (Figure 3.4). If the gas supply was further increased a point was reached where the pressure gradient in the downcomer became equal to that of the FBs. A transition from a moving bed flow to a FB flow of solids then occurred in the downcomer.

The solids downflow in the FB region decreased with air supply. Voids seen in the downcomer hindered the solids downflow. The same observation was made by Knowlton[30] *et al*. At much higher air velocities the downcomer became a pneumatic conveyor with solids transported from the bottom to the top FB.

Experiments to determine the amount of air travelling up the downcomer showed that:

(a) For a given downcomer and FB cross section areas,if the solids height in the FBs is fixed, increasing the solids level in the downcomer resulted in a non-linear decrease in gas passing through the downcomer. The FBs were just fluidized (Figure 3.5).

(b) In the moving bed regime if the solids level in the downcomer was increased this caused an increase in solids downflow for the same total gas rate to the system.

(c) The fraction of gas travelling up the downcomer for a selected solids height in the downcomer remained constant for the moving bed regime of solids and was independent of gas supply rate to the system (Figures 3.6,3.7).This can be explained if one considers that a FB can expand at a constant pressure. In contrast, with the downcomer still in the moving bed regime, no extra gas can travel up the downcomer because it would be met with an increasing resistance. Based on the same argument this gas fraction would be equal to the gas

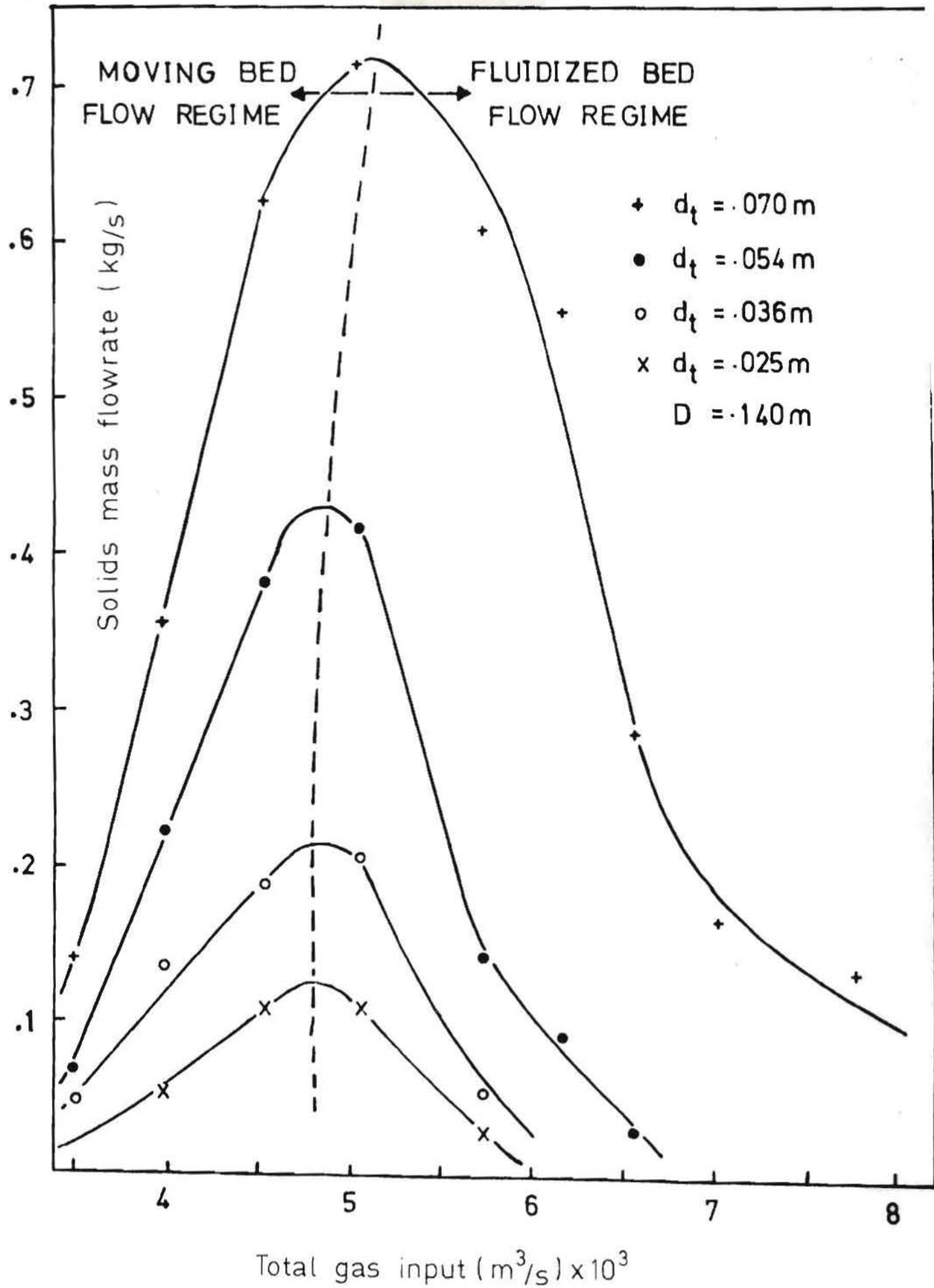

Figure 3.4 : Solids mass flowrate through the downcomers and its relation to the total gas throughput

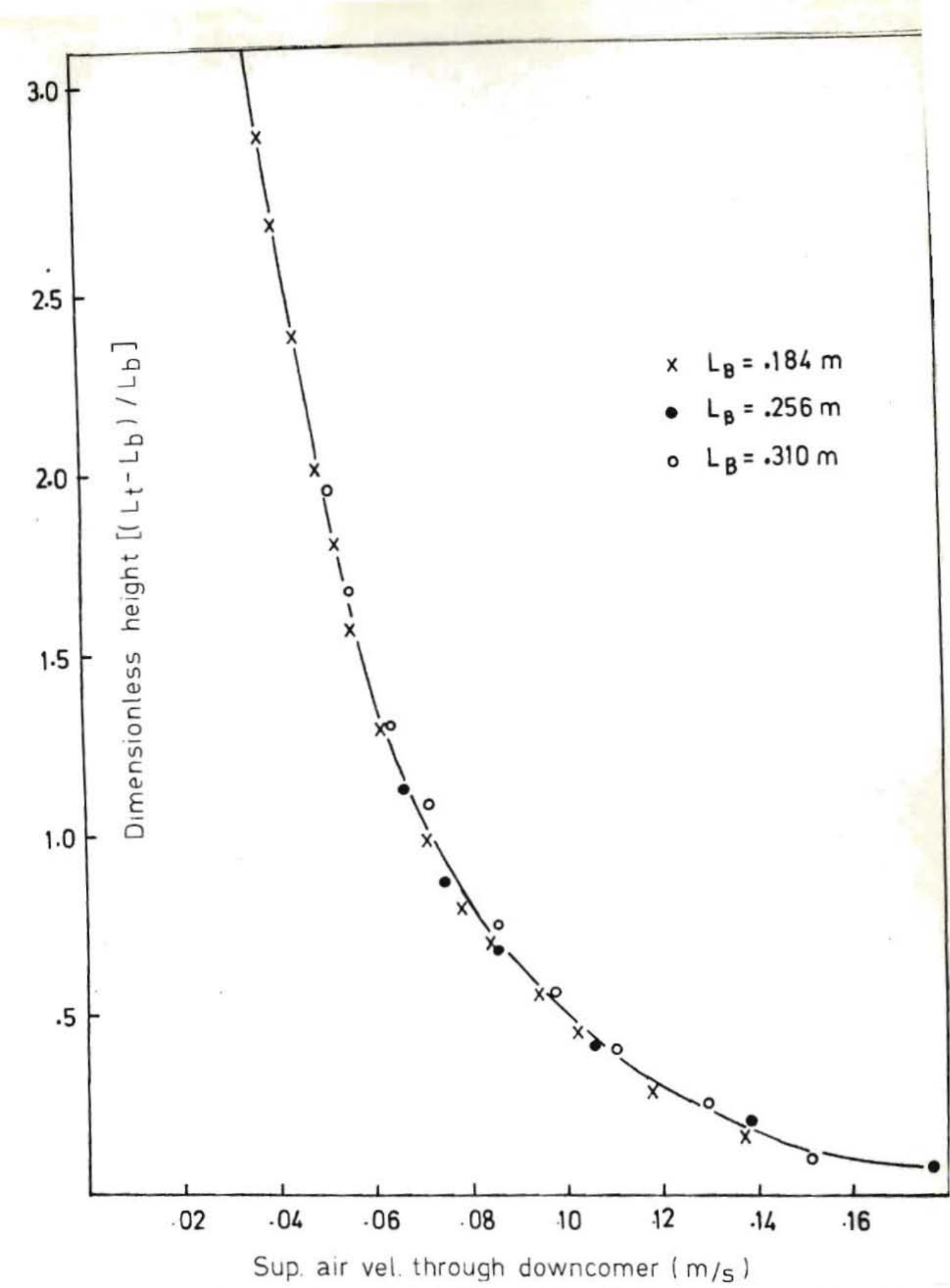

Figure 3.5 : Dimensionless solids height and its relation to the gas velocity through the downcomer when the FBs are at minimum fluidizing conditions

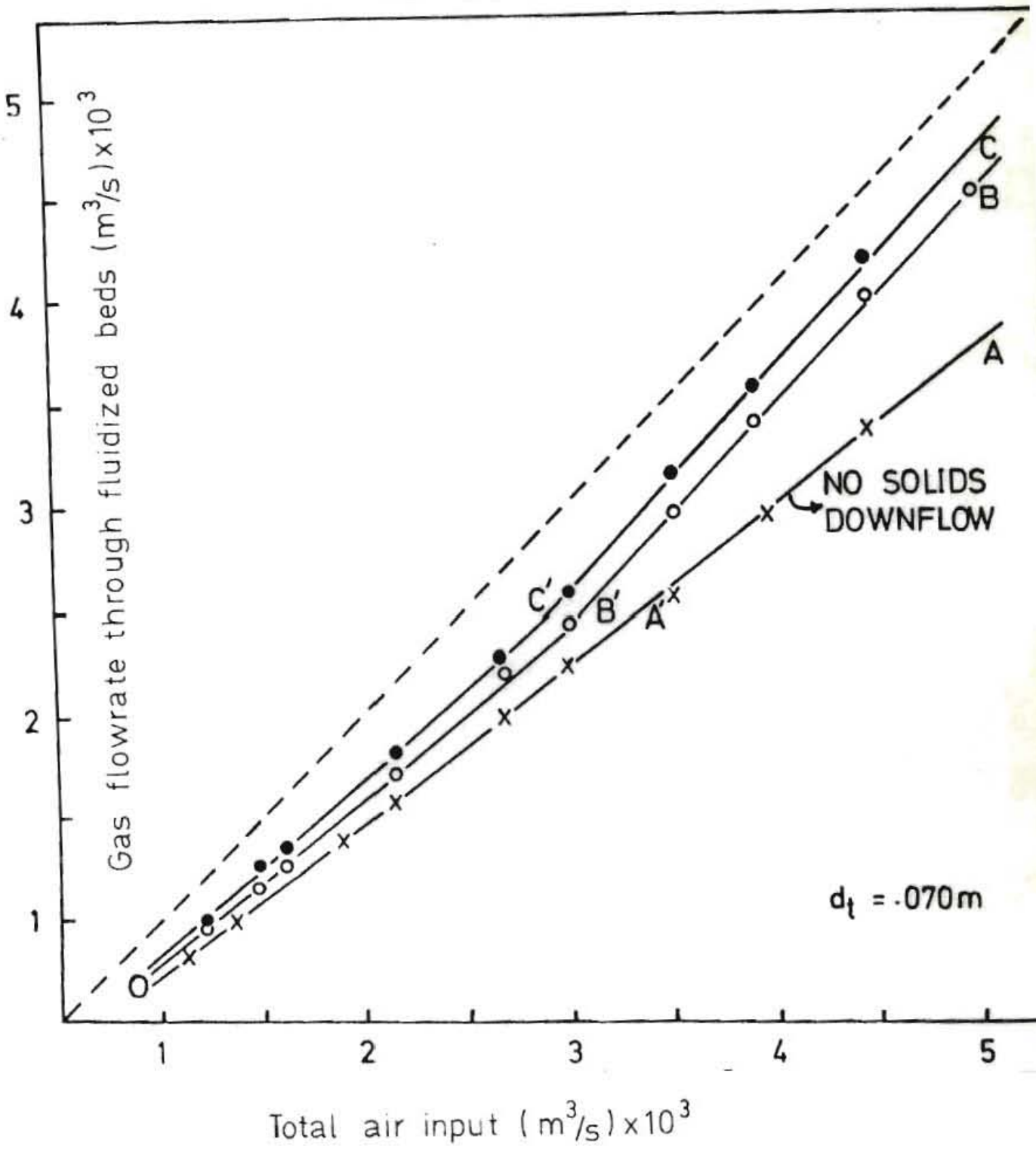

Figure 3.6 : Volumetric flowrate of gas through the FBs and its relation to the total gas supply for downcomer with an internal diameter, d_t = 0,070m

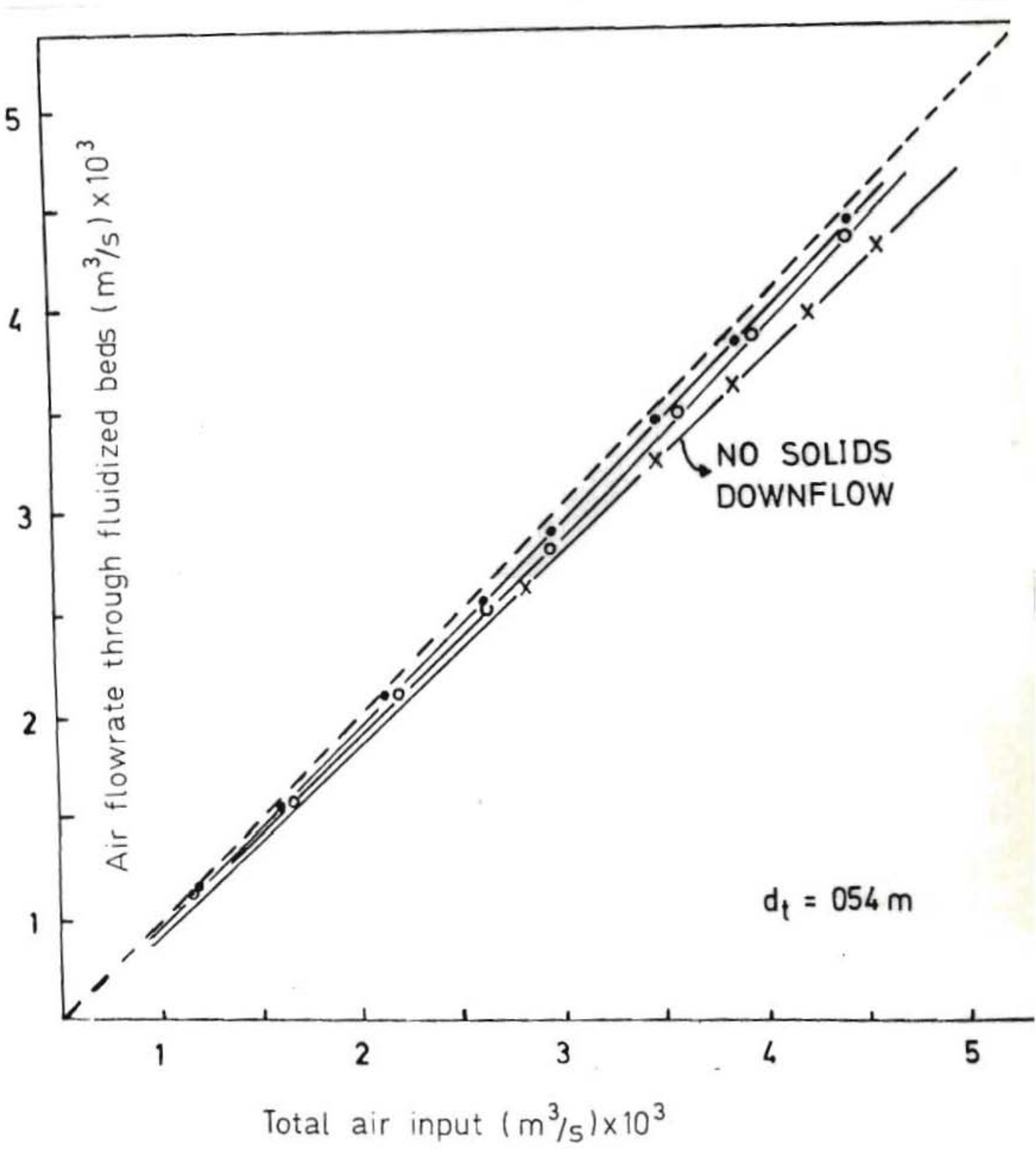

Figure 3.7 : Volumetric flowrate of gas through the FBs and its relation to the to gas supply for downcomer, with an internal diameter, d_t = 0,054m

passing through the downcomer when the FBs are just fluidized (pts B', C', Figure 3.6).

(d) If there was no solids supply to the top FB then the solids level in the downcomer settled to an equilibrium position depending on the pressure drop across the two FBs (and distributor). Under these conditions the fraction of gas travelling through the downcomer was a function only of the downcomer area (OA'A, Figure 3.6).

The pressure gradient in the downcomer for the moving bed region is plotted in Figure 3.8, against the solids velocity. Recall that the gas velocity and voidage remained constant in this region. This Figure confirms work done by Yoon and Kunii[37] on moving beds.

The friction factor f_s for the moving bed region is estimated from the experimental data given in Table A.1.2. and is plotted as a function of u_s in Figure 3.9. The empirical equation relating the two parameters is:

$$f_s = 0{,}049\ u_s^{-2{,}4} \qquad \text{E.3.5}$$

3.1.4. Design of downcomers

In order to design a fluidized bed system its duty must be specified. This fixes the gas throughput as well as the solids circulation rate for a circulating system. The design therefore of the interstage downcomers reduces to finding the required diameter to accommodate these solids mass rates. The proposed downcomer design procedure is included in Appendix 1 and illustrated with a numerical example. The same procedure was also used for the design of the downcomers for our PFBC. (The full investigation on the downcomers can be found in Reference 38)

3.2 USE OF A NON-MECHANICAL CONTROL VALVE TO CONTROL SOLIDS CIRCULATION IN A MULTISTAGE FB SYSTEM

In Section 3.1 the downcomers joining vertically staged FBs

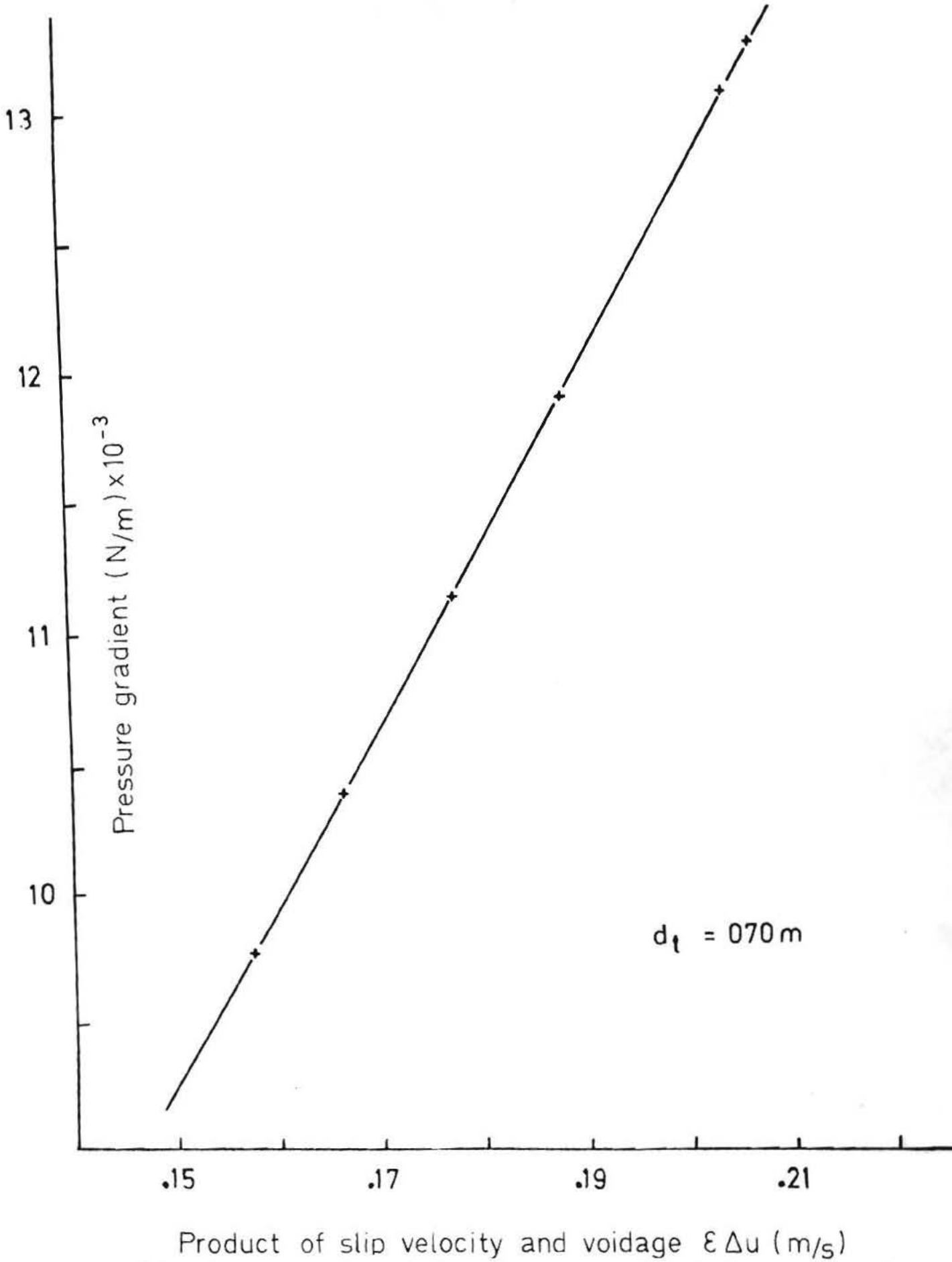

Figure 3.8. Pressure gradient in the downcomer and its relation to the product of the voidage and slip velocity

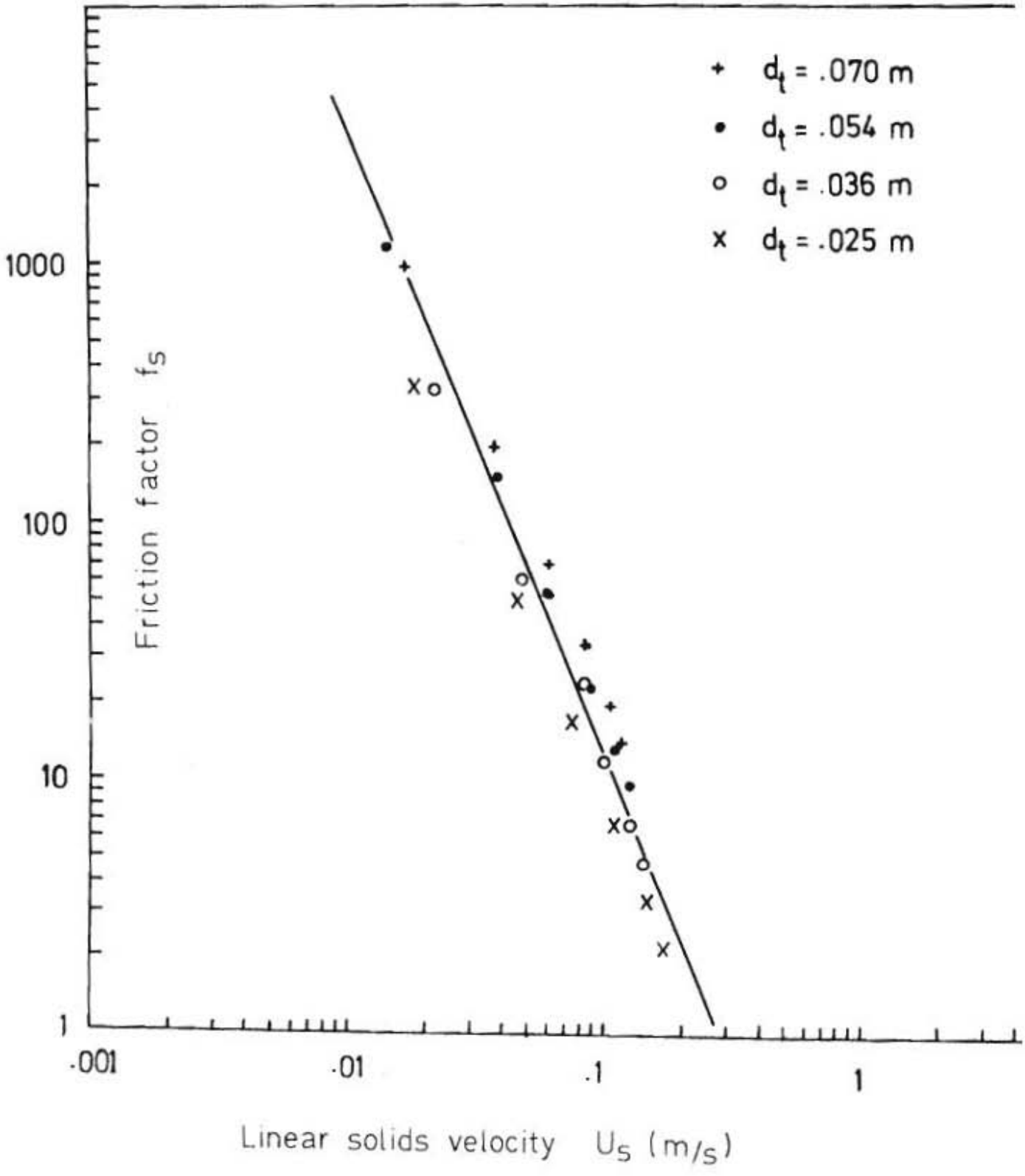

Figure 3.9 : The friction factor and its relation to the solids velocity through the downcomers

were investigated and a design method was suggested for determining the most suitable interstage downcomer for a given maximum solids downflow rate. It was also shown that solids flowrates in the downcomers could be varied by altering the flow of the fluidizing gas. However, if a multistage fluidized system is to be used as a reactor with the fluidizing gas being one of the reactants then it may be necessary to achieve solids control other than by varying the fluidizing air. The use of a mechanical solids control valve positioned outside the reactor seemed a better way to control the flow of solids in an FB system. Thus solids leaving the bottom FB entered the control valve and then a pneumatic lift line which returned them to the top FB.

Non-mechanical solids flow control valves have been investigated by Knowlton *et al.*[29,30]. Initial work though on a modular valve of this type showed that the solids passing through the valve were so aerated that added aeration (that would normally be needed for control of the solids flowrate[29,30]) did not have much effect on the flowrate.

Furthermore we observed that once a certain high solids flowrate was reached the flow could not be stopped. Thus the use of this type of valve for external control of solids circulation in our PFBC needed further investigation.

3.2.1. Theoretical analysis

For the purpose of the analysis which follows the 'non-mechanical' valve having a shape of the letter λ was divided into three regions (Figure 3.10).

(a) The entry region to the λ valve.

(b) The region between the entry and aeration point, and

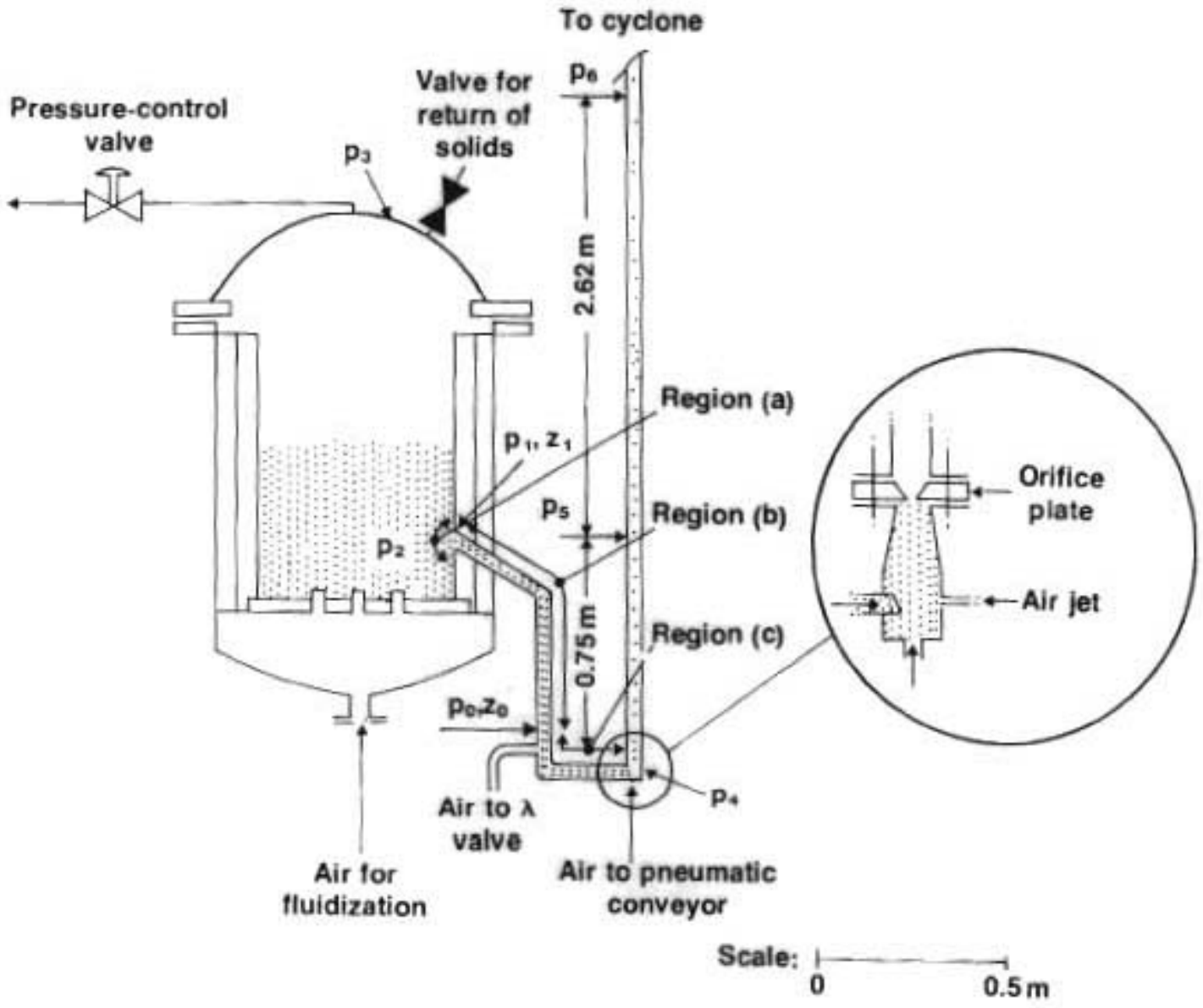

Figure 3.10. Apparatus used for experiments on the non-mechanical λ valve

(c) the region between the aeration point and the discharge into the pneumatic conveyor.

Experimental data were obtained for all three regions, and a theoretical interpretation is presented for the first two regions. For the third region, further experimental work and a more complicated theoretical approach are necessary to account for the air injected at the aeration point on the side and for the change in momentum and loss of energy of the aerated solids as they travel through the 90^{o} bend.

3.2.1.1. The entry region (a) to the λ valve

For this region, two different approaches were used. The first is based on a simple type of model to describe the discharge of the solids by use of the following equation:

$$\Delta p_a = \frac{W_s^2}{2c_d^2 \rho_s(1-\varepsilon)} , \qquad \text{E.3.6.}$$

where Δp_a is (loosely speaking) the drop in pressure between the bulk of the FB and the opening to the λ valve, W_s is the mass flux of the solids, $\rho_s(1-\varepsilon)$ is the bulk density in the FB, and c_d is a discharge coefficient with a value in the region of 0.5 to 0.6. This model was shown by Jones and Davidson[39] and later by Burkett *et al.*[40] to be a remarkably adequate description of a highly complicated two-phase flow system.

The second approach, which is based on the work of De Jong and Hoelen[41], relates the drop in pressure, Δp_a, to the radial distance from the opening to the λ valve by use of the Ergun equation.

$$-\frac{dp}{dr} = K_1 \Delta u + K_2 \Delta u \, |\Delta u| \quad , \qquad \text{E.3.7}$$

where $K_1 = 150 \frac{(1-\varepsilon)^2}{\varepsilon^2} \frac{\mu_g}{\phi_s^2 d_p^2}$,

$K_2 = 1{,}75 \frac{\rho_g}{\phi_s d_p} (\frac{1-\varepsilon}{\varepsilon})$, and

$\Delta u = u_g - u_s$

With r increasing with distance from the entry to the λ valve and into the FB, and from the continuity equation (on the assumption that the voidage of the fluidized bed, ε, is constant and does not change near the entry to the valve):

$$u_{g_r} = \frac{u_{g\lambda} r_\lambda^2}{r^2} \qquad \text{and} \qquad u_{s_r} = \frac{u_{s_\lambda} r_\lambda^2}{r^2} \qquad \text{E.3.8}$$

where subscript λ refers to conditions at the entry to the λ valve. The integration of E.3.8 (as per De Jong and Hoelen[41]) with respect to r from $r=r_\lambda$ (the radius of the entrance to the λ valve) to $r=\infty$ leads to the following equation:

$$\Delta p_a = K_1 (\Delta u)_\lambda r_\lambda + K_2 \frac{(\Delta u)_\lambda^2}{3} r_\lambda \qquad \text{E.3.9}$$

where $(\Delta u)_\lambda = |-u_{g_\lambda} + u_{s_\lambda}|$

3.2.1.2. The region between the entry region of the valve and the aeration point

By the incorporation of interparticle stresses[42,43] and use of a

balance on the segment of the λ valve between the entry region and the aeration point, the following relation can be postulated:

$$\frac{d\sigma_z}{dz} + \frac{dp}{dz} + \rho_s(1-\varepsilon)g + C_1\rho_s(1-\varepsilon)\frac{d}{dz}(u_{sz})^2 + \frac{4\tau_w}{D_\lambda} = 0 \qquad \text{E.3.10}$$

where σ_z is the normal stress and u_{sz} the velocity of the solids at height z averaged over the cross-section of the λ valve, C_1 is a constant depending on the velocity profile (for a flat profile $C_1 = 1$), and τ_w is the solids shear at the wall. According to Walters[42],

$$\tau_w = B_1 D_1 \sigma_z, \qquad \text{E.3.11}$$

where B_1 and D_1 are constants expressed in terms of the effective angle of internal friction of the solids (δ) and the angle of wall friction (φ). Their product is as follows:

$$B_1 D_1 = \frac{\tan\phi \cos^2\delta}{(1+\sin^2\delta) \pm 2y \sin\delta}$$

where $$y = \frac{2}{3c}\left(1 - (1-c)^{\frac{3}{2}}\right)$$

and $$c = \left(\frac{\tan\phi}{\tan\delta}\right)^2$$

The positive and negative signs refer to the respective static and dynamic conditions in the λ valve[42].

Substitution of τ_w from E.3.11 into E.3.10 and the integration of E.3.10 from z_1 to z of region (b) of the λ valve with the following boundary conditions gives

$\sigma_z = 0$ at $z = z_1$. ($z < z_1$ in Figure 3.10)

$$\Delta\sigma_z = e^{-\alpha(z_1-z)}\left[\int_{z_1}^{z} [\rho_s(1-\varepsilon)g + \frac{dp}{dz} - \rho_s(\frac{1-\varepsilon}{C_1})\frac{d}{dz}(u_{sz})^2]e^{\alpha(z_1-z)}dz, \right. \qquad \text{E.3.12}$$

where $\alpha = \frac{4B_1D_1}{D_\lambda}$.

Since region (b) as given in Figure 3.10, is defined by pressure tapping, p_1 and p_o, and heights z_1 and z_o, and it has been shown that, while region (a) was being examined, the solids had reached their maximum speed at level z_1, it follows that, in region (b), there is no acceleration and the voidage ε is constant. In addition, dp/dz is a constant and $d(u_{sz})^2/dz$ is zero.

E.3.12 can therefore be evaluated for the entire region (b), and the value of normal stress between particles $\Delta\sigma_{z_o}$ at $z = z_o$ (Figure 3.10), written as

$$\Delta\sigma_{z_o} = \frac{1}{\alpha}\left[\rho_s(1-\varepsilon)g + \left(\frac{\Delta p}{\Delta z}\right)_{z_o \text{ to } z_1}\right]\left[1-e^{-\alpha(z_1-z_o)}\right], \qquad \text{E.3.13}$$

(σ_{z_1} is taken as zero.)

The mathematical approach that led to E.3.12 is compared with that applied to the downcomers examined in a previous investigation[38]. If the flow in region (b) of the λ valve is treated in the same manner as that through the downcomers, the dynamic behaviour of this system could be described instead in terms of a friction factor, f_s, as given by the following equation:

$$\left(\frac{\Delta p}{\Delta z}\right)_{z_1-z_o} - 2f_s\frac{W_s^2}{D_\lambda\rho_s(1-\varepsilon)} + \rho_s(1-\varepsilon)g = 0, \qquad \text{E.3.14}$$

where $W_s = u_s\rho_s(1-\varepsilon)$.

E.3.13 and E.3.14 represent two different correlations of the same region (b) of the λ valve. In the first instance, energy losses are expressed in terms of interparticle stresses, whereas, in the second instance, an overall friction factor is introduced.

It should be emphasized that, although both E.3.13 and E.3.14 deal

with the energy losses of the same system, E.3.13 does not depend on a knowledge of the velocity of the solids. It is known that, in an ideal FB there are no interparticle stresses; the evidence of such stresses is therefore an indication of a departure from the ideal and of energy losses. E.3.13 can thus be used as an indication of these losses in an FB where the net velocity of the solids is zero.

3.2.1.3 Losses of energy within an FB

If the procedure followed in Section 3.2.1.2 for derivation of the force-momentum equation is applied to an FB, and it is borne in mind that the pressure gradient decreases with height, the normal stress between particles can be expressed as

$$\Delta\sigma_z = \frac{1}{a}\left[\rho_s(1-\varepsilon)g - \left(\frac{\Delta p}{\Delta z}\right)_{z_o \text{ to } z_1}\right]\left[1-e^{-a(z_1-z_o)}\right], \qquad \text{E.3.15}$$

where (z_1-z_o) is the height of the FB.

The significance of E.3.15 is that the normal stress between particles is zero if the observed pressure gradient is equal to the weight per unit volume of the fluidizing solids. This is the case in an ideal FB. In contrast, the larger the difference between these two terms, the greater the departure from an ideal system.

3.2.2. Apparatus and procedure

The experimental apparatus used consists of a single FB, a non-mechanical control valve, and a pneumatic conveyor in which the flow-rate of the solids can be measured, and via which the solids can be returned to the FB.

Higher flow-rates for the solids can be achieved if the pressure in the FB is increased by use of the pressure-control valve shown in Figure 3.10. The purpose in increasing the pressure was to simulate the other FBs and the effect they have on the circulation of the solids in a

multistage system. The flow-rates of the solids were measured direct by weighing, or determined from the calibration curve for the conveyor (Figure 3.11) Pressure readings were taken direct from water or mercury manometers. The pressure tapping p_o was placed 0,03m above the side aeration; p_1 was placed at the entrance to the λ valve and 0,71m above p_o, and p_2 was placed in the FB 0,2m away from the entry to the λ valve. The pressure tappings for the conveyor were placed 2,62m apart and 0,75m from the receiver of the conveyor.

During each experimental run , the system pressure p_3 was fixed , by use of the pressure control valve and all the other pressures were recorded for various values of aeration through the λ valve. The same procedure was followed with a different pressure, p_3 in the system.

In a different set of experiments, the pneumatic lift line (conveyor) was removed, and aerated solids discharging from the λ valve were collected and weighed in a container with a rotameter attached to it for measuring the expelled air. These experiments were also repeated for different pressures in the system. The properties of the solids used are listed in Table A.2.1.

3.2.3. Results and discussion

During the experimental work the following observations were made.

(1) The pressure p_2 within the FB and near the entrance to the λ valve was always higher than the pressure p_o near the injection point. This is essentially the difference between our work and that of Knowlton and Hirsan[29] and Knowlton *et al.*[30]. They found that the pressures in the FB were low and that the slip was such that the pressure at the aeration point was always the highest.

(2) The FB was fluidized with air at 1.4 U_{mf}, and, in all cases investigated, the amount of air that escaped from the FB through the

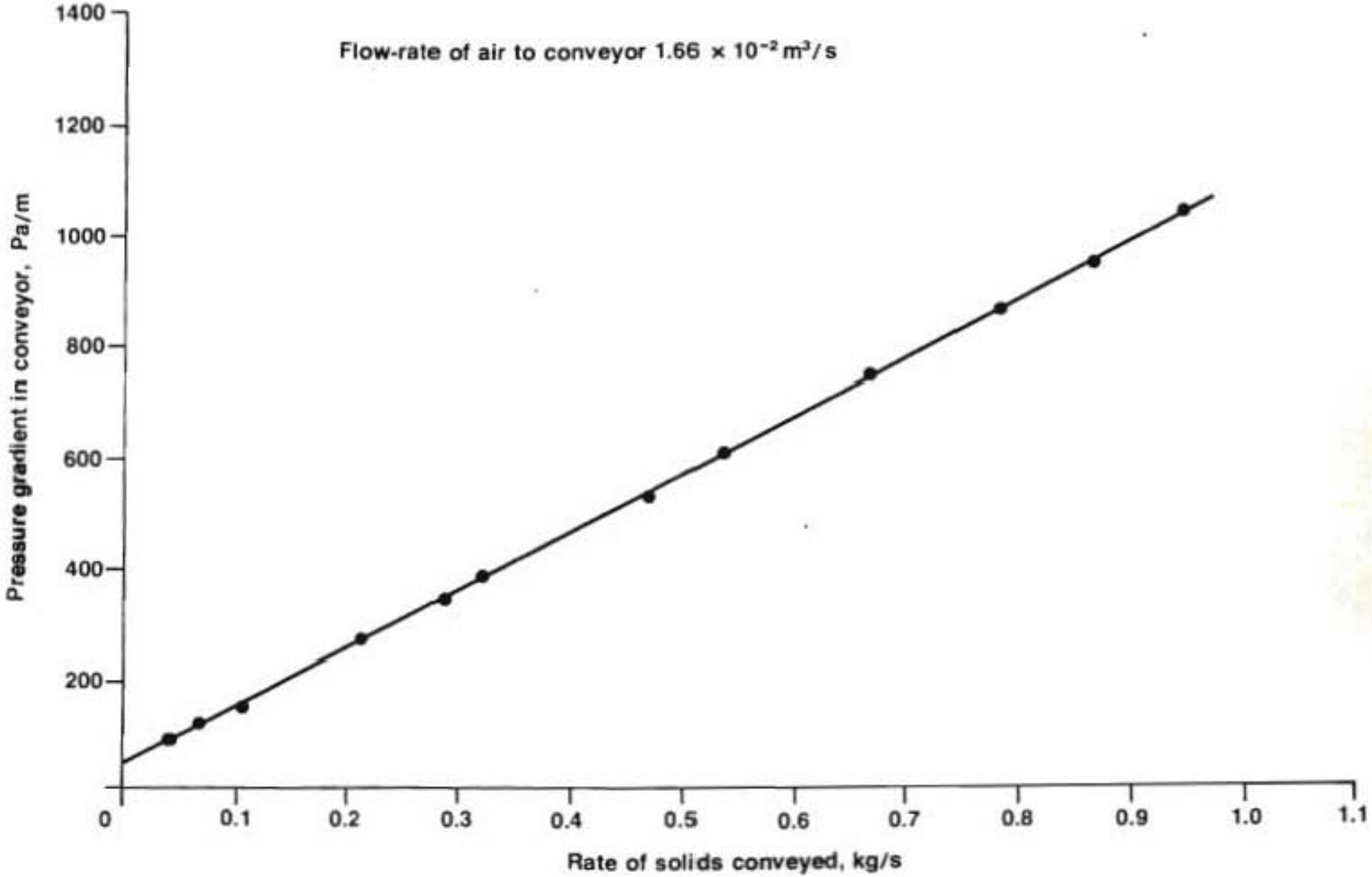

Figure 3.11. The experimental relation between the pressure gradient in the conveyor and the mass velocity of solids through the pneumatic conveyor

λ valve was very small compared with the fluidizing air passing through the bed and the air supplied to the pneumatic conveyor.

(3) The interstitial velocity of the air in the λ valve was always greater than the linear velocity of the solids and dragged the solids with it (Figure 3.12). Data for Figure 3.12 were obtained from the second set of experiments, for which the pneumatic conveyor was removed (Section 3.2.2.)

(4) For each pressure in the FB system, there was a minimum flow of solids through the valve for low aeration, and this minimum increased with increase in the pressure p_3 in the system.

When the pressure in the system was equal to atmospheric pressure, and the pressure p_2 was reduced to below approximately 2700 Pa(gauge) by lowering of the amount of the solids in the FB, it was found that, in spite of the aeration through the valve , no solids entered the valve. This might be because the pressure exerted by the solids head was not great enough to overcome the resistance offered by the λ valve due to its shape, or because a local bridge was formed in the vicinity of the bend.

(5) At very high pressures in the system (greater than about 10800 Pa(gauge)) it was observed that there was no control of the flow of solids through the λ valve if the conveyor was lifting the solids away. The aeration was apparently needed to initiate the flow of solids in the uncontrolled region.

(6) In the region of uncontrolled flow of the solids, increasing pressures in the system resulted in even larger increases in the drop in pressure at the entrance $(p_2 - p_1)$, corresponding to a high solids flux, whereas the drop in pressure in region (b), $(p_1 - p_0)$ appeared to remain constant at the expense of an increase in voidage. Only a few data were recorded for the uncontrolled region because of the

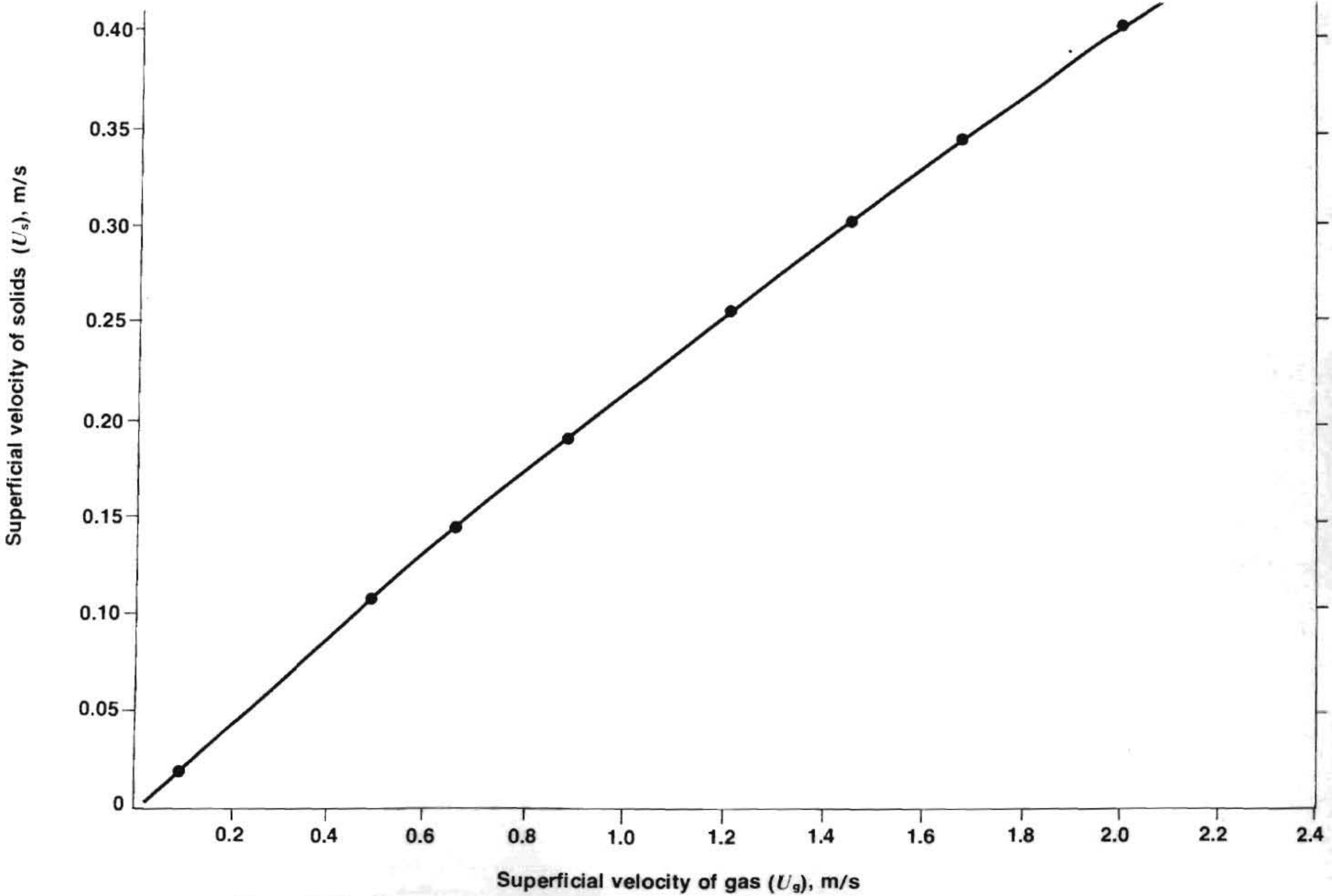

Figure 3.12. Superficial co-current velocities for the solids and the gas through the λ valve. The values were obtained experimentally

very high velocity of the solids, which resulted in the complete emptying of the FB within a very short period.

These observations can be verified from the experimental data included in Table A.2.2 and A.2.3. The region of uncontrolled flow of the solids occurred at pressures p_3 in the FB system of above about 10 800 Pa (gauge). The importance of the transition to the uncontrolled flow of solids is also covered in a later section.

3.2.3.1. Region (a) of the λ value

On the assumption that the voidage at the entry to the λ valve is the same as that of the FB at minimum fluidizing conditions ($\epsilon_{mf} = 0,5$), E.3.6. and E.3.9 were solved for the drop in pressure, Δp_a, by use of the measured flow-rates of the gas and of the solids, and then compared with the drop in pressure ($p_2 - p_1$) measured experimentally with pressure probes placed within the FB and at the entry to the λ valve. The results from E.3.9 are given in Table A.2.4 and compare favourably with the drop in pressure Δp_a obtained experimentally. The results from the orifice equation E.3.6 were compatable only at higher pressures in the FB system and higher flow-rates of the solids. This indicates that, for the low flow-rates of the solids, E.3.6 does not include the downstream 'solids-restraining effect' of the λ valve and the influence that it may have on the behaviour of the solids on their entry to the λ valve. At higher flow-rates for the gas and the solids near the region of uncontrolled flow, aeration through the λ valve became less effective for control of the solids. Losses of energy due to the increasing speeds of the particles in the entry region to the valve determined the flow behaviour of the solids, whereas downstream conditions and the 'solids-restraining effect' had lesser effect on the flow of the solids. Under these conditions the behaviour of the λ valve can simulate that of an orifice plate.

3.2.3.2. Region (b) of the λ valve

By use of the Ergun equation E.3.7, the solids voidage (ε) was determined iteratively for region (b) of the valve for each set of conditions based on the observed values of superficial solids and gas velocities (Figure 3.12) and the observed pressures p_1 and p_0 (Table A.2.2.). For consistency with E.3.14 the normal stress between particles, $\Delta\sigma_{z_0}$, was then calculated from equation E.3.13 and plotted in Figure 3.13 against the linear velocities of the solids for the controlled and uncontrolled flows respectively. The same experimental data were then used in E.3.14 for determination of the friction factor, f_s. The resulting empirical relation between f_s and the linear velocity of the solids (Figure 3.14) is given by

$$f_s = 0{,}29u_s^{-1{,}9} \qquad \text{E.3.16.}$$

E.3.16 differs from that obtained from work on downcomers[38] ($f_s = 0{,}049u_s^{-2{,}4}$) in that it shows less dependence on the linear velocity of the solids. This is possibly due to the fact that, in region (b) of the λ valve, the voidage is somewhat higher than that found in a downcomer.

The high value of the estimated voidage found in region (b) of the λ valve (Table A.2.3) is consistent with work done on gas-solid jets leaving fluidized systems. For example, Massimilla *et al.*[44] found that the voidage in the jet was higher than that in the FB, and Jones and Davidson[39] calculated exit voidages of between 0.6 and 0.9.

The Ergun equation is admittedly meant for low voidage systems. However, it has been shown here that the Ergun equation provides a reasonably good description of systems with a voidage greater than the incipient value as long as the stream of gas and solids can be treated as a uniform medium. A similar view is also held by Stockel[45], who used

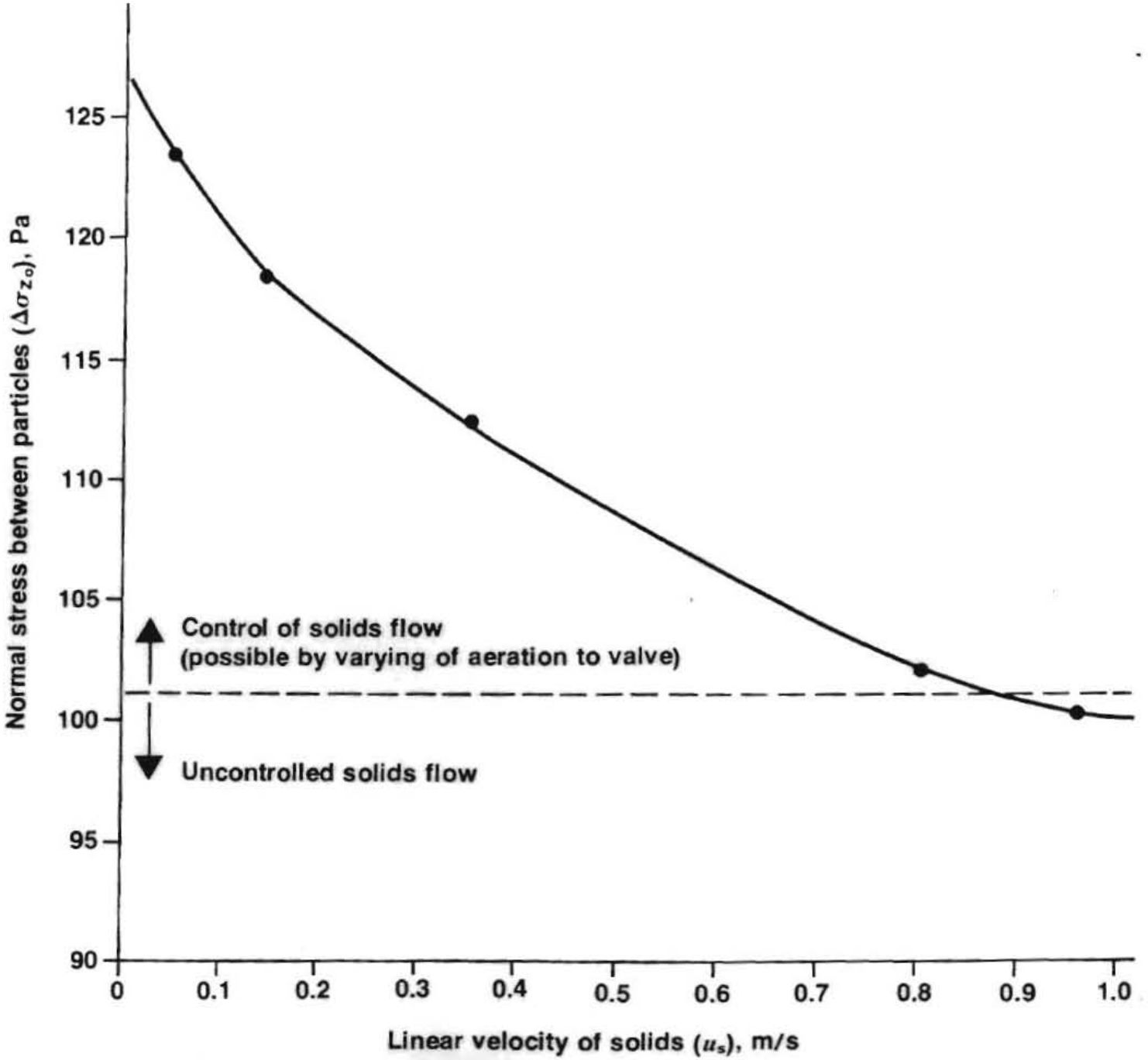

Figure 3.13. Calculated normal stress between particles for region (b) of the λ valve, and its relation to the linear velocity of the solids

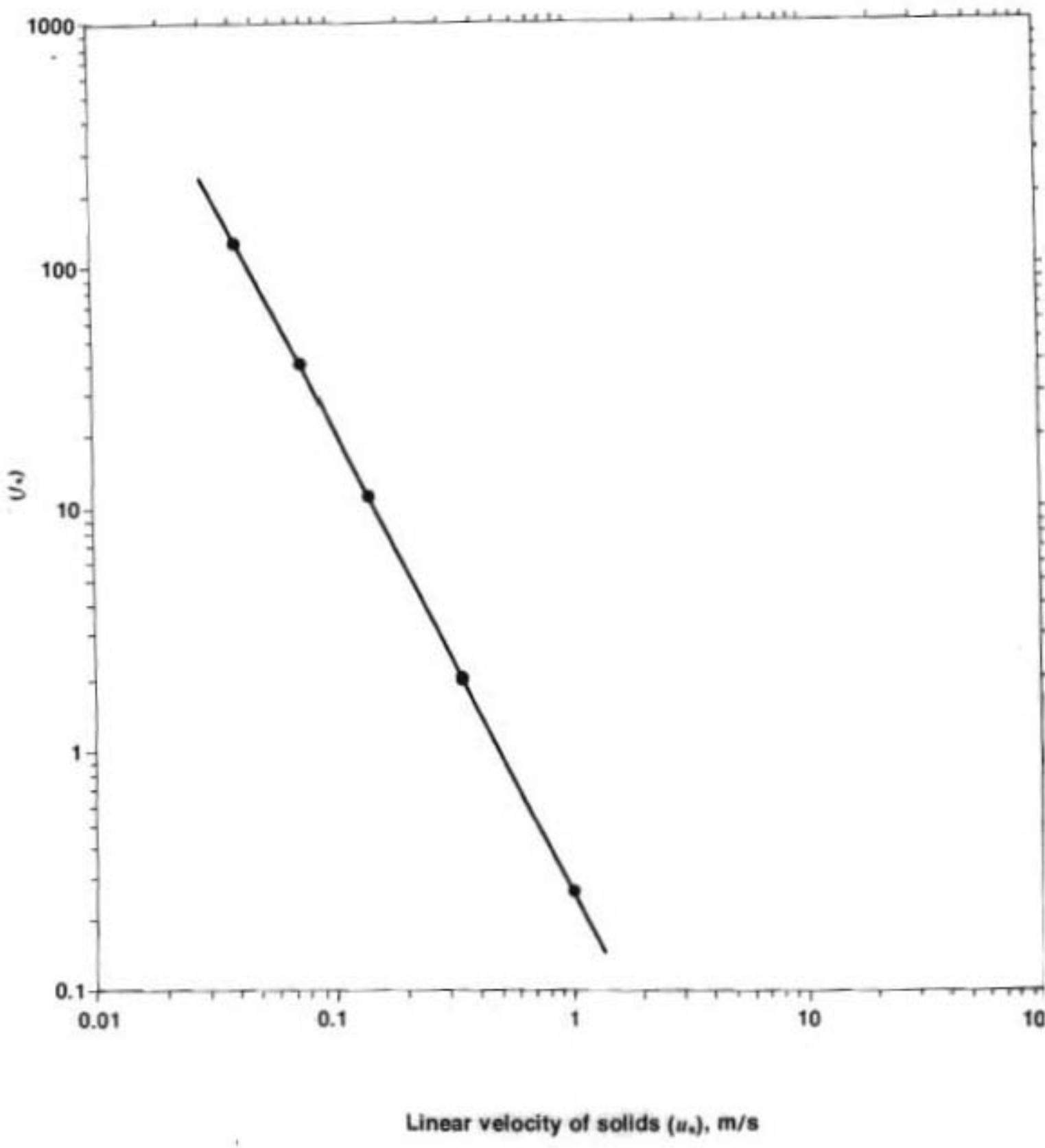

Figure 3.14. The relation between the friction factor and the linear velocity of the solids, the downcomer model being used, for region (b) of the L valve

the Ergun equation for very dilute systems.

In the region of uncontrolled flow, the slip velocity and the linear velocity of the solids became essentially independent of the pressure gradient of the λ valve (Figures 3.15 and 3.16), whereas the friction factor and interparticle stresses became relatively small and less dependent on the velocity of the solids, indicating a much more dilute stream of gas and solids (Figures 3.13 and 3.14,)

Once the uncontrolled region was reached, control at these high pressures in the system could again be re-established by the introduction of back-pressure to the λ valve. The introduction of the back-pressure should be regarded as a means to counteract the effect of a higher pressure in the system by reduction of the flow-rate of the solids and therefore the drop in pressure (p_1 to p_o) measured at the aeration point of the λ valve. This was achieved by the use, in the receiver of the conveyor of an air jet facing the exit of the λ valve to the receiver (Figure 3.10.) Data on these experiments are included in Table A.2.2.

3.2.4. Design of a non-mechanical solids valve

Though a general stepwise procedure for the design of a non-mechanical solids valve fed with solids from an FB is not possible unless different size valves are considered, this was not required at this stage because the solids flowrates in the current investigation were of the same magnitude as the anticipated solids circulation rates in the PFBC.

However, a theoretical approach and a model are presented in this study that can be applied to any other similar system. The back pressure technique re-instating solids flow control if higher operating pressures are required, can be used to increase the pressure

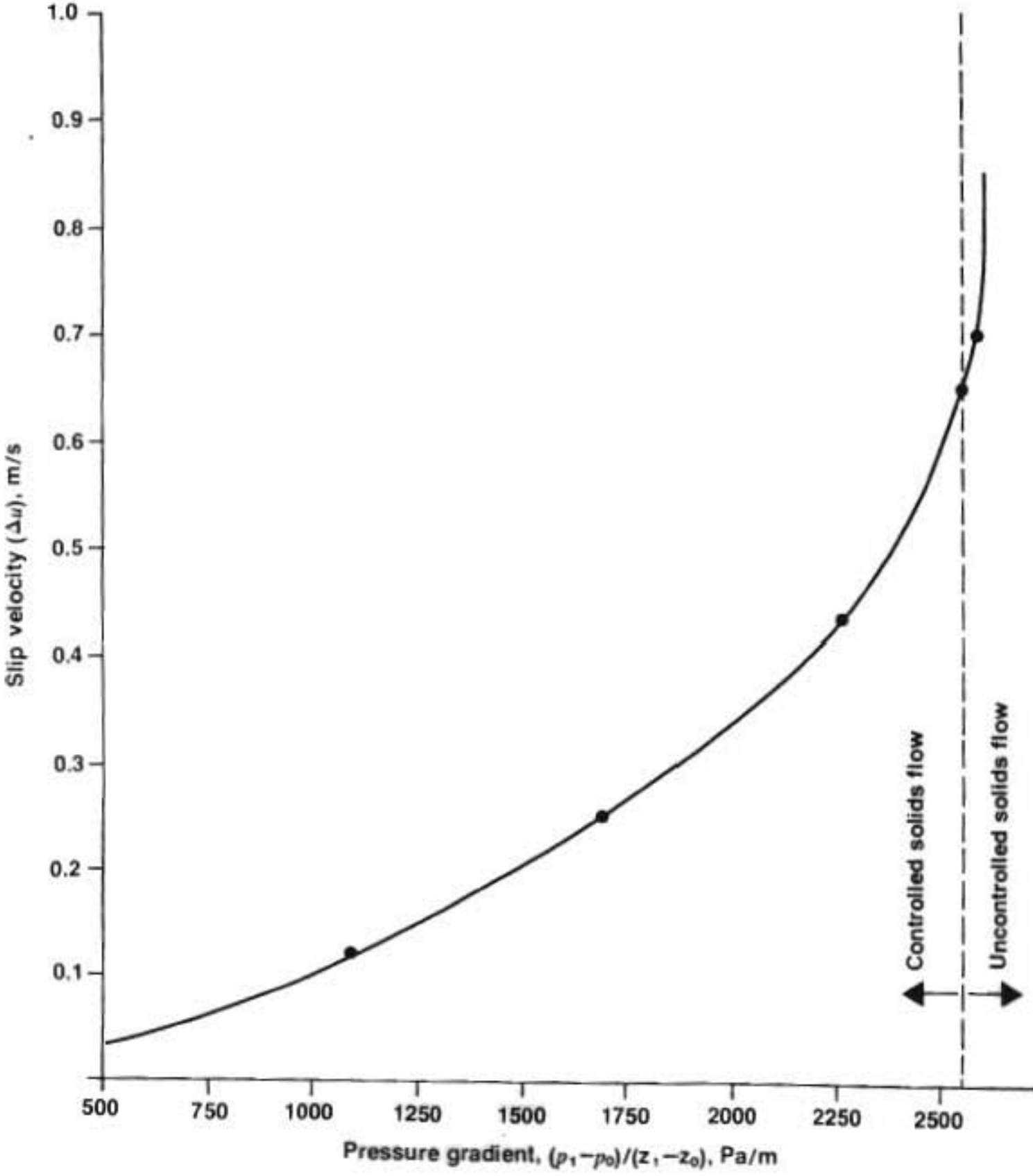

Figure 3.15. The relation between the pressure gradient and the slip velocity for region (b) of the λ valve

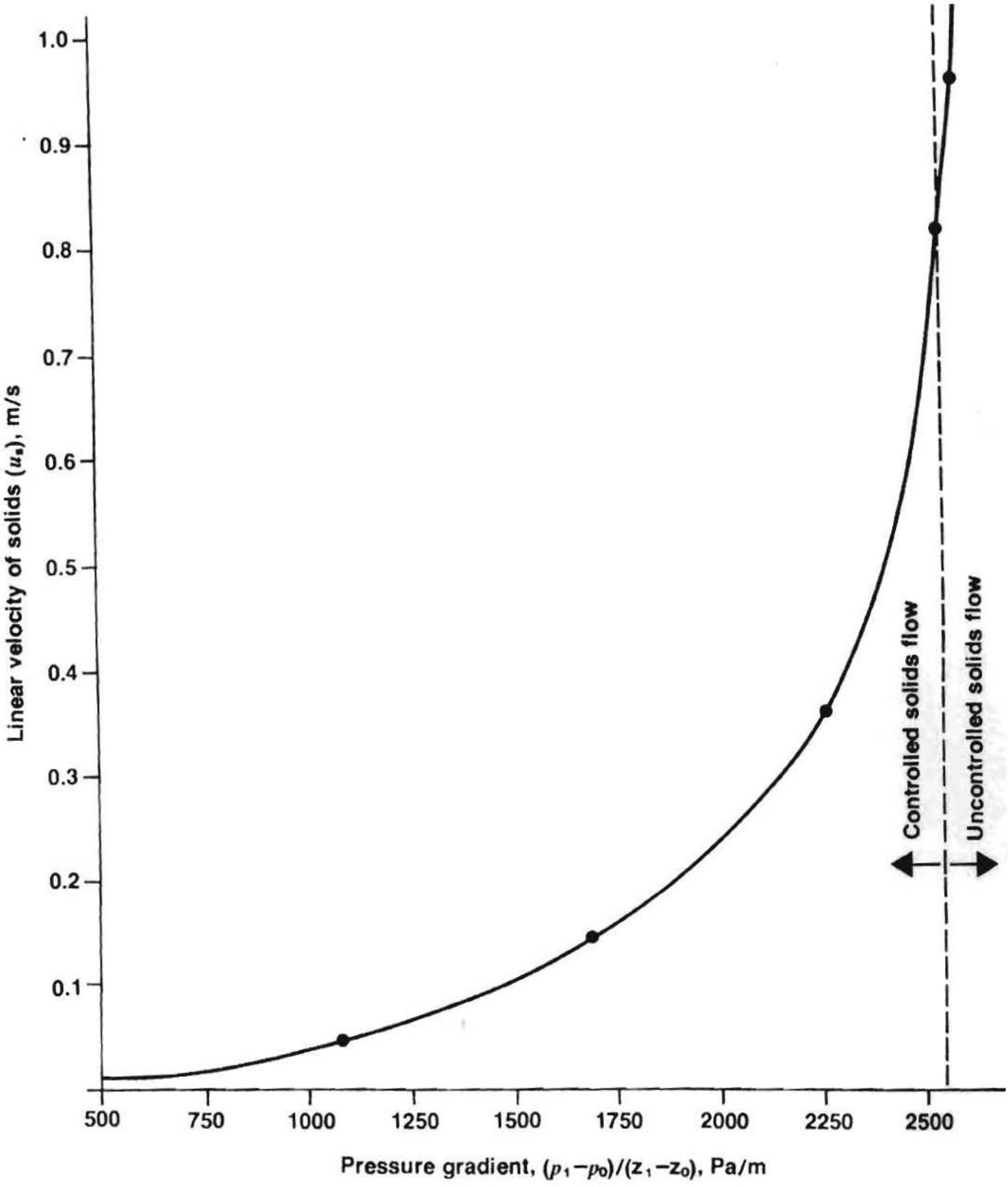

Figure 3.16. The relation between the pressure gradient and the linear velocity of the solids for region (b) of the λ valve

range of operation of the λ valve and eliminate uncontrolled regions of operation. (The entire work on the non-mechanical solids control valve was also submitted for publication to the Chem. Engng Science Journal in April 1981)

3.3. INTERSTAGE DISTRIBUTOR PLATES

The importance of the distributor plate on the quality of fluidization has already been outlined in Section 2.3.2. In a multistage system however, there is a special requirement, and that is, that sand and unburned coal should flow downwards from stage to stage. Also combustion of coal should take place in the lower stages and the unburned coal fines and ash should be able to pass freely through the distributor to higher stages where they would be completely burnt.

The necessity to look for a distributor that can let high quantities of fines pass through it while maintaining good quality of fluidization led to this investigation. In a series of experiments which are described below tests were carried out on a porous distributor and on a distributor with a new type of cyclonic-tuyeres,for comparison purposes, and in order to determine the suitability of the tuyere-distributor as an interstage plate for the multistage PFBC. The experimental results were correlated by adopting existing theoretical and experimental correlations (Section 2.3.2.).

3.3.1 Apparatus and procedure

A plexiglass cylinder with a 0,298m internal diameter and a seven tuyere distributor (Figure 3.17) were used in a series of experiments to determine the distributor characteristics, the FB pressure recovery and the effect that different solid sizes had on the quality of fluidization. For comparison with the work using the tuyere-distributor, similar tests were carried out on the same apparatus using instead, a porous-distributor (30μm pores)which had a very high pressure drop

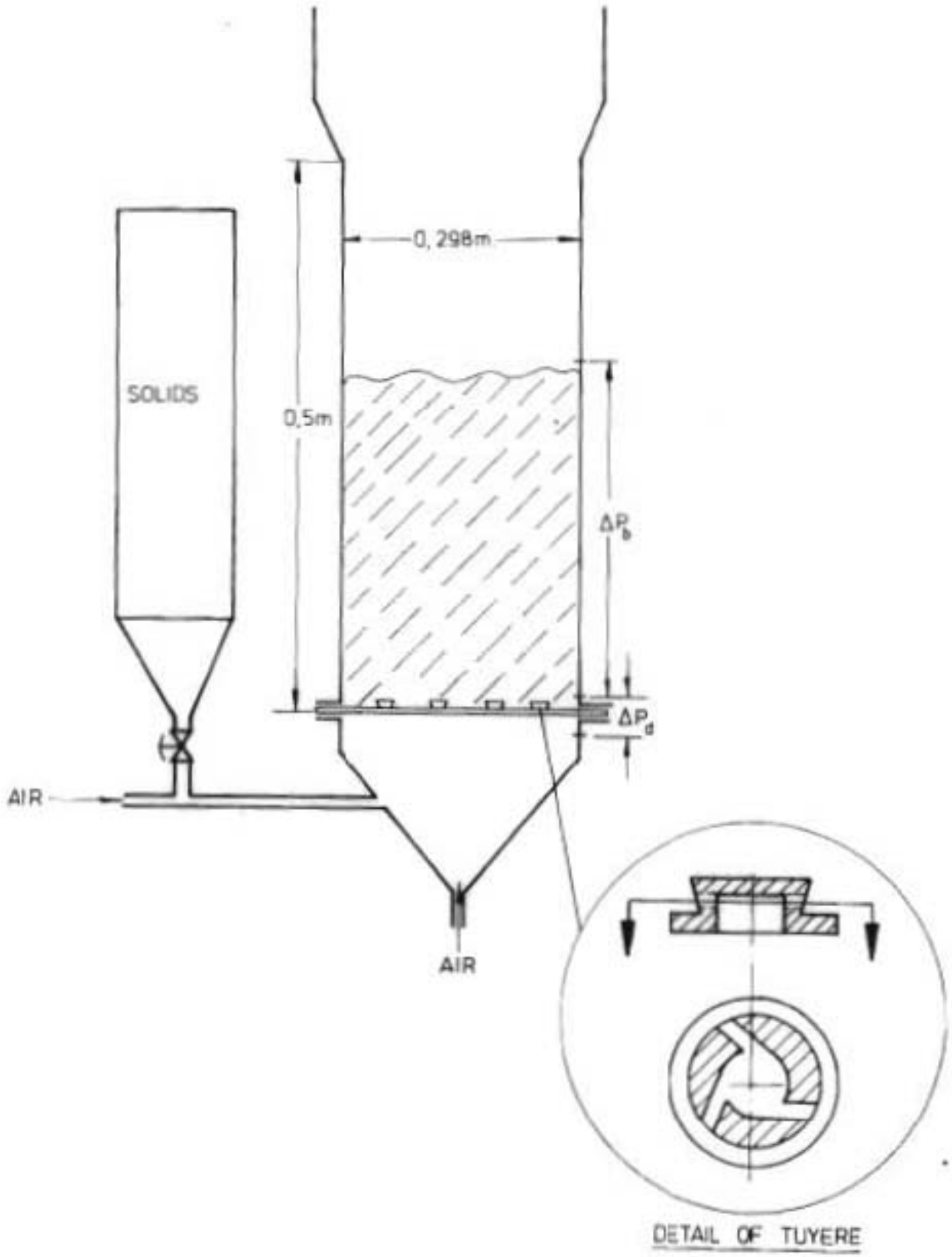

FIGURE 3.17 - Schematic drawing of the plexiglass FB showing details of the tuyere

across it. This ensured good quality fluidization. Finally, in a different set of experiments, various quantities of fine particles with a 30μm mean diameter were introduced in the gas plenum below the tuyere distributor to test its ability to convey particulate fines.

Each tuyere had three orifices symmetrically positioned round the top part of the tuyere (Figure 3.17). Tuyeres with three different orifice diameters were used, namely 6,3 7 and 8 mm. Two different size distribution particles were used as the fluidizing materials (Table A.3.1.). Pressures were measured using water manometers.

3.3.2. Results and discussion

(1) Initial experiments using the tuyere-distributor in the absence of solids showed that the distributor pressure drop (Δp_d) was linearly related to the square of the superficial air velocity (U) (Figure 3.18) and the square of the gas velocity through the orifice (U_{or}) (Figure 3.19). This indicates that the equation of the gas flow through an orifice (E.2.2) is valid for this type of tuyere too. The calculated discharge coefficient is independent of the tuyere orifice diameter and has a value of c_d = 0,63.

(2) The pressure drop across the distributor loaded with solids differs significantly from the unloaded distributor when lower superficial gas velocities are used. However, at higher velocities the two pressure drops are exactly the same (Figure 3.20). The different pressure drops observed at lower gas velocities are characteristic only of the tuyere-distributor and are caused by defluidized solid particles blocking some of the orifices. It was found that E.2.3 derived by Whitehead and Dent[22] can be satisfactorily used to determine the minimum superficial gas velocity above which all tuyeres were operational. It is also clear from Figure 3.20 that when entering

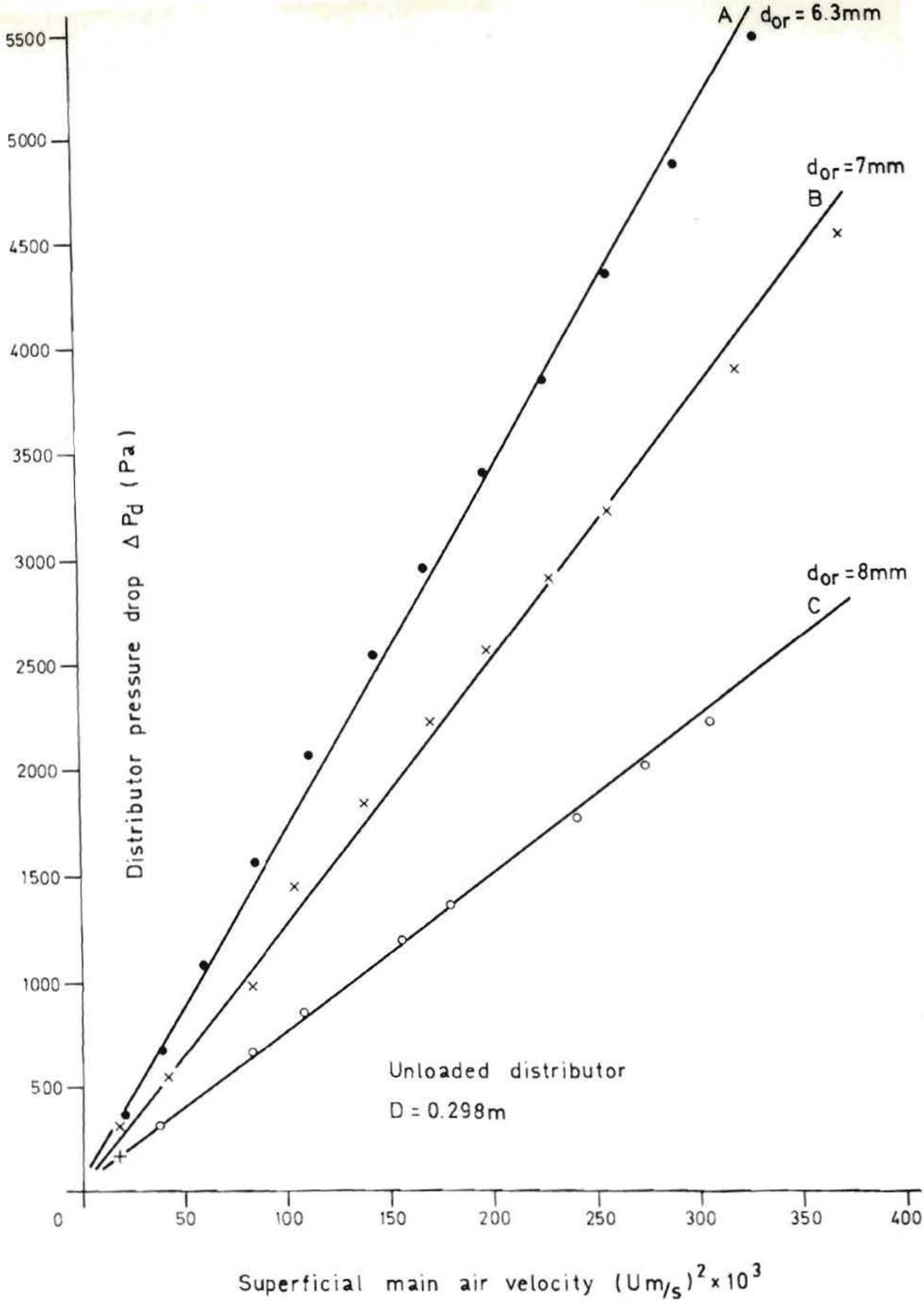

Figure 3.18. The relation between the distributor pressure drop and the superficial gas velocity through the FB system in the absence of fluidizing solids

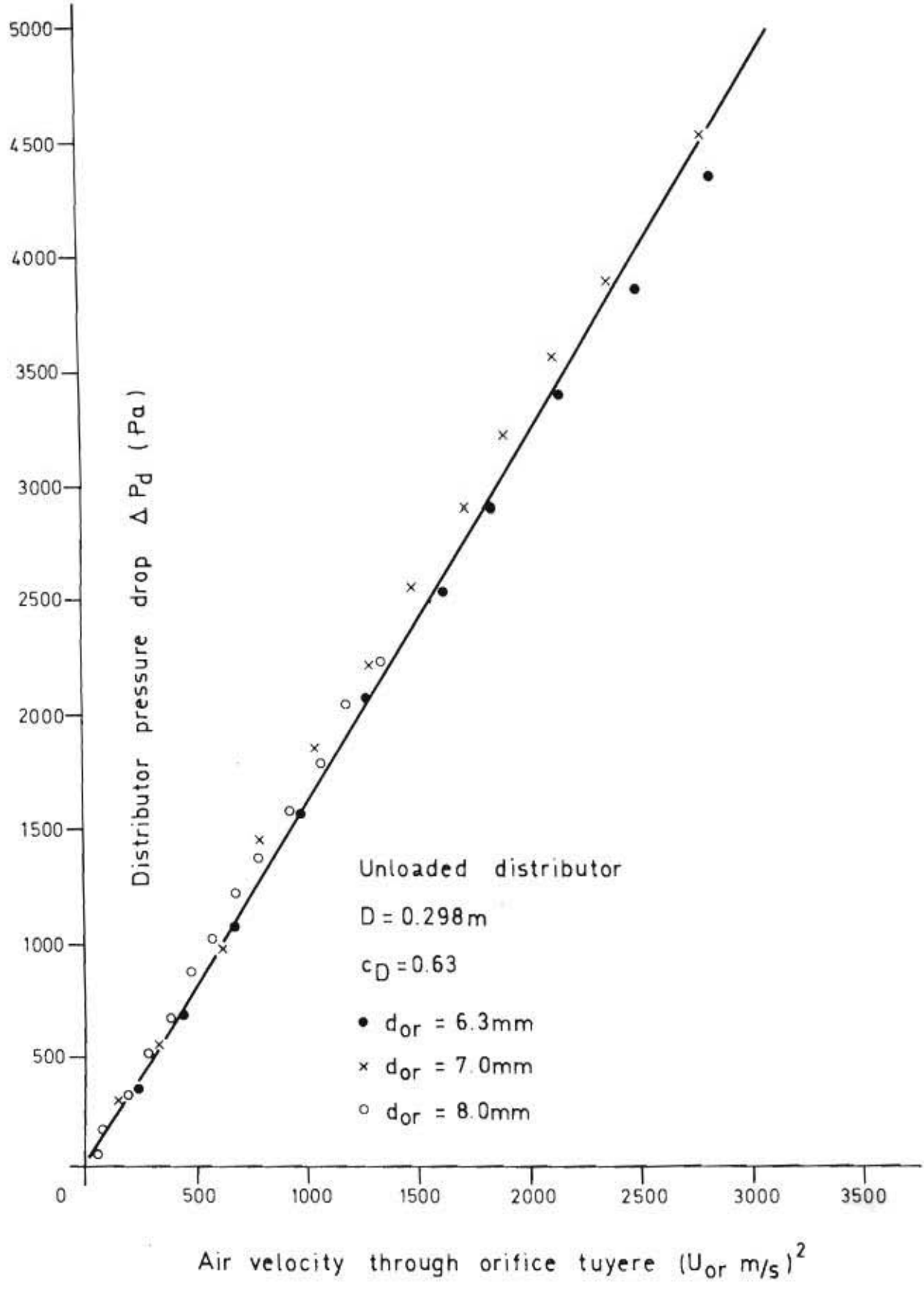

Figure 3.19. The relation between the distributor pressure drop and the square of the gas velocity through an orifice of the tuyere in the absence of fluidizing solids

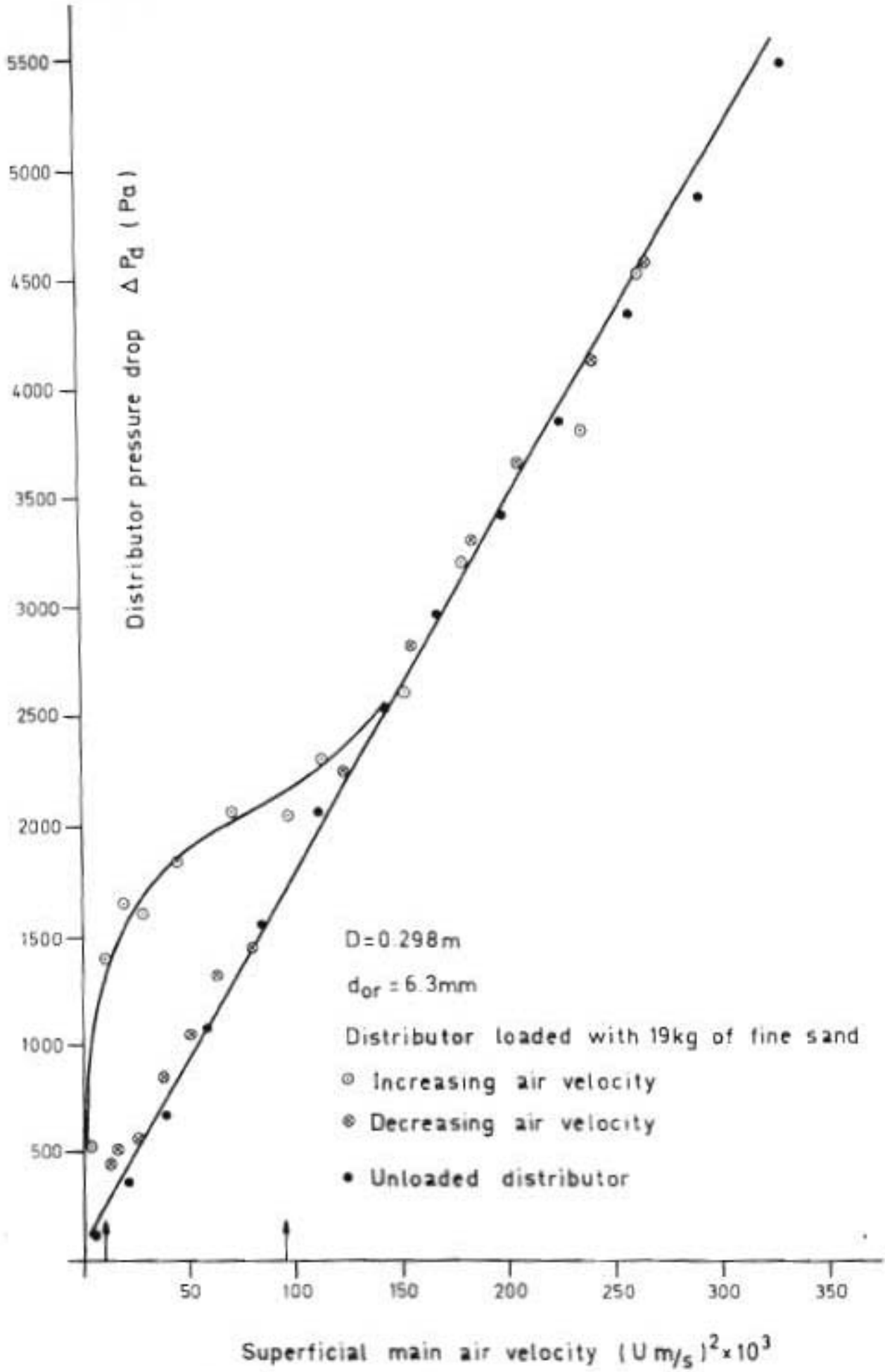

Figure 3.20. Distributor pressure drop obtained experimentally in the absence and presence of fluidizing solids plotted against the square of the superficial air velocity

the region where some tuyeres were not operating, moving from higher to lower gas velocities, the pressure drop across the tuyere distributor were the same as that of the porous distributor.

(3) From the experiments on the pressure drop across the FB it was found that the tuyere distributor was associated with an amount of defluidized solids resting permanently on the plate between the tuyeres. The effect of the defluidized solids can be seen in Figure 3.21 which gives the relationship between observed and theoretical pressure drops. It is also clear that for both the distributors the slope of the theoretical pressure drop-line differs from the slope of the experimental line. The lower experimental pressure drops, may be attributed to interparticle and other frictional losses within the FB. The pressure recovery in an FB has already been investigated in section 3.2.1.3. Substituting the data obtained from this investigation into E.3.15 and plotting the results in Figure 3.22 a graph is obtained which shows the relationship of the interparticle normal stress and the weight of solids per distributor area in the FB. To normalize the theoretical pressure drop obtained from the porous and tuyere-distributors the amount of fluidized solids resting between the tuyeres was subtracted from the total bed weight. The line in Figure 3.22 shows that the interparticle stress and thus the energy losses increase with the FB height. Alternatively in deep FBs there are higher frictional losses and a lower pressure recovery. This is true if one considers the low quality of fluidization that exists in deep FBs.

(4) From experiments to determine the transport of fine particles through the tuyere distributor, solids up to $50g/Nm^3$ of fluidizing gas were introduced into the gas plenum. No choking or accumulation

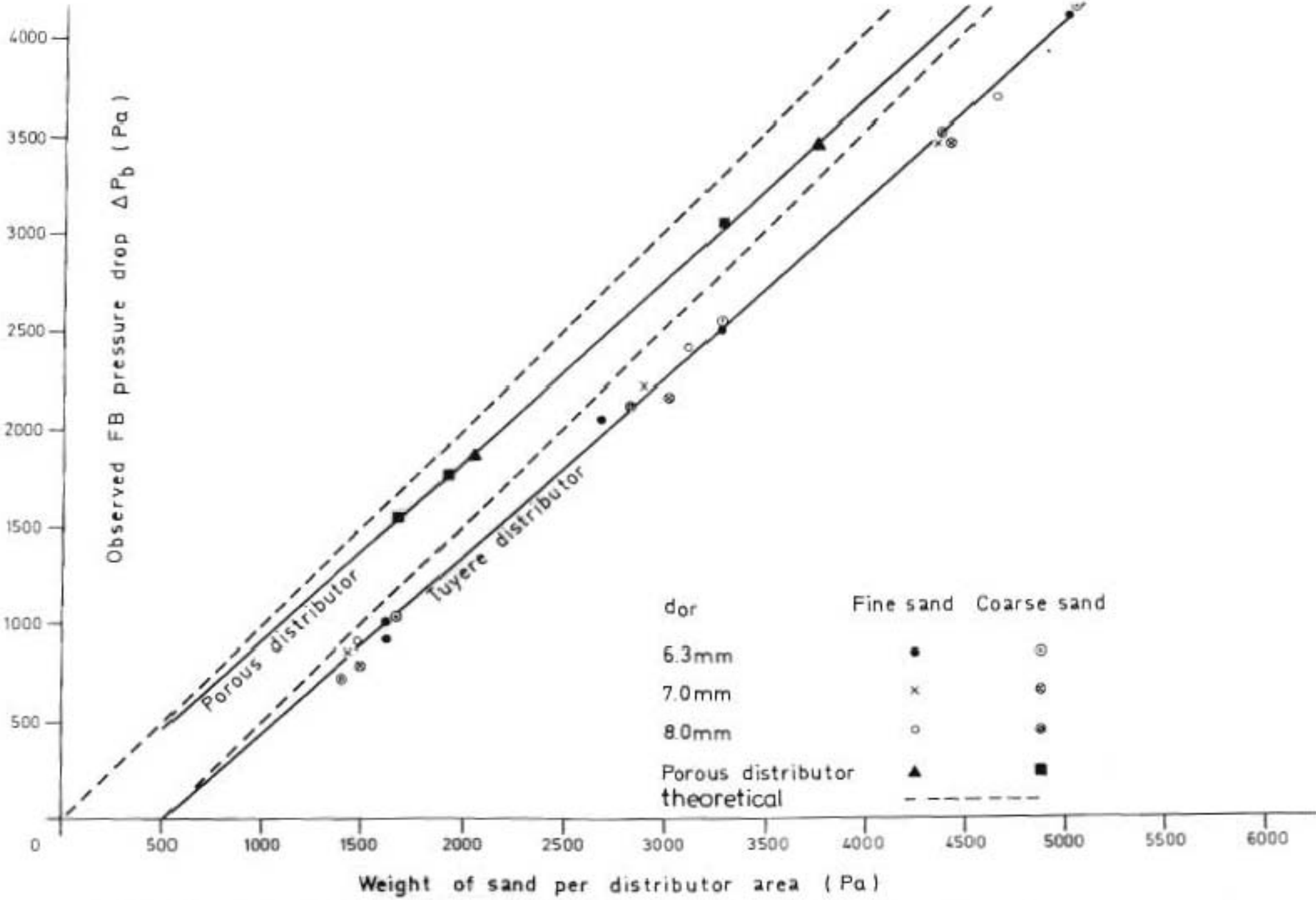

Figure 3.21. The relation of the observed pressure drop and the theoretical pressure drop for the porous and tuyere distributor

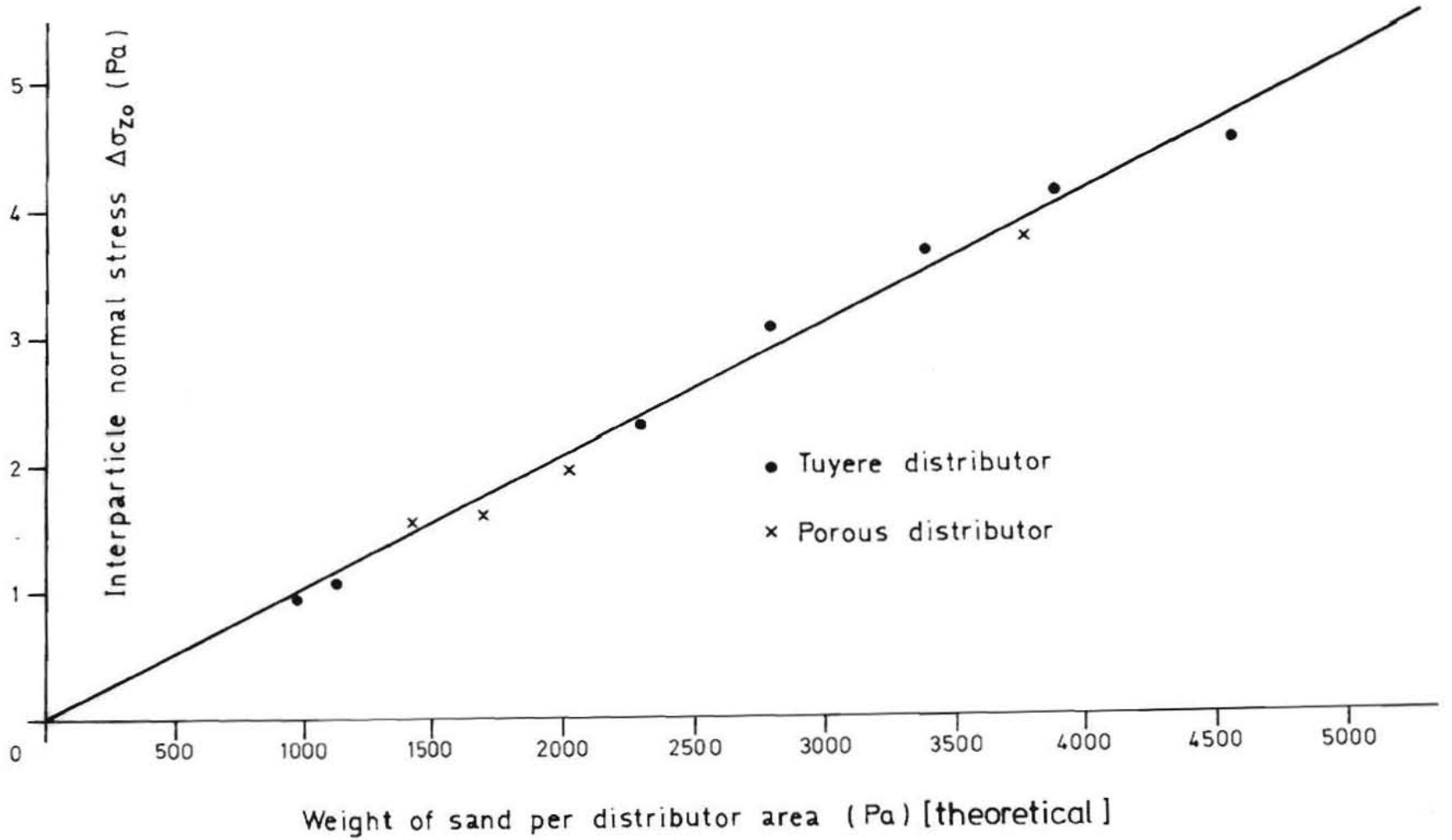

Figure 3.22. The FB interparticle normal stress using both the tuyere and porous distributor plotted against the theoretical pressure drop across the FB

of solids in the tuyeres were observed and the distributor pressure drop and FB pressure recovery were not significantly different from the ones obtained by not introducing solids in the entry gas stream.

3.3.3. Design of interstage distributor plates

The investigation on the tuyere-distributor proved its suitability for our multistage PFBC and revealed that for design purposes its behaviour can be predicted by existing theoretical and experimental correlations. It was also shown that fine solids can be transferred through it without blocking the tuyeres and without changing the predicted pressure drop across the distributor.

The final design of the distributor plate can therefore be fixed by the following general distributor requirements:

(a) No flowback of solids through the tuyeres is permitted. The choice therefore of the orifice length (l_{or}) and orifice diameter (d_{or}) has to obey the following relation:

$$\tan^{-1}\left(\frac{d_{or}}{l_{or}}\right) < \phi_R \qquad \text{E.3.17}$$

where ϕ_R is the angle of repose of silica sand.

(b) The pressure drop across the distributor has to be at least one third[19] of the pressure drop across the FB of solids (E.2.1).

3.4. THE IMMERSED BURNER

Some of the methods used for heating up FBs have already been discussed in Section 2.3.2. The necessity to minimize heat losses, avoid the creation of hot zones in the combustor and the requirement to supply heat to the PFBC,if needed,during its normal operation at high pressure,led to the concept of a solids immersed type burner. The burner consisted of two concentric chambers to avoid direct contact of the flame with the solids. It was believed that this kind of burner could supply heat to the solids while immersed under the FB surface without causing sintering or fusion of the solids.

A small FB was built and this type of burner was used to determine the flame stability of the burner in the presence of solids and its suitability as a start up burner for the multistage PFBC.

3.4.1. Description of apparatus and procedure

A schematic representation of the immersed burner is shown in Figure 3.23. The burner designed for flame stability had the form of a venturi. It was surrounded by a concentric tube through which the secondary air was introduced in the burner for cooling the venturi and for controlling the temperature of the combustion gases. An outer sleeve placed over the burner ensured the complete mixing of the combustion gases and secondary air, prevented any solids from falling into the venturi and protected the bed material from direct contact with the flame. The primary air and Liquid Petroleum Gas (LPG), (Table A.3.2) were ignited using a long reach electrode. The diluted exhaust gas left the burner through orifices positioned round the lower end of the outer sleeve.

In a series of experiments a single burner made of 304 ss with a 0,06m outside diameter was used immersed under the solids in a 0,2m diameter FB. The design and shape of the burner nozzle was based on the LPG-air flame speed data and on the stoichiometry of combustion (Table A.3.2.). Various LPG and primary air flowrates were tried keeping the two flowrates at a given ratio. Different flowrates of secondary air were also used.

The temperature of the gases was recorded using a thermocouple placed inside the outer sleeve and near the gas exit orifices. The burner also acted as a distributor, with the exhaust gas leaving the burner, fluidizing the solids in the bed.

3.4.2. Results and discussion

(1) The highest permissible temperature of the hot gases leaving the

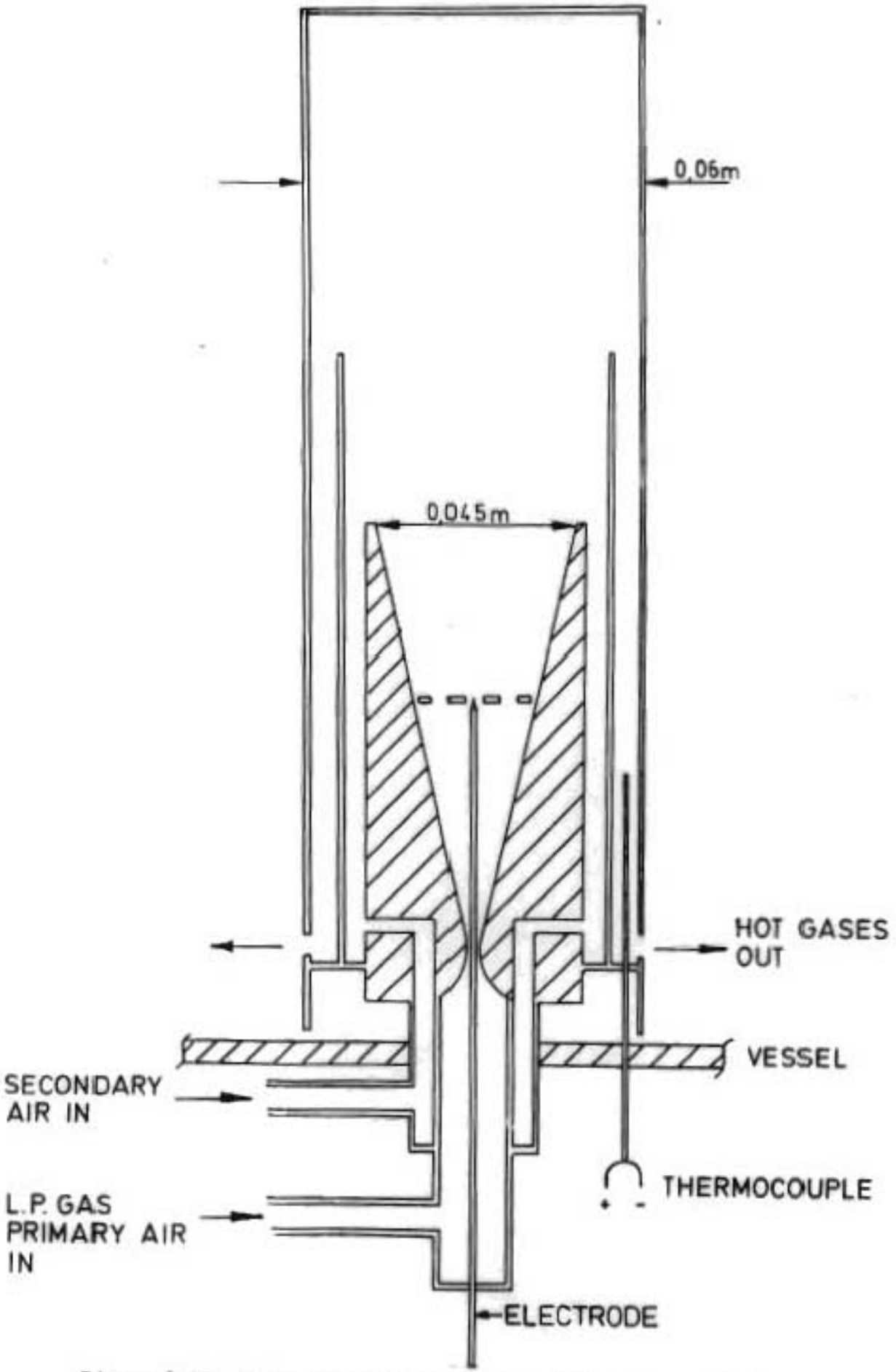

Figure 3.23. Schematic drawing of the solids immersed burner

burner was fixed by the heat transfer properties of the burner material and fluidized solids. It was observed using coarse and fine sand as a fluidizing medium, that for a given exhaust gas velocity sufficient to fluidize the fine but not the coarse particles (Table A.3.1.), the FB got very hot and solids fusion was detected near the burner. This was due to the fact that the defluidized solids were acting as an insulator, rather than a heat carrier as was the case with the experiments where the solids were fluidized, creating a very hot region close to the burner.

(2) The bulk of the experimental work on the immersed burner, for exhaust gas flowrates securing fluidization of solids, is represented in Table A.3.3. and plotted in Figure 3.24. The burner was operated at LPG flowrates of $2,83 \times 10^{-5}$ to $6,70 \times 10^{-5}$ Nm^3/s which are equivalent to a generated heat rate of 2,8 to 6,8 kW. The temperature of the exhaust gases was maintained between 280°C and 985°C. It is important to note from Figure 3.24 that the exhaust gas temperature can be selected by either fixing the burner heat output and changing the secondary air or vice versa. This is very useful in cases where there are restrictions on the exhaust gas velocity through the bed or alternatively the amount of required heat.

(3) The burner flame was stable for the whole range of designed LPG flowrates and did not seem to be effected by the bubbling solids and the pressure fluctuations of the FB. Solids height levels of up to five times the FB diameter were used and the immersed burner seemed to be operating very smoothly particularly under higher solids levels.

(4) It was clear that with the burner immersed under the solids all the generated heat was supplied directly to the solids and no heat losses occurred as in the case of a freeboard burner.

3.4.3. The design of immersed burners

The current investigation using a 0,06m diameter burner showed

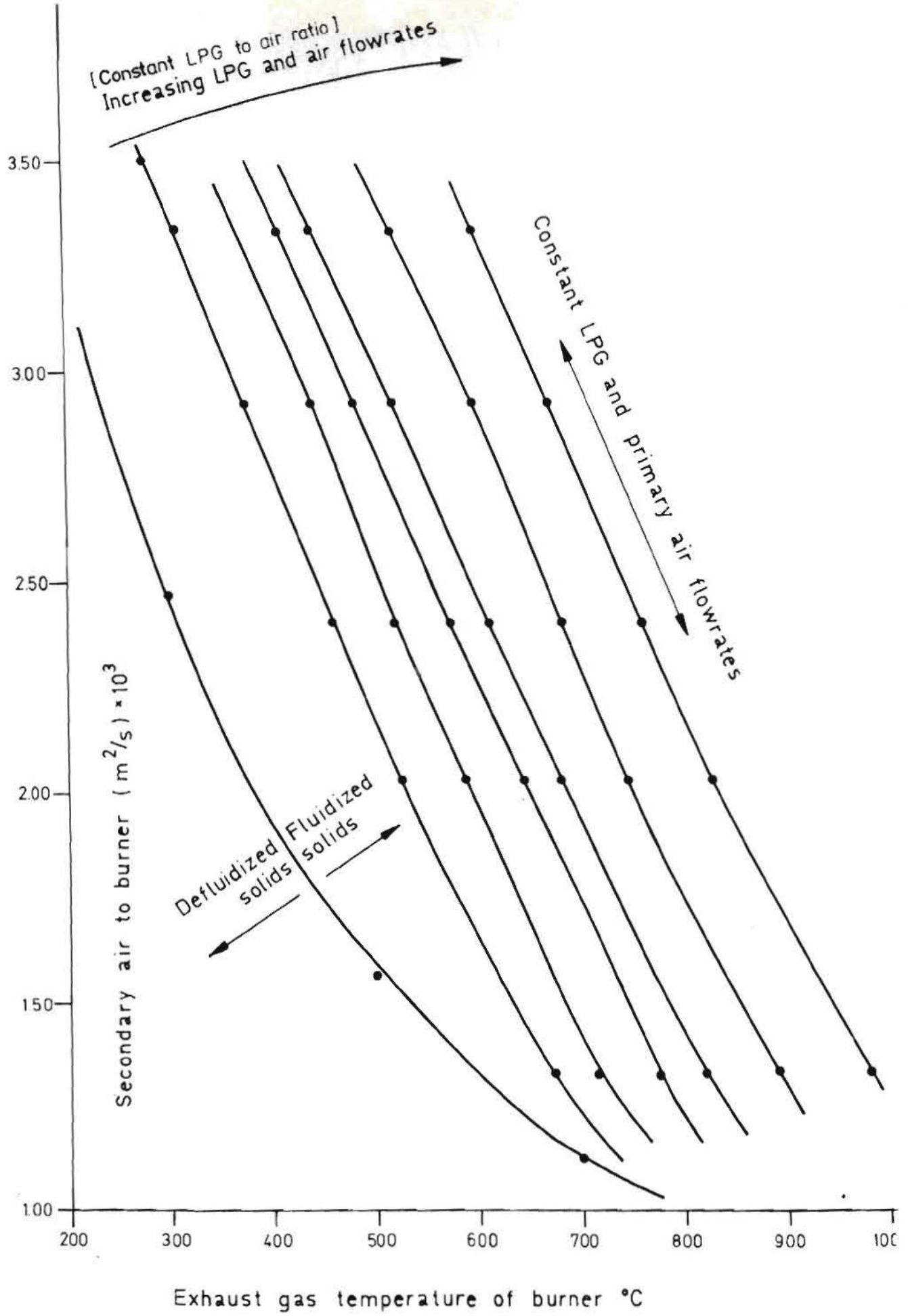

Figure 3.24. The relation between the secondary air flowrate and exhaust gas temperature for various LPG and air flowrates. (Ratio of LPG to primary air was kept constant at 0,038)

that this type of burner could be successfully used submerged under the solids, to supply heat and fluidize the solids as a multiorifice tuyere. The observation that the back pressure,due to the presence of solids, improved the operation of the burner, makes the design of the exhaust gas orifices round each burner easier. It is also possible to design a distributor for any specified pressure drop without this to have any effect on the performance of the burner. It must be borne in mind that during the design of an immersed burner the limiting factors on the performance and range of the heat output of the burner are firstly, the shape of the venturi which determines the maximum velocity of the premixed gas, secondly,the material of construction of the burner and thirdly,the physical and heat transfer properties of the fluidizing solids.

In order to preheat our PFBC, an assembly of these burners were used which were arranged on a plate to form a multiburner distributor. Each burner on the plate acted as a multiorifice tuyere.

To design our PFBC and give its dimensions and power rating,a series of combustion studies were carried out, using South African coals, which provided us with the combustion kinetics. To generalize these combustion studies and be able to use them to design and predict the behaviour of our PFBC mathematical models were written which are presented in the following chapter with a description of the investigations carried out.

CHAPTER FOUR

PRELIMINARY COAL COMBUSTION TRIALS UNDER BATCH CONDITIONS AND MATHEMATICAL MODEL FOR THE CONTINUOUS COMBUSTION OF COAL

Concepts like plug flow and complete mixing, developed for reactors in which homogeneous reactions take place, were originally used as a basis for FB combustion studies. The effect of gas bubbles rising through the emulsion phase led to the two-phase and three-phase models[46] which include gas exchange between the phases. Fryer and Potter[47] in their theoretical model of a catalytic FB, used the concept of solids backmixing, which is caused by the continuous uplifting of solids to the surface by the bubble wakes.

Consideration of the change in size of the solid reactant led to the application of the shrinking core model to coal combustion and the modelling of a carbon-air diffusion controlled reaction in a batch FBC[48]. For the continuous FB system Levenspiel *et al.*[49] developed a model that incorporates a general solids population balance for both increasing and decreasing size particles. This model formed the basis of a number of recent theoretical studies[50,51] and prompted a series of experimental investigations[52,53] aimed to produce a realistic model that correlates key parameters like carbon loading, excess air, bed temperature, and combustor efficiency.

The purpose of our preliminary combustion trials was to investigate the combustion of our coals in a small FB under batch conditions and use existing theoretical models or updated versions to describe the combustion characteristics of South African coals. These theoretical investigations later formed the basis of the theoretical model for combustion of coal in our PFBC.

The combustion studies on the small FB also provided valuable practical experience on the operation of such a system.

4.1 COMBUSTION OF COAL PARTICLES USING A SMALL FB UNIT

In a heterogeneous system the overall rate expression often accounts for more than one process involving both physical and chemical steps. However, the choice of a mathematical model which closely describes the actual kinetics often warrants experimentation to determine the rate controlling process and produce a simplified overall rate expression.

In the case of combustion of coal particles two different theoretical approaches may be used depending on the following:

(a) Coal particles burn with the reaction zone moving towards the centre of the particle and the unreacted core shrinking leaving behind it the ash.

(b) Coal particles burn and shrink in size with the ash continuously removed.

In addition, it is necessary to determine for both cases whether the reaction is controlled by gas diffusion through the ash layer or gas film, or by chemical reaction.

The rate controlling step can be determined by noting the progressive conversion of coal particles and their size. To determine these parameters, a series of batch tests were carried out on a small FB using South African coals.

4.1.1. Description of apparatus for batch burnout tests

The small FB used for these experiments consisted of two chambers positioned vertically one above the other separated by a porous silicon carbide plate which acted as an air distributor. The two chambers were built out of fireclay bricks* , with culite bricks* used on the outside for thermal insulation (Figure 4.1). Each chamber on a plan view had the shape of a square, with a side measuring 0,15m. The depth of each chamber was 0,45m.

The bottom chamber acted as an electric air preheater. A total of fourteen silicon carbide elements giving a maximum power output of 9kW were used. The heating elements were wired in series in two separate circuits of six and eight elements. A 380V-15A, phase angle thyristor controller was connected to the set of eight elements, regulating the supply of heat by sensing the temperature of the top chamber. The set of six elements, acting as a base heat load, were joined to a 220V-15A, voltage regulator.

The top chamber was used as the combustion chamber for coal. Quartz windows were built on the same level as the distributor plate of the top chamber. These windows were used to observe the combustion of coal particles and their behaviour during the initial evolution and combustion of the volatiles.

The pressure drop across the FB and distributor was calculated from water manometers. Type K (Cr/Al) thermocouples were used to indicate the top and bottom chamber temperatures.

---

*Manufactured by Cullinan Refractories Ltd, Olifantsfontein, Transvaal.

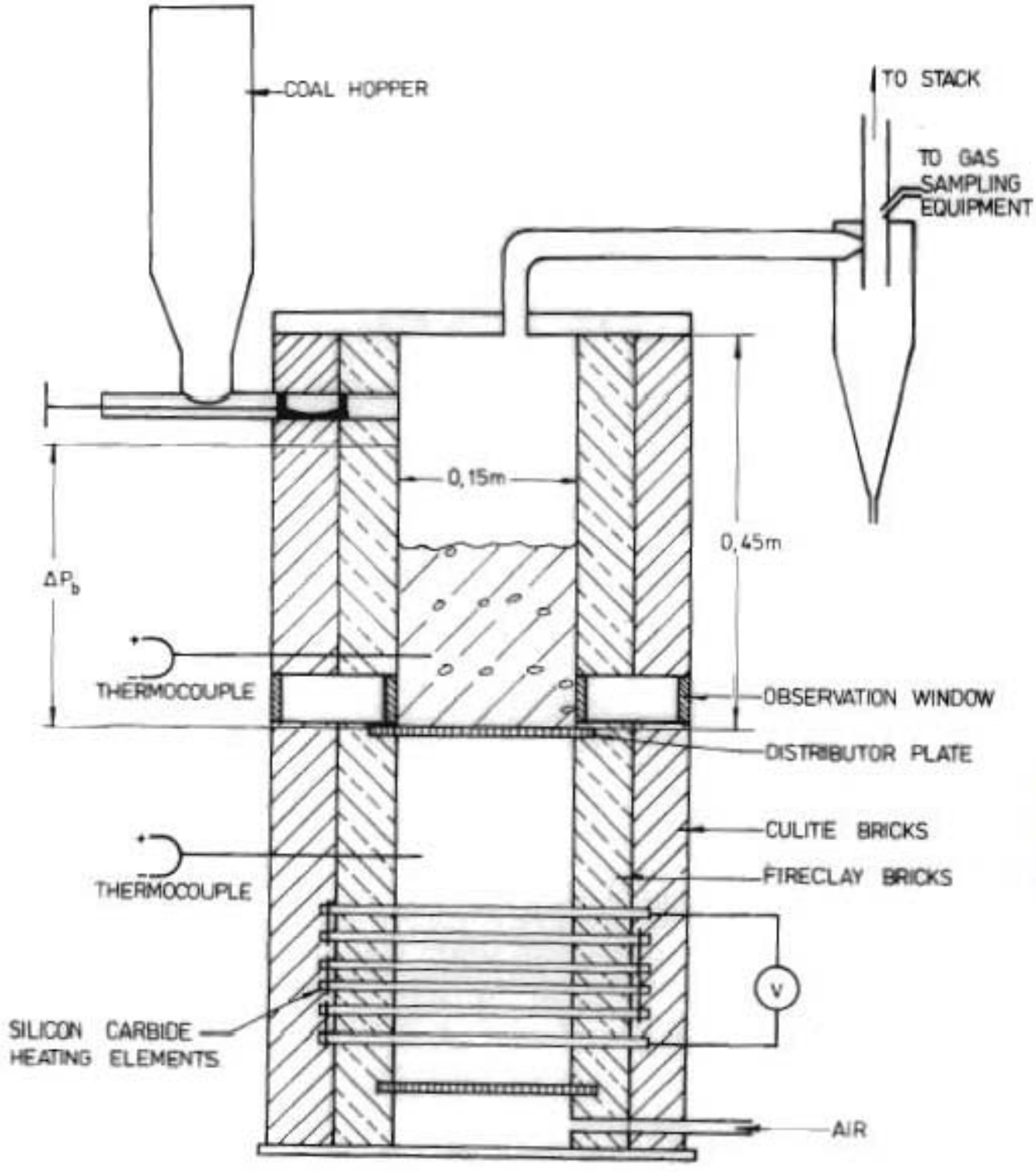

FIGURE 4.1 - Schematic drawing of the small square FB combustor used for batch burnout tests on South African coal and char.

The exhaust gas after the removal of all entrained solids was analysed using an infra red CO/CO_2 analyser (Infra Red Industries, model IR 702) and a fuel cell O_2-analyser (Teledyne, model 326B). A chart recorder was used to record the percentage of CO_2 and O_2 in the exhaust gas.

Coal was fed to the top chamber through the side of the combustor using a plunger type feeder connected to an airtight coal hopper. The plunger was operated manually.

Two different investigations were carried out on the small-scale FB, one dealing with combustion of coal on the distributor plate, and the other with combustion in an FB of solids. The purpose of the first set of experiments was to determine whether coal particles break during their devolatilization. Both coal and char were used in these experiments.

4.1.2. Experimental procedure

The combustor was initially preheated. During this period a constant flowrate of air, measured on a rotameter, was passed through the combustor to achieve a uniform reactor temperature. When the top chamber reached a desirable temperature for the combustion of coal, known weights of coal particles were introduced into the combustion chamber. During the combustion process, the percentage volumes of CO, CO_2, O_2 in the flue gas, and the temperatures were continuously monitored by the instruments. The quartz windows were used to observe, either the behaviour of coal particles on the distributor plate, or how well the coal particles mixed with the solids in the FB during combustion.

During the entire experimental work an excess concentration of oxygen was maintained inside the combustor whenever possible. Two different coal sizes were used (Table A.4.1).

4.1.3. Interpretation of experimental results

The observations from the tests on burning coal particles on the distributor in a hot stream of air can be summarized as follows:

(1) When coarse particles were dropped onto the distributor at 800°C the volatiles were immediately driven off and ignited in a yellowish flame that lasted for a few seconds. The O_2-analyser indicated no oxygen present in the flue gas during this period and a low carbon monoxide (CO < 1 per cent) was detected. The remaining devolatilized coal continued burning with a layer of ash covering the unreacted core.

(2) The ash remained attached to the unreacted core until even after the completion of the reaction.

(3) No breakage of particles was observed during the entire experimental work.

(4) To compare the effect of the volatiles during combustion, char particles were also used, derived from pyrolysis of the same type of coal in a coke oven (Table A.4.1). Its combustion characteristics were similar to that of coal with the exception that the very low volatiles in the char did not create the initial shortage of oxygen in the gas stream.

(5) If the temperature of the combustion region was decreased to temperatures between 600°C and 650°C devolatilization and combustion of the particles was prolonged due to lower reaction kinetics.

(6) The increasing thickness of the ash layer round the burning particle reduced the rate of oxygen diffusion to the core of the particle and the rate of carbon dissipation.

(7) Using the finer coal particles, the burnout time was reduced due to the higher available area per weight of sample.

The oxygen concentration in the flue gas was plotted against time for both fine and coarse particles and is shown in Figure 4.2.

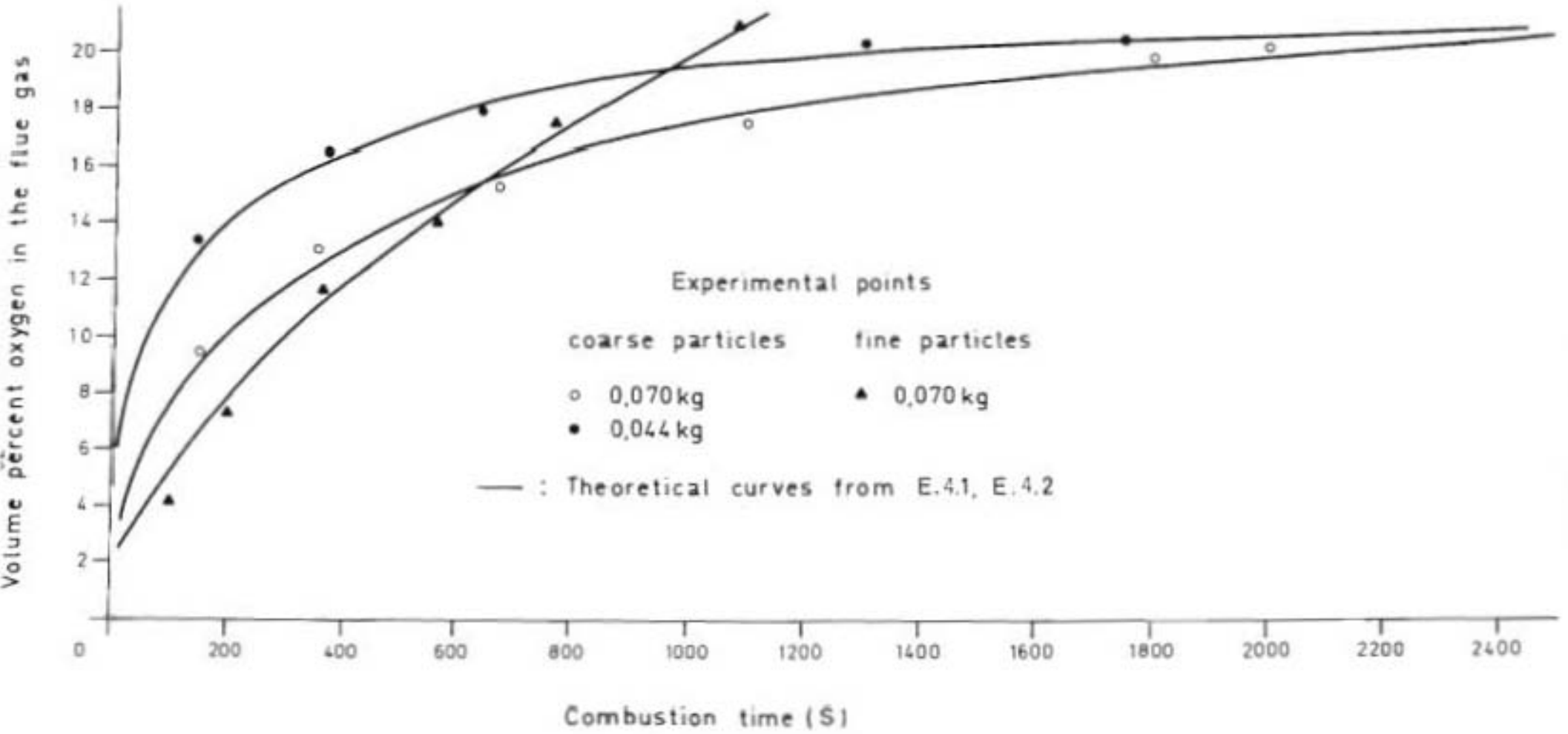

Figure 4.2. Experimentally and theoretically predicted percentage of oxygen for coal combustion in a stream of hot air and in the absence of fluidized solids, plotted against time

At higher time values the experimental points for the coarse particles become asymptotic with the horizontal axis which indicates the increasing resistance of the ash to gas diffusion. The fine particles do not show this kind of behaviour due to the thinner layer of ash and higher available surface areas.

The observations from the experiments on coal burning in an FB of solids can be summarized as follows:

(1) Combustion occurred throughout the FB and there was good mixing between burning coal particles and fluidizing solids.

(2) The ash was continuously removed from the surface of the burning particle. This can be verified from Figure 4.3 where the experimental points obtained do not show the asymptotic behaviour as it happened when dealing with the combustion of coal on the distributor. Figure 4.3 relates the experimentally obtained percentage oxygen in the flue gas with time.

It may be concluded from the experiments in the small FB that coal combustion in the absence of a fluidizing material can be represented by a model based on a reacting particle of unchanging size. However, a model assuming a shrinking particle should be used if it is required to represent coal combustion in a bed of solids. Furthermore, the volatile content of coal may be neglected since it was observed, that the volatiles were immediately driven off and burnt in a period much shorter than the burnout time of the particles considered. The volatiles did not seem to affect the subsequent burning of the devolatilized coal.

For a better understanding of the combustion behaviour of South African coals, which was observed experimentally, the combustion of coal under batch conditions both in the absence and presence of fluidized solids was examined and presented below in the form of mathematical models.

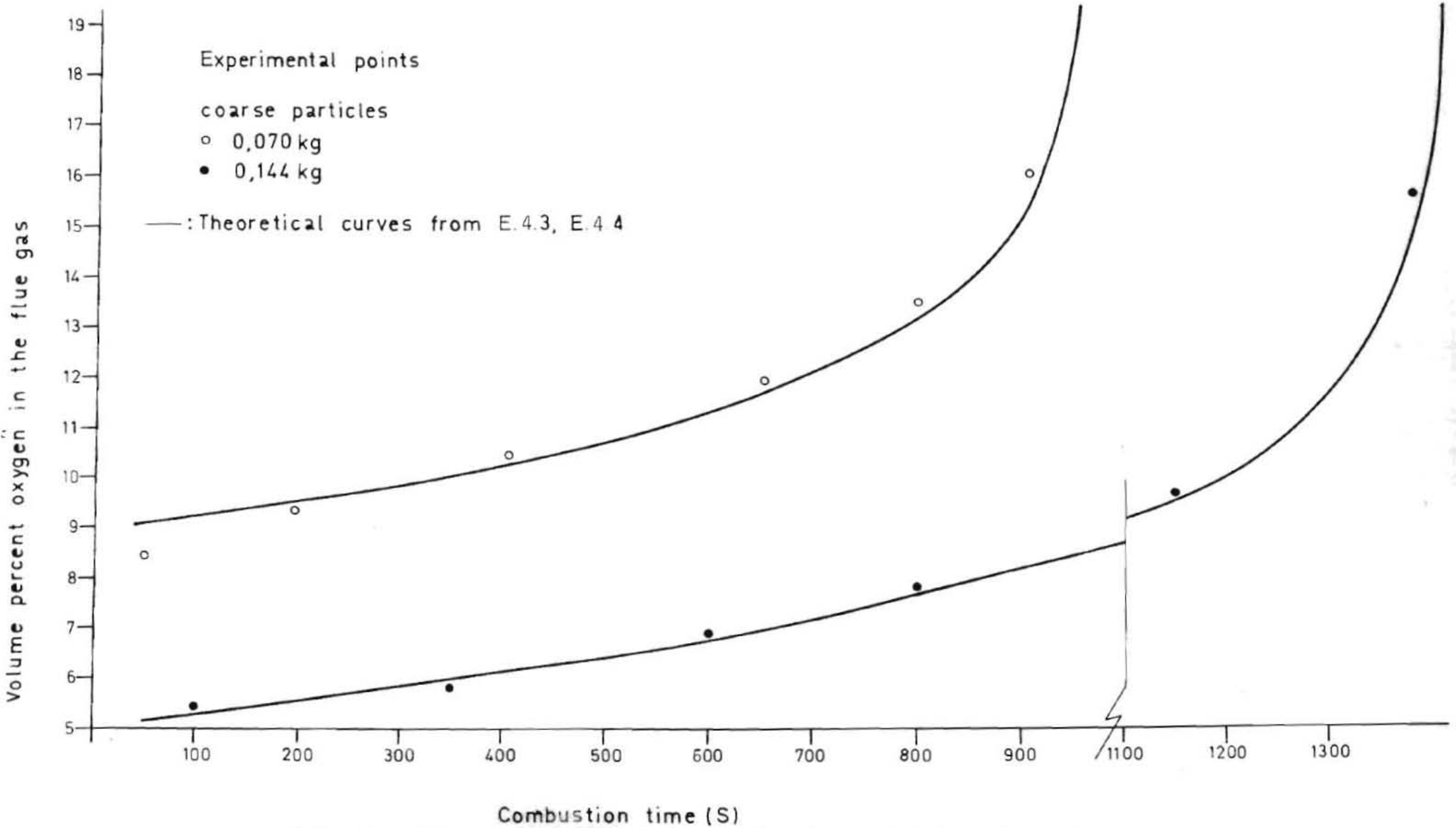

Figure 4.3. Experimentally and theoretically predicted percentage of oxygen in the flue gas for coal combustion in the FB, plotted against time

4.1.4. Mathematical model for combustion of coal on the distributor under batch conditions, in a stream of hot air and in the absence of fluidizing solids.

An updated version of the mathematical model, originally developed by Yagi and Kunii[54], for the reaction of a single particle of unchanging size, was used here to predict the burning rate of batches of coal particles in a hot stream of air.

The assumptions listed below formed the basis for this mathematical model.

(a) Coal is treated as char and no account is made of the volatiles.

(b) The resistance to gas diffusion through the ash controls the reaction and the oxygen concentration at the unreacted core surface is assumed to be zero.

(c) At steady state the oxygen consumption at any instant is given by its rate of diffusion through the ash layer.

The actual derivation of the mathematical equations for the combustion of coal on the distributor plate is presented in Appendix 4.1. The final two equations which form the basis of this model are written below. These are firstly, the equation relating the unreacted particle radius (r_c) and time (t) and the equation for the overall oxygen concentration balance:

$$t = \frac{mF_c}{C_o Q M_c}\left[1 - \left(\frac{r_c}{R}\right)^3\right] + \frac{\rho F_c R^2}{6 C_o D_G M_c}\left[1 - 3\left(\frac{r_c}{R}\right)^2 + 2\left(\frac{r_c}{R}\right)^3\right] \qquad \text{E.4.1.}$$

$$Q(C_o - C_p) = -3m \frac{F_c}{M_c}\left(\frac{r_c}{R}\right)^2 \frac{d}{dt}(r_c/R) \qquad \text{E.4.2.}$$

where $m = N\frac{4}{3}\pi R^3 \rho$, the initial mass of coal sample (kg)

N = the number of coal particles in a batch sample

F_c = fixed carbon in coal

C_o = the inlet oxygen concentration (kg mol/m^3)

C_p = the oxygen concentration in the flue gas (kg mol/m^3)

Arithmetic values were substituted in the theoretical equations as shown in Appendix 4.1. The predicted percentage of oxygen in the flue gas is compared with the corresponding one obtained experimentally and is plotted against time in Figure 4.2. The agreement between theory and the experimental results is an indication that the assumption of an ash diffusion control reaction is correct. E.4.1 and E.4.2 can therefore be used to predict the exit oxygen concentration or extent of reaction at any time (t), when coal is burnt on the distributor in the absence of fluidizing solids.

4.1.5. Mathematical model for the combustion of coal in an FB under batch conditions

The experiments on the combustion of coal in an FB, (observations (1) and (2) Section 4.1.3) indicated that the combustion process may be represented theoretically by assuming a reaction of a shrinking spherical particle. This mathematical model was based on the work carried out by Davidson and Harrison[46] and Avedesian and Davidson[48]. The assumptions made for its derivation are the following.

(a) The reaction is controlled by the diffusion of the reactant and product gases from the coal surface.

(b) The particles shrink in size and the ash is continuously removed.

(c) All particles are considered to be of the same average size.

(d) No account is made of the volatiles.

The derivation of the mathematical equations for the combustion of coal in an FB under batch conditions is presented in Appendix 4.2.

The derived equation relating the unreacted particle radius (r_c) and time (t) and the equation for the overall oxygen concentration balance are listed below:

$$t = \frac{mF_c}{C_o M_c A[U-(U-U_{mf})\exp(-X)]}\left[1 - \left(\frac{r_c}{R}\right)^3\right] + \frac{F_{c^o}}{2C_o M_c Sh D_G} R^2\left[1-\left(\frac{r_c}{R}\right)^2\right] \qquad \text{E.4.3.}$$

and

$$(C_o - C_p)A[U-(U-U_{mf})\exp(-X)] = -\frac{3mF_c}{R^3 M_c} r_c^2 \frac{dr_c}{dt} \qquad \text{E.4.4.}$$

where X is the number of times a bubble is swept out during its stay in the bed

Other parameters as in E.4.1 and E.4.2.

Arithmetic values were substituted in these equations which were used to determine theoretically the percentage of oxygen in the flue gas and its relation to time, as shown in Appendix 4.2. The results between the theoretically predicted and experimentally obtained values are presented in Figure 4.3. From the agreement between theory and the experimental results it may be concluded that this mathematical model can be used to describe the combustion of coal particles in an FB which is operated under batch conditions.

4.2 A MATHEMATICAL MODEL FOR CONTINUOUS COMBUSTION OF COAL IN A MULTISTAGE FB

The combustion experiments on the small FB showed that our coals can be combusted in an aerated bed of solids and their behaviour under batch conditions can be predicted by a simple mathematical model. For the derivation of a theoretical model to predict the continuous combustion of coal, a rather more complex system was considered that takes into account the fluidizing features of the FB. This mathematical model was based on the works by Levenspiel *et al*[49], Chen and Saxena[50],

and Fryer and Potter[47]. The assumptions made for the derivation of this model are the following:

a) Silica sand is used as the fluidizing medium with coal comprising not more than five per cent by weight in the bed.

b) The fluidization characteristics of the reactor are based on the inert material with coal evenly distributed in the emulsion and cloud-wake phases.

c) The cloud-wake and emulsion phases are at minimum fluidizing conditions.

d) The emulsion phase is well mixed while in the bubble and cloud-wake phases, gas moves in plug flow.

e) The temperature is constant throughout the FB and there is no change in gas volume because of the reaction.

f) Combustion occurs only in the cloud-wake and emulsion phases and solids and gas can interchange between phases.

g) Coal is continuously fed, and on entry to the FB the coal particles are charred. The volatiles burn instantly. When the coal particles diminish to a certain size they get elutriated and burn in the top FB.

h) The feed consists of a wide size-distribution of coal particles. During combustion the coal particles shrink in size and the generated ash is continuously removed.

The model developed here uses a population balance of reacting coal particles with fresh coal entering through the feed. For reasons which will be dealt with in the following chapters interstage circulation of solids was not considered during the derivation of the theoretical model. Instead a two stage non-circulating FB system was assumed, where

the bottom FB acted as the main combustion stage and the top bed as a burn out stage for all elutriated coal particles. The derivation of the mathematical model follows below.

4.2.1. Reactions involving the solid phase

4.2.1.1. Reaction of a single particle

To consider a material balance it is necessary to determine the coal mass change due to the reaction. The mass m_p of a single coal particle assumed to be spherical can be written as:

$$m_p(R) = \frac{4}{3}\pi R^3 \rho \qquad E.4.5$$

The rate of mass change for a single particle is dependant on the radius of the particle, the oxygen concentration and temperature[50].

$$\frac{dm_p(R)}{dt} = 4\pi R^2 \rho \frac{dR}{dt} = \phi_1(R,C,T) \qquad E.4.6$$

and

$$\frac{dR}{dt} = \frac{\phi_1(R,C,T)}{4\pi R^2 \rho} = \phi_2(R,C,T) \qquad E.4.7$$

(ϕ_1 and ϕ_2 are negative functions)

Since coal particles react only in the cloud-wake and emulsion phases, the average rate of combustion, can be expressed in terms of the contribution of the two phases. (The dependance of ϕ_2 on C and T is not considered at this stage).

$$\overline{\frac{dR}{dt}} = \frac{1-\epsilon_B(1+f_W)}{1-\epsilon_B}\phi_2(R) + \int_0^H \frac{1}{H}\frac{\epsilon_B f_W}{1-\epsilon_B}\phi_2(R)dh = \phi_3(R) \qquad E.4.8$$

Similarly the average mass change in the FB is

$$\overline{\frac{dm_p(R)}{dt}} = \frac{1-\epsilon_B(1+f_W)}{1-\epsilon_B}\left(\frac{dm_p(R)}{dt}\right) + \int_0^H \frac{1}{H}\left(\frac{\epsilon_B f_W}{1-\epsilon_B}\right)\left(\frac{dm_p(R)}{dt}\right)dh \qquad E.4.9$$

From E.4.6, E.4.7, E.4.8 and E.4.9

$$\overline{\frac{dm_p(R)}{dt}} = 4\pi R^2 \rho \phi_3(R) \qquad E.4.10$$

4.2.1.2. Overall mass balance equation to determine the total weight of reacting particles in an FB

A stream of coal particles F_o(kg/s) with a size distribution $P_o(R)$ enters the bottom stage of an FBC consisting of sand particles and a small amount of resident coal particles (W_{pb}). The total bed weight of the bottom stage is W_b.

The coal particles in the FB have a size distribution $P_B(R)$. A portion of the reacting particles F_1 gets entrained and carried into the top FB by the fluidizing gas.

The particles elutriation constant is defined by the following equation:

$$k_e(R) = \frac{F_1 P_1(R)}{W_{pb} P_B(R)} \qquad \text{E.4.11}$$

For any size interval dR the material balance for shrinking coal particles can be expressed as:

(particles entering in feed) − (particles leaving in entrainment) + (particles shrinking in interval from larger size)

− (particles shrinking out of the interval to a smaller size) + (depletion of mass because of combustion) = 0

In mathematical terms the following equation gives the material balance for coal particles in a size interval dR.

$$F_o P_o(\bar{R})dR - F_1 P_1(\bar{R})dR + W_{pb} P_B(R)\frac{\overline{dR}}{dt}\Big|_{R+dR} - W_{pb} P_B(R)\frac{\overline{dR}}{dt}\Big|_{R} +$$

$$\frac{W_{pb} P_B(\bar{R})}{m_p(\bar{R})} \frac{\overline{dm_p(\bar{R})}}{dt} dR = 0 \qquad \text{E.4.12}$$

where $\bar{R}$ is the mean radius in the interval dR.

Replacing the second term in E.4.12 by E.4.11 and the terms $\overline{\frac{dR}{dt}}$ and $\overline{dm_p(\bar{R})/dt}$ by E.4.8 and E.4.10 then dividing by dR and taking limits as dR→0 E.4.12 becomes:

$$F_o P_o(R) - k_e(R) W_{pb} P_B(R) - W_{pb} \frac{d[P_B(R)\phi_3(R)]}{dR} + \frac{3 W_{pb} P_B(R)\phi_3(R)}{R} = 0 \qquad \text{E.4.13}$$

To solve E.4.13 it is necessary to define the boundary conditions. Considering a single size feed or $P_o(R) = \delta(R_o)$ and taking an interval dR of radius (R) not including $R=R_o$ the first term of E.4.13 becomes zero. Dividing throughout by $\phi_3(R)P_B(R)$ and integrating E.4.13 from R to R_o (but not including R_o) gives:

$$-\frac{k_e(R)}{\phi_3(R)} dR - \frac{d\phi_3(R)}{\phi_3(R)} - \frac{dP_B(R)}{P_B(R)} + 3\frac{dR}{R} = 0, \text{ and}$$

$$\ln \frac{P_B(R|R_o)}{P_B(R_o)} + 3 \ln \frac{R_o}{R} - \ln \frac{\phi_3(R_o)}{\phi_3(R)} - \int_R^{R_o} \frac{k_e(R)}{\phi_3(R)} dR = 0 \qquad \text{E.4.14}$$

where $P_B(R|R_o)$ is the frequency distribution of coal particles in the FB originated from a size of feed particles, R_o.

In order to calculate the value of $P_B(R_o)$, equation E.4.12 is applied to the feed size interval, R_o to $R_o + dR$. Since all particles in the bed are shrinking $P_B(R|R_o) = 0$ for $R>R_o$ and only the first and fourth terms in E.4.12 will remain. Taking the limit as $R \to R_o$ E.4.12 becomes

$$P_B(R_o) = -\frac{F_o}{W_{Pb}\phi_3(R_o)} \qquad \text{E.4.15}$$

Substituting E.4.15 into equation E.4.14 and rearranging it gives:

$$P_B(R|R_o) = -\frac{F_o}{W_{pb}\,\phi_3(R)}\,\frac{R^3}{R_o^3}\exp\left[\int_R^{R_o}\frac{k_e(R)}{\phi_3(R)}\,dR\right] \qquad \text{E.4.16}$$

For a wide size distribution feed the following equation for coal particles is true

$$P_B(R) = \int_{R_o=R_{min}}^{R_o=R_M} P_B(R|R_o)P_o(R_o)dR_o = \int_{R_o=R}^{R_o=R_M} P_B(R|R_o)P_o(R_o)dR_o \qquad \text{E.4.17}$$

where $P_B(R|R_o)$ is given by E.4.16

To determine the weight of reacting particles in the FB (W_{pb}), E.4.17 must be integrated again over all particle sizes within the FB. So that:

$$\int_{R=R_{t\to\infty}}^{R_M} P_B(R)dR = 1$$

$$W_{pb} = -\int_{R=R_{t\to\infty}}^{R=R_M}\int_{R_o=R}^{R_o=R_M}\frac{F_o R^3}{\phi_3(R)}\,\frac{P_o(R_o)}{R_o^3}\exp\left[\int_R^{R_o}\frac{k_e(R)}{\phi_3(R)}\,dR\right]dR_o\,dR \qquad \text{E.4.18}$$

4.2.1.3. The rate of total mass change of reacting particles

From the weight (W_{PB}) of coal particles in the FB defined by E.4.18 it is possible to determine the number of reacting particles for a radius interval dR in the cloud-wake and emulsion phases.

For the emulsion phase the number of reacting particles (N_E), is:

$$N_E = \frac{1-\varepsilon_B(1+f_w)}{1-\varepsilon_B} \quad \frac{W_{pb}P_B(R)dR}{4/3\pi R^3\rho} \qquad E.4.19$$

For the cloud-wake phase the number of reacting particles (N_C) within a height interval (dh) is:

$$N_C = \frac{\varepsilon_B f_W}{1-\varepsilon_B} \quad \frac{W_{pb}P_B(R)dR}{4/3\pi R^3\rho} \quad \frac{dh}{H} \qquad E.4.20$$

where H is the FB height.

The rate of mass change for a single particle, ϕ_1 was defined by E.4.6. The rate of change of mass of all reacting coal particles (M_R), can therefore be written as:

$$M_R = \int_R N_E \phi_1 + \int_R \int_h N_C \phi_1 \qquad E.4.21$$

The overall mass balance on the coal particles in the FB is given as:

$$F_1 - F_o = M_R \qquad E.4.22$$

4.2.2. Fluidization and the existence of countercurrent backmixing in the FB

The internal circulation of solids and the downward movement

of gas within the FB has been explained in terms of a countercurrent backmixing model[47]. For backmixing to occur the slip velocity which is defined as the resultant velocity of gas and solids in the particulate phase must have the same magnitude as the gas velocity at incipient fluidizing conditions, i.e.,

$$u_{gE} + u_{sE} = \frac{U_{mf}}{\epsilon_{mf}} \qquad \text{E.4.23}$$

4.2.2.1. Solids circulation within the FB

The superficial gas velocity (U) may be expressed in terms of the superficial gas velocities through the emulsion, bubble and cloud-wake phases by the following equation:[47]

$$U = U_{gE} + U_{gB} + U_{gC} \qquad \text{E.4.24}$$

Expressing (U) in terms of the bubble rise velocity (u_B) E.4.24 becomes:

$$U = u_{gE}(1-\epsilon_B(1+f_w)\epsilon_{mf}+u_B\epsilon_B+u_B\epsilon_B f_w\epsilon_{mf} \qquad \text{E.4.25}$$

Due to the solids velocity in the emulsion phase the bubble rise velocity (U_B) as given by Chen and Saxena[50] is

$$u_B = U-U_{gE} + 0{,}711(g\ D_B)^{\frac{1}{2}}-u_{sE} \qquad \text{E.4.26}$$

From the assumption that the coal particles are evenly dispersed in both the emulsion and cloud wake phases, the mean density of a particle in the FB, ($\bar{\rho}$), can be written in terms of the densities of coal and the inert solids acting as the fluidized medium by

$$\bar{\rho} = \frac{W_{pb}}{W_b}\rho + \frac{W_b-W_{pb}}{W_b}\rho_s \qquad \text{E.4.27}$$

Assuming that there is solids circulation within the FB, by treating the cloud-wake and emulsion phases separately, it was shown[50] that for an envelope around the cloud wake phase:

$$F_o+\bar{\rho}u_{sE}\,A(1-\epsilon_B(1+f_w))(1-\epsilon_{mf})=\bar{\rho}u_B\epsilon_B Af_w(1-\epsilon_{mf})-(\frac{\epsilon_B f_w}{1-\epsilon_B})M_R \qquad E.4.28$$

and similarly for the emulsion phase that:

$$\bar{\rho}u_B\epsilon_B Af_w(1-\epsilon_{mf})-F_1=\bar{\rho}u_{sE}A(1-\epsilon_B(1+f_w))(1-\epsilon_{mf})-(\frac{1-\epsilon_B(1+f_w)}{1-\epsilon_B})M_R \qquad E.4.29$$

From E.4.29, E.4.25 and E.4.28, u_{sE} can be expressed in terms of U, U_{mf}, F_o and M_R by the following relationship:

$$u_{sE}=\frac{f_w}{1-\epsilon_B(1+f_w)}U-f_wU_{mf}-[\frac{1+f_w\epsilon_{mf}}{\bar{\rho}A(1-\epsilon_{mf})(1-\epsilon_B(1+f_w))}]F_o-$$

$$[\frac{\epsilon_B f_w(1+f_w\epsilon_{mf})}{\bar{\rho}A(1-\epsilon_B)(1-\epsilon_{mf})(1-\epsilon_B(1+f_w))}]M_R \qquad E.4.30$$

For solids circulation the solids must move downwards in the emulsion phase, i.e., the velocity of solids (u_{sE}) must be positive.

From E.4.30 the solids velocity is positive under the following condition:

$$F_o<F_o^{\cdot}=[\frac{\bar{\rho}A(1-\epsilon_{mf})f_w}{1+f_w\epsilon_{mf}}]U-[\frac{\bar{\rho}Af_w(1-\epsilon_{mf})(1-\epsilon_B(1+f_w))}{1+f_w\epsilon_{mf}}]U_{mf}-\frac{\epsilon_B f_w}{1-\epsilon_B}M_R \qquad E.4.31$$

If there is no nett solids velocity through the emulsion phase then $u_{sE}=0$ and a portion (q) of the coal particles in the feed will enter the emulsion phase and remain while the rest of the coal will stay in the cloud-wake phase. If there is no nett solids velocity then E.4.28 and E.4.29 will become:

For the cloud wake phase:

$$F_o - q = \bar{\rho} u_B \varepsilon_B A f_w (1-\varepsilon_{mf}) - \frac{\varepsilon_B f_w}{1-\varepsilon_B} M_R \qquad \text{E.4.32}$$

For the emulsion phase:

$$\bar{\rho} u_B \varepsilon_B A f_w (1-\varepsilon_{mf}) - F_1 + q = \frac{1-\varepsilon_B(1+f_w)}{1-\varepsilon_B} M_R \qquad \text{E.4.33}$$

The possibility of a negative solids velocity through the emulsion phase (u_{sE}) is not considered because no solids are added to the FB and consequently the quantity of solids in the FB remains constant.

4.2.2.2. Gas circulation within the FB

Gas circulates within the FB if E.4.23 is satisfied. Eliminating the solids velocity (u_{sE}) from E.4.30 and E.4.23 the equation for the gas velocity in the emulsion phase (u_{gE}) is given as:

$$u_{gE} = U_{mf}\left(f_w + \frac{1}{\varepsilon_{mf}}\right) - \frac{f_w}{1-\varepsilon_B(1+f_w)} U + \left[\frac{1+f_w \varepsilon_{mf}}{\bar{\rho} A (1-\varepsilon_{mf})(1-\varepsilon_B(1+f_w))}\right] F_o +$$

$$\left[\frac{\varepsilon_B f_w (1+\varepsilon_{mf} f_w)}{(1-\varepsilon_B)\bar{\rho} A (1-\varepsilon_{mf})(1-\varepsilon_B(1+f_w))}\right] M_R \qquad \text{E.4.34}$$

For gas circulation u_{gE} must be negative (notation: u_{gE} is positive if directed upwards). This is true if:

$$U > U' = \left[\frac{1-\varepsilon_B(1+f_w)(1+f_w \varepsilon_{mf})}{f_w \varepsilon_{mf}}\right] U_{mf} + \left[\frac{1+f_w \varepsilon_{mf}}{\bar{\rho} A (1-\varepsilon_{mf}) f_w}\right] F_o +$$

$$\left[\frac{\varepsilon_B (1+f_w \varepsilon_{mf})}{\bar{\rho} A (1-\varepsilon_B)(1-\varepsilon_{mf})}\right] M_R \qquad \text{E.4.35}$$

The conditions therefore for the existence of gas, and solids circulation within the FB are given by E.4.31 and E.4.35 respectively.

4.2.3. Gas phase reactions

The oxygen concentration within the FB changes because of the reaction with the coal particles in the cloud-wake and emulsion phases, and the continuous gas exchange between the three phases.

4.2.3.1. Gas exchange between phases

The gas within the FB exchanges freely between the three phases. The volumetric gas exchange rate per unit bubble volume is given by the following equations[47].

Exchange of gas between bubble and cloud-wake phases:

$$k_{BC} = 4{,}5 \frac{U_{mf}}{D_B} + 5{,}85 D_G^{\frac{1}{2}} g^{\frac{1}{4}} / D_B^{5/4} \qquad \text{E.4.36}$$

Exchange of gas between cloud-wake and emulsion phases.

$$k_{CE} = 6{,}78 \left(\frac{D_G \varepsilon_{mf} U_B}{D_B^3}\right)^{\frac{1}{2}} \qquad \text{E.4.36}$$

4.2.3.2. Mass balance on gaseous reactant

Since combustion takes place only in the cloud-wake and emulsion phases the oxygen concentration in the bubble phase will be affected only by the amount of gas which is exchanged with the cloud-wake phase. An oxygen balance for the bubble phase thus gives:

$$-u_B \frac{dC_B}{dh} = k_{BC}(C_B - C_C) \qquad \text{E.4.37}$$

If $\phi_4(R)$ (kg/mol/s) is defined as the oxygen consumption due to the reaction with a single coal particle then the oxygen balance for the cloud-wake phase is given as:

$$-f_w \varepsilon_{mf} u_B \frac{dC_c}{dh} = k_{CE}(C_C - C_E) + k_{BC}(C_C - C_B) +$$

$$+ \frac{1}{AH\varepsilon_B}\left(\frac{\varepsilon_B f_w}{1-\varepsilon_B}\right) \int_R \frac{W_{pb} P_B(R)}{4/3\ \pi R^3 \rho}\ \phi_4(R)dR \qquad \text{E.4.38}$$

From the assumption that the emulsion phase is well mixed, the oxygen concentration in this phase (C_E) can be obtained from an overall oxygen balance (C_E does not change with height). For the solution of a similar set of equations as E.4.37 and E.4.38 Fryer and Potter[47] have assumed that at the distributor plate all the bubble phase gas was derived from the incoming gas. Chen and Saxena[50], however, assumed that at the distributor level the cloud wake and bubble phase gas comes from both the recirculating and incoming gas stream (for gas backmixing).

Using the latter approach, the boundary conditions therefore are:

At height h = 0 (the distributor level):

$$U\ C_o = (U - U_{gE})C_{Bo} + U_{gE}\ C_E \qquad \text{E.4.39}$$

and $\quad C_{Bo} = C_{Co} \neq C_o$

At a height h = H (the total height of the FB):

$$AU\ C_o - \frac{AU}{1+f_w \varepsilon_{mf}} C_{BH} - \frac{AUf_W\ \varepsilon_{mf}\ C_{CH}}{1 + f_w\ \varepsilon_{mf}} =$$

$$\int_R \int_h \frac{1}{H} \frac{f_W \varepsilon_B}{1-\varepsilon_B} \frac{W_{pb} P_B(R)}{4/3\pi R^3 \rho}\ \phi_4(R)\ dR dh\ +$$

$$\int_R \frac{1-\varepsilon_B(1+f_W)}{1-\varepsilon_B} \frac{W_{pb} P_B(R)}{4/3\pi R^3 \rho}\ \phi_4(R)dR \qquad \text{E.4.40}$$

If there is no gas backmixing then the cloud wake and bubble phase gas comprises only of incoming gas, therefore:

$$C_{bo} = C_o \quad \text{and} \quad C_{Co} = C_o$$

and the overall gas balance at height h = H can be written now as:

$$U\,AC_o - U_{gE}AC_E - U_{gB}AC_{BH} - U_{gC}AC_{CH} =$$

$$= \int_R \int_h \frac{1}{H} \frac{f_w \varepsilon_B}{1-\varepsilon_B} \frac{w_{pb} P_B(R)}{4/3\pi R^3 \rho} \phi_4(R)\,dR\,dh + \int_R \left(\frac{1-\varepsilon_B(1+f_w)}{1-\varepsilon_B} \right.$$

$$\left. \frac{w_{pb} P_B(R)}{4/3\pi R^3 \rho} \phi_4(R) \right) dR \qquad \text{E.4.41}$$

As mentioned in Section 4.2 the derived mathematical model for the combustion of coal particles of a wide range of sizes was used to simulate the behaviour of the two-stage PFBC with no interstage circulation of solids.

Due to the complexity of the integral equations, a computer was used for their solution. A flowchart of the entire computational procedure is shown in Appendix 5 and explained below.

4.2.4. Description of the computational procedure used for the combustion of coal in a two FB system.

The computer programme treats the two FBs separately. Based on the input data the dynamic behaviour of the bottom FB is determined. The exit gas stream which is laden with fine coal particles then acts as the coal and gas feed to the top FB.

At the beginning of the programme values for the oxygen concentration in the emulsion and cloud-wake phases at the exit point from

the bottom FB are chosen (Appendix 5.). A value for the fraction of bubbles in the FB (ϵ_B) is also assumed. From E.4.18 the weight of coal particles resident in the FB (X_{pb}) is calculated. The size distribution of coal particles ($P_B(R)$) and the total rate of combustion of coal (M_R) in the FB are then calculated from E.4.17 and E.4.21. The rate of elutriation of coal particles (F_1) from the FB is then determined from the overall balalnce on coal (E.4.22).

To establish if there is backmixing of solids in the FB a comparison is made between the value of coal feedrate (F_o) and the value of an estimated coal feedrate (F_o') which forms the criterion for the existence of backmixing of solids in the FB, (E.4.31). In the case where there is solids backmixing, the values of the bubble rise velocity (u_B), the gas velocity in the emulsion phase (u_{gE}), the value of the solids velocity in the emulsion phase (u_{sE}) and the fraction of bubbles in the FB are calculated by solving E.4.23, E.4.25, E.4.26, and E.4.28. For the case of 'no solids backmixing' the solids interstitial velocity (u_{sE}) is set equal to zero, and the values of (u_B), (u_{gE}), (ϵ_B), and the fraction of feed coal (q), which enters and remains in the emulsion phase, are determined by the simultaneous solution of E.4.23, E.4.25, E.4.26 and E.4.32.

An iteration then follows which compares and reduces the difference between the calculated and assumed values of the volumetric fraction of the bubbles (ϵ_B) in the FB until convergence.

To determine the existence of backmixing of gas in the FB a comparison is made between the incoming gas velocity (U) accounting for the pressure and temperature conditions in the FB and the estimated gas velocity (U') which forms the criterion for gas backmixing in the FB (E.4.35). If there is backmixing of gas the oxygen concentrations for the bubble phase and cloud-wake phase at the exit from the FB

(C_{BH}) and (C_{CH}) and the oxygen concentration in the emulsion phase (C_E) are determined by solving simultaneously the differential equations E.4.37 and E.4.38 with boundary conditions given by E.4.40. If there is no gas backmixing then the oxygen concentrations, (C_{BH}), (C_{CH}) and (C_E) are obtained by the simultaneous solution of E.4.37, E.4.38 with boundary conditions given by E.4.41.

An iteration is then carried out using the initial guessed values of oxygen concentrations (C_{CH}) and (C_E) and the calculated values from E.4.37 and E.4.38 until convergence.

Until this stage of computation the programme dealt with the behaviour of the bottom FB. To deal with the top FB the same computational procedure is followed after setting:

a) The values of (F_o), and $P_o(R)$ equal to (F_1) and ($P_1(R)$) respectively, and

b) the composition of the gas entering the top FB equal to the gas composition leaving the bottom FB.

The dimensions of our PFBC presented in the following chapter and the various conditions under which it was operated covered in Chapter 6, were substituted in this model and a comparison is made in a later chapter between the results determined theoretically and the ones obtained experimentally.

Our research work presented in the current and the previous chapter provided us with the necessary information which was required for the final design of our PFBC plant. This is presented in the following chapter.

CHAPTER FIVE

DESIGN AND FABRICATION OF OUR MULTISTAGE PFBC

5.1 THE DESIGN OF OUR PFBC

The contribution of our research work described in the last two chapters to the design of our PFBC is described below. A number of constraints which had to be accounted for in the design of our combustor are also included in this section. The final design of our PFBC plant was thus fixed by the constraints and research findings which are given below.

(1) The advantages of a multistage combustor with countercurrent contact between the coal and air have already been covered in Chapter 3. However, the decision to use a three stage system was prompted by the necessity to build a simple enough multistage system while still being able to realize the effects of multistaging.

(2) The thermal power of the combustor was chosen as a result of the following:

(a) A combustor with a 1 MW(t) power was considered a realistic one

(b) A 2 MW shell and tube heat exchanger was available and could be used for condensing the superheated steam generated in the FBC.

(3) The height of the combustor which included the coal feeding system could not exceed 6 m (the height of the central area of our laboratory). As a consequence of this, the height of the main combustor vessel which included the cyclone and coal hopper was chosen to be 4 m. This was also determined by consideration of the kinetics of coal combustion (Section 4.1), the calorific value of coal (10 to 28 MJ/kg) and the required power generation of the combustor (1 MW(t)). The total weight of inert solids was fixed at approximately 300 kg, (100g of silica per stage). A circulation of up to 60 kg/min was necessary to give the chosen types of

coal a residence time of not less than 5 minutes. To accommodate this base load of solids, to achieve the required solids circulation and allow the solids fluidizing velocity, determined on the basis of an inert material with a mean diameter of 0,5 mm, the internal diameter of the combustor was chosen to be D = 0,45m and the interstage distance between the distributors 0,7m.

(4) A pressurized combustor was chosen for reasons already explained in Chapter 3. The combustor was designed for a maximum operating pressure of 8 bar(abs) due mainly to the unavailability and delivery time of compressors with a supply pressure of 16 bar(abs), (this pressure of operating an FBC is recommended by the Americans), as well as the stringent safety requirements associated with the higher pressure system. A rotary screw-type compressor (Atlas Copco, model GA708) rated at 7,3 Nm^3/min (258 Ncfm) and a pressure of 8 bar(abs) was therefore purchased.

(5) A wet scrubber with a capacity which was sufficient to treat the gases leaving the PFBC boiler was available and could be easily connected in series with the combustor.

Looking closer at the combustor its final design was determined by the following factors.

(6) The importance of a suitable pressure drop across the distributor plate which can ensure a good quality of fluidization and the satisfactory operation of the downcomers was covered in Section 3.3. It was also shown that a distributor with an assembly of the new type of cyclonic tuyeres could be treated in the same way as any other type of distributor.

Based on the information on our PFBC given in Section 3.3, each distributor was designed with 16 cyclonic type tuyeres arranged in a near square pattern with each tuyere having four orifices for symmetry (d_{or}=

6,2mm) as shown in Figure 5.1.

(7) The investigation on the use of downcomers for interstage transfer of solids (Section 3.1) showed that the downflow of solids could be satisfactorily controlled by altering the flowrate of the fluidizing air. However, in the case of our PFBC, where it was intended to use air as the oxidant, the use of the non-mechanical λ valve (Section 3.2) to achieve control of circulation of the solids and avoid any interference with the combustion of coal in the FB seemed by far the best method of control. For this reason the downcomers were designed so that even at the lowest gas velocity through the combustor, the maximum required downflow of solids could be achieved. The dimensions of the two downcomers were thus determined: The downcomer length l_t = 0,92m and the internal diameter d_t = 0,05m.

(8) It was shown in Section 3.4 that an immersed type burner could be used to preheat a multistage FB system reliably and efficiently. In the design of our PFBC provision was made to use either the immersed type burner or preheat the combustor using the combustion of a stoichiometric mixture of air and LPG in the FB. This gave the opportunity to compare the two preheating methods.

(9) The problem of removing heat from the PFBC was solved by using both, water jackets in each stage and internal cooling coils. The cooling coils were designed to remove up to 0,3MW with the remainder of the generated heat removed by the exhaust gas and through the water jackets (one in each of the three stages). Two different shapes of coil were designed. A horizontal coil with a total length of 10,6m and an outside loop diameter of 0,44m, and a vertically orientated coil having the shape of a double serpentine. This coil had a length of 4m. The coil pipe outside

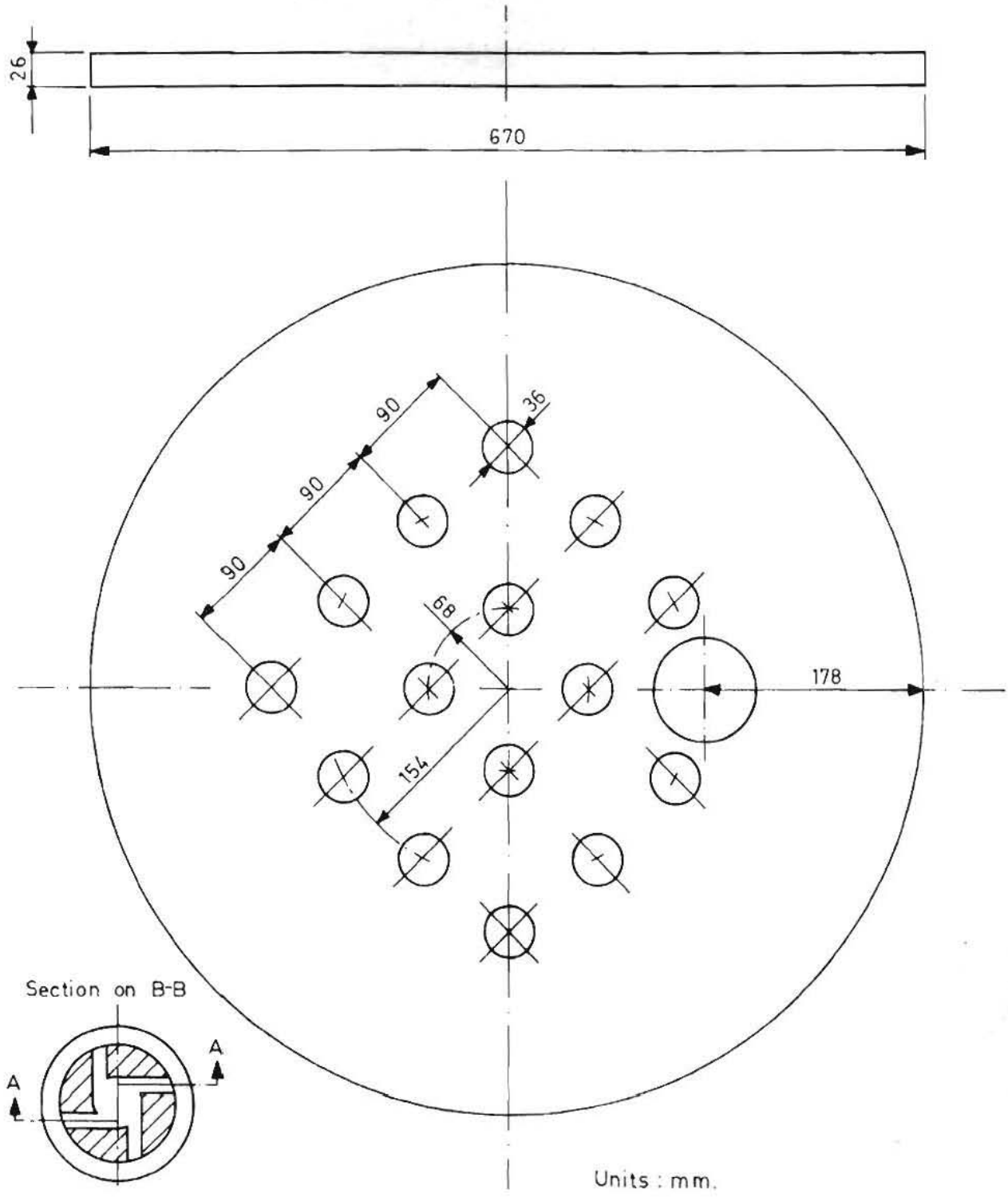

Figure 5.1. Schematic drawing of the distributor plate showing the downcomer position and details of the ceramic tuyere

diameter was 13mm and had a wall thickness 1,5mm.

(10) A double entry high-efficiency cyclone was designed for removing the fine coal particles and fluidizing material from the flue gas, as well as returning solids coming from the pneumatic conveyor. The cyclone entries for the flue gas and circulating solids were positioned in such a way as to induce a unidirectional stream of gas and solids within the cyclone, as shown in Figure 5.2. The cyclone was designed to have a cut-off particle size of 30um and an operating temperature of 500^{o}C.

(11) Two coal hoppers rated at a working pressure of 10 bar(abs) were designed to hold each one up to 90 kg coal. A baffle was placed at the bottom of each hopper to stop bridging of coal particles as shown in Figure 5.3. To achieve a continuous feed of coal to the combustor at high pressures the hoppers were designed to operate, positioned vertically one above the other with a connecting valve placed between them to form a double lock system. Coal could be fed into the combustor by using a screw feeder which was designed to deliver up to 2 kg/min of coal at a 110 r.p.m.

To enable the continuous monitoring of the experimental parameters and achieve control of the combustion process during the operation of the PFBC, all necessary sensing devices and instrumentation were ircorporated in the design of the plant, as explained below.

5.2 SAMPLING AND INSTRUMENTATION

Four sampling nozzles for gas analysis were designed, with three of them located each at 0,7m above each distributor plate and one at the flue gas line after the cyclone (Figure 5.4). These nozzles were designed to accommodate a gas sampling probe which could continuously supply gas for analysis to an O_2 and a CO and CO_2 analyser .

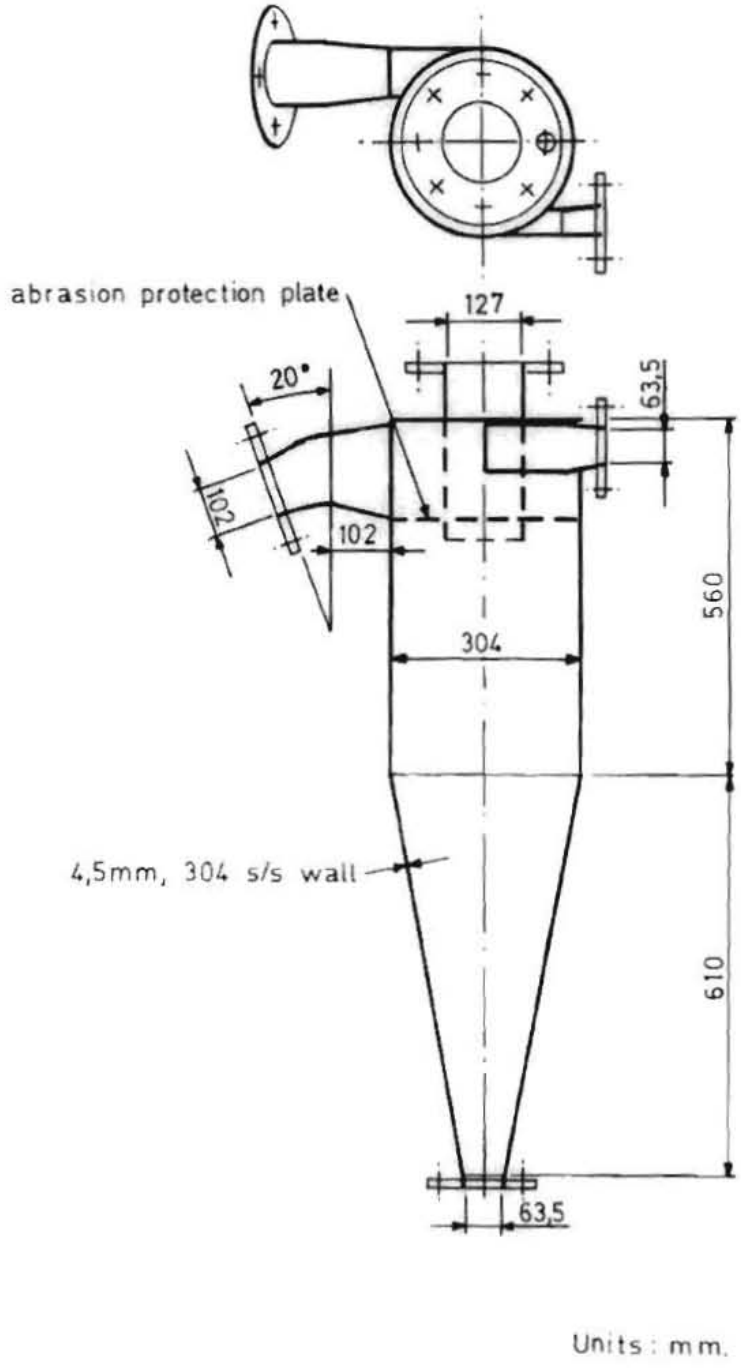

Figure 5.2. Schematic drawing of the high-pressure double-entry cyclone

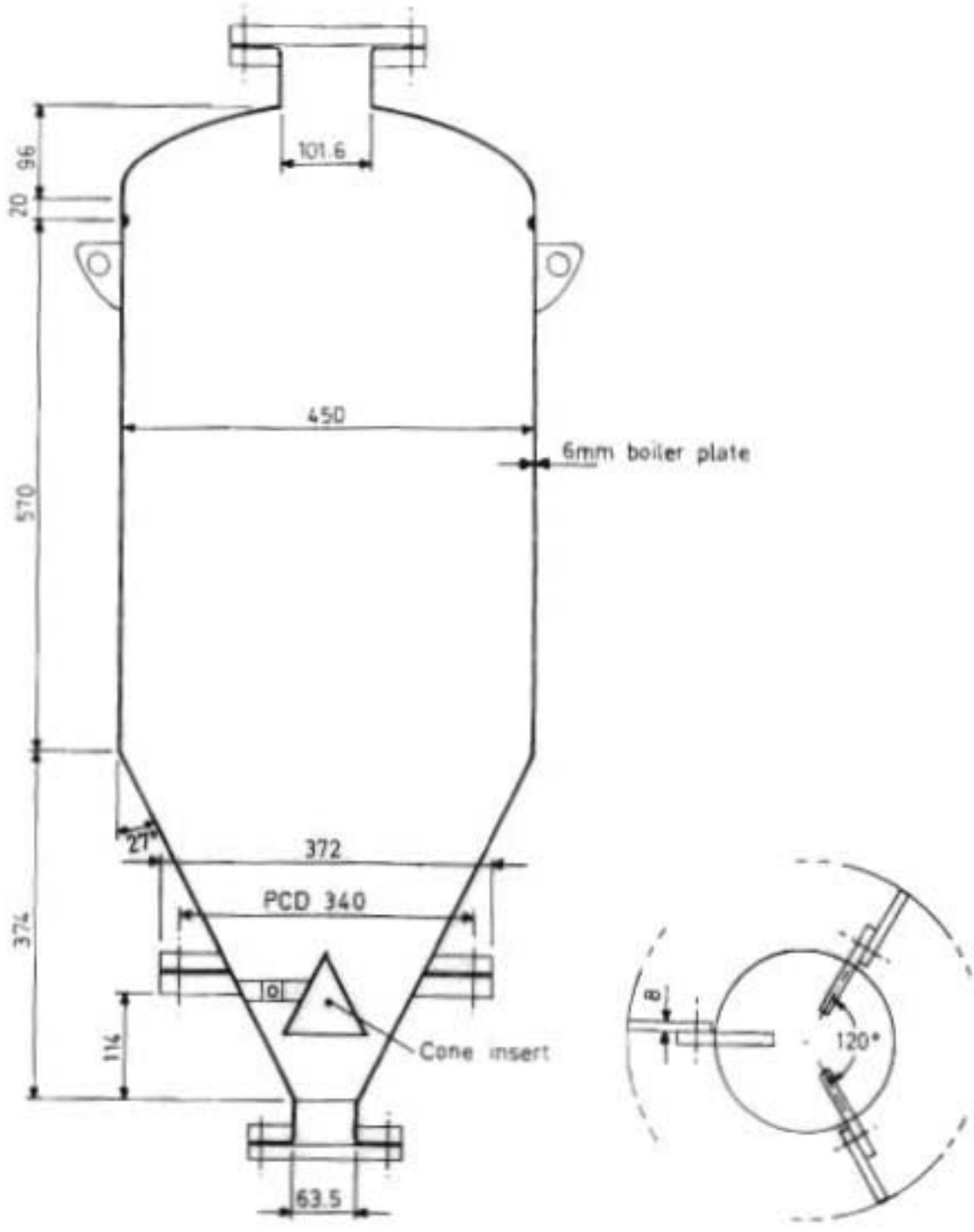

Figure 5.3. Schematic drawing of the high-pressure coal hopper

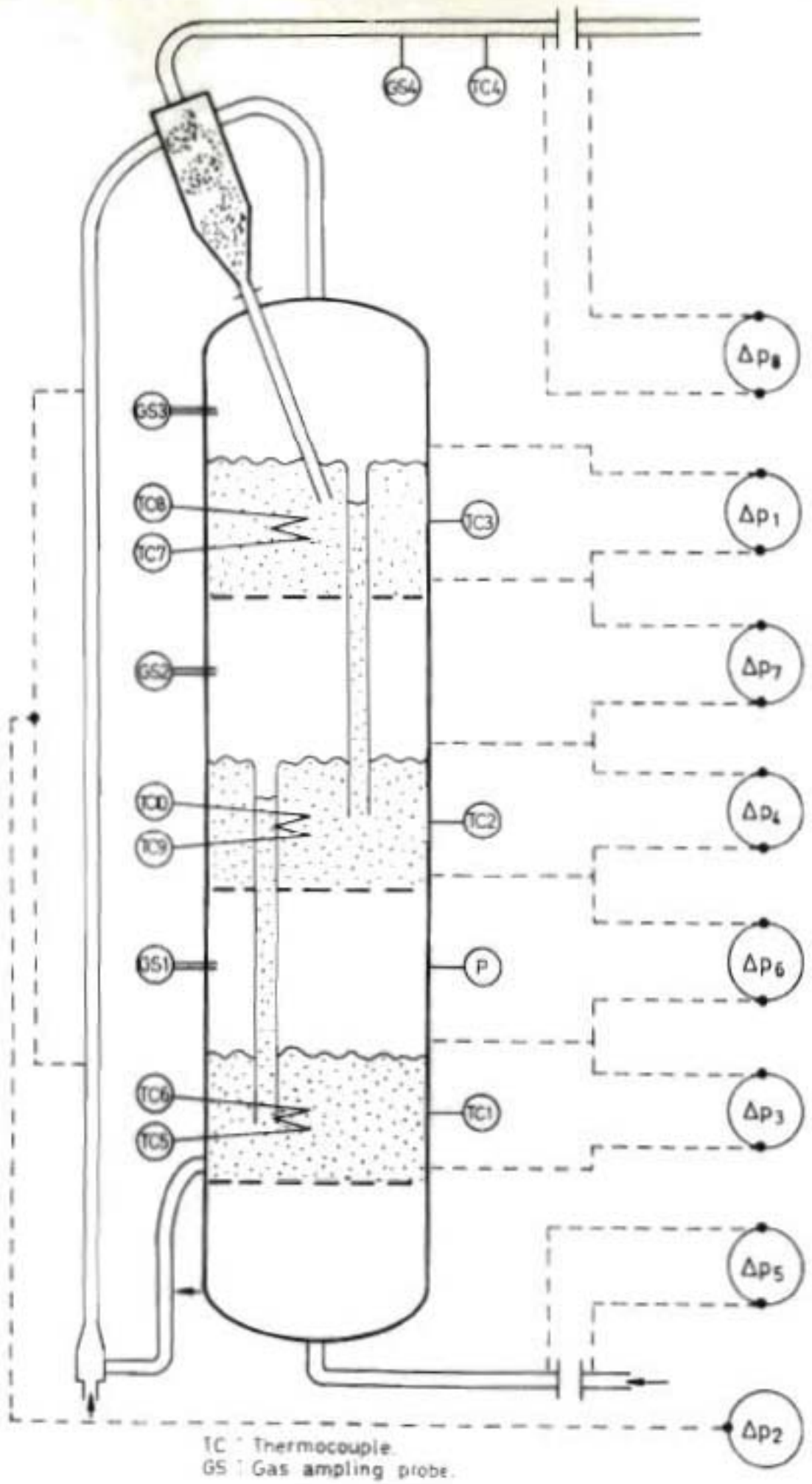

Figure 5.4. Gas sampling and instrumentation diagram of the PFBC

These analysers had already been used in a series of combustion experiments on the small FB combustor (Section 4.1).

Six pressure tappings were placed at regular intervals along the length of the combustor and were designed to measure the pressure drops across each FB and each distributor plate. Pressure tappings were also located across the orifice plates, designed to measure the incoming and flue gas flowrates, as well as along the pneumatic conveyor to enable the measurement of the circulating solids.

Three K-type thermocouples positioned 0,14m above each distributor were provided to measure the temperature in each FB. The inlet and outlet coil temperatures, as well as,the flue gas temperature could be measured using the same type thermocouples connected as shown in Figure 5.4.

All instruments used for monitoring the performance of the PFBC were chosen with the intention of coupling them up,at a later stage, with the departmental computer for data logging and processing. The computer link up with the PFBC plant is covered in the last section of this Chapter.

Allowing for instrumentation, the engineering drawing of the main combustor and ancillary equipment, which was based on the constraints and findings in research as described in Section 5.1, was sent to the manufacturers for the fabrication of the PFBC.

5.3 FABRICATION OF THE PFBC

5.3.1. The combustor vessel, hoppers and cyclone

The main combustor vessel, the hoppers, and cyclone, classified as pressure vessels were designed according to ASME VIII DIV 1-1977 code for pressurized systems.

All dimensions and specifications for the manufacture* of the main combustor vessel comprising of three separate stages were detailed in numbered engineering drawings[55]. The material used was 304 stainless steel except for the interstage flanges and water jackets, where mild steel was used. The inner diameter of the vessel was 0,74m and the thickness of the stainless-steel wall was 5mm. The two stainless-steel dished ends had a thickness of 8mm. The width of the water jacket for cooling the cylindrical walls of the vessel and the top dished end was 0,03m. Separate water inlet and outlets were used for each stage.

The thickness of each interstage flange was 0,04m and twenty 32mm (1¼in) bolts were used for joining two stages together. The interstage flanges were welded flush with the wall of the vessel and a stainless-steel ledge was welded on the inside of each flange to support the firebrick lining. Each section could thus be lifted complete with its lining. Each stage was lined with three layers of twenty-two fireclay bricks† per layer and the bricks were bonded together with a high temperature mortar¶. The bricks had the shape of a wedge and had an internal radius of curvature of 0,46m. A high alumina castable cement§ was used for lining the two dished ends. To protect the stainless-steel shell from excessive heat, which is transferred across

---

*A. Chalmers & Co. (Pty) Ltd, Clairmont, Natal, S.A.

†Normal duty fireclay bricks, manufactured by Cullinan Refractories, Olifantsfontein, Transvaal, S.A.

¶Hiluset 35, manufactured by Cullinan Refractories.

§AF66 castable cement, manufactured by Carborundum Universal, Port Elizabeth, S.A.

the hot phase fireclay bricks, a high alumina fibre* was used between the bricks and the shell. This narrow gap, packed with the loose insulating fibre,was also used as a space where the bricks could expand into, when hot, without damaging the water-cooled shell.

To position the thermocouples, gas sampling and pressure probes, holes were drilled through the firebrick walls of the combustor at the designed locations.

Dimensions and specifications for the manufacturers† of the cyclone and coal hoppers were detailed in numbered drawings[56].

The cyclone was made of 304 stainless steel to withstand the high temperature of the gases and had a wall thickness of 5mm. A 2mm thick plate was welded inside the top section of the cyclone to protect the stainless-steel shell from abrasion caused by the high velocity of the incoming gas and solids.

The two hoppers were made of mild steel and had a diameter of 0,45m. The wall thickness was 6,3mm.

All vessels after they had been manufactured were individually pressure tested by an engineering inspection company¶ and numbered certificates were issued[57].

5.3.2. The distributor plates, tuyeres and downcomers

A 0,72m diameter wooden mould,with mild-steel rods,used in place of the sixteen tuyeres,was made in our laboratory at the University of Natal and sent to a company§ specializing in refractory materials, to cast the distributor plates. The refractory material used for the

*Fibrefrax, manufactured by Carborundum Universal.

†A.J. Howes, Rossburgh, Durban, S.A.

¶SGS Engineering Inspection Company, Durban, S.A.

§Carborundum Universal, Port Elizabeth, S.A.

fabrication of the distributors had a high alumina content and was previously used for lining the dished ends of the combustor. After drying in air refractory distributors were heat cured in a pottery kiln in which the temperature was slowly raised to 150^{o}C and then increased to 1200^{o}C and held there for 6 hours.

Longitudinally splitting plaster moulds were used for moulding the tuyeres. Four 6,2mm thick brass pins, one for each tuyere orifice, were pushed into the mould in such a way as to induce the gas swirling effect when gas was forced through the tuyere. After drying in air the pins were removed, and the tuyeres, still in their plaster moulds, were placed in a furnace where the same heat curing procedure as the one used for the distributors was employed. At these high temperatures the plaster mould broke off and released the cured tuyere. The reason for heat curing the tuyeres in their plaster moulds was that the chosen castable mortar for the tuyeres had a low mechanical strength at ambient temperature but set very hard after heat curing. The downcomers were cast out of the same refractory material as the one used for the distributor plates. The tuyeres and downcomers were then cemented on the distributors and heated in a kiln to cure the bonding mortar. Each downcomer was cemented on the distributor plate in such a way so as to act as the overflow of the FB above the distributor while forming a solids seal 0,22m below the solids surface of the FB immediately below the distributor.

5.3.3. The cooling coils

Two sets of holes were drilled through the walls of each stage of the combustor and the cooling coils were suspended inside each stage, using stainless steel couplings (Figure 5.5). The same type of stainless steel (304) was used for the manufacture of the two different shapes of coils.

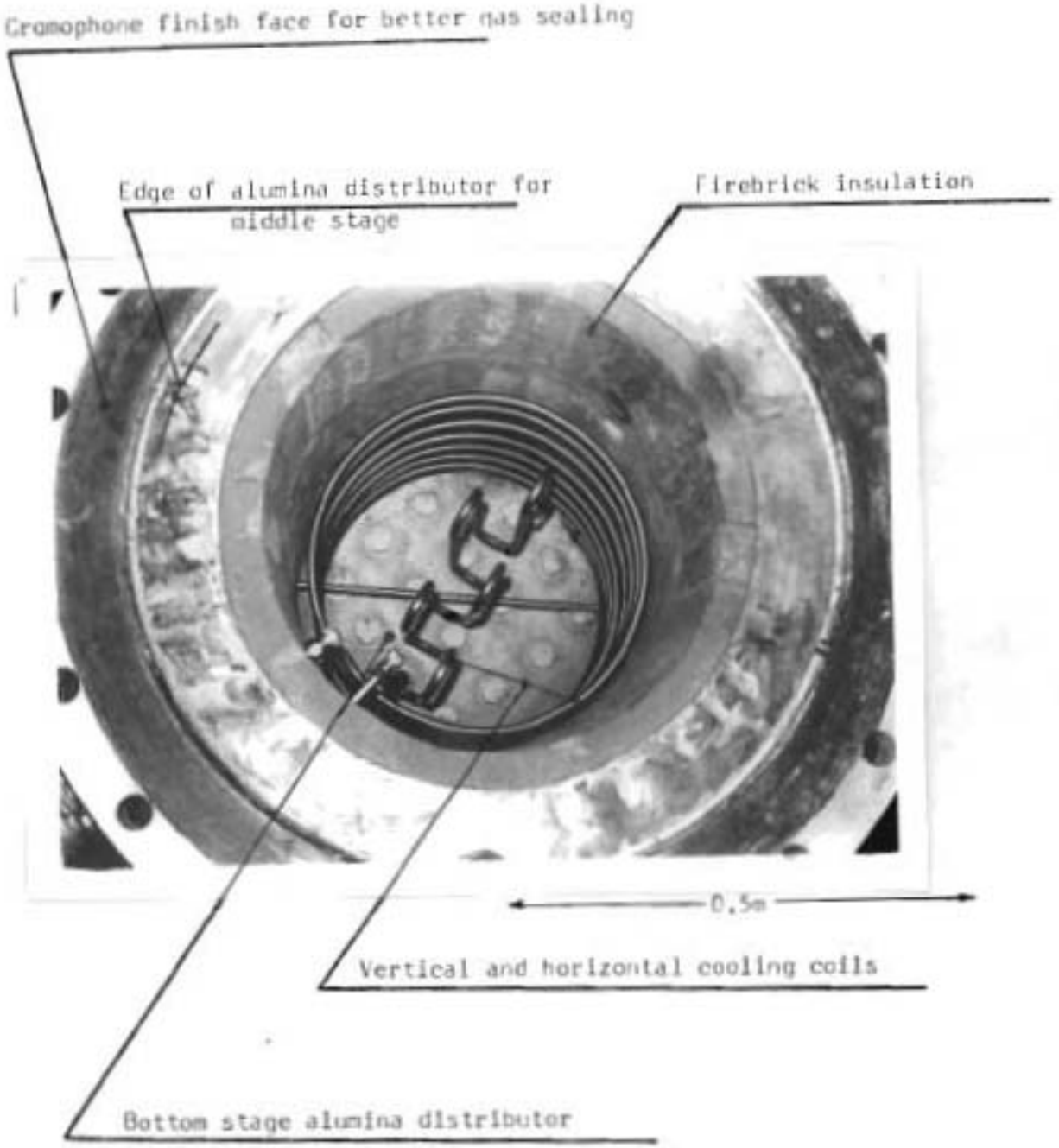

Figure 5.5. The bottom stage of the PFBC showing the firebrick lining, cooling coils and distributor plate.

After the fabrication of the main combustor vessel and all the ancillary equipment the PFBC plant was temporarily assembled.

5.4 INITIAL ASSEMBLY OF THE PFBC

The purpose of the initial assembly of the PFBC was to pressure test the plant as a unit,check all sensing devices and link the PFBC with the departmental computer for data logging.

The combustor positioned in the central area of the laboratory was assembled using a one-ton mechanical hoist. Each stage was lifted into position using the hoist with the interstage distributors positioned between the flanges. High temperature gaskets were used for sealing the flanges. To avoid any bypassing of gas the distributors were made air tight at the edges,between the stages,by filling the gap with a refractory fibre. The coal hoppers and double entry cyclone were bolted on the combustor and supported onto the framework surrounding the vessel.

The scrubber was positioned 6m away from the combustor close to the north facing wall of the laboratory where the exhaust gases could be easily purged to the atmosphere. A 304 stainless-steel pipe,with an internal diameter of 82,2mmand a wall thickness of 3,3mm having a length of 6,2m,was used to connect on one end the top of the double entry cyclone and the other the pressure control valve. The control valve was positioned above the gas entry to the wet scrubber. The scrubber was fitted with a slurry pump for pumping the slurry to a nearby settling tank where the ash could be removed.

The three sets of cooling coils one from each stage of the combustor were connected to a common exit manifold and from there a single pipe was used to carry the coolant to the heat exchanger. The heat exchanger was placed very close to the combustor to reduce heat losses and the danger involved with the transport of a high temperature and pressure fluid. It was possible to use either steam, water or air as a coolant

for the coils. The flowrates for air and water could be measured using rotameters while for the steam electronic turbine flowmeters were used. The PFBC plant and the three-FB combustor are shown in Figures 5.6 and 5.7.

All sensing devices were positioned in their locations on the PFBC plant and were tested. The pressure probes were made of thin stainless-steel tubes and had stainless-steel sintered discs welded at their tip to prohibit solids entering the probes. All pressure probes were linked to a set of electronic differential pressure cells. The gas sampling probes were made of stainless-steel tubes which protruded 50mm into the freeboard area of each stage. Each sampling probe could be kept clean of any solids by regularly backflushing the probes with air using solenoid valves. To protect the gas analysis instruments from particulate matter, a gas conditioning unit which included a series of filters and a moisture trap was located before the instruments. The signals from the thermocouples were transformed into temperatures and displayed on a panel next to the combustor.

To enable the continuous monitoring of all temperatures, pressures, and have a continuous recording of the analyses of gas streams, all electronic instruments, connected to the combustor, were linked with the departmental computer (CDC 1700). A computer programme was thus written, for the regular scanning of all instruments and thermocouples, and for the logging of all corresponding data. The programme requests initially the time interval between successive scans. It then sets up all channel addresses, scans all instruments and thermocouples, and stores all data as physical variables. Data from previous runs can also be recalled from storage for an assessment of the performance of the combustor, if required. Once the programme is loaded onto the computer, control of data logging can be transferred to a remote control panel positioned next to the PFBC. A flowchart of the computer programme

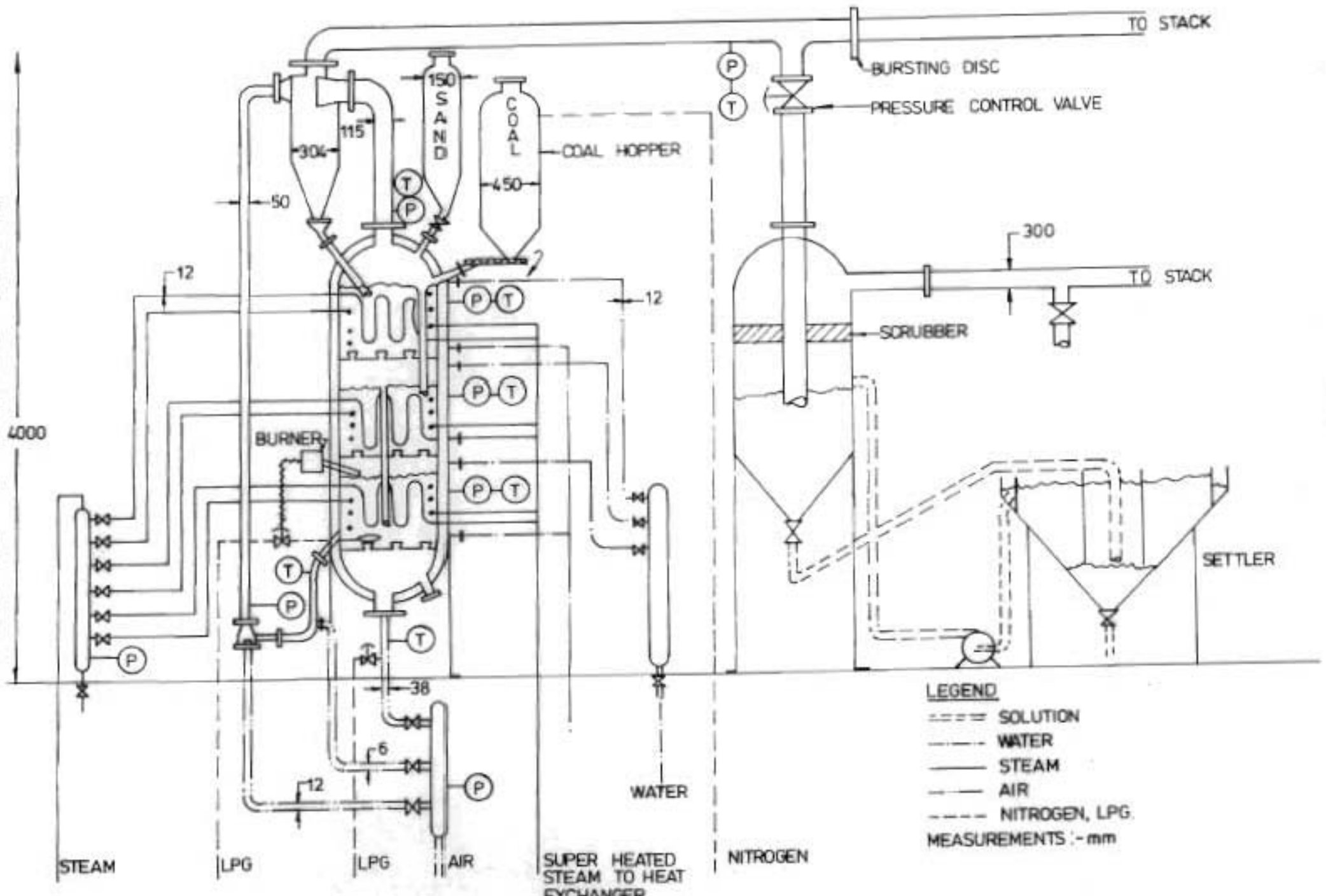

Figure 5.6. Schematic drawing of the PFBC plant

Figure 5.7 Photograph of the three-FB combustor

is included in Appendix 6. The computer channel addresses with the corresponding instruments on the PFBC, are also included in the same Appendix.

The entire PFBC plant was pressure tested using the control valve in the exhaust line (Figure 5.6). During the pressure test which was performed with the combustor empty of solids and at ambient temperature, a close look was maintained on all instruments,differential pressures and flowrates. Any gas leaks and other minor problems which were detected were rectified.

CHAPTER SIX

COMMISSIONING AND COMBUSTION TRIALS

After completion of the preliminary work and tests on the PFBC the main combustor vessel was dessembled and the firebrick insulation and cooling surfaces were inspected for any possible damages.

Commissioning of the plant and combustion trials were then conducted in the following sequence.

(1) The combustor was loaded with silica sand and cold runs were carried out using the three-FB configuration. These were followed by,

(2) Hot trials using the three-FB configuration with solids circulation.

(3) Hot trials using the single deep FB configuration, and

(4) Hot trials using the two-FB configuration.

6.1 COLD TRIALS USING THE THREE-FB CONFIGURATION

The cold trials on the three-FB system began by slowly assembling the combustor and testing every stage of assembly to determine if the design specifications were satisfied, until the combustor was fully assembled. In this way any problems associated with the functioning and behaviour of each FB could be solved before the system was fully assembled.

The bottom stage was initially assembled and investigated by testing the pressure drop across the unloaded distributor. The same testing procedure was followed for a loaded distributor using silica sand as a fluidizing material. Circulation of solids was also tested by connecting the λ valve and pneumatic conveyor to the bottom FB. The cyclone at the top of the conveyor was supported by using the overhead hoist and during circulation the solids were returned to the FB in the bottom stage, via an extension pipe attached

to the underflow of the cyclone. Finally, with the bottom stage completely open to atmosphere, a stoichiometric mixture of LPG and air was passed through the FB and ignited to test the safety and operation of the preheating system. The main features of the preheating system included a control device which continuously monitored the flame via an ultra-violet light (UV) detector, a solenoid valve which controlled the flow of LPG, and a pilot burner. The preheating system had built in it all the required safety features and operated in the same way as an oil fired burner in a conventional boiler.

On completion of the tests on the bottom stage, without emptying the solids, the middle FB distributor with the downcomer and the middle stage were placed on top of the bottom stage and secured by bolting the flanges together. After connecting all instruments to this stage, a similar testing procedure was followed. The pressure drop across the seccnd stage distributor and the FB were observed and the circulation of solids and operation of the downcomer were tested. The downcomer was transfering solids from the FB in the middle stage to the one in the bottom stage.

Finally all three stages were put together and the entire system was tested.

6.1.1 Cold trials: observations

From the cold trials on the PFBC the following observations were made

(1) The pressure drops across the distributor and FB were in agreement with the designed values and circulation of solids was possible and could be controlled by varying the air flowrate to the λ valve. The designed solids circulation rate of 60 kg/min was achieved and a pressure height diagram obtained while the system was operating at

this circulation rate is shown in Figure 6.1.

(2) The test on the preheating system was successful though as observed by Baskakov *et al.*[26] at lower FB temperatures, combustion occurred near the solids surface with bubbles, filled with a flammable gas mixture, igniting near the solids surface.

As a result of the irregular burning of LPG in the FB, which was also visible if one looked through the observation port on to the surface of the FB, the UV detector was continuously tripping off the preheating system and was interrupting the supply of LPG to the FB. To overcome this problem the UV detector was placed in a position directly opposite the pilot burner where it could monitor the pilot burner instead. However, it was subsequently ascertained that the pilot burner, which was positioned in the freeboard area between the two stages, was also put out by the solids if the superficial velocity of the gas mixture reached a value which was eight times greater than the velocity required for minimum fluidizing conditions. These velocities however, were not likely to be reached during the preheating period. For this reason no further modifications were made. Furthermore, this problem did not affect the safety of the system.

6.2 HOT TRIALS USING THE THREE-FB CONFIGURATION

The coal combustion trials using this configuration of the combustor were divided into two different sets of experiments. In the first set, coal was supplied to the top FB while in the second set of experiments, coal was supplied to the middle FB. The purpose of these experiments was trifold:

a) To study the effect of countercurrent solids flow on the combustion of coal.

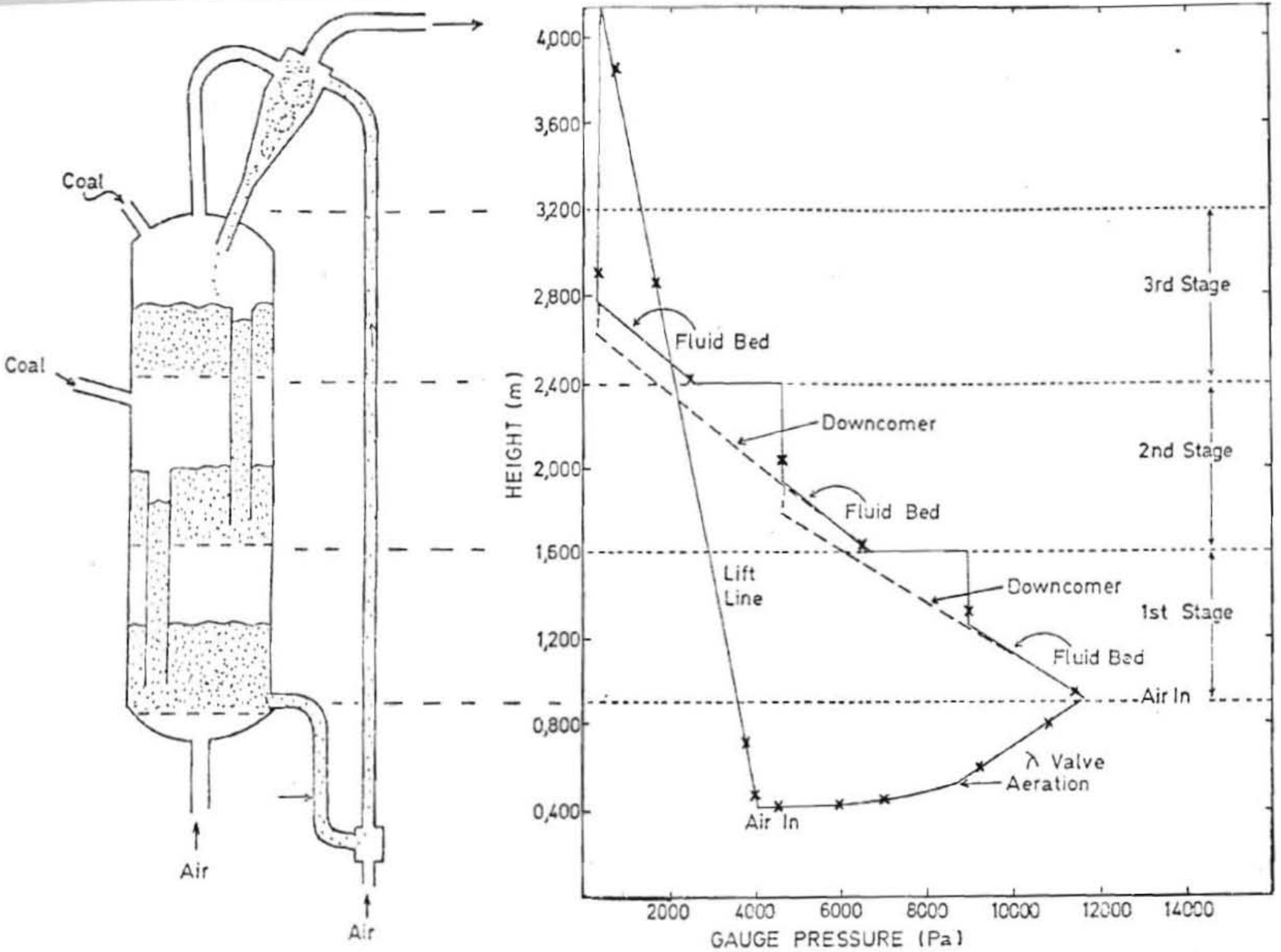

Figure 6.1 Pressure - height diagram of the three-stage configuration of the PFBC

(b) To investigate the possibility of controlling the temperature of the FBs, and

(c) To reduce the coal in the flue gas.

Before coal was introduced into the PFBC for combustion, a preliminary run was carried out using an LPG-air mixture to cure the refractory mortar and drive off the moisture still in the system. During this preliminary run the temperature of the reactor was raised very slowly to the 100°C mark and kept there for two hours. The temperature was then raised by 100°C per hour until the system reached 900°C. It was then kept at 900°C for three hours in accordance with the instructions of the refractory manufacturers. To avoid overheating of the immersed cooling surfaces a low air flowrate was passed through the cooling tubes.

In the experiments on the PFBC both Rand Carbide char and Rooifontein coal were burnt in the combustor. The ash content in the char and coal was 20 and 30 per cent respectively. Their chemical analyses and size distributions are included in Appendix 7. A single coal hopper was used in these tests and the coal was loaded into the hopper using a 500 kg hydraulic hoist.

For all the combustion trials a standard start up and shut down procedure was followed. This is listed in Appendix 8.

6.2.1. Overbed coal feed in top stage FB

The combustor was initially brought up to temperature with the help of the preheating system. To reduce the preheating time, coal was fed into the top stage and transferred with the solids down to the bottom stage. The solids circulation was then stopped and the temperature in the bottom FB raised to 650°C. After the coal ignited in the bottom FB,solids circulation was renewed and more coal was fed

into the top stage until the system was operating in a steady state.

Various temperatures in each FB were attempted by regulating the amount of heat removed from each FB and the circulation of solids. Air was used as a coolant through the coils

6.2.2. Overbed coal feed in middle stage FB

In this set of combustion trials, the coal feed was removed from the top stage and placed in the stage below,so as to feed coal to the middle FB (Figure 6.2).

The same preheating procedure, followed in Section 6.2.1., was also used here. In these experiments both coal and char were combusted.

6.2.3. Combustion trials: observations

A number of observations were made when operating the PFBC with coal being fed either in the top stage or middle stage of the combustor. These observations are listed below.

(1) In an attempt to protect the cooling coils in the bottom stage from the excessive heat generated during the preheating period, the solids were kept well fluidized and the flowrate of LPG to the FB was reduced considerably. This resulted in a preheating period of nearly five hours. Allowing for the time needed for the system to reach a steady state, which was approximately four hours after the coal was ignited, each full run lasted for a minimum of twelve hours.

(2) The main objectives of circulating the solids and feeding coal in the top FB were, to achieve coal devolatilization and combustion of elutriated fines in the top stage, combustion in the middle stage and final burnout of descending coal particles in the bottom stage as already explained in Chapter 3. Although the system did not incorporate facilities for treating or monitoring the amount and quality of coal volatiles leavin the PFBC heavier hydrocarbons were collected in the wet scrubber.

(3) Control of the temperature and removal of heat from anyone of the FBs was easier achieved by transferring solids in and out of

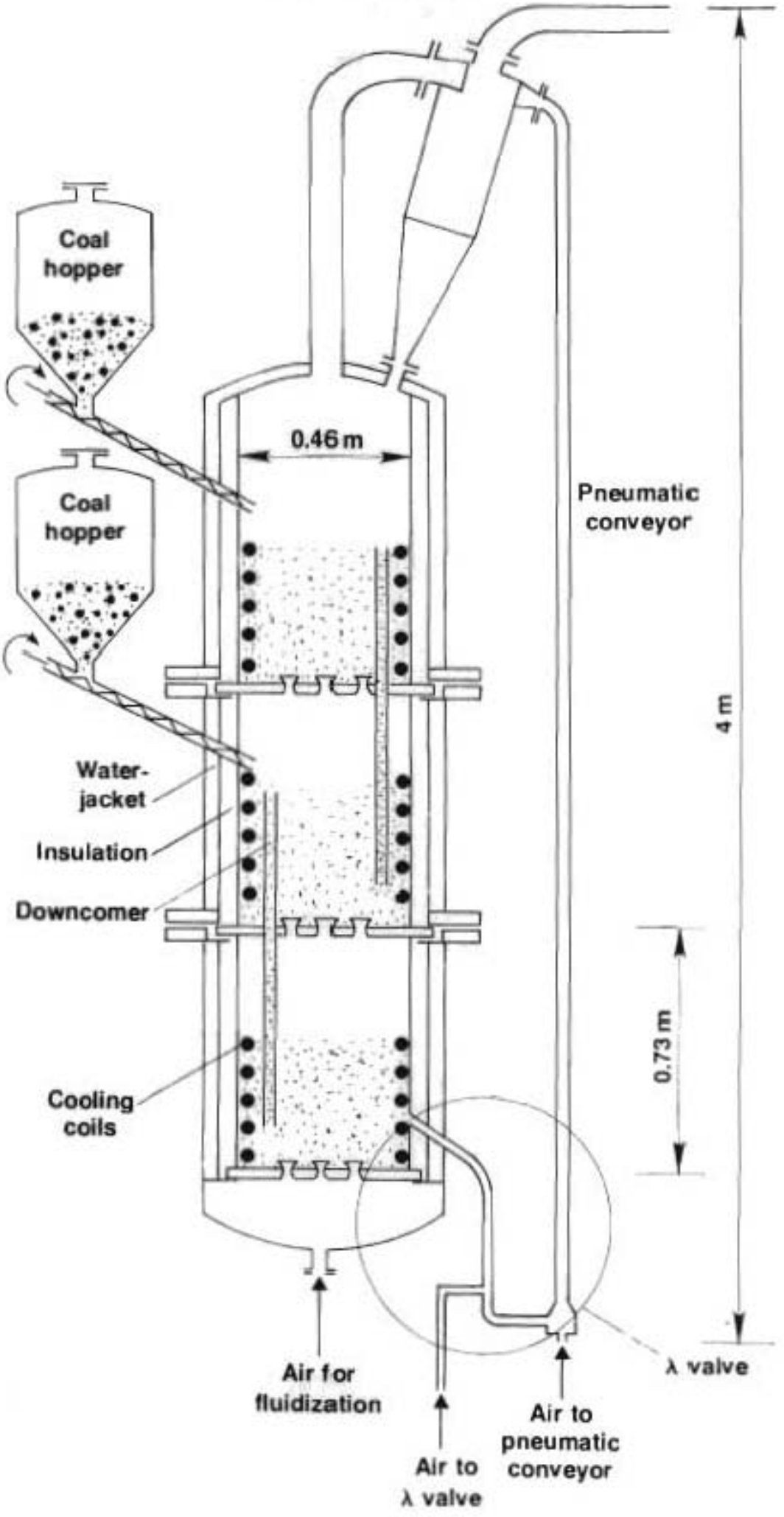

Figure 6.2. Schematic drawing of the PFBC

the bed rather than by removing heat through the cooling coils. However, it was not easy to control the temperatures of all three FBs or vary their temperature independently, particularly if combustion in the top FB was also required.

(4) The temperature in the lower two FBs had to be kept above 600°C otherwise the devolatilized coal,descending into the lower FB, could not be combusted.

(5) Since all downcomers were acting as overflow pipes, it was not possible, say for instance, for the solids and the coal to be transferred from the top FB to the middle FB and kept there until the required degree of combustion was achieved, before transferring them to the bottom stage for the final burnout.

(6) Tests on the ash recovered from the flue gas indicated a combustibles content in the ash over 10 per cent by weight. With high solid circulation,the combustibles in the ash increased to over 20 per cent. This pointed towards reduced solids circulation or preferably intermittent circulation in order to reduce the loss of combustibles.

(7) Feeding of coal into the middle FB reduced the amount of elutriated coal. This indicated that not all the combustibles, escaping from the PFBC, originated from the circulating solids. Further an increase in the loss of combustibles was detected when transfer of coal and solids from the bottom to the top FB was attempted via the pneumatic conveyor. In conclusion, the loss of combustibles from the three-FB system may be attributed to the following factors:

(a) The size distribution and quantity of coal in the top FB and to a lesser extent, to the coal loading in the bottom FB.

(b) If the coal was fed into the top FB, to the fines present in the feed, and finally,

(c) The frequency of circulation of solids.

(8) Combustion of char in the top FB and control of the temperature in all three FBs of the combustor was not easily achieved mainly because of the higher ignition temperature of char and the low residence time of char in the top FB.

(9) It was possible to operate the three-FB combustor as described in paragraph (2) of this section satisfactorily only after the finer fraction of coal particles, with a diameter less than 600 μm, was removed from the coal feed.

(10) The flue gas clean-up system operated as designed and no SO_2 or particulates were detected in the stack gas. All the ash was collected in the wet scrubber and then pumped into the settler. The flocculant was very effective when the solution in the settler was at a pH of between 8 and 10.

After the completion of this set of hot trials using the three-FB configuration which lasted for a total of three weeks, the combustor was dessembled for inspection and the following observations were made:

(a) A crack developed across the distributor of the middle FB. This was attributed, firstly, to small LPG air mixture explosions which occurred below this distributor during the preheating period and secondly, to localized high stress zones developed during the same period.

(b) Signs of erosion were observed on all horizontal parts of the cooling coils because of the vertical movement of the solids caused by solids backmixing and circulation. The effects of the excessive heat, incurred during the pre-heating period, were visible in the freeboard area and the distributor above the bottom FB.

(c) Some of the orifices on the tuyeres were blocked by sand particles and fine ash. This kind of problem was not encountered in the experimental tests using these type of tuyeres (Section 3.3). It is believed that this blockage occurred when coal was combusted at low fluidizing gas velocities (less than U_{MIN} of E.2.3.). Due to the properties of the fine hot ash the non-operational orifices could not be cleared even if high gas fluidizing velocities were used.

6.2.4. Sequential action

As a result of the observations made during the combustion trials on the three-FB PFBC and the inspection of the main combustor after it was dessembled, the following changes were made:

(1) The alumina distributors and downcomers were replaced with ones made of 430 stainless steel. These distributors were made larger in diameter for better heat removal. They stretched beyond the gramophone finish faces of the interstage flanges. It was believed that the good heat transfer properties of the stainless steel distributors would keep them relatively cool. The design of the tuyeres was based on the same principle as the one used for the design of the alumina tuyeres, though the new tuyeres had only three orifices and were arranged on the distributor plate in a triangular pattern as shown in Figure 6.3. To avoid the problem of blockage of the tuyere orifices with ash and silica, the top section of the tuyeres was modified so that no solids could enter the orifices when the bed was defluidized.

(2) To reduce the high loss in combustibles,which amounted to 10 to 20 per cent by weight of the ash,small fluidizing pots were positioned under the discharge ends of the downcomers as shown in Figure 6.4. The supply of air to these pots could be remotely controlled thus making it possible to control the solids transfer within the combustor. In this way the solids residence time in each FB could be determined independently.

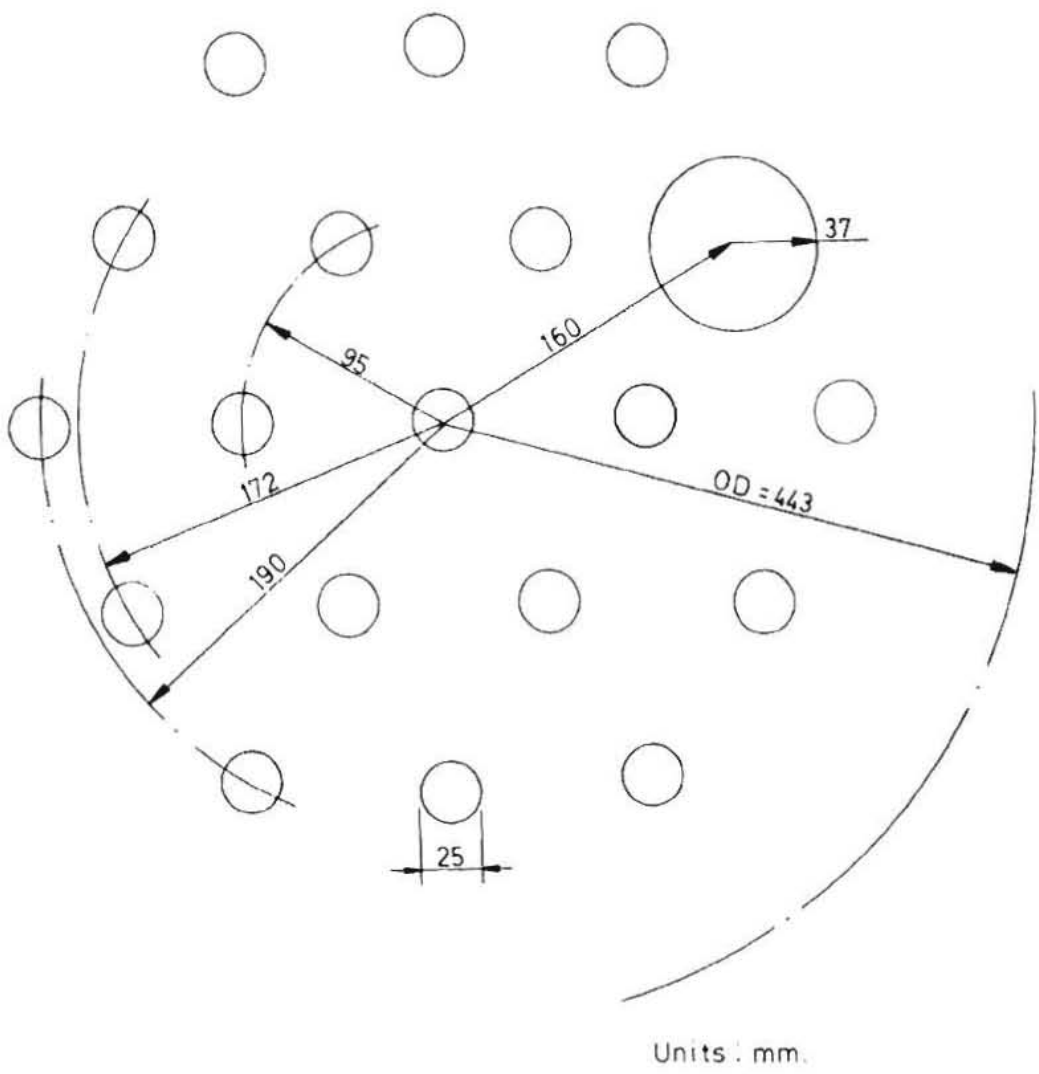

Figure 6.3 : Schematic drawing of the stainless-steel distributor showing the position of the downcomer and tuyeres

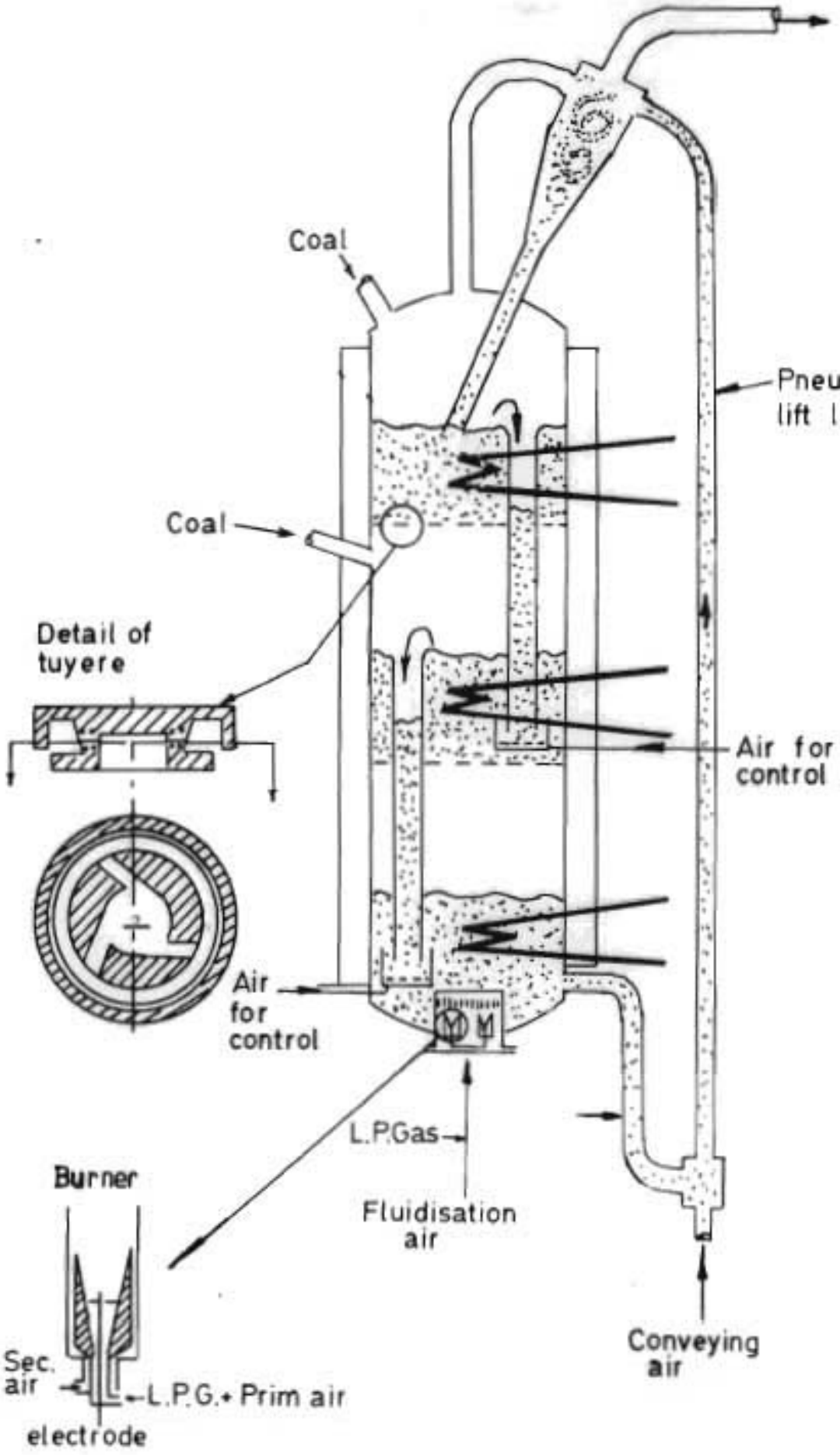

Figure 6.4 : Schematic drawing of the three-stage PFBC showing the immersed burner assembly, the fluidizing pots under the downcomers and the final version of the cyclonic tuyere

(3) The problems of overheating during the preheating period, which could have worse effects on the stainless steel distributors, were solved by the incorporation of the immersed type burner, which could offer better temperature control during preheating. Four burners of a similar design as the one investigated in Section 3.4 were positioned in place of the bottom FB distributor (Figure 6.4). The burners were rated at a heat output of 15kW each and a common ignition system, secondary air and outer sleeve were used for all four burners.

6.2.5. Combustion trials on the modified three-FB combustor

The combustor was reassembled and a series of tests were carried out by feeding coal in the middle FB. The pressure of the combustor was raised to 4 bar (abs) and solids were circulated through the system to test the new downcomers and evaluate the effect of the fluidizing pots. As has been previously mentioned the height of solids in the middle and top stage FBs was fixed by the corresponding downcomers acting as overflow pipes. However, the solids in the bottom FB could be drained completely through the λ valve which was acting as an underflow drainage pipe. To minimize the possibility of such a situation occurring, which could destroy the seal formed between the downcomer and the solids in the bottom FB, an extra 50 kg of solids was added to the PFBC. This was also aimed at making the solids circulation easier and relaxing the stingent conditions governing the timing of this operation. The procedure followed for the circulation of solids is listed below:

(a) The PFBC was initially preheated and the extra weight of solids was transferred to the middle FB. Coal was then introduced into the middle FB until the oxygen in the gas leaving this bed was reduced to

less than 2 per cent by volume. The coal supply was then interrupted.

(b) After the oxygen in the same gas stream had increased to 8 per cent by volume, the excess bed material was transferred to the bottom FB and coal was again introduced into the middle FB. Once the oxygen in the gas leaving the bottom FB had reached 16 per cent by volume the excess bed material was withdrawn from the bottom FB and lifted up to the top FB.

(c) Finally, the solids were transferred from the top back to the middle FB once the oxygen in the flue gas leaving the system had risen above 5 per cent by volume.

6.2.6. Combustion trials on the modified combustor: observations

(1) The immersed burner operated satisfactorily. Preheating periods of four hours were achieved by decreasing the secondary air to the burners. However, to increase the burner lifetime,lower exhaust gas temperatures leaving the burners were used, thus averaging a pre-heating period of five hours.

(2) The elutriated combustibles were reduced to between 5 and 10 per cent by weight of the elutriated fines leaving the top FB. The fluidizing pots operated successfully and the solids level in each FB was individually controlled. Combustion of coal was concentrated in the middle stage and little coal was allowed to reach the bottom stage. In this way less coal was transported through the pneumatic conveyor and almost none was lost from the cyclone,as was verified from the ash analysis. Thus combustion in the top FB depended on the elutriated coal from the middle FB rather than the circulated coal via the pneumatic liftline. It was also observed that some combustion took place in the liftline and cyclone because of the supplied air used for aeration of the λ value and for lifting the solids.

(3) The weight of elutriated combustibles increased with the gas velocity through the combustor and at gas velocities in excess of $6 \times U_{mf}$, the stainless steel cyclone began to glow indicating inflight combustion of the fines with the excess oxygen in the flue gas.

(4) In spite of the modifications made to the PFBC it was still difficult to maintain all three FBs at temperatures above 600°C and at the same time reduce the amount of combustibles lost from the system.

(5) Circulation of solids was also possible at higher system pressures and the thermal power of the PFBC could be varied from 150 kW(t) at 1.2 bar (abs) to 300 kW(t) at 4 bar (abs).

(6) In a different set of experiments solids circulation was completely stopped and the bottom FB left to cool. The power output of the system was drastically reduced because coal was burning in the middle FB only with a very small portion of the feed coal getting elutriated and burnt in the top FB. The loss of combustibles, estimated from total carbon burnout tests on the ash was remarkably low. Values of 2 to 4 per cent by weight of carbon in the ash were detected. This indicated an overall coal conversion of over 99 per cent.

6.2.7. Sequential action, following the tests on the modified three-FB PFBC

Following the high coal combustion efficiency achieved when the PFBC was operated without solids circulation, it was decided to investigate the non-circulating system closer and report on its performance. The three-FB system combustor could be used under non-solids circulation conditions if a second coal feeder is used to supply coal to the bottom FB (feeding of coal in the top FB was undesirable due to elutriation losses). However, due to the complexity of such a system a two-FB configuration was chosen instead. The distributor of the middle FB was removed changing the three-FB system to a combustor with a deep

bottom FB and the previously used top FB. To improve the efficiency of this system the coal feeder was removed from the middle stage and placed in the bottom stage so that coal could be fed in-bed and particles with less than 1 mm in diameter could also be used as a feed to the PFBC A schematic drawing of the two FB configuration of the PFBC is shown in Figure 6.5. To study the results from the hot trials using a two FB system, a series of tests were also carried out, using a single deep FB. This was achieved by removing both the interstage distributors.

6.3 HOT TRIALS USING THE TWO-FB CONFIGURATION

The aim of these trials was to verify the use of the top FB as a smuts burnout stage and determine its contribution to the overall efficiency of the PFBC. Pressures of up to 7 bar (abs) were used. For consistency of the results most of the experiments were carried out using one type of coal (Appendix 7(B)). A coal with a very high ash content (70 per cent ash, Appendix 7(C)) was also burnt using this configuration. Each experimental run lasted between 2 and 8 days. The two interlocking hoppers were used placed vertically one above the other, to enable the continuous operation of the PFBC. Coal was fed into the bottom deep FB. (Figure 6.5)

Heat was removed from the combustor using mainly air, though steam and water were also used as the coolant for the immersed cooling coils.

Combustion trials using a single deep FB were also carried out in conjunction with these experiments. Comparison of the two systems is included in the following section.

6.3.1. Combustion trials: Observations and their interpretation

(1) Analysing the gas leaving the bottom and top FBs for O_2 and CO_2 and performing an overall heat and mass balance on the system it was possible to determine the heat output of the system, as well as

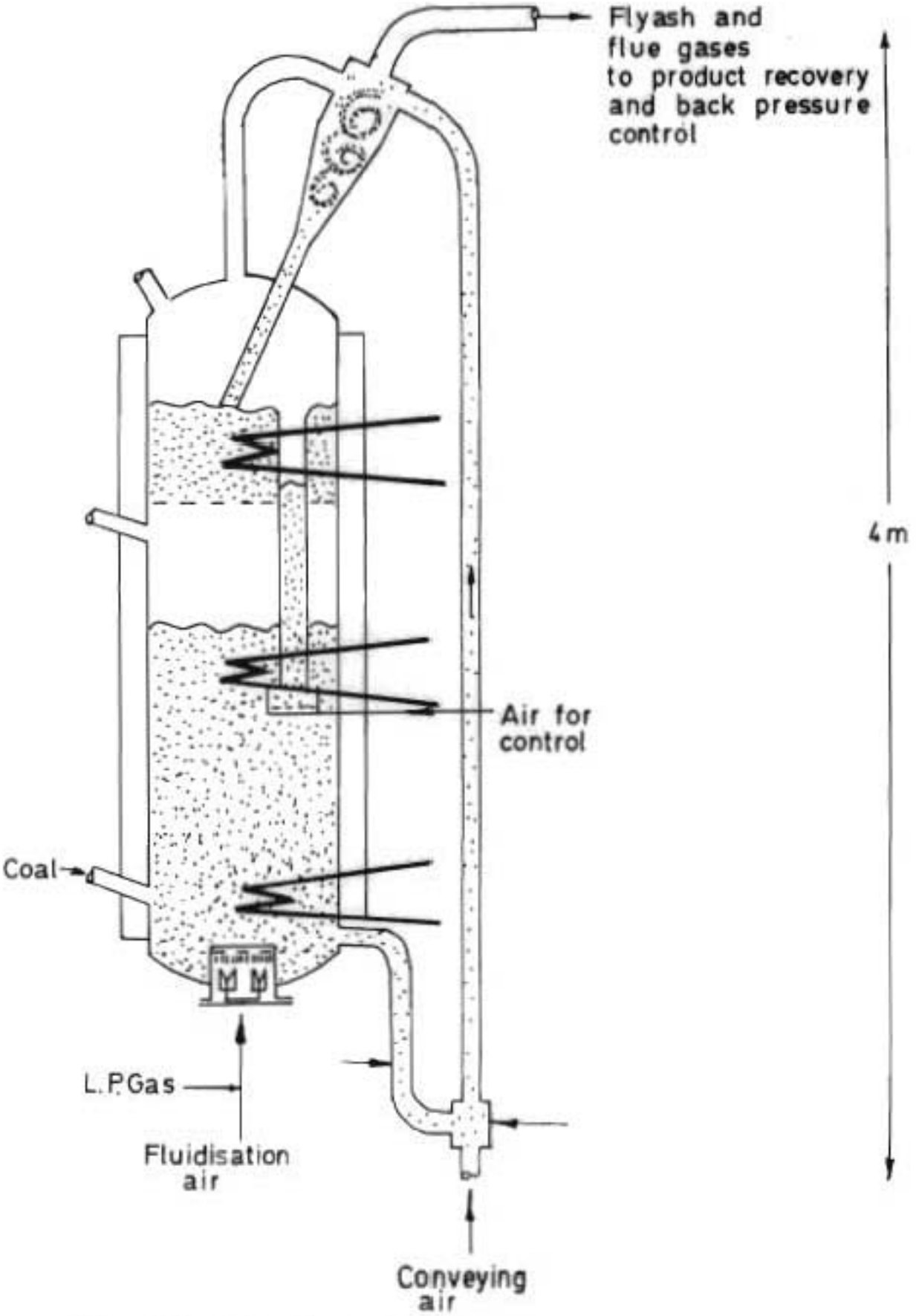

Figure 6.5 : Schematic drawing of the two-FB configuration of the PFBC showing the bottom deep FB and shallow top FB

the heat output of the bottom FB. Some of the results on the heat balance are shown in Figure 6.6. The lower curve shows the output of the bottom bed as the coal feed rate was increased at constant air rate and constant pressure. The top curve shows the total heat generation of the system, and the lenticular region in between the curves shows the contribution made by the top bed. The theoretical results are explained in the following chapter. From Figure 6.6 it may be concluded that:

(a) At low coal feed rates and thus with plenty of excess air, the top bed contributed very little to the combustion process.

(b) As the coal feed rate was increased the elutriated coal increased and with it the contribution of the top FB.

(c) A drop in the contribution of the top bed occurred at higher coal feedrates. This might be due to limitations on the amount of coal carried by the gas stream leaving the bottom FB or the high rate of intense heat released as the stoichiometric conditions are approached.

(2) The range of temperatures and pressures explored and the effect on the relative combustion of the bottom deep bed and the top bed are shown in Figures 6.7 and 6.8. The interaction between the variables is complex; however, the plots served to show that the top bed contributed about 10 per cent to the total combustion with the burnout of smuts and also that the higher the operating pressure the greater the contribution. This was probably related to the increased elutriation rate, or the coal loading of the gas stream, as pressure went up as well as other factors.

For the top bed to sustain combustion the temperature had to be above a certain minimum temperature, which in the case of the various coals we have looked at can be seen from Figure 6.7 to be about 580^{o}C. This temperature was probably related to the auto-ignition temperature of the devolatilised smuts which were elutriated into the top bed. The rate of combustion in the top bed was dependent on both temperature and

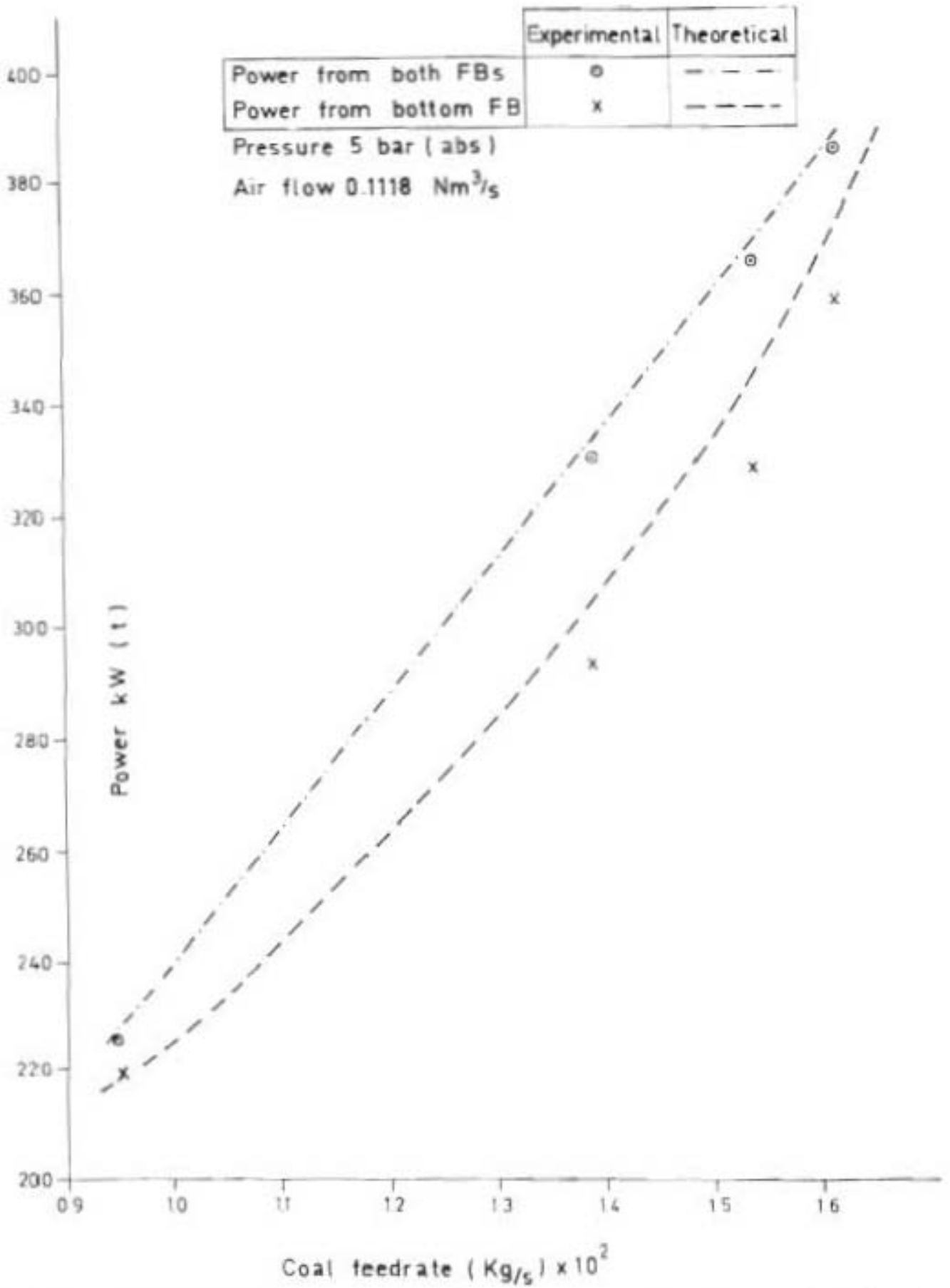

Figure 6.6. Thermal power of the two-FB PFBC at a constant pressure and fluidizing gas velocity. The experimental results were obtained from a simple mass balance on the coal supplied to the reactor. The theoretical results were calculated using the FBC computer programme.

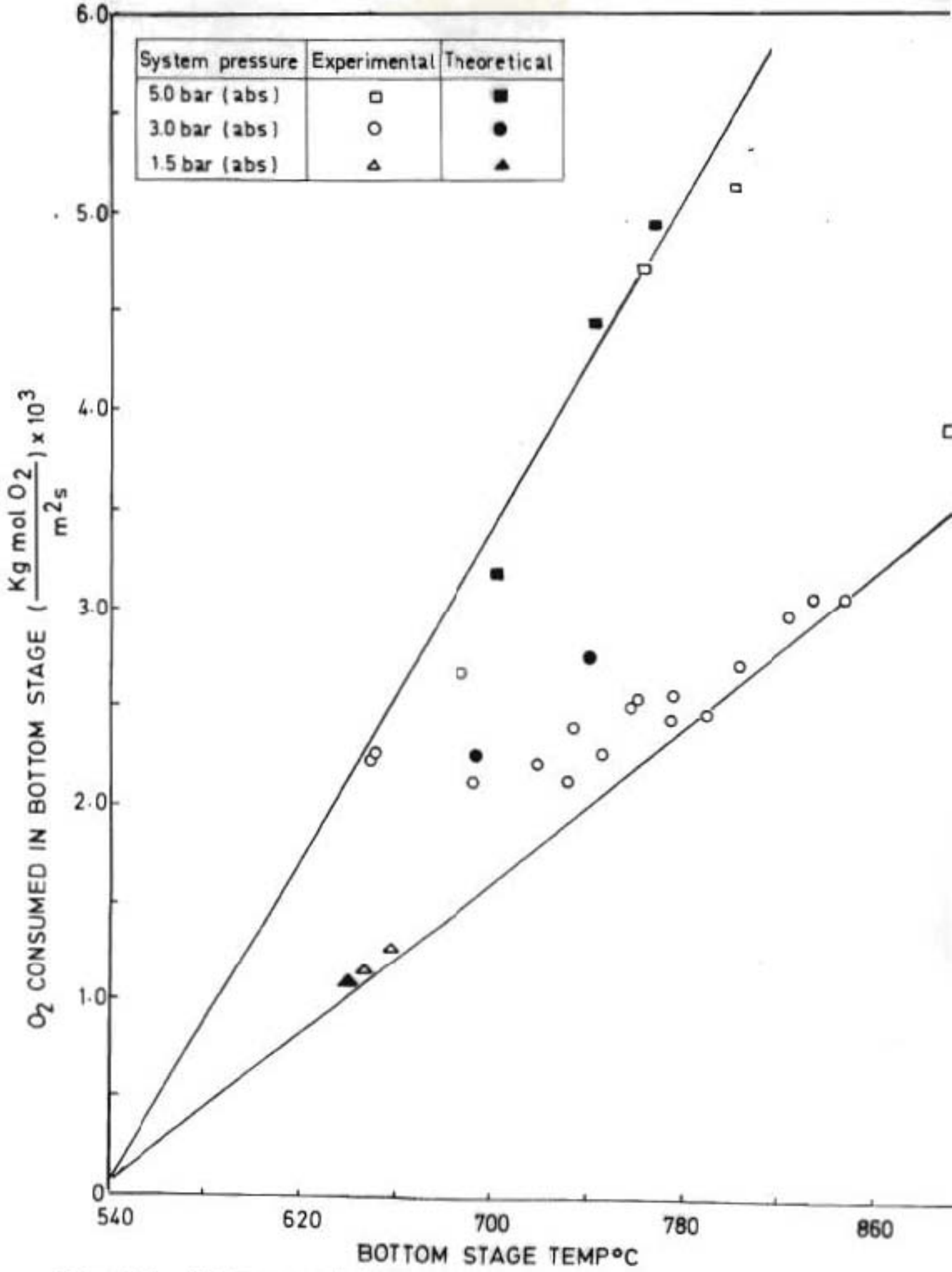

Figure 6.7. Oxygen consumed in the bottom FB determined experimentally and its dependance on the bottom FB temperature for different PFBC pressures. The theoretical points were obtained using the computer programme applied to the two-FB reactor

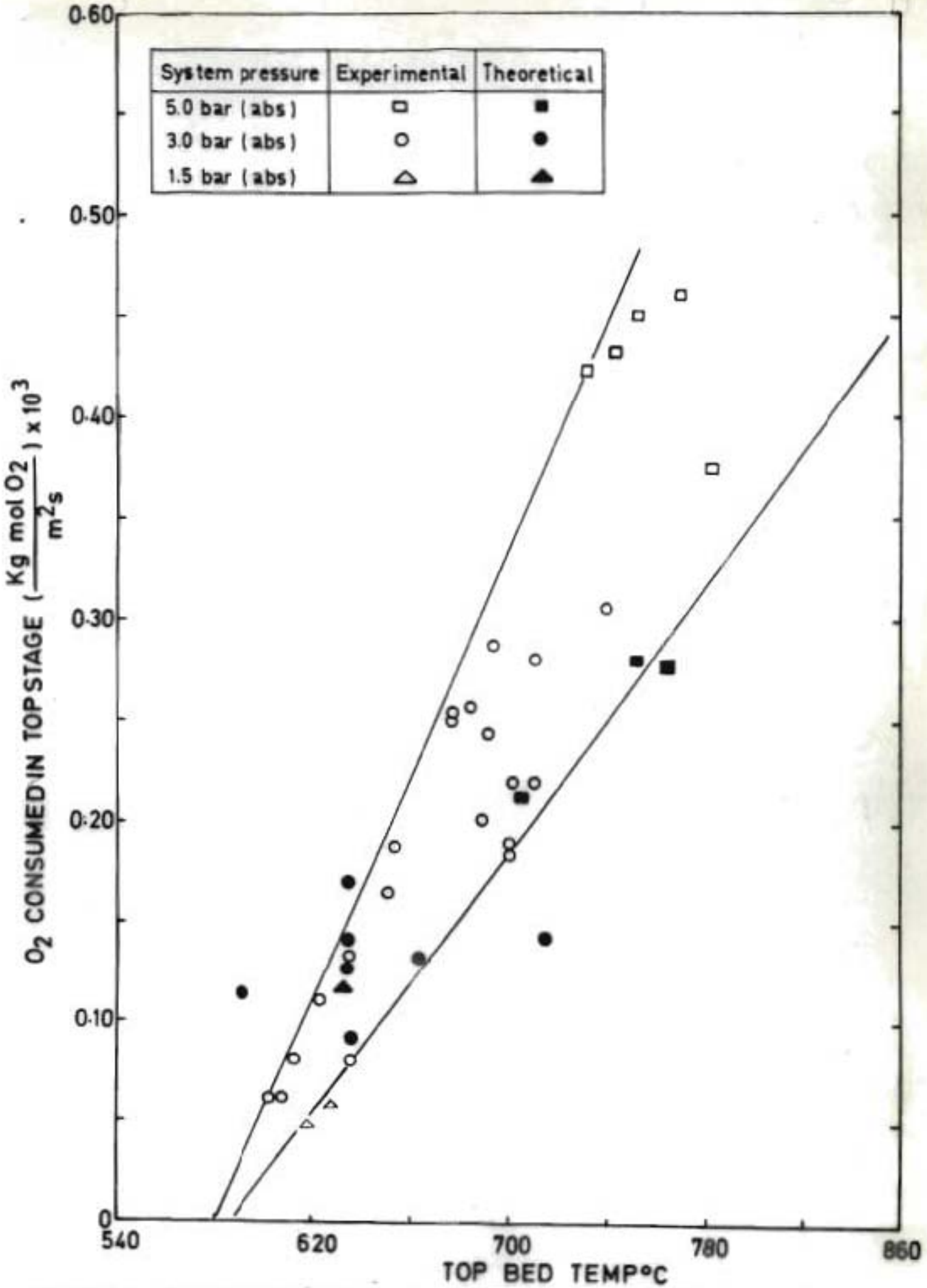

Figure 6.8. Oxygen consumed in the top FB determined experimentally and its dependance on the top FB temperature for different PFBC pressures. The theoretical points were determined using the computer programme applied to the two-FB reactor.

pressure and if one assumed that the rate was proportional to the pressure, and had a simple power-dependence on temperature (Figure 6.9) all the data for a reactor pressure equal to 3 bar(abs) could be roughly collapsed on to a single curve through the empirical transformation

$$R_{O_2} = R'_{O_2} \times \frac{51}{(T-580)^{0,88}} \times \frac{3}{p} \qquad E.6.1$$

where R'_{O_2} is the rate of combustion expressed as kg mol oxygen consumed per sec per m^2 bed area, p is the combustor pressure in bar (abs) and T is the bed temperature in ^{o}C.

The data for the top bed from Figure 6.8 was plotted with this normalisation on to Figure 6.10 as a function of the oxygen content of the gases leaving the bottom bed. The resultant curve shows a distinct maximum at around 7,5 per cent oxygen in the gases leaving the bottom bed. One would expect this shape heuristically - at low oxygen concentration from the bottom bed there is not enough oxygen for combustion in the top bed - a high oxygen concentration from the bottom bed would imply that combustion in the bottom bed is essentially complete, or alternatively that the coal hold up and hence entrainment rate from the bottom bed is small.

In any event, whatever the detailed mechanism might be, the top bed was most effective at an oxygen input concentration of about 7,5 per cent. This figure corresponded to about 30 to 40 per cent excess air to the bottom bed. One would not normally operate at an excess air level much greater than this, and what we are in effect saying is that our top bed was fortunately most efficient at the normal sort of excess air rate used in FB combustion.

(3) The tests using high ash coal (Appendix 7(c)) showed that the PF

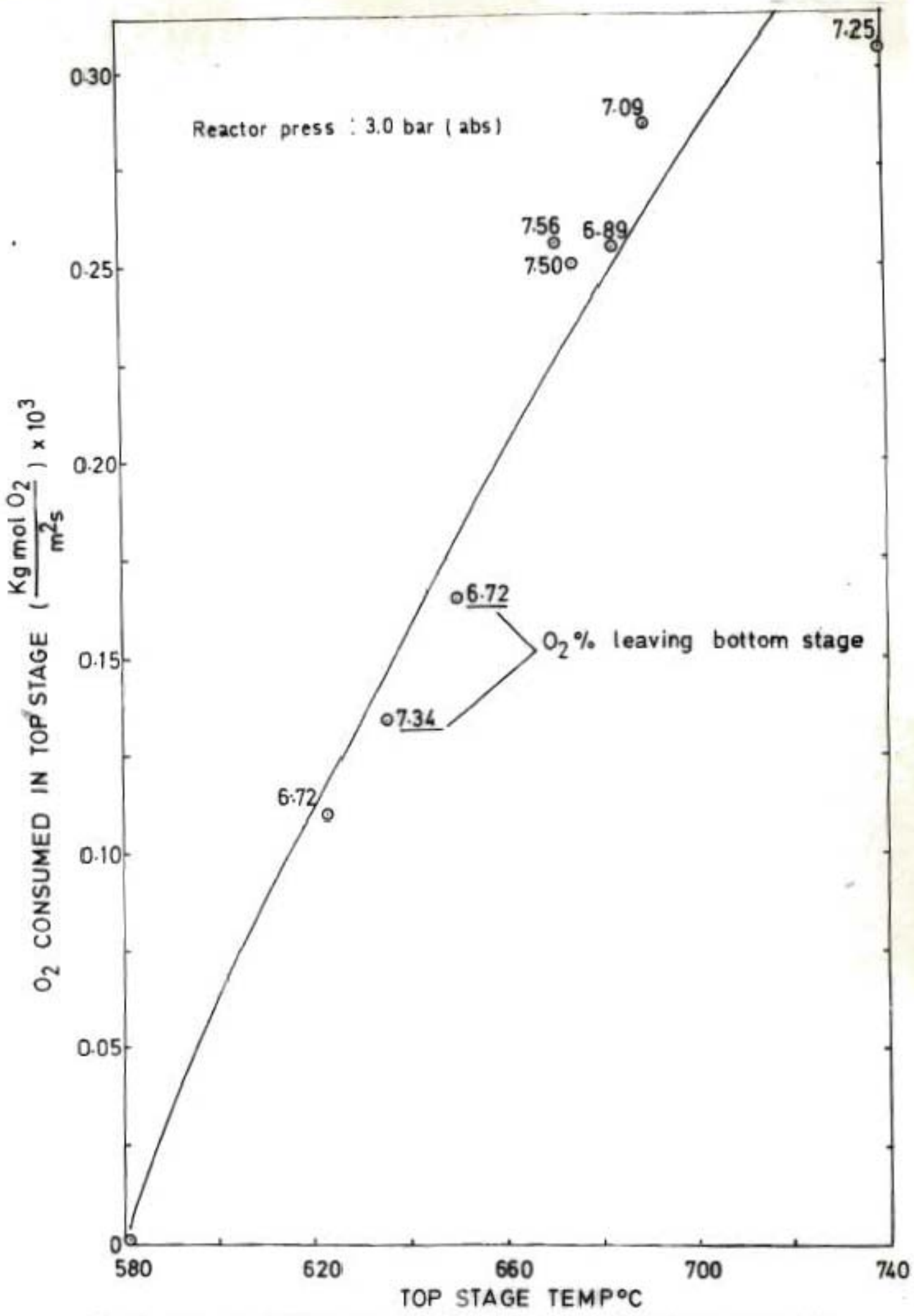

Figure 6.9. Oxygen consumed in the top FB and its relation to the top FB temperature for a constant oxygen concentration entering the top FB

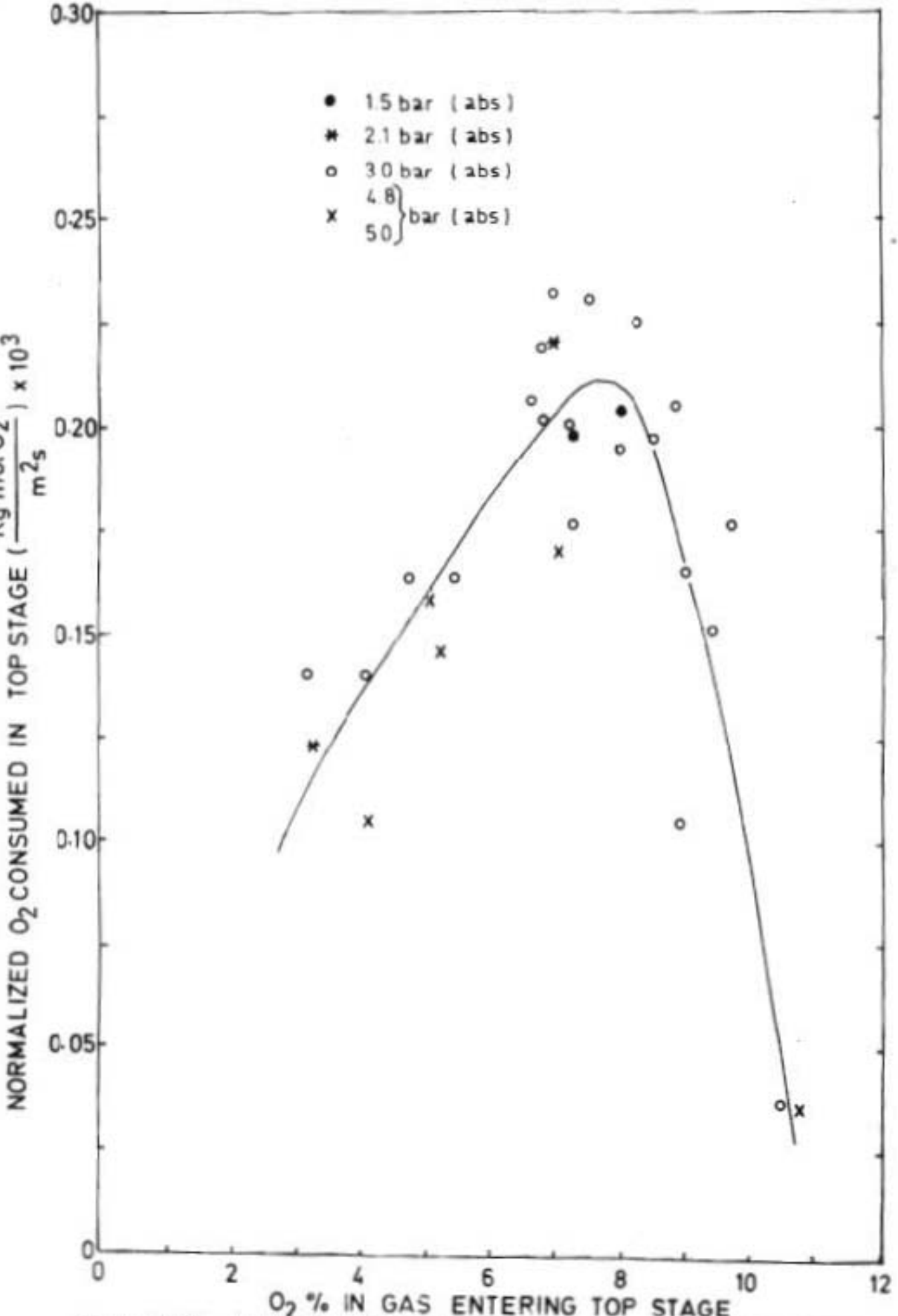

Figure 6.10. Oxygen combustion rate in the top FB normalized for temperature and pressure and its relation to the percentage of oxygen in the gas entering the top FB

could be operated successfully with coal of very low colorific value (8,5 MJ/kg). The overall coal conversion, however, was reduced due to the high volume of coal required to sustain combustion in the FB and the fineness of the coal particles in the feed. From fly ash analysis the overall coal conversion was always below 90 per cent.

(4) Comparing the performance of the single and two-FB system, operated under similar conditions it may be concluded that :

(a) Overall combustion with the two-FB system was never below 98 per cent while the coal combustion in the single FB was below 96 per cent (efficiency based on total carbon in feed and exhaust gas).

(b) A higher carbon content in the elutriated fines from the single FB combustor was observed in the large particle sizes as shown in the fly ash analysis in Table 6.1. With the two-FB configuration the carbon distribution amongst the particles of fly ash was almost independent of particle size as shown in the same Table. The top bed was therefore most effective in burning up the carbon in the larger fly ash particles.

The full report on the combustion tests using the two FB system can be found in Reference 58.

Summarizing the experimental work, cold trials and a series of combustion experiments lasting for up to eight days were carried out on the PFBC. The combustor was successfully operated with three FBs and subsequently by the removal of one or both interstage distributors as a two- and a one-FB combustor respectively. These experiments have shown that the two-FB combustor offered the best solution to the problem of combustibles lost in the flue gas by using the shallow top FB as a smuts burnout cell. It was also shown that circulation of solids was not required if this type of combustor configuration was chosen. However, an important use of these results was to test the mathematical model, derived specifically for this type of combustor, and its ability to

TABLE 6.1

Sizing and carbon content of ash leaving with the combustor off-gas from the two-FB PFBC

Ash particle size micron (Note 1)	Reactor configuration					
	One-FB system			Two-FB system		
	Mass % in size fraction	Analysis carbon % in size fraction	Total carbon % in ash sample	Mass % in size fraction	Analysis carbon % in size fraction	Total carbon % in ash sample
+ 39	1,6	12,9		4,8	2,4	
- 39 + 20	1,1	9,5		4,4	3,9	
- 30 + 21	3,5	5,8	9,9	7,2	3,9	3,8
- 21 + 15	8,4	4,9		9,2	3,2	
- 15 + 12	8,6	6,5		8,2	3,0	
- 12 (Cal.)	76,8	11,0		66,2	4,1	
TOTAL	100,0			100,0		

Note 1. Sizing analyses were carried out using a Warman Cyclosizer. Particle sizes refer to Quartz equivalent diameter. Low density (high carbon) particles report to a much finer size fraction than their true diameter (approx. one half diameter).

predict the performance of combustors with similar features. A comparison between the experimental and theoretical results for the two-FB configuration is presented in the following chapter. The use of the mathematical model for the prediction of the heat transfer to the cooling coils is also included in the same chapter.

CHAPTER SEVEN

APPLICATION OF THE THEORETICAL MODEL FOR COMBUSTION OF COAL IN A TWO-FB PFBC. COMPARISON BETWEEN EXPERIMENTAL AND THEORETICAL RESULTS FOR THE COMBUSTION OF COAL IN THE TWO-FB COMBUSTOR AND FOR THE HEAT TRANSFER TO THE COOLING COILS

7.1 APPLICATION OF THE THEORETICAL MODEL FOR COMBUSTION OF COAL IN THE TWO-FB COMBUSTOR

The derivation of the mathematical model for coal combustion in a non-circulating two-FB combustor was presented in Section 4.2. In this Chapter the mathematical model was considered again and some simplifications were made to it based on our research finding and on other investigators.

The computational procedure described in Section 4.2.4 was applied to the two-FB system in which coal combustion follows the shrinking core model. Experiments on batch combustion of coal in a small FB (Section 4.1.3) showed that, coal can be treated as char and the presence of volatiles in the coal can be neglected if the time for evolution and combustion of the volatiles is much shorter than the burnout time of the average size coal particle. The rates of particle shrinkage obtained experimentally, as coal burns in the presence of solids, were between 2×10^{-6} and 5×10^{-6} m/s depending on conditions and the type of coal introduced in the small FB. Figure A.4.2 shows the shrinkage rate for two different quantities of coal of radius R = 0,0034m burnt in the small FB. Though the same type of coal and size distribution was used, two different curves were obtained. This may be attributed to the dependance of the shrinkage rate of the particles on the concentration of oxygen in the FB which is determined by the FB coal loading.
A theoretical expression of the particle shrinkage rate and its relation to parameters like concentration of oxygen in the vicinity of the coal particle and temperature was developed by Stanmore and

Junk[59]. They experimented on brown coal char using a small FB assuming gas diffusion through the pores of the char. Their expression for the particle shrinkage rate is given below:

$$\frac{dR}{dt} = -2635 \frac{\varepsilon_c}{\rho_a} (k_y C)^{\frac{1}{2}} (T + 273)^{\frac{1}{2}} \quad (mm/s) \qquad E.7.1$$

where ε_c is the char voidage

ρ_a the char apparent density (g/mm^3)

C is the oxygen concentration in the vicinity of the burning particle [mol/mm^3]

T is the temperature of the particle (^oC), and

k_y is the intrinsic rate constant for combustion ($mol/mm^2 s$) and is given by $k_y = 0{,}0112 \exp(-16400/T)$

E.7.1 was adapted and used in our computational model in place of E.4.7 to predict the shrinkage rate of coal particles in the emulsion and cloud wake phases. The two different concentrations of oxygen in the emulsion and cloud wake phase were used in place of C in E.7.1. It is clear from this equation that the particle shrinkage rate is independent of the particle radius. Therefore, the function $\phi_2(R,C,T)$ of E.4.7 which is explicitly given by E.7.1 is no longer dependent on R. If E.7.1 is substituted in E.4.8 then this equation can be integrated to give $\phi_3(C,T)$ which denotes the shrinkage rate of coal particles in the FB. This presupposes the integration of the second term of E.4.8 over the total height of solids in the FB. To achieve this the mean oxygen concentration in the cloud wake phase was assumed. In the computer program, this mean oxygen concentration was calculated from an overall mass balance and its numerical value altered at the end of each iteration until convergence.

The elutriation constant k_e was arbitrarily assumed to be proportional to the superficial gas velocity through the FB and inversely proportional to the radius of the burning particles, i.e.

$$k_e = \frac{1}{c_1}\frac{U}{R} \qquad \text{E.7.2}$$

where $1/c_1$ is the proportionality constant with c_1 having a value of $10^5 < c_1 < 10^7$ (as obtained from Reference 49).

Introducing the special forms of ϕ_3 and k_e in E.4.18 this equation becomes

$$W_{PB} = \frac{-F_o}{\phi_3} \int_{R=R_{t=\infty}}^{R=R_o} \int_{R_o=R}^{R_o=R_M} P_o(R_o)\left(\frac{R_o}{R}\right)^{c_2-3} dR_o\,dR \qquad \text{E.7.3}$$

where $c_2 = \dfrac{U_o}{\phi_3 c_1}$

Similarly E.4.17 becomes

$$P_B(R) = \frac{-F_o}{W_{pB}\phi_3} \int_{R_o=R}^{R_o=R_M} P_o(R_o)\left(\frac{R_o}{R}\right)^{c_2-3} dR_o\,dR \qquad \text{E.7.4}$$

If FUNC2(R) (a term used in the computer program) is defined as:

$$\text{FUNC2}(R) = \int_{R_o=R}^{R_o=R_M} P_o(R_o)\left(\frac{R_o}{R}\right)^{c_2-3} dR_o \qquad \text{E.7.5}$$

Substitution of E.7.5 into E.7.4 gives

$$P_B(R) = \frac{-F_o}{w_{PB}\phi_3} \text{FUNC2}(R) \qquad \text{E.7.6}$$

From E.4.11 and E.7.6 the rate of elutriated coal (F_1) and its size distribution ($P_1(R)$) can be expressed as follows.

$$F_1 = \frac{-F_o U_o}{c_1 \phi_3} \int_{R=R_1}^{R=R_M} \frac{\text{FUNC2}(R)}{R} \, dR \qquad \text{E.7.7}$$

$$\text{and} \quad P_1(R) = \frac{-F_o U_o}{F_1 c_1 \phi_3} \frac{\text{FUNC2}(R)}{R} \qquad \text{E.7.8}$$

If it is assumed that all carbon burns to carbon dioxide and there are only traces of carbon monoxide then the gas consumption rate $\phi_4(R,C)$ (kg mol/s) can be written in terms of the reaction for a single particle burning in the cloud wake phase or emulsion phase, as follows:

$$\phi_4(R,C_c) = c_3 \frac{4\pi R^2 \rho}{M_c} \phi_2(C_c) \qquad \text{E.7.9}$$

$$\text{and } \phi_4(R,C_E) = c_3 \frac{4\pi R^2 \rho}{M_c} \phi_2(C_E) \qquad \text{E.7.10}$$

where M_c is the molecular weight of carbon

c_3 is the fraction of fixed carbon in the coal

If $B_2 = \frac{1-\epsilon_B(1+f_w)}{1-\epsilon_B} = \frac{B_1}{1-\epsilon_B}$

$B_3 = \frac{\epsilon_B f_w}{1-\epsilon_B}$

and if PBOR (a term used in the computer program) is defined as

$$PBOR = \int_R^{\infty} \frac{P_B(R)}{R} = \frac{-F_o}{\phi_3 W_{PB}} \int_R^{\infty} \frac{FUNC2(R)}{R} \qquad E.7.11$$

Substituting E.7.9 and E.7.11 into E.4.38 it becomes

$$-f_w c_{mf} u_B \frac{dC_C}{dh} = k_{CE}(C_C - C_E) + k_{BC}(C_C - C_B) + \frac{3c_3 B_3 W_{PB} \phi^2}{AHc_B M_c} PBOR \qquad E.7.12$$

The boundary conditions given by E.4.40 and E.4.41, are also simplified as follows:

At height h = H (with gas recirculation)

$$AUC_o - \frac{AU}{1+f_w c_{mf}} C_{BH} - \frac{AUf_w c_{mf}}{1+f_w c_{mf}} C_{CH} = (B_3+B_2)\left(\frac{3c_3 W_{PB}\phi^2}{M_c} PBOR\right) \qquad E.7.13$$

and at height h = H (without gas recirculation)

$$AUC_o - U_{gE}AC_E - U_{gB}AC_{BH} - U_{gC}AC_{CH} = (B_3+B_2)\left(\frac{3c_3 W_{PB}\phi^2}{M_c} PBOR\right) \qquad E.7.14$$

In this Section 7.1 the mathematical model derived in Section 4.2 has been simplified on the basis of our experimental observations and using an equation for the coal particle skrinkage rate derived by Stanmore and Junk[59]. Although different shrinkage rate expressions

have been tried, the good agreement between the theoretical and experimental results, as is shown in this Chapter 7, is the reason for the adoption of the shrinkage rate equation given by Stanmore and Junk.

In the following section a comparison is made between the experimental results which are listed in Table 7.1 and the theoretical results obtained from the computer programme applied on the two-FB PFBC.

7.1.1. Comparison between theoretical and experimental results

The procedure, used to recall and execute the mathematical model on the computer, and a printout of this programme are included in Appendix 9.

The computer programme was executed a number of times and the theoretical results were compared with the ones obtained experimentally. The experimental runs were simulated on the computer by using the correct data which corresponded to a particular set of experimental conditions. The complete list of input variables required for the execution of the computer programme is presented in Appendix 9. Table 7.2 shows a list of a number of theoretical computer runs which include both the input data taken from the experimental runs and the results obtained from the theoretical model.

In this section the theoretical results generated from the mathematical model of the two-FB PFBC are compared with the experimental results. Some of these experimental results have already been presented in graphical form in Chapter 6. However, to achieve a better comparison between theory and experiment and avoid the presentation of the same experimental results in both the previous and current chapter, some of the theoretical results have already been plotted with the experimental

TABLE 7.1.

A list of experimental results obtained from the tests on the two-FB PFBC

Experimental results averaged	PFBC pressure bar(abs)	Bottom FB temp. t°C	Top FB temp. t°C	Coal feedrate (kg/s)x10^3	Air feedrate (Nm^3/s)x10^2	Oxygen percentage		Oxygen burn rate		Combustibles in ash	Power (t)	
						Bottom FB	Top FB	Bottom FB (kgmol/s)x10^3	Top FB (kgmol/s)x10^5	wt %	Bottom FB kW	Total kW
1	1,50	644	628	3,62	3,28	8,19	7,16	0,188	10	5	79,6	83,8
1	1,50	656	618	3,75	3,28	7,25	6,72	0,201	8	5	86,1	88,5
1	2,10	783	690	5,62	4,39	6,78	5,21	0,279	31	3	118,2	131,3
1	2,10	816	698	5,59	4,39	3,34	2,41	0,346	18	3	146,6	154,2
8	3,00	745 ±55	667 89	7,99 ±1,13	6,60 ±0,23	7,16 ±1,7	3,06 ±1,36	0,408 ±0,049	31 ±12	3 ± 1	172,8 ±20,7	185,8 ±5,58
1	4,80	894	741	15,55	11,08	5,06	3,63	0,788	71	3	333,8	363,8
1	4,80	891	731	13,02	11,03	7,57	6,56	0,644	70	3	272,8	302,4
1	5,00	701	708	9,90	11,18	10,61	10,31	0,518	15	3	219,4	225,8
1	5,00	730	753	13,91	11,18	7,17	5,69	0,690	74	3	292,3	323,6
1	5,00	759	769	15,38	11,18	5,49	3,97	0,773	76	3	327,4	359,6
1	5,00	796	784	16,30	11,18	4,17	2,97	0,840	60	3	355,8	381,2

TABLE 7.2

A list of theoretical computer runs for the two-FB PFBC showing the input data taken from experimental runs and the obtained theoretical results. These results were used for comparison purposes between theory and experiment

Run no.	PFBC* pressure bar (abs)	Bottom* FB temp. T°C	Top FB* temp. T°C	Coal feedrate* (kg/s)x10^3	Air flowrate* (Nm^3/s)x10^2	Constant in (E.7.2), C_1	Intrinsic Rate constant k_y (E.7.1) (mol/min^{2}s)x10^9 Bottom FB	Top FB	Oxygen percentage Bottom FB	Top FB	Oxygen burn rate Bottom FB (kg mol/s)x10^3	Top FB (kg mol/s)x10^6
22A	1,5	644	628	3,62	3,28	0,5x10^7**	0,1915	0,1394	7,12	7,06	0,2015	0,8980
22	1,5	644	628	3,62	3,28	0,1x10^7**	0,1915	0,1394	7,34	7,07	0,1984	3,862
23	1,5	644	628	3,62	3,28	0,5x10^6**	0,1915	0,1394	7,59	7,11	0,1947	7,033
21	1,5	644	628	3,62	3,28	0,1x10^6	0,1915	0,1394	9,06	7,60	0,1731	21,360
20C	1,5	644	628	3,62	3,28	0,1x10^6	0,7660 **	0,5576**	8,23	7,27	0,1853	14,058
21	1,5	644	628	3,62	3,28	0,1x10^6	0,1915	0,1394	9,06	7,60	0,1731	21,379
21C	1,5	644	628	3,62	3,28	0,1x10^6	0,0213 **	0,0155**	11,02	9,15	0,1443	27,452
20	1,5	644	628	3,62	3,28	0,1x10^5	0,0077 **	0,0056**	12,07	10,24	0,1290	26,882
19B	1,5	644	628	3,62	3,28	0,1x10^5	0,0039 **	0,0028**	12,74	11,03	0,1191	25,093
29C	3,0	690	628	7,99	6,68	0,1x10^5	0,4499	0,1394	7,18	6,22	0,4086	28,670
29A	3,0	745	628	7,99	6,63	0,1x10^6	1,129	0,1394	6,78	6,12	0,4207	19,711
29B	3,0	780	628	7,99	6,68	0,1x10^5	1,929	0,1394	6,57	6,07	0,4268	15,118
29	3,0	690	628	6,86	6,45	0,1x10^6	0,4499	0,1394	8,61	7,80	0,3534	23,477
24	3,0	745	580	7,99	6,68	0,1x10^5	1,129	0,0500	6,78	6,17	0,4207	18,081
25	3,0	745	667	7,99	6,68	0,1x10^5	1,129	0,2966	6,78	6,07	0,4207	21,122
26	3,0	745	590	7,99	6,68	0,1x10^6	1,129	0,7526	6,78	6,03	0,4207	22,431
31B	5,0	701	708	9,90	11,18	0,8x10^7	0,5453	0,6150	10,52	9,86	0,5171	33,308
30B	5,0	730	753	13,91	11,18	0,8x10^7	0,8873	0,1280	6,32	5,39	0,7271	46,294
32B	5,0	759	769	15,38	11,18	0,8x10^7	1,405	1,636	4,65	3,75	0,8103	45,223

* Data taken from the experimental runs used as input data for the theoretical model

**Values of the intrinsic rate constant k_y and constant c_1 selected to show the effect of these parameters on the oxygen burning rate

Table 7.2 (continued)

(Oxygen consumption rate)/m^2		Power (thermal)		Coal in FB	
Bottom FB (kg mol/m^2s)x10^3	Top FB (kg mol/m^2s)x10^3	Bottom FB kW	Top FB kW	Bottom FB kg	Top FB kg
1,227	0,00547	85,4	0,4	0,33	0,0021
1,208	0,0235	84,0	1,6	0,32	0,094
1,185	0,0428	82,5	3,0	0,31	0,017
1,054	0,1301	73,3	9,1	0,25	0,057
1,128	0,0856	78,5	5,9	0,14	0,018
1,054	0,130	73,3	9,1	0,25	0,057
0,879	0,167	61,1	11,6	0,52	0,23
0,785	0,163	54,6	11,4	0,67	0,38
0,726	0,153	50,5	10,6	0,78	0,50
2,489	0,175	173,1	12,1	0,29	0,058
2,562	0,120	178,2	8,3	0,19	0,040
2,599	0,0921	180,8	6,4	0,14	0,030
2,152	0,143	149,7	9,94	0,24	0,042
2,562	0,110	178,2	7,7	0,19	0,060
2,562	0,128	178,2	8,9	0,19	0,028
2,562	0,138	178,2	9,5	0,19	0,018
3,149	0,203	219,0	14,1	0,22	0,017
4,428	0,282	308,0	19,6	0,29	0,023
4,935	0,275	343,3	19,1	0,28	0,023

results in the same figures already presented in Chapter 6.

A comparison of theory and experiment with some reference to the figures in the previous chapter follows below:

(a) The overall thermal power of the two-FB PFBC for various reactor pressures determined both theoretically and experimentally is shown in Figure 7.1. From this figure, the power of the combustor increases with pressure and the range of thermal power at any given pressure increases as the system pressure increases. The theoretical and experimental results show the same behaviour and they are in a very good agreement.

(b) Figure 6.6 shows the contribution of the top FB as a smuts burnout cell. Using the same reactor pressure and superficial air velocity the thermal power generated in the bottom deep-FB and top FB increases with increasing coal feedrate. The top FB, as it has already been explained in Section 6.3.1, contributes the most to the burnout of smuts, at intermediate coal feedrates and at excess oxygen levels of between 30 and 40 per cent. The theoretical results predict the same behaviour for the top FB and are in agreement with the experimental results.

(c) The theoretical and experimental results for the oxygen consumption rate and its relation to temperature for the bottom and top FB are shown in Figure 6.7 and 6.8 respectively. The oxygen consumption rate increases with bed temperature and combustor pressure and, as previously, the theoretical and experimental results are in good agreement. The theoretical results show a relatively higher oxygen consumption in the bottom FB which seems to be compensated by a relatively lower consumption rate in the top FB.

(d) The effect of the arithmetic value of the proportionality factor $(1/c_1)$, taken from the equation of the elutriation constant (k_e), (A. 7 .2), on the oxygen consumption rate for the bottom deep FB and

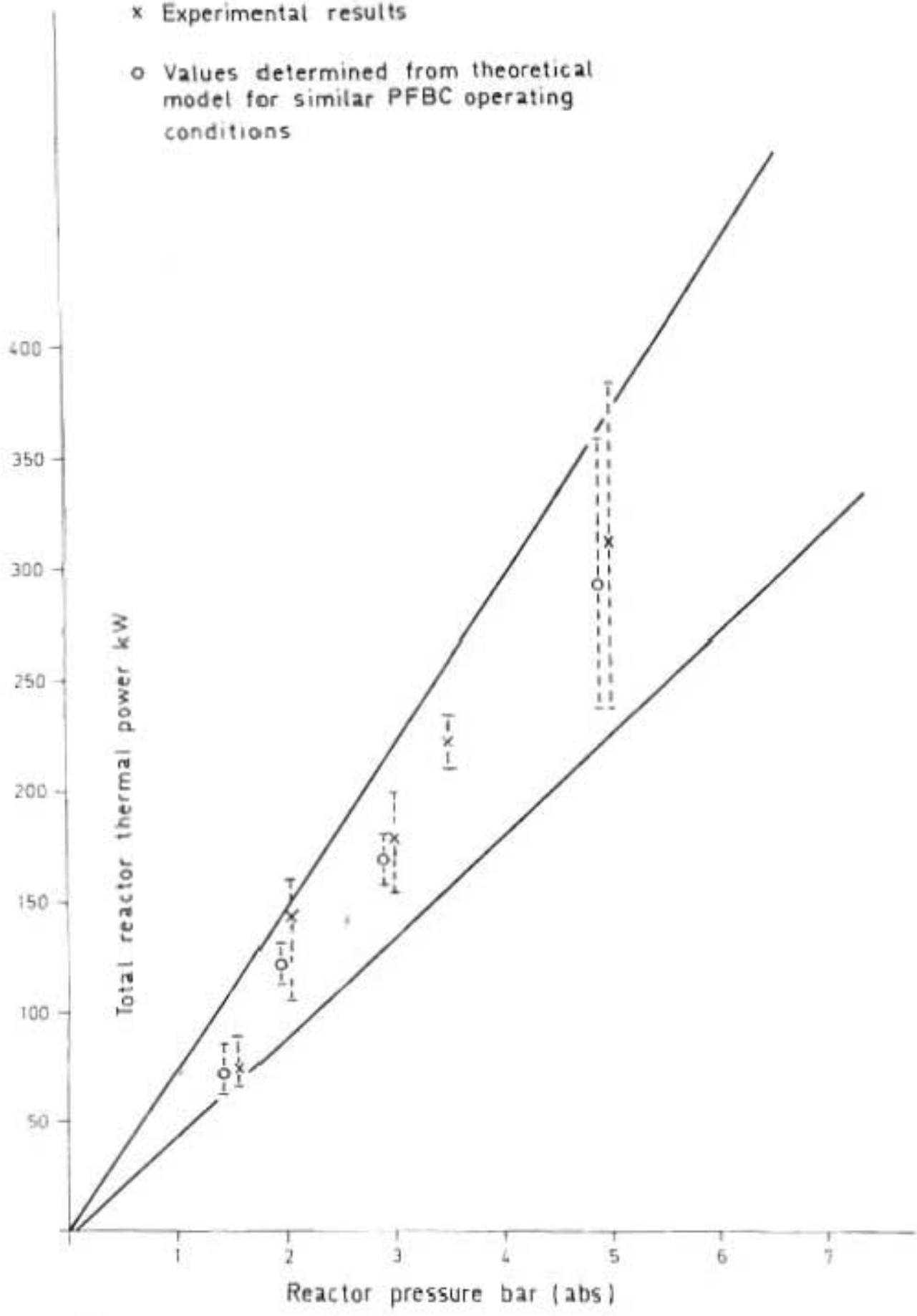

Figure 7.I. Thermal power of the PFBC determined experimentally and plotted with the corresponding computer calculated value against the absolute reactor pressure.

top FB is shown in Figure 7.2. From this figure, as the proportionality constant ($1/c_1$) increases, the contribution of the top FB increases by burning the elutriated smuts. At the same time the oxygen consumption rate in the bottom FB decreases as it can be expected. In the same Figure 7.2, the percentage of carbon burnt in the PFBC, based on the inlet carbon feed was plotted against the proportionality constant ($1/c_1$). This figure shows that although the carbon burnt in the top FB increases with ($1/c_1$) the overall percentage of carbon burnt in the PFBC decreases with increasing ($1/c_1$). From chapter 6 acceptable values of c_1 lie in the region of $10^5 < c_1 < 10^7$. The value of c_1 chosen for our mathematical model was $c_1 = 1 \times 10^5$ (Figure 7.2).

(e) The oxygen consumption rate was finally plotted against different values of the intrinsic rate constant k_y as shown in Figure 7.3. The value of k_y for the bottom and top FB was calculated using the equation for k_y (E. 7 .1). To see the effect of k_y on the oxygen consumption rate, multiples of the calculated k_y value were used,(Table 7.2 Run nos 20c, 21, 21c, 20, 19B),$0,10k_y < k_y < 10\ k_y$. Figure 7.3 shows that the oxygen consumption rate increases with increasing values of k_y while the oxygen consumption rate for the top FB reaches a maximum and then decreases. This shows that if different proportionality constants were used in the equation for the expression of k_y, the two FBswould behave differently.

To conclude, in this section the theoretical results derived from the application of the mathematical model were compared with the experimental results. The good agreement between the results showed that the mathematical model can sucessfully predict the performance of our PFBC. This model was put onto the computer and is presented in a form that can be easily used to predict the behaviour of other FBCs which are used in similar operations.

A mathematical model was also written to predict the heat transfer

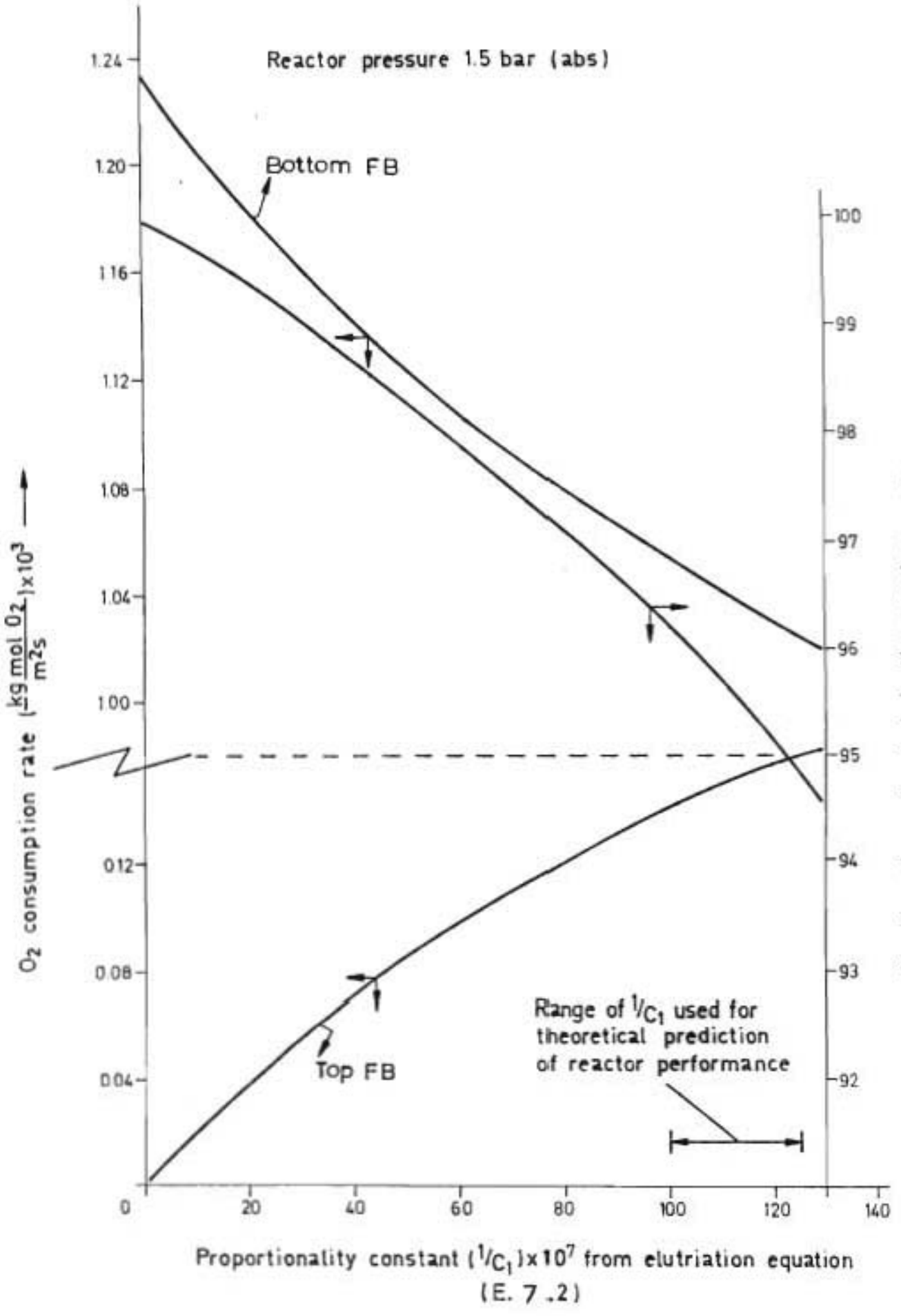

Figure 7.2. Theoretical relation of the oxygen consumption rate for the top and bottom FB and the proportionality constant taken from the elutriation equation (E. 7 .2.). Also showing the corresponding percentage of coal burnt in the PFBC.

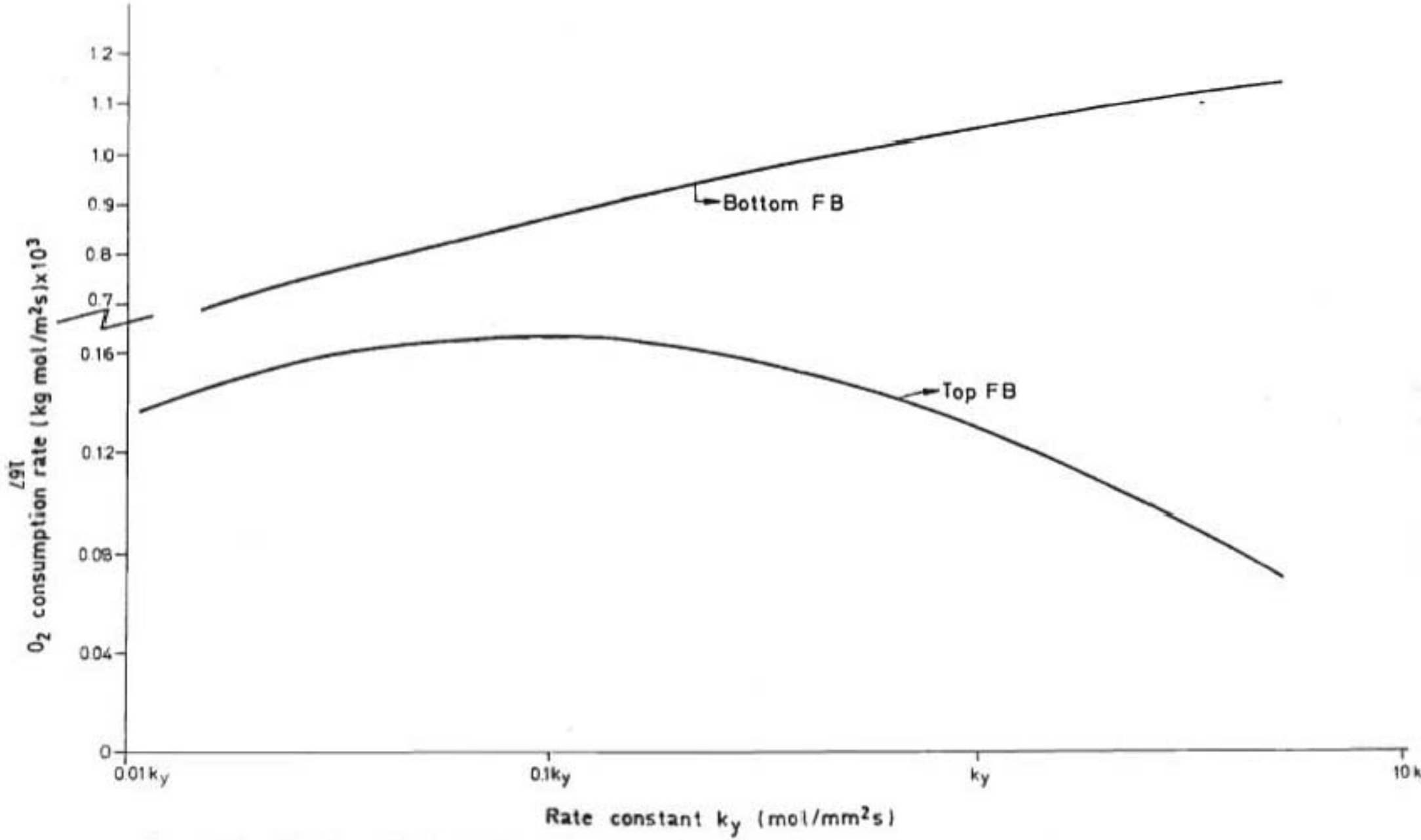

Figure 7.3. The theoretical relation of oxygen consumption rate and the coal particle rate constant k_y given in (E. 7.1.) obtained from the computer programme when applied to the two-FB configuration.

to the cooling coils. As it was done in this section,a comparison between the experimental and theoretical results for the cooling coils was also carried out and the results are presented in the following section.

7.2. HEAT TRANSFER TO THE COOLING COILS IN AN FB

As it was not the intention of this investigation to utilize the heat generated in the PFBC, the coolant leaving the cooling coils of the PFBC was immediately cooled in the heat exchanger and the exhaust gases were cooled by radiation through the long exhaust line before reaching the pressure control valve and wet scrubber. The heat transfer to the cooling coils was calculated by measuring the fluid flow through the horizontal and vertical coils and the inlet and outlet temperatures of the coils. A mathematical model was written which calculates the heat transferred to the cooling coils from the FB, due to both convection and radiation. This model is presented in Appendix 10. Water, steam or air may be used as the coolant. The model is based on a stepwise heat and mass balance along the length of the cooling coils. In order to improve the accuracy of the results which can be achieved by increasing the number of steps or elements, the departmental computer was used for the execution of the mathematical model. A flowchart of the computational procedure is included in Appendix 10 along with the list of the input data.

Initially, the programme computes the effective emissivity, $\varepsilon\varepsilon_s$ of silica sand (E.A.10.7) and that of the cooling coils $\varepsilon\varepsilon_t$ (E.A.10.8) and then, based on the inlet conditions to the cooling coils, it estimates the outlet temperature and wall temperature of the coil for an element of coil of length ($d\ell$). Depending on the coolant used, the heat transferred to the element is calculated and the outlet and wall

temperatures for the next element of coil are estimated. As successive elements of the coil are considered the difference between the inlet and outlet temperature of the coolant becomes smaller. If the difference between successive outlet temperatures is greater than a set value the computation continues. Otherwise the calculating procedure is interrupted. If the total length of the coil has been considered then the programme is terminated, otherwise the calculated heat flux to the element is compared with another set value. If the calculated flux is smaller than the set value the computation is terminated otherwise the inlet and outlet temperatures of the element are set equal to each other and the computation is continued until the end of the coil is reached.

7.2.1. Comparison between theoretical and experimental results

The computer output includes a temperature profile along the coil and the total heat removed up to any point along the coil as well as the radiative and convective heat removed by each successive element of coil. An abbreviated version of the computer results applied to the horizontal coils only,with water and air being used as coolants is included in Table 7.3. The calculated and experimentally obtained outlet temperatures from the cooling coils for a FB temperature of 800°C are very similar which indicate agreement between the theoretical approach and the experimental results. Due to the radiative heat losses to the PFBC water jacket and the position where the exit temperature of the hot air was measured,this temperature is lower than the temperature calculated from the mathematical model.

Although the actual heat flux per unit length of cooling coil was different from the values obtained when the mathematical model was applied to the vertical coils, no changes were made to the computer programme to distinguish between the two types of coils. This was mainly due to the following reasons:-

TABLE 7.3

Computer results based on the theoretical model for the prediction of the heat transferred from the FB to the immersed cooling coils (horizontal coils)

INPUT DATA

TB = 1073,0	TIN = 298,0	DT = 1,0
H = 380,00	ES = 0,620	ET = 0,650
HI = 1,00	K = 16,30	DI = 0,00940
DO = 0,01265	L = 10,37	DL = 0,100
TOL= 0,010	FTOL= 20,000	

A. AIR USED AS COOLANT

Air flowrate : 8,333 x 10^{-3} Nm^3/s

FB temperature: 1073,0 K

Temperature of coil at length ℓ		Cooling coil length ℓ	Heat transferred to element at length ℓ		Cooling coil cumulative heat
Experimental	Theoretical		Convective	Radiative	
K	K	m	W	W	W
298,0	298,0	0,0	0,0	0,0	0,0
	350,5	0,1	441,8	132,0	573,8
	691,3	1,0	228,2	101,2	4428,7
	985,2	3,0	51,0	31,7	7926,3
	1063,7	6,0	5,4	3,7	8884,9
	1072,0	9,0	0,6	0,5	8986,4
1049,0	1072,7	10,3	0,2	0,2	8994,9

At ℓ = L

Total heat transferred : 8995,3 W

Total convective heat : 6175,8 W

Total radiative heat : 2819,5 W

B. WATER USED AS COOLANT

Water flowrate : 0,5 kg/s

FB temperature : 1073,0 K

Temperature of coil at length ℓ		Cooling coil length ℓ	Heat transferred to element at length ℓ		Cooling coil cumulative heat
Experimental	Theoretical		Convective	Radiative	
K	K	m	W	W	W
298,0	298,0	0,0	0,0	0,0	0,0
	298,3	0,1	582,8	137,0	719,8
	301,4	1,0	580,5	137,0	7186,6
	308,3	3,0	575,3	136,9	21481,4
	318,4	6,0	567,7	136,8	42728,8
	328,5	9,0	560,1	136,6	63744,3
331,0	332,7	10,3	556,9	136,6	72779,6

At ℓ = L

Total heat transferred = 73472,9 W

Total convective heat = 59242,9 W

Total radiative heat = 14230,0 W

(a) Although there was a difference between the theoretical and experimental results for the vertical coil, this was not significantly big probably due to the length of the vertical coil (4.2m). It might be that because of this coil being relatively short, its better heat transfer rates did not appear significant.

(b) The position of the two types of coils in the FB was considerably different (Figure 5.5) and it was evident that more experimental tests on the cooling coils would have to be carried out in order to formulate the significance of their position in the FB. Only if this was completed could the effect of different shapes of cooling coils be investigated.

In conclusion, the mathematical model on the cooling coils can be further modified to include the positional effect and the shape of the cooling coils. We believe that this model can form a sound basis for a wide spectrum of models dealing with heat transfer and heat exchanger surfaces and that changes to it resulting from further experimental tests can be easily incorporated.

The following chapter is the summary of our research findings, derived from our preliminary work and the experimental runs on our PFBC. The success of our theoretical models to predict our experimental work is also covered.

CHAPTER EIGHT

SUMMARY

Our theoretical and experimental work on the design aspects and operation of our multistage PFBC are summarized in this chapter.

8.1 PRELIMINARY INVESTIGATIONS

I. A 0,15 m square FB was initially used to determine the kinetics of combustion of South African coals and their behaviour as they burn in the absence of a fluidizing medium and in an FB of solids. The batch combustion tests indicated good mixing of the solids and coal and no breakage of coal particles was observed during these trials. On the assumption that the volatiles were immediately driven off the coal particles on their entry to the FB, a simple mathematical model was derived using the skrinking core approach. The results from this theoretical model were in good agreement with the experimental results. This experimental work later formed the basis for a more complex mathematical model which described the continuous combustion of coal in the two-FB PFBC.

II. The downcomers transfering solids internally from the higher to the lower FBs of the PFBC were also investigated and a mathematical model was presented for the design of downcomers. The importance of parameters such as fluidizing gas velocity, the height of the free board area, the distributor pressure drop and the downcomer diameter on the design of downcomers were included in the mathematical model. Two downcomers were subsequently designed and successfully used to transfer solids within the PFBC. These downcomers were in fact purposely overdesigned because as it was later discovered it was of greater importance to control the solids circulation using the non-mechanical solids control valve.

III. A separate investigation was carried out on the non-mechanical λ valve. Preliminary tests showed that the behaviour of this valve, used

to control the flow of solids leaving an FB, could not be predicted by correlations taken from Knowlton and Hirsan's work[29]. The experimental investigation which followed confirmed this and a mathematical model was derived to describe the flow of solids through this valve. Though the mathematical equations in this model cannot be readily applied to other similar systems the theoretical approach has a wider scope.

The same λ-valve was successfully used to control the solids circulation in the pilot scale PFBC.

IV. A novel distributor plate able to transmit relatively high loads of particles (up to 60 g/Nm^3) without choking was designed and tried in a small FB. A seven tuyere distributor was used, with the tuyeres operating individually as a multientry cyclone. The behaviour of the distributor was in every other respect similar to a conventional distributor and its behaviour could be predicted by existing empirical equations[21,22]. Larger diameter distributors of the same design were later successfully used as the interstage distributors of the pilot scale PFBC.

V. An LPG-air burner operating immersed under the surface of the fluidized solids, was investigated in a small FB. On the basis of this work four burners of a similar design were fabricated and were successfully used for preheating the pilot scale PFBC. The burners operated successfully at a thermal output of up to 60 kW. The temperature of the hot gases leaving the burner assembly was regulated by the addition of secondary air. These burners were also used when the PFBC was pressurized. (During preheating,the system pressure had to be kept below the LPG supply pressure.) No sintering of solids or fouling was observed as long as the solids were kept fluidized during preheating. The burner assembly was specially designed to act as the bottom FB distributor as well.

8.2 EXPERIMENTAL RUNS ON THE PFBC

The three-stage PFBC fabricated out of stainless steel with external mild steel water jackets and internally lined with refractory bricks,was used in a series of experiments to prove the most suitable and practical combustor configuration for burning high in ash South African coals. The PFBC had an internal diameter of 0,45 m and a height of 4 m and was operated as a three, two or one-FB system by simply removing the interstage distributors.

I. Low combustion efficiencies and high carbon losses were achieved when the PFBC was operated as a circulating system with three-FBs. The concept of countercurrent processing,though theoretically sound and extremely successful when applied to other operations , could not be used in practice to burn coal efficiently in a multistage system. The main reasons for this are given below.

(a) When coal was fed in the top FB any fine particles in the feed were immediately driven off the combustor by the fluidizing gas, sometimes before they even reached the fluidized solids.

(b) Combustion in the top FB also meant reduction in size of coal particles. This was therefore a source of fines since these fines could be easily lifted off the FB by the fluidizing gas.

(c) Fine coal particles were also lost through the overflow of the double entry cyclone due to the low density and small size of the coal particles mixed with the circulating solids.

(d) Inflight combustion of the elutriated fines was limited because of a limited amount of oxygen present in the exhaust gas. (It was essential to run the PFBC with a low excess oxygen).

II. Screening off the fines from the coal feed or preferably feeding coal in the middle FB improved the combustion efficiency of the PFBC. The use of just any size of coal particles was one of the main

objectives of this investigation, therefore, the screening off of fines was unacceptable. When the PFBC was operated with coal fed to the middle FB, the coal losses which occurred were only dependent on the circulating load of solids and the weight of coal present in the top FB at any instant. To eliminate any coal losses, caused by the circulation of solids, a series of experiments were carried out without any solids circulation. As a consequence of this no combustion took place in the bottom FB while the middle FB acted as the main combustion FB and the top FB as a burnout cell for the elutriated fines. It became clear from these experiments that the loss in combustible fines was drastically reduced and that up to 99 per cent coal combustion efficiencies could be achieved.

Although high efficiencies were achieved when the three-FB PFBC was operated with no solids circulation the overall thermal output of the combustor was very low because of the under utilization of the bottom and top FB . This problem was solved by operating the PFBC with a bottom deep FB and a shallow top FB with, again, no solids circulation. Coal was fed in the bottom FB under the solids surface.

II. When the combustor was operated as a two-FB system the coal combustion efficiencies achieved were of the order of 99 per cent. Combustion of coal took place in the bottom FB while the top FB acted as a smuts burnout cell. The vital contribution of the top FB was realized when the PFBC was operated at pressures above 3 bar (abs). Higher combustor pressures meant higher amounts of air input to the bottom FB and higher quantities of elutriated particles from this FB. The top FB seemed always capable of handling the ever increasing quantity o elutriated coal particles as long as the oxygen concentration in the fluidized gas was maintained at not less than 2 per cent by volume. Best results were obtained when the gas entering the top FB contained 7,5 per cent oxygen by volume.

Although extra air could have been introduced into the top FB to supplement the free oxygen in the fluidizing gas, in almost all cases this was not necessary.

III. Different kindsof coal with different particle sizes, all under 15 mm (maximum particle size fixed by coal screw feeder), and with an ash content of up to 70 per cent were successfully burnt in the two FB PFBC. Since the elutriated coal particles as well as the carbon removed with coarser ash, increased with the coal in the bed (also observed by Cammarota *et al.*[64]), lower overall coal efficiencies were obtained when higher in ash coal particles were burnt in the PFBC. Typically for the 70 per cent ash coal, the overall coal conversion was never more than 90 per cent (based on carbon in feed and exhaust gas).

IV. The size of the ash leaving the PFBC was 80 per cent -15μm and the flue gas had a particle loading of 30 to 50 g/Nm^3. Whether the flue gas from the PFBC can be used to drive a gas turbine is not yet clear. Conflicting information have been published on the performance of turbine blades when exposed to gases carrying with them particles less than 30μm[16,17]. It is becoming clearer that if our PFBC is to be used in combined cycle operations the size of the ash particles may have to be reduced.

V. Some erosion was detected on the cooling coils which was mainly located on the horizontal parts of the cooling surfaces. It was not though significant and compared favourably with erosion figures released on cooling tubes used in a conventional boiler.

VI. Atmospheric pollution was not seriously considered as it did not form part of this work. All solid pollutants were though successfully removed by the wet scrubber while all SO_2 reacted with the caustic solution which was added to the scrubber. For an industrial size FBC

the use of caustic to remove the SO_2 is uneconomical. The use of dolomite or limestone fed with the coal is generally practised.

VII. PFBC Pressures of up to 7 bar (abs) were used and the achieved thermal output of the system was as high as 0,6 MW(t). The combustor was operated smoothly for periods of between 2 and 8 days. The two-FB PFBC proved to be the combustor which offered easy operation, a trouble free operation, and a highly efficient utilization of all types of coal.

8.3. THEORETICAL MODELS

The mathematical models predicting the combustion of coal in the PFBC and the heat transfer to the cooling coils were written, firstly, to establish how well these processes could be represented theoretically and by choosing the right set of experiments, how to gain greater knowledge of their behaviour and secondly, to provide means of predicti the performance of other FBCs and heat exchangers operated under similar conditions.

8.3.1. Combustion of coal in the PFBC

The mathematical model on the combustion of coal in the PFBC was based on a shrinking core type model where the rate of shrinkage of a coal particle was expressed in terms of parameters like the oxygen concentration and the temperature of the particle. The overall mass balance was based on a population balance over all the coal particles, assuming that, combustion takes place in the emulsion and cloud-wake phases. Backmixing of gas and solids was also incorporated in the mathematical model.

On selection of the correct value of the constant in the elutriati equation the results derived from the theoretical model were in good agreement with the experimental results obtained from the operation of the two-FB combustor. The methematical model was also used to supplement

the experimental work and create a better understanding of the behaviour of the PFBC. It is presented here in a general form and it may be used as is with the replacement of a few statements to predict the performance of other FBCs of a single or a multi-fluidized bed type.

8.3.2. Heat transfer through the cooling coils

The mathematical model on the cooling coils which were used to extract heat from the PFBC, was based on a stepwise heat and mass balance along the length of the cooling coils assuming that all surfaces were grey.

The theoretical results compared favourably with the experimental results although,the mathematical model did not dintinguish between the two different shapes of cooling coils. For this reason,if the mathematical model is to be used for other types of cooling surfaces it should be changed to include the effect of the shape of the coils and their position in the FB.

CHAPTER NINE

SUGGESTIONS FOR FURTHER RESEARCH

In this investigation it was shown that all types of South African coals can be efficiently burnt in the PFBC operated as a two-FB combustor and that solids circulation was not necessary.

It is suggested that work shall now be directed towards the preparation of the PFBC, to be used in a combined cycle operation. It may be necessary to reduce the particle size in the exhaust gas stream below the values which were obtained experimentally. To achieve this a multicell cyclone may have to be added in series with the existing double entry cyclone to remove the coarser particles from the flue gas. Alternatively , the size of the larger particles may be reduced if their carbon is burnt by either using the top FB more effectively, or by using a principle similar to the one employed in FB sulphide roasting, where hot oxygenated air is introduced into the hot flue gas stream leaving the reactor. In this way some of the larger particles may break up due to combustion of the remaining carbon molecules. If the research which is currently directed towards the use of particle laden gases to drive gas turbines, solves the problem of fouling of the turbine blades,then the PFBC can be coupled up to a gas turbine.

It is suggested that the PFBC shall be properly insulated and further experiments, orientated towards reducing heat losses and improving thermal efficiency of the combustor, shall be carried out. This will enable an overall heat balance to be performed.

Finally the theoretical model on the cooling coils must be further improved by incorporating results from experiments on different shapes of cooling coils using only one of the three FBs of the PFBC to carry out the experiments.

APPENDIX 1

DERIVATION OF DESIGN EQUATIONS AND NUMERICAL ILLUSTRATION OF THE PROPOSED THEORETICAL MODEL FOR DOWNCOMERS

A.1.1. DERIVATION OF EQUATIONS

A.1.1.1. The Force-momentum Balance Equation

From Figure A.1.1 (Appendix 1), based on the assumptions already outlined and taking all physical quantities positive if increasing in the upward (z) direction, the force-momentum equation can be written as:

$$\rho_s(1-\varepsilon)\frac{d}{dz}\left(\frac{u_s^2}{2}\right) = -\frac{dp}{dz} - \frac{1}{r}\frac{d}{dr}(r\tau_{rz}) + \rho_s(1-\varepsilon)g \qquad \text{E.A.1.1.}$$

Noting that for axial symmetry,

$$(\tau_{rz})_{r=0} = 0, \text{ and writing } (\tau_{rz})_{r=R} = \tau_w$$

E.A.1.1 can be integrated over the downcomer cross section and over its total length L_T to give:

$$p_2 - p_1 + C_1\rho_s(1-\varepsilon)(\bar{u}_{s_2}^2 - \bar{u}_{s_1}^2) + \frac{4\tau_w L_T}{d_t} - \rho_s(1-\varepsilon)gL_T = 0 \qquad \text{E.A.1.2.}$$

where $\bar{u}_s$ is the averaged value of the solids velocity across the cross-section and the factor C_1 is included to account for the radial velocity profile $u_s = u_s(r)$.

From the assumption that the initial solids velocity is zero either $\bar{u}_{s_1}$ or $\bar{u}_{s_2}$ is zero.

Substituting into E.A.1.2. the solids mass rate (W_s) and writing the wall shear stress rather in terms of a friction factor (f_s), the

generalized form of the force-momentum balance equation becomes:

$$\Delta p + C_1 \frac{W_s|W_s|}{\rho_s(1-\epsilon)} + 2f_s \frac{L_T W_s|W_s|}{d_t \rho_s(1-\epsilon)} - \rho_s(1-\epsilon)gL_T = 0 \qquad \text{E.A.1.3.}$$

A.1.1.2. The Gas Drag Equation

The Ergun equation can be used for calculating the pressure gradients for systems where no bubbles are present and the overall voidage (ϵ) does not thus exceed the minimum fluidizing voidage.

Based on the same sign convention used for the force-momentum balance equation the general form of the Ergun equation[36] for a moving bed situation is:

$$-\frac{\Delta p}{\Delta L} = 150\left(\frac{1-\epsilon}{\epsilon}\right)^2 \frac{\mu_g . u}{\phi_s^2 d_p^2} + 1{,}75\left(\frac{1-\epsilon}{\epsilon}\right)\frac{\rho_g}{\phi_s d_p} \Delta u|\Delta u| \qquad \text{E.A.1.4.}$$

where

$$\Delta u = u_g - u_s = \frac{U_g}{\epsilon} + \frac{W_s}{\rho_s(1-\epsilon)}$$

$\epsilon \leq \epsilon mf$

While a force-momentum balance equation can be written to cover all systems of solids transport, the general Ergun equation must be restricted to systems with voidage less than or equal to ϵmf.

The forms of E.A.1.3 and E.A.1.4 for describing the behaviour of downcomers joining fluidized beds for the moving bed regime are thus:

$$-\Delta p - C_1 \frac{W_s^2}{\rho_s(1-\epsilon mf)} - 2f_s \frac{L_T W_s^2}{d_t \rho_s(1-\epsilon mf)} + \rho_s(1-\epsilon mf)gL_T = 0 \qquad \text{E.A.1.5.}$$

$$-\frac{\Delta p}{L_T} = 150\left(\frac{1-\varepsilon mf}{\varepsilon mf}\right)^2 \frac{\mu_g \Delta u}{\phi_s^2 d_p^2} + 1{,}75\left(\frac{1-\varepsilon mf}{\varepsilon mf}\right) \frac{\rho_g}{\phi_s d_p} (\Delta u)^2 \qquad \text{E.A.1.6.}$$

where

$$\Delta u = u_g - (-u_s) = \frac{U_g}{\varepsilon mf} + \frac{W_s}{\rho_s(1-\varepsilon mf)} \qquad \text{E.A.1.7.}$$

A.1.2. NUMERICAL ILLUSTRATION OF PROPOSED DESIGN MODEL FOR DOWNCOMERS

Consider the design of a three-stage FB pilot plant for coal combustion, using sand as a circulating load. It is required to find the smallest size downcomer that will convey solids at a mass rate of 0,167 kg/s. The design requirements are specified on Table A.1.3. Note that a safety factor is included to allow for expected solids fluctuations.

The procedure is:

(a) Choose the level of the solids in the downcomer to be equal to the length of the downcomer pipe. (Recall observation (b) (Section 3.1.3, Chapter 3).

(b) From the given total gas input of 5,910 x 10^{-2} m^3/s estimate the FB voidage ($\bar{\varepsilon}$) from Figure 3.1.

(c) Determine the pressure gradient of solids in the FB using E.3.4.

(d) From Figure 3.5 obtain the velocity of gas through the downcomer based on the downcomer length (L_T) and the combined height of the two FBs (L_B). (The pressure drop across the distributor is neglected.) Note that heights (L_T and L_B) must be reckoned relative to the foot of the downcomer (Figure 3.2 level '0'.)

To estimate d_t an iterative solution of E.3.1, E.3.2, and E.3.5 is necessary.

(e) Guess a value of downcomer diameter, d_t.

(f) Determine the linear solids velocity u_s in the downcomer and calculate the solids friction factor (f_s) from E.3.5.

(g) Determine the pressure gradient in the downcomer from E.3.2, and compare with that of the FBs.

(h) Estimate the pressure drops across the downcomer (L_T) and the combined FBs (L_B).

(i) Substitute in E.3.1.

If E.3.1. is satisfied then (d_t) is the required minimum value.

The results of such an iterative scheme are shown in Table A.1.3. for which it can be concluded that the minimum downcomer size for the required duty is 0,0265m.

TABLE A.1.1.

Size analysis of solids used for the experiments on downcomers

Particle size mm	Cumulative less than size % wt	Minimum fluidization velocity ms^{-1}
0,40	0,5	
0,45	21,5	
0,50	47,5	0,224
0,55	81,0	
0,60	99,6	

TABLE A.1.2.

Experimental results showing the superficial velocity of gas through the FB, the solids flux rate through the downcomers and the pressure gradient corresponding to the FB and downcomers. The calculated values of the friction factor are also included (solids level in downcomers was L_T = 0,33m)

Gas veloc in FB (superficial) ms^{-1}	Solids flux rate $kgm^{-2}s^{-1}$				Pressure gradient, Nm^{-1}				
					For FB	For downcomer			
	d_t 0,070	d_t 0,054	d_t 0,036	d_t 0,0254		d_t 0,070	d_t 0,054	d_t 0,036	d_t 0,0254
0,225	25,98	21,83	32,71	27,15	14 481	9 768	9 668	9 895	9 780
0,239	56,30	56,76	72,01	67,90	14 156	10 395	10 411	10 736	10 651
0,258	90,94	93,13	111,31	108,54	13 711	11 139	11 188	11 583	11 523
0,276	125,59	130,99	148,90	161,03	13 456	11 891	12 017	12 377	12 679
0,294	160,20	165,92	186,60	213,14	13 284	12 260	12 787	13 244	13 872
0,313	177,56	187,75	211,20	246,69	12 944	13 047	13 269	13 804	14 592

Friction factor				Solids linear velocity in downcomer, ms^{-1}			
d_t 0,070	d_t 0,054	d_t 0,036	d_t 0,0254	d_t 0,070	d_t 0,070	d_t 0,054	d_t 0,036
983,5	110,7	316,1	327,0	0,0175	0,0148	0,0221	0,0184
197,2	149,2	60,1	48,1	0,0381	0,0384	0,0487	0,0459
69,6	51,0	22,9	17,1	0,0615	0,0630	0,0753	0,0734
33,5	23,5	11,7	6,8	0,0850	0,0886	0,101	0,109
19,4	13,3	6,6	3,3	0,108	0,112	0,126	0,144
14,3	9,6	4,7	2,2	0,120	0,127	0,143	0,167

ε_{mf} = 0,465

ρ_s = 2762 kgm^{-3}

D = 0,14m

TABLE A.1.3.

Numerical illustration of design model on the use of downcomers for transporting solids between FBs

Specification

D = 0,457m

d_p = $0,5 \times 10^{-3}$m

Length of downcomer = 0,965m

L_B = 0,622m

ρ_s = 2762 kgm^{-3}

ρ_g = 1,8 kgm^{-3}

nominal solids mass rate : 0,167 kgs^{-1}

safety factor : 10%

design solids mass rate : 0,183 kgs^{-1}

gas supply : $5,91 \times 10^{-2} m^3 s^{-1}$

ϕ_s = 0,715

Design Calculation

Iteration number	Downcomer diameter d_t, m	Linear solids velocity u_s ms^{-1}	Friction factor f_s (E.3.5)	Pressure grad Nm^{-1}		Pressure drop Nm^{-2} across		Value of L.H.S. of (E.A.1.5
				for downcomer (E.A.1.6)	for FB (E.3.4)	L_T	L_B	
1	0,040	0,0988	12,670	8 608	12 585	8 307	7828	4666
2	0,030	0,175	3,911	11 021	12 585	10 635	7828	1778
3	0,027	0,217	1,924	12 341	12 585	11 909	7828	283
4	0,0265	0,225	1,759	12 601	12 585	12 161	7828	-13

Therefore choose $d_t \simeq$ 0,0265m

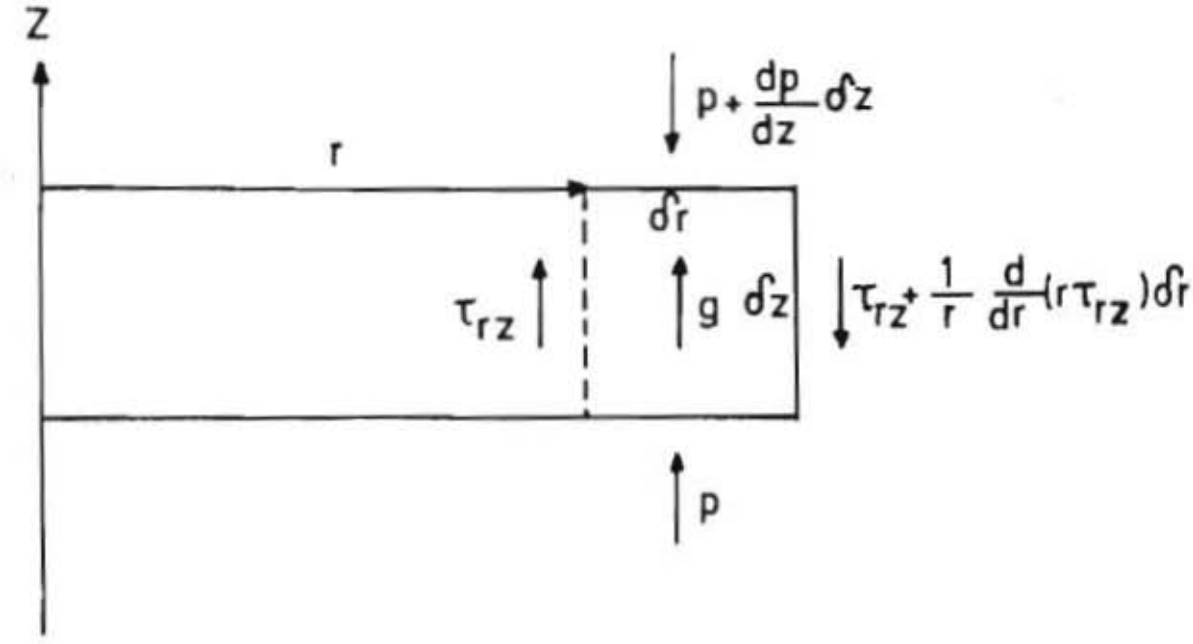

Figure A.1.1. Annular element used for the derivation of the force-momentum balance equation

APPENDIX 2

THE NON-MECHANICAL SOLIDS FLOW CONTROL VALVE - EXPERIMENTAL DATA

TABLE A.2.1

Physical properties of solids used in the experiments on the λ valve

ρ_s = 2650 kg/m^3

ϕ = 28° } (Reference 8)

δ = 36° }

B_1 = 0,639 } dynamic conditions

D_1 = 1,576 } (Reference 42)

$$a = \frac{4B_1D_1}{D_\lambda} = 95,99 \text{ m}^{-1}$$

d_p = 0,56 x 10^{-3} m

Particle size μm	Cum. fraction less than size Mass, %
212	0,8
300	2,4
425	11,1
600	54,0
850	99,2

Important dimensions:

Diameter of λ valve, D_λ = 0,042 m

Diameter of fluidized bed, D_b = 0,46 m

Diameter of pneumatic conveyor, D_L = 0,055 m

TABLE A.2.2

Experimental results showing the pressure in the FB system, the pressure profile, and the flow-rate of the solids through the λ valve. Results obtained with an orifice plate and an air jet are included for the region of uncontrolled flow

Aeration via λ valve $m^3/s \times 10^3$	P_3 = 3334 Pa					P_3 = 4952 Pa				
	P_0-P_4 Pa	P_1-P_0 Pa	P_2-P_1 Pa	P_5-P_6 Pa	W_s kg/m².s	P_0-P_4 Pa	P_1-P_0 Pa	P_2-P_1 Pa	P_5-P_6 Pa	W_s kg/m².s
0	441	2746	78	147	0	932	3824	176	147	0
0,3	2353	706	59	275	42,1	2726	1000	118	465	91,5
0,47	2334	716	59	294	42,1	2667	1079	127	490	107,1
0,62	2334	745	59	314	45,9	2628	1128	147	588	122,7
0,77	2314	755	59	343	48,1	2608	1206	147	647	144,4
0,92						2550	1236	157	686	156,4
	P_3 = 7550 Pa					(Transition to uncontrolled region) P_3 = 10 884 Pa				
	P_0-P_4 Pa	P_1-P_0 Pa	P_2-P_1 Pa	P_5-P_6 Pa	W_s kg/m².s	P_0-P_4 Pa	P_1-P_0 Pa	P_2-P_1 Pa	P_5-P_6 Pa	W_s kg/m².s
0	1471	5683	275	147	0	2157	8041	490	196	0
0,3	3235	1510	235	1039	252,7	2501	1785	588	2255	509,6
0,47	3197	1569	255	1079	262,3	2501	1794	588	2275	577,6
0,62	3140	1589	265	1226	288,8	2452	1804	608	2314	539,6
0,77	3040	1628	275	1275	312,8	2452	1824	618	2351	601,6
0,92	3001	1637	294	1373	326,9	2353	1824	628	2340	598,2
Aeration via λ valve $m^3/s \times 10^3$	Use of orifice plate (orifice diameter = 19 mm) P_3 = 10 884 Pa					Use of air jet (8×10^{-3} m^3/s) P_3 = 10 884 Pa				
	P_0-P_4 Pa	P_1-P_0 Pa	P_2-P_1 Pa	P_5-P_6 Pa	W_s kg/m².s	P_0-P_4 Pa	P_1-P_0 Pa	P_2-P_1 Pa	P_5-P_6 Pa	W_s kg/m².s
0	2255	8237	294	196	0	2942	7060	490	294	0
0,3	3432	1461	226	1030	188,2	6531	1442	245	961	217,8
0,47	3383	1559	255	1128	231,4	6423	1471	255	1020	231,1
0,62	3344	1569	275	1177	294,6	6315	1510	275	1079	259,9
0,77	3216	1608	265	1226	312,9	6178	1579	275	1128	276,8
0,92	3138	1638	284	1255	315,3					

TABLE A.2.3

The normal stress between particles, friction factor, and voidage calculated for region (b) of the λ valve. (Aeration = $0,77 \times 10^{-3}$ m^3/s)

Pressure in fluidized bed p_3 Pa	Flow-rate of solids through λ valve W_s $kg/m^2.s$	$Q_\lambda \times 10^4$ m^3/s	$\frac{p_1 - p_0}{z_1 - z_0}$ Pa/m	u_s m/s	ε	$\Delta\sigma_{z_0}$ Pa	f_s
3 334	48,1	1,337	1065	0,0439	0,585	123,48	118,32
4 952	144,4	3,450	1680	0,145	0,627	118,42	11,32
7 550	312,8	7,343	2256	0,358	0,670	112,78	2,03
10 884	601,6	14,550	2544	0,811	0,720	102,25	0,422
12 040	683,7	16,597	2580	0,952	0,729	100,20	0,310

TABLE A.2.4

Observed and calculated drops in pressure for the entry region (a) of the λ valve. (Aeration = $0,77 \times 10^{-3}$ m^3/s)

Pressure in fluidized bed p_3 Pa	Flow-rate of solids through λ valve W_s $kg/m^2.s$	$Q_\lambda \times 10^4$ m^3/s	Observed drop in pressure Δp_a Pa	Calculated drop in pressure Δp_a Pa	
				E.3.6	E.3.9
3 334	48,1	1,337	59	3	56
4 952	144,4	3,450	147	31	162
7 550	312,8	7,343	275	147	314
10 884	601,6	14,550	618	546	680
12 040*	683,7	16,597	720	705	789

*Uncontrolled region

APPENDIX 3

THE IMMERSED BURNER - SOLIDS SIZE ANALYSIS, PROPERTIES OF LPG AND EXPERIMENTAL DATA

TABLE A.3.1.

Size analysis of silica sand used in tests with immersed burner and tests with the new type distributor

Coarse silica sand:

Particle size μm	Cumulative less than size % weight	Mean particle diameter μm
212	0,1	
300	0,4	684
425	0,7	(U_{mf} = 0,27 m/s)
600	18,4	
850	99,3	

Fine silica sand :

Particle size μm	Cumulative less than size % weight	Mean particle diameter μm
150	1,1	
212	6,2	396
300	17,9	(U_{mf} = 0,13 m/s)
425	61,1	
600	99,6	
850	99,9	

TABLE A.3.2.

Properties of LPG used for design and tests

on immersed burner*

1. Composition: C_3H_8 : 60%, C_4H_8 : 40%

2. Inflammability limits in air :

Component	Upper mole, %	Lower mole, %
C_3H_6	9,5	2,4
C_4H_8	8,4	1,85

3. Stoichiometric mixture:

Ratio of LPG to air is 3,75 to 100

4. Flame speed data in air

Component	Maximum speed composition mole %	Maximum speed m/s	Maximum speed for LPG m/s
C_3H_6	4,71	0,45	0,41
C_4H_8	3,65	0,37	

*Data supplied by Shell South Africa

TABLE A.3.3.

Data from tests on a 0,06m outer diameter immersed burner

Primary air $m^3/sx10^4$	LPG $m^3/sx10^4$	Secondary air $m^3/sx10^4$	Heat of combustion kW	Exhaust gas T^oC
7,50	0,283	35,0	2,90	280
		29,2		375
		24,0		460
		20,3		525
		13,3		670
8,83	0,333	33,3	3,41	360
		29,2		440
		24,0		518
		20,3		586
		13,3		715
10,56	0,400	33,3	4,09	410
		29,2		482
		24,0		572
		20,3		646
		13,3		775
11,90	0,450	33,3	4,60	442
		29,2		520
		24,0		614
		20,3		680
		13,3		820
14,5	0,550	33,3	5,63	520
		29,2		599
		24,0		682
		20,3		742
		13,3		890
17,6	0,671	33,3	6,82	600
		29,2		670
		24,0		758
		20,3		826
		13,3		980

APPENDIX 4

MATHEMATICAL MODELS FOR COAL COMBUSTION IN A STREAM OF HOT AIR ON THE DISTRIBUTOR, AND IN AN FB

A.4.1. COMBUSTION OF COAL ON THE DISTRIBUTOR IN A STREAM OF HOT AIR IN THE ABSENCE OF FLUIDIZED PARTICLES

A.4.1.1. Derivation of equations

Considering a burning particle and taking a mass balance at a radius r_c within the ash layer then:

$$-\frac{dN_{O_2}}{dt} = -4\pi r_c^2 D_G \frac{dC}{dr} = \text{constant} \qquad \text{E.A.4.1.}$$

Integrating E.A.4.1. across the ash layer from the unreacted core radius r_c to the initial particle radius R, it yields:

$$-\frac{dN_{O_2}}{dt}\left(\frac{1}{r_c} - \frac{1}{R}\right) = 4\pi D_G C_p \qquad \text{E.A.4.2.}$$

where C_p is the oxygen concentration near the particle.

From the stoichiometry assuming that oxygen goes to carbon dioxide:

$$-dN_{O_2} = -dN_c = -4\pi \frac{\rho}{M_c} F_c r_c^2 dr_c \qquad \text{E.A.4.3.}$$

where ρ and M_c are the coal density and carbon molecular weight, and F_c is the fraction of fixed carbon in the coal or char.

From the last two equations:

$$4\pi D_G C_p = -4\pi\rho \frac{F_c}{M_c} r_c^2 \left(\frac{1}{r_c} - \frac{1}{R}\right)\frac{dr_c}{dt} \qquad \text{E.A.4.4.}$$

For a number of particles N or a mass of sample $m = N\frac{4}{3}\pi R^3 \rho$ the overall rate of oxygen consumption must equal the rate of carbon consumption ($\frac{kg\ mol}{s}$), i.e.:

$$Q(C_o - C_p) = -\frac{3m}{R^3}\frac{F_c}{M_c} r_c^2 \frac{dr_c}{dt} \qquad \text{E.A.4.5.}$$

where Q is the air volumetric flowrate through the reaction chamber.

Elimination of C_p between E.A.4.4 and E.A.4.5 gives an equation, in which the only variables are, r_c and t. Integrating this equation noting that $r_c = R$ at $t = 0$ gives:

$$t = \frac{mF_c}{C_o Q M_c}\left(1 - \left(\frac{r_c}{R}\right)^3\right) + \frac{\rho (F_c)_R^2}{6 C_o D_G M_c}\left[1 - 3\left(\frac{r_c}{R}\right)^2 + 2\left(\frac{r_c}{R}\right)^3\right] \qquad \text{E.A.4.6.}$$

A.4.1.2. Application of theoretical model

To make a comparison between the experimental results and the values predicted theoretically the derived equations were used to predict the exit oxygen concentration for the combustion of 0,07kg of the coarse coal particles on the distributor.

Experimental data:

$m = 0{,}07kg$

$C_o = 2{,}6 \times 10^{-3}$ kg mol/m^3 (at 800^{o}C)

$Q = 2{,}7 \times 10^{-3}$ m^3/s (at 800^{o}C)

$F_c = 0{,}535$

$M_c = 12$ kg/kg mol

$\rho = 1715$ kg/m^3

$\tau = 2610s$

$R = 0{,}0034m$

Using E.A.4.6 the effective diffusivity D_G is calculated by replacing (t) with the burnout time(τ) and setting the particle radius (r_c) equal to zero, ($D_G = 2{,}61 \times 10^{-5}$ m^2/s). Using E.A.4.6 the time (t) is then calculated for a number of ratios of $(\frac{r_c}{R})$ and plotted in Figure A.4.1. The slope $d(r_{c/R})/dt$ at any time (t) is then determined graphically from Figure A.4.1 and substituted in E.A.4.5 which gives the exit oxygen concentration at any time during the combustion period. The same procedure is followed for the combustion of 0,07kg of fine size coal particles. The calculated values of the percentage of oxygen in the flue gas for fine and coarse particles were plotted along with the experimental values in Figure 4.2.

A.4.2. COMBUSTION OF COAL IN AN FB OF SOLIDS

A.4.2.1. Derivation of equations

Working as in the case of particles burning in the absence of fluidizing solids (Section A.4.1) the overall rate of oxygen consumption must be equal to the coal consumption rate. From the assumption that gas in excess of what is required for incipient fluidization passes through the bed as bubbles the overall mass balance on oxygen can be written as:[48]

$$(C_o - C_p)A[U-(U-U_{mf})\exp(-X)] = -\frac{3m}{R^3}\frac{F_c}{M_c} r_c^2 \frac{dr_c}{dt} \qquad \text{E.A.4.7.}$$

where A is the bed cross-sectional area, and

X is the number of times a bubble is swept out during its time in the bed.

The mass balance round a single particle is given by[48]:

$$4\pi Sh D_G r_c C_p = -\frac{4\pi\rho}{M_c} F_c r_c^2 \frac{dr_c}{dt} \qquad \text{E.A.4.8.}$$

Elimination of (C_p) from E.A.4.7 and E.A.4.8 gives an equation in which the only variables are (r_c) and (t). Integrating this equation

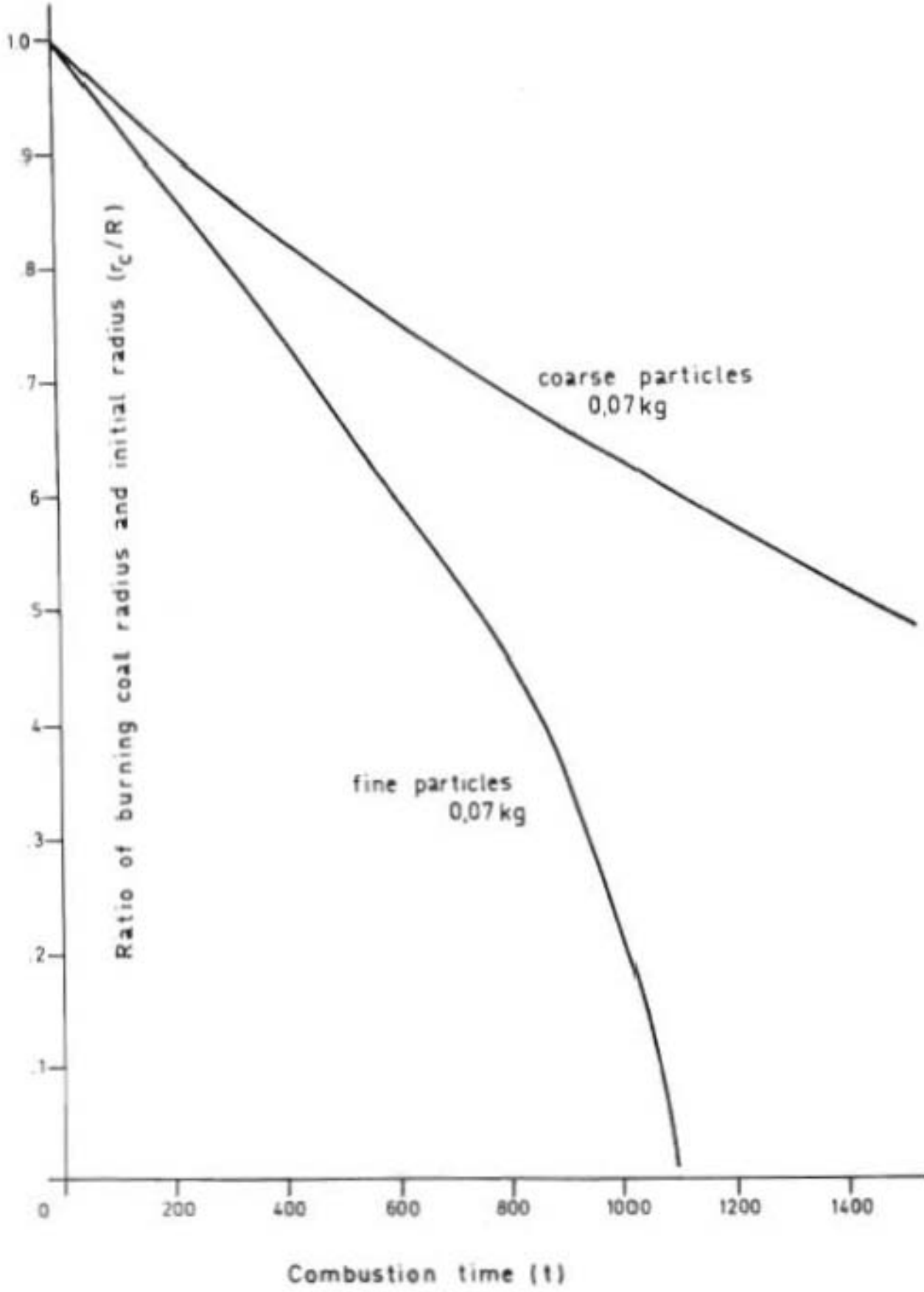

Figure A.4.1 : The relation of the ratio of the burning coal radius and the initial coal radius and the combustion time. Coal is burnt in the absence of solids under batch conditions

with $r_c = R$ at $t = 0$, gives:

$$t = \frac{mF_c}{C_o M_c A[U-(U-U_{mf})\exp(-X)]}\left[1-\left(\frac{r_c}{R}\right)^3\right] + \frac{\rho F_c R^2}{2C_o M_c Sh D_G}\left[1-\left(\frac{r_c}{R}\right)^2\right] \qquad \text{E.A.4.9.}$$

A.4.2.3. Application of theoretical model

To compare the experimental results and the values predicted theoretically, the derived equations were used to predict the exit oxygen concentration, for the combustion of 0,07kg of coarse coal particles in the FB.

For the calculations the following data were used:

C_o = $2{,}6 \times 10^{-3}$ kg mol/m^3 (at 800°C)

Q = $2{,}7 \times 10^{-3}$ m^3/s (at 800°C)

m = 0,07kg

F_c = 0,535

M_c = 12

ρ = 1715 kg/m^3

A = $2{,}25 \times 10^{-2}$ m^2

H = 0,2m

U_{mf} = 0,094 m/s (at 800°C)

Sh = 2

τ = 966s

R = 0,0034m

Initially the value of X is calculated from equation (15) of Reference 48, which gives X = 3,1. The same calculating procedure is then followed, as the one used for the combustion of coal particles in the absence of fluidizing solids. The calculated value of the diffusion coefficient obtained from E.A.4.9 for $t = \tau$ and $r_c = 0$ is $D_G = 1{,}61 \times 10^{-4}$ m^2/s. This is comparable with the value of D_G obtained by Avedesian and Davidson[48] ($D_G = 2{,}08 \times 10^{-4}$ m^2/s). The comparison between experimental

and theoretically predicted percentage of oxygen, is shown in Figure 4.3. Figure A.4.2 shows the relationship of (r_c/R) and time (t), calculated from E.A.4.9, as used in this calculating procedure.

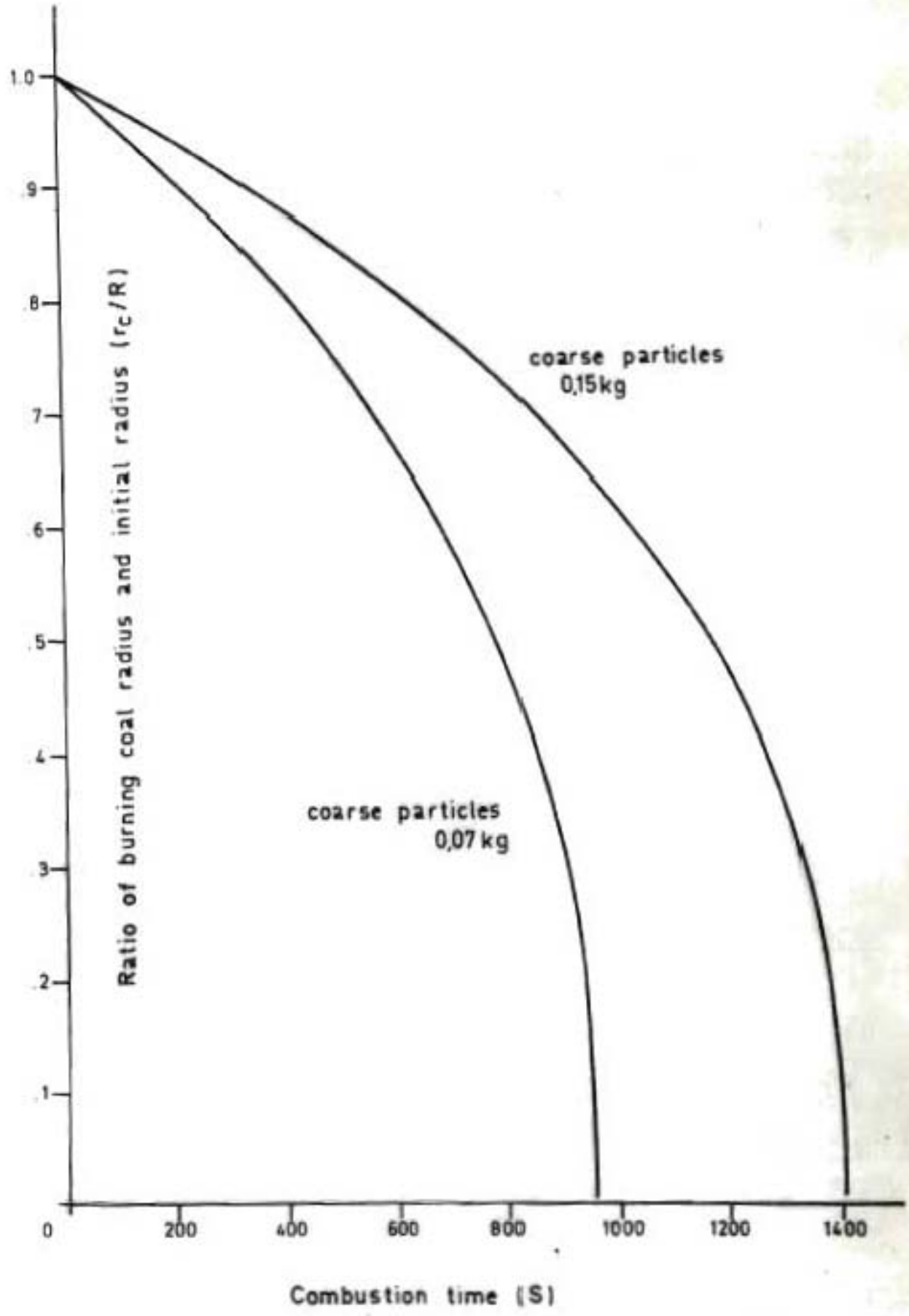

Figure A.4.2 : The relation of the ratio of the burning coal radius and the initial radius and the combustion time. Coal is burnt in the FB under batch conditions

TABLE A.4.1

Proximate analysis and grading analysis of Rand Carbide coal and char product used for combustion tests in the small FB combustor

Proximate analysis:

	Coal %	Char product %
Fixed carbon	53,5	74,9
Ash	13,8	20,0
Volatile matter	30,1	3,5
Moisture	2,5	1,5
Sulphur	0,7	0,7

Grading analysis:

Sieve size	Cumulative mass % smaller than size	
um	Fine coal	Coarse coal
600	3,0	0,5
1 180	7,0	2,2
2 360	25,5	7,9
4 750	95,6	25,4
6 300	100,0	47,0
9 400		90,1
14 200		100,0

APPENDIX 5

Flowsheet of computational procedure for the continuous combustion of coal in an FB

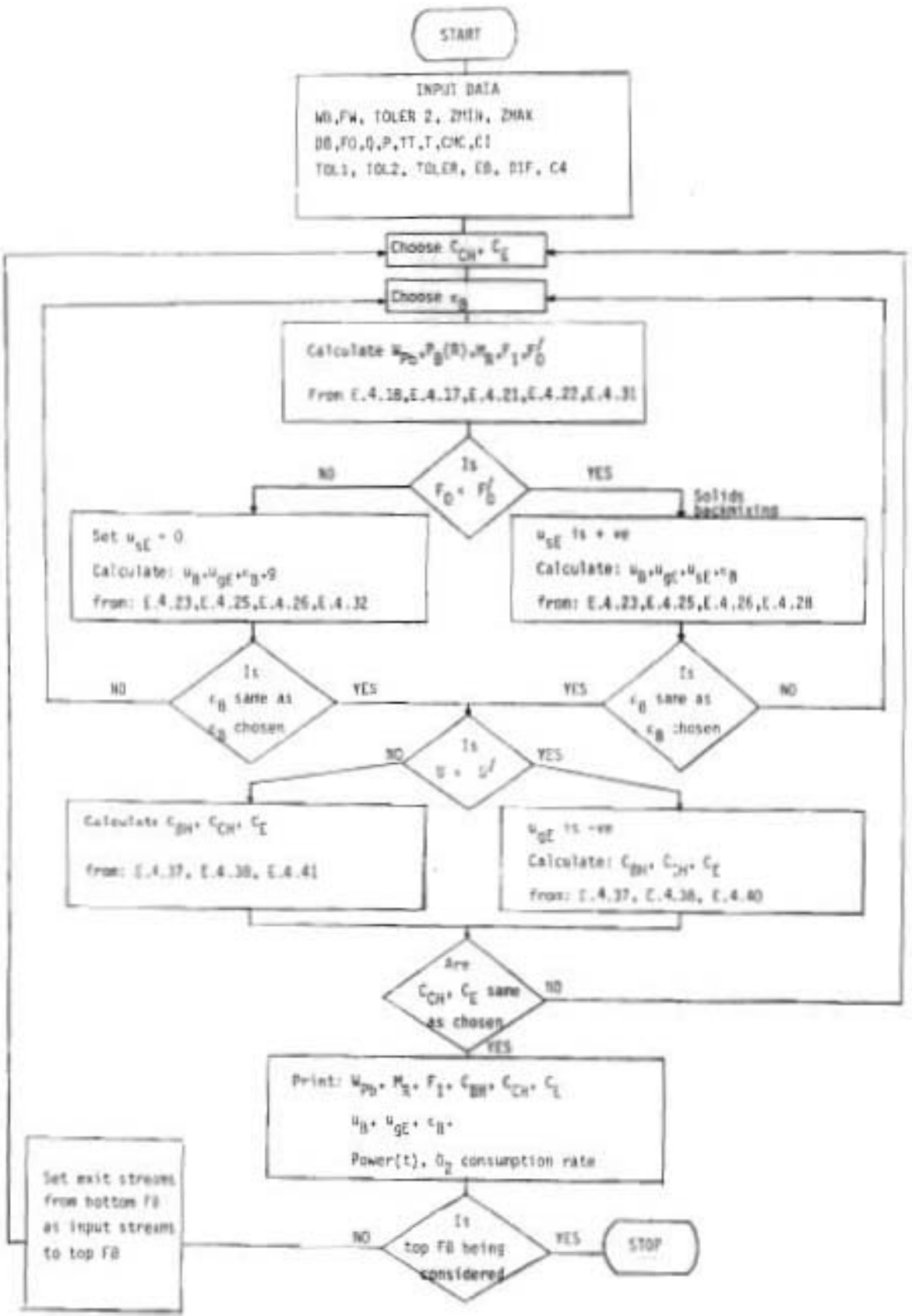

APPENDIX 6

FLOWCHART OF THE COMPUTER PROGRAMME FOR REAL TIME DATA LOGGING AND LISTING OF COMPUTER CHANNEL ADDRESSES WITH THE CORRESPONDING INSTRUMENTS

1. Flowsheet of real time computer program for data analysis and storage on memory disc

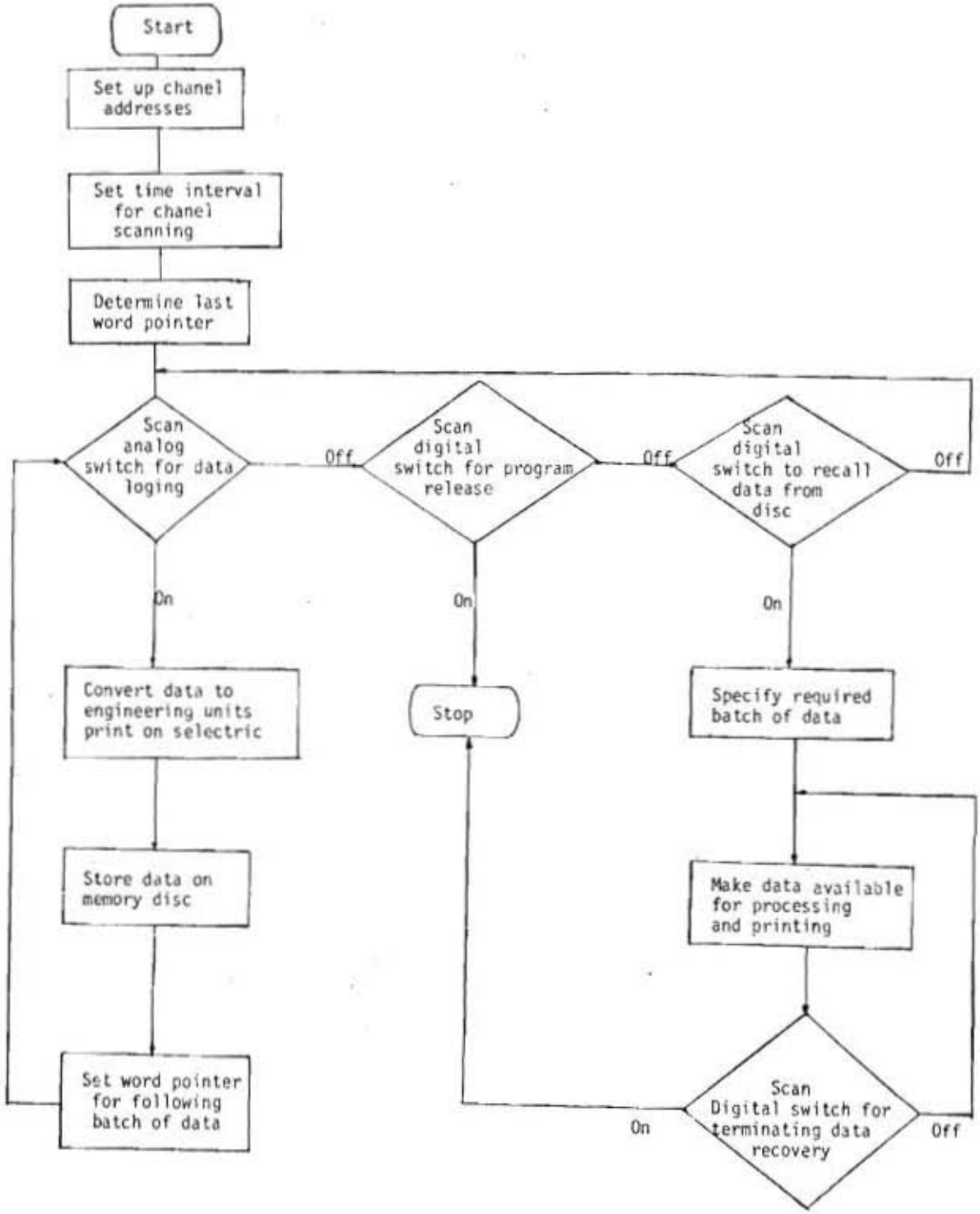

2. List of instruments and corresponding computer channel addresses

Instrument	Input signal	Output signal	Terminal junction	Wire connection	Computer address	Function
Δp_5	0/20" H_2O	4/20 mA	7A	Blue+ White-	87F	Main air supply Δp
Δp_2	0/20" H_2O	4/20 mA	5A	Blue- Red+	87E	Conveyor Δp
Δp_3	0/20" H_2O	4/20 mA	6A	White- Brown+	87D	Bottom bed Δp
Δp_6	0/40" H_2O	4/20 mA	1A	White- Green+	83B	Middle distr. Δp
Δp_1	0/20" H_2O	4/20 mA	4A	Red- Orange+	879	Top bed Δp
Δp_4	0/25" H_2O	10/50 mA	2A	Orange- White+	83C	Middle bed Δp
Δp_7	0/25" H_2O	2.5/11.5 V	3A	White- Blue+	878	Top distr. Δp
Δp_8	0/25" H_2O	2.5/11.5 V	8A	White- Grey+	83D	Flue gases flow Δp
Oxygen analyz.	0/25%	IV	10A	Orange+ Red-	87A	Combust gas O_2
CO_2 Analyz.	0/10%	100mV	11A	Orange+ White-	87C	Combust gas CO_2
CO Analyz.	0/5%	100mV	12A	Green+ White-	87B	Combust gas CO
Ch/Al T/C	0/1200°C	50mV	1B		870	TC1
Ch/Al T/C	0/1200°C	50mV	2B		871	TC2
Ch/Al T/C	0/1200°C	50mV	3B		872	TC3
Ch/Al T/C	0/1200°C	50mV	4B		873	TC4
Ch/Al T/C	0/1200°C	50mV	5B		874	TC5
Ch/Al T/C	0/1200°C	50mV	6B		875	TC6
Ch/Al	0/1200°C	50mV	7B		876	TC7
Ch/Al T/C	0/1200°C	50mV	7B		876	TC7
Ch/Al T/C	0/1200°C	50mV	8B		877	TC8

APPENDIX 7

PROXIMATE AND SIZE ANALYSIS OF DIFFERENT KIND OF COALS USED FOR THE COMBUSTION EXPERIMENTS IN THE PFBC. SIZE ANALYSIS OF SILICA SAND USED AS THE FLUIDIZING MEDIUM

A) RAND CARBIDE CHAR

Proximate analysis :

Fixed carbon	= 74,9%
Ash	= 20,1%
Volatile matter	= 3,5%
Moisture	= 1,5%
Sulphur	= 0,7%

Calorific value: = 25,7 MJ/kg

Grading analysis :

Sieve size µm	Cumulative mass % smaller than size
150	10,1
300	20,1
600	29,1
1180	42,3
2360	51,4
4750	78,1
6300	86,1
9500	98,8

B) ROOIFONTEIN COAL

Proximate analysis :

Fixed carbon	= 43,7%
Ash	= 30,1%
Volatile matter	= 24,8%
Moisture	= 1,4%
Sulphur	= 1,5%

Calorific value : = 23,7 MJ/kg

Grading analysis :

Sieve analysis µm	Cumulative mass % smaller than size
150	12,0
300	21,1
600	34,2
1180	50,8
2360	68,2
4750	84,5
6300	90,0
9400	99,1

C) HIGH IN ASH FILTER CAKE COAL

Proximate analysis:

	Coal, %
Fixed carbon	= 24,0
Ash	= 69,7
Volatile matter	= 5,2
Moisture	= 1,0
Sulphur	= 1,1

Calorific value: = 8,5 MJ/kg

Grading analysis:

Sieve size µm	Cumulative mass % smaller than size
75	48,2
150	76,6
210	92,3
300	98,4
420	100

D) SILICA SAND

Grading analysis:

Sieve size µm	Cumulative mass % smaller than size
75	0,49
106	2,34
150	6,56
212	14,78
300	25,89
425	36,56
600	50,41
850	100,00

APPENDIX 8

OPERATING PROCEDURE

(1) All valves closed.

(2) Switch on power supply to the electronic instruments and solenoid valves.

(3) Purge gas analysers with nitrogen and test against calibration gas. Check gas sampling line and gas conditioning unit and clean filters.

(4) Start up screw compressor.

(5) Supply air to cooling tubes and water to water jackets.

(6) Purge all pressure tappings and sampling ports with air.

(7) Supply a small quantity of nitrogen to the coal hopper (approximately 200 cc/min).

(8) Supply cooling water to the heat exchanger.

(9) Check flue gas cleaning system, and start up the liquor circulating pump. Adjust the liquor flow to the settler and the addition of caustic and flocculant (Allied Colloids 156).

(10) Open valve for main air supply to the combustor.

(11) Power on the departmental computer and load the data logging program (Program XTOS, file S@98,5) and transfer control of logging to the operators panel by the combustor. Set the time interval for the scanning of instruments and initialize data logging.

(12) Preheating procedure

Switch power to the controller. Press the reset button which initializes a number of steps in the following sequence - purging of the system, ignition of pilot flame and switching on of the solenoid valve which introduces the main LPG for combustion.

If the pilot flame fails to ignite the combustor is purged and the ignition procedure is repeated.

(13) The combustor is heated up. The temperature rise can be set at between 100°C and 180°C per hour.

(14) When a desired temperature is reached which is between 500°C and 650°C, depending on the type of coal used, the LPG supply to the pilot burner and combustor is turned off.

(15) Coal is then screw-fed to the combustor starting with a high coal feedrate for a period of a few minutes which is then reduced to the desired feedrate. The coal feedrate is controlled by a timer switch which regulates the on-off time of the motor driving the screw-feeder.

(16) Shut down

Stop coal feedrate and after ten minutes reduce air to the combustor. Reduce the system pressure if it is operating at high pressures trying to keep the solids in the combustor in a fluidized state.

When the combustor is cooled down to 200°C turn off the main air supply and the coolant to the water jacket, heat exchanger and cooling coils. Isolate all electronic instruments and purge the gas analysers with nitrogen.

Release program and power down the computer then switch off the compressor. When system is *cold* close all valves.

APPENDIX 9

EXECUTION AND LISTING OF THE COMPUTER PROGRAM FOR THE COMBUSTION OF COAL IN THE TWO-FB PFBC

1. EXECUTION OF THE COMPUTER PROGRAM

To execute the computer program code named NIMFBM on one of the computer terminals (HP 1600A) which is linked with the University central computer (UNIVAC 1100) the following statements have to be supplied

```
BREAK, F
XQT   ST.NIMFBM
ADD,E  ST.XTSDAT
BREAK, P.
```

The program will then be executed using the data already in XTSDAT. The data in this file can be altered by calling the editor as follows

```
ED,U  ST.XTSDAT
insert new data
.
.
.
EXIT
```

The data stored in XTSDAT which are used for the execution of the NIMFBM are listed below in the sequence they are called by NIMFBM.

WB	weight of material in bottom FB (kg)
FW	fraction of cloud wake to total bubble volume
TOLER2	convergence tolerance
ZMIN	minimum coal particle radius in feed (m)
ZMAX	maximum coal particle radius in feed (m)
DB	bubble diameter (m)
FO	coal feedrate (kg/s)
Q	air volumetric flowrate at STP (m^3/s)
P	combustor pressure (bar (abs))
TT	temperature of top FB (^oC)
T	temperature of bottom FB (^oC)

CMC	molecular weight of coal
C1	elutriation factor
EB	fraction of bubble phase to total volume of FB
DIF	gas diffusivity (m^2/s)
TOL1	convergence tolerance
TOL2	convergence tolerance
TOLER	convergence tolerance

```
FTN,S ST.NIMFBM
FTN 8R1  *11/20/81-16:21(27,)
      1.     C
      2.     C
      3.     C
      4.     C       LISTING OF PROGRAM NIMFBM FOR THE COMBUSTION OF COAL IN THE
      5.     C       TWO-FB PFBC STORED ON THE CENTRAL COMPUTER OF THE UNIV.OF NATAL
      6.     C       ON FILE CHEN-DBROUCK*ST.
      7.     C
      8.     C
      9.     C
     10.     C       PROGRAM NIMFBM
     11.     C
     12.     CCC       THIS COMPUTER PROGRAM PREDICTS THE COMBUSTION OF COAL IN THE
     13.     CCC     PFBC. IT DEALS FIRSTLY WITH THE COAL COMBUSTION IN THE BOTTOM
     14.     CCC     FB AND THEN AFTER CALCULATING THE INPUT PARAMETERS FOR THE TOP
     15.     CCC     FB ,THE COMBUSTION OF COAL IN THE TOP FB. THE THEORETICAL MODEL
     16.     CCC     IS BASED ON A SHRINKING CORE MODEL ,ON THE ASSUMPTION THAT COAL
     17.     CCC     PARTICLES BURN IN THE EMULSION AND CLOUD-WAKE PHASE  THE MASS
     18.     CCC     BALANCE IS CARRIED OUT ON THE BASIS OF A POPULATION BALANCE
     19.     CCC     OVER ALL THE COAL PARTICLES
     20.     CCC     IN THE PRINTOUT THE PROGRAM GIVES INPUT/OUTPUT PARAMETERS
     21.     CCC     COAL CONSUMPTION RATE,POWER (THERMAL) OF EACH FBAND RESIDENT
     22.     CCC     COAL IN EACH FB.
     23.     CCC
     24.     CCC     SIGNIFICANCE OF INPUT SYMBOLS
     25.     CCC
     26.     CCC       WB       WEIGHT OF CONTENTS OF BOTTOM FB (KG)
     27.     CCC       FW       FRACTION OF CLOUD-WAKE TO TOTAL BUBBLE VOLUME
     28.     CCC       ZMIN     MINIMUM COAL PARTICLE RADIUS IN FEED (M)
     29.     CCC       ZMAX     MAXIMUM              "
     30.     CCC       DB       BUBBLE DIAMETER (M)
     31.     CCC       F0       COAL FEEDRATE  (KG/S)
     32.     CCC       Q        AIR VOLUMETRIC FLOWRATE AT STP (M3/S)
     33.     CCC       P        RPESSURE OF PFBC (BAR (ABS))
     34.     CCC       TT       TEMPERATURE OF TOP FB (0C)
     35.     CCC       T          "          BOTTOM   "
     36.     CCC       CMC      MOLECULAR WEIGHT OF CARBON
     37.     CCC       C1       CONSTANT IN ELUTRIATION EQUATION
     38.     CCC       FB       FRACTION OF BUBBLE PHASE TO TOTAL VOLUME OF FB
     39.     CC        DIF      GAS DIFFUSIVITY (M2/S)
     40.     C         TOL1     =0.04     INTEGRATION TOLERANCE
     41.     C         TOL2     =0.0003       "          "   (FINAL ITERATION)
     42.     C         TOLER2   =1.E-06  CONVERGENCE TOLERANCE
     43.     C         TOLER3   =0.005       "          "   (FINAL ITERATION)
     44.     C         TOLER4   =0.005       "          "
     45.     C
     46.     C
     47.             DIMENSION OBJ(2),GUESS(2),TEMP(31),PBR(51),OBJ1(2),GUESS1(2)
     48.             COMMON TOL,HMIN,ZMIN,ZMAX,B1,B2,B3,C1,C2,C3,R4,HT,T,C0,CKY,
     49.            +CCH,CE,F0,WPB,PBOR,CMR,A11,A12,A21,A22,A23,CC0,CB0,CBH,U0,
     50.            1ISTAGE
     51.             COMMON /COMM1/ WB,Q,F1,CBB,F0D,U0D,SBM,GBM,QR1,QR2,CHQCC0,CHQCB0,
     52.            1NSKRYF,NB,NH,NCALL
     53.             COMMON /DISTRB/ SIZE(9),FRACT(9),SPLINE(9),RR(31),P1R(31),RS(31)
```

```
C---------- SET UP INTERPOLATION FOR FEED SIZE DISTRIBUTION
      CALL GSPN(9,SIZE,FRACT,SPLINE,2,0.,0.,0.,0.,0.,1.,0.,0.,TEMP)
      NB=0
      NH=1
      NCALL=0
      IOUT=6
      IIN=5
C---------THE NEXT 3 CARDS REQUEST UNIVAC 1100 TO REPORT ARITH.ERR.
      CALL DIVSET(1)
      CALL UNDSET(1)
      CALL OVFSET(1)
C------READ IN INPUT DATA
      READ(IIN,333) WB,FW,TOLER2,TOLER3
      WRITE(IOUT,338) WB,FW
  338 FORMAT(' WB,FW -',2(1X,G13.5))
      READ(IIN,333)ZMIN,ZMAX,DB,F0,Q,P
  333 FORMAT(6F8.6)
      READ(IIN,433)TT,T,CMC,C1
  433 FORMAT(3F8.1,F10.1)
      WRITE(IOUT,939)ZMIN,ZMAX,DB,F0,Q,P,TT,T,CMC,C1
  939 FORMAT(' ZMIN,ZMAX,DB,F0,Q,P,TT,T,CMC,C1',2(/,6(1X,G15.4)))
      READ(IIN,333) TOL1,TOL2,TOLER4,ER,DIF,C4
      WRITE(IOUT,335) TOL2,TOLER3,TOLER2
      WRITE(IOUT,336) DIF,C4
  336 FORMAT(' DIF,C4 -',2(1X,G12.4))
  335 FORMAT(' INTEGRATION TOLERANCE TOL2 = ',G15.4,/
     +  ' CONVERGENCE TOLERANCE TOLER3 = ',G15.4,/,' TOLER2 = ',G15.4)
      T1=T
      F00=F0
      TT1=TT
      DO 3112 I3112=1,1
      T=T1
      F0=F00
      TT=TT1
      NSKRYF=0
      NB=0
      NCALL=0
C     COAL ANALYSIS
      FIC=43.7
      VOLC=12.1
      VOLH=4.0
      VOLO=6.0
      VOLN=1.2
      CMOIST=1.4
      VOLS=1.5
      TVOL=VOLC+VOLH+VOLO+VOLN+VOLS
      A=0.1642
      EMF=0.49
      RHOA=1715.0
C     DENSITY OF CHARRED COAL RHO IS:
      RHO=RHOA*(100.0-TVOL-CMOIST)/100.0
      RHOS=2650.0
      RHOG=1.21
      DP=0.0006
      HMIN=0
      WT=0.2*WB
      GR=9.81
C
C-----------------------------------------------------------------------
C
```

```
C        EXPANSION OF INLET ON ENTRY TO THE FB
         DO 3111 ISTAGE=1,2
         TOL = TOL1
         TOLER = TOLER4
         IF(ISTAGE.EQ. 1) GO TO 21
         COIN = COUT
         QIN  = QOUT
         C0=CBB*(273.0+T)/(273.+TT)
         F0=F1
         RHOG=RHOG*(273.0+T)/(273.0+TT)
         WB=WT
         U0=U0*(273. +TT)/(273.9+T)
         Q0 = Q0*(273.+TT)/(273.+T)
         VMOIST = VMOIST*(273.+TT)/(273.+T)
         I=TT
         GO TO 31
C
C-------------------------------------------------------------------
C
C        INITIAL DEPLETION OF OXYGEN BECAUSE OF COAL VOLATILIZATION
C        AND COMBUSTION OF VOLATILES AS COAL ENTERS FB. EVOLUTION OF STEAM
C
21       C0=0.209/22.4
         COIN = C0
         QIN = Q
         C0=C0-F0/(Q*100.)*(VOLC/12.+VOLH/4.+VOLN/14.+VOLS/32-VOLO/32.)
         C0=C0*P*(298.0/(273.+T))
         Q0=Q*(273.+T)/(P*298.0)
         VMOIST=F0*CMOIST*22.4*(273.0+T)/(100.0*18.0*P*298.0)
C        THE CONCENTRATION OF O2 AT OPERATING CONDITIONS IS:
         C0=C0*Q0/(Q0+VMOIST)
         F0=F0*(100.-TVOL-CMOIST)/100.
         U0=(Q0+VMOIST)/A
         RHOG=RHOG*Q0/(Q0+VMOIST)+0.8*VMOIST/(Q0+VMOIST)
         RHOG=RHOG*P*298.0/(T+273.)
 31      IF(ISTAGE.EQ.1) CCH = 0.51*C0
         IF(ISTAGE.EQ.2) CCH = 0.95*C0
         IF(ISTAGE.EQ.1) CE = 1.2125*CCH
         CMG=(T+630.0)/333.3*1.E-5
         UMF=0.0079*(RHOS-RHOG)*DP*DP/CMG
         E = EMF*(1-EB)+EB
         HT=WB/(A*RHOS*(1-EMF)*(1-EB))
         C3=RHOA/RHO*FIC/100.
         KOUNT3=0
         KOUNT1 = 0
 210     KOUNT3=KOUNT3+1
         IF(KOUNT3.GT.15)GO TO 999
C
C-------------------------------------------------------------------
C
C----------ITERATION ON EB UNTIL CONVERGENCE FOR SOLIDS BACKMIXING CON-
C----------DITIONS IN THE FLUIDIZED BED
 100     KOUNT1=KOUNT1+1
         IF(KOUNT1.GT.75 )GO TO 999
C
C-------------------------------------------------------------------
C
C----------ITERATION ON EB UNTIL CONVERGENCE FOR ZERO NETT SOLIDS VELO-
C----------CITY IN THE FLUIDIZED BED
         E = EMF*(1.-EB)+EB
```

```
      1-EB*(1+FW)
      B2=B1/(1-EB)
      B3=EB*FW/(1-EB)
      B4 = 2635.0*E/RHO*1.E6
      CKY=0.0112*EXP(-16400.0/(T+273.0))
      CCD = (C0+CCH)*0.5
      R3CC=-B4*SQRT(CKY*CCD*1.E-6)*(T+273)**0.25/C4
      R3CE=-B4*SQRT(CKY*CE*1.E-6)*(T+273)**0.25/C4
      R4=B2*R3CE + B3*R3CC
      C2 = U0/(C1*R4)
C
C-----------------------------------------------------------------------
C
C----------CALCULATION OF COAL RESIDENT IN THE BED WPB
      CALL CALWPB
C     WRITE(IOUT,9753) WPB
 9753 FORMAT(' COAL IN BED, WPB = ',G12.4)
C
C-----------------------------------------------------------------------
C
C----------CALCULATION OF INTEGRAL OF PB(Z) OVER Z WRT Z
      CALL CAPBOR
      F3=WPB*U0*PBOR/C1
      CMR=3*B3*WPB*R3CC*PBOR+3*B2*WPB*R3CE*PBOR
C     CMR = -CMR
      F1=F0+CMR
C     WRITE(IOUT,1357) F0,F1,F3,PBOR,CMR
 1357 FORMAT(' F0,F1,F3,PBOR,CMR = ',5(1X,G11.4))
C
C-----------------------------------------------------------------------
C
C----------CALCULATION OF F0 DASH TO COMPARE WITH F0 AND DETERMINE IF
C       THERE IS SOLIDS BACKMIXING OR NOT
      D3=WPB/WB*RHO+(WB-WPB)/WB*RHOS
      UMF = 0.0079*(D3-RHOG)*DP*DP/CMG
      D1=A*(1-EMF)*FW*U0/(1+FW*EMF)
      D2=D1*B1*UMF/U0
      F0D=D3*(D1-D2)-B3*CMR
      HT = WB/(A*D3*(1-EMF)*(1-EB))
      HEMF = WB/(A*D3*(1-EMF))
C
C-----------------------------------------------------------------------
C
C----------IS F0 LESS THAN F0D - IF YES THERE IS BACKMIXING OTHERWISE SOL . IDS
C----------VELOCITY USE IS SET TO ZERO
      IF(F0.GE.F0D)GO TO 400
      D4=D3*A*EB*FW*(1-EMF)
      D5=(1-EB)*D4
      D6=F0/D4
      D7=EB*FW*CMR/D5
      D8=EMF/(1-EMF)
      D9=1/(B1*(1-EMF))
      D10=1/(EB*FW*(1-EMF))
      USE=(D6+D7+UMF*B1-0.711*SQRT(GR*DB)-U0)/(D8-D9-D10)
      UB=U0+USE*(D8-D9)-UMF*B1+0.711*SQRT(GR*DB)
      UGE=U0-UB+0.711*SQRT(GR*DB)-USE*D9
      EEB=(U0-UGE)/(UB*FW*EMF+UB)
      IF(KOUNT1.GT.1)GO TO 200
      OBJ1(1)=EB-EEB
      GUESS1(1)=EB
```

```
      EB=EB*0.95
      GO TO 100
  200 OBJ1(2)=EB-EEB
      IF(ABS(OBJ1(2)).LT.TOLER)GO TO 300
      GUESS1(2)=EB
      IF(ABS(OBJ1(2)-OBJ1(1)).LT.1.E-5)GO TO 999
      EB=(OBJ1(1)*GUESS1(2)-GUESS1(1)*OBJ1(2))/(OBJ1(1)-OBJ1(2))
      OBJ1(1)=OBJ1(2)
      GUESS1(1)=GUESS1(2)
C     CHECK IF EB IS TOO HIGH IN WHICH CASE  UGE GETS-VE  WHILE U0 IS SM . ALLER
C     THAN U0D.
      U0D=B1*(1+FW*EMF)*UMF/(FW*EMF)+((1+FW*EMF)*F0)/(D3*A*(1-EMF)*FW)
     ++EB*(1+FW*EMF)*CMR/(D3*A*(1-EB)*(1-EMF))
      IF((UGE.LE. 0.0).AND.(U0.LE. U0D)) GO TO 1490
      GO TO 100
  400 UGE=UMF*B1
      U0=U0-UMF*B1+0.711*SQRT(GR*DB)
      FC=F0-D3*A*U0*EB*FW*(1-EMF)+B3*CMR
      EEB=(U0-UGE)/(U0*(1+FW*EMF))
      IF(KOUNT1.GT.1)GO TO 500
      OBJ1(1)=EB-EEB
      GUESS1(1)=EB
      EB=EB*0.95
      GO TO 100
C-----------------------------------------------------------------------
C
  500 OBJ1(2)=EB-EEB
      GUESS1(2)=EB
      IF(ABS(OBJ1(2)).LT.TOLER)GO TO 300
      IF(ABS(OBJ1(2)-OBJ1(1)).LT.1.E-5)GO TO 999
      EB=(OBJ1(1)*GUESS1(2)-GUESS1(1)*OBJ1(2))/(OBJ1(1)-OBJ1(2))
      OBJ1(1)=OBJ1(2)
      GUESS1(1)=GUESS1(2)
      GO TO 100
C----------POSSIBILITY OF GAS BACKMIXING IN THE FLUIDIZED BED AND SOLUTI . ON OF
C----------CLOUD-WAKE AND BUBBLE PHASE DIFFERENTIAL EQUATIONS TO DETERMI . NE
C----------OXYGEN CONCENTRATIONS IN THE FLUIDIZED BED UNDER BACKMIXING
C----------OR NO BACKMIXING CONDITIONS
  300 CONTINUE
      U0D=B1*(1+FW*EMF)*UMF/(FW*EMF)+((1+FW*EMF)*F0)/(D3*A*(1-EMF)*FW)
     ++EB*(1+FW*EMF)*CMR/(D3*A*(1-EB)*(1-EMF))
      CKBC=4.5*UMF/DB+5.85*SQRT(DIF)*GR**0.25/DB**1.25
      CKCE=6.78*SQRT(DIF*EMF*UB/DB**3)
       UGB=EB*UB
      A1=EB/UGB
      A2=EB/(UGB*FW*EMF)
      A7 = -1
      A3=3.*B3*A7*WPB*R3CC*PBOR/(A*HT*EB*CMC)*C3
      A11=-A1*CKBC
      A12=A1*CKBC
      A21=A2*CKBC
      A22=-A2*CKCE-A2*CKBC
      A23=CE*A2*CKCE-A2*A3
C-----------------------------------------------------------------------
C
C----------IF U0 IS GREATER THAN U0D THEN THERE IS GAS BACKMIXING OTHER-
C----------WISE THE GAS IN EMULSION PHASE IS MOVING UPWARDS
      IF(U0.LE.U0D)GO TO 700
```

```
C
C-----------------------------------------------------------------------
C
C----------BOUNDARY CONDITIONS FOR GAS BACKMIXING
      CB0=(U0*C0-UGE*CE)/(U0-UGE)
      CC0=CB0
      GO TO 800
C
C-----------------------------------------------------------------------
C
C----------BOUNDARY CONDITIONS FOR NO GAS BACKMIXING
 700  CC0=C0
      CB0=C0
 800  CALL CCHCBH
C
C-----------------------------------------------------------------------
      IF(U0.LE.U0D)GO TO 900
      IF (KOUNT3.GT.1)GO TO 110
      BC1=A*U0*C0-A*U0/(1+FW*EMF)*(CBH+FW*EMF*CCH)+(3*R3CC*B3*WPB/CMC+3*
     *B2*WPB*R3CE/CMC)*PBOR*C3
      OBJ(1)=BC1
      GUESS(1)=CE
      CE=CE*0.95
      GO TO 210
 110  OBJ(2)=BC1
      IF(ABS(OBJ(2)).LT.TOLER)GO TO 410
      GUESS(2)=CE
      IF(ABS(OBJ(2)-OBJ(1)).LT.1.E-5) GO TO 999
      CE=(OBJ(1)*GUESS(2)-GUESS(1)*OBJ(2))/(OBJ(1)-OBJ(2))
      IF(CE.LT.0.) CE=0.
      OBJ(1)=OBJ(2)
      GUESS(1)=GUESS(2)
      GO TO 210
 900  UGC = EB*FW*EMF*UB
      BC2=U0*A*C0-UGE*A*CE-UGB*A*CBH-UGC*A*CCH+(B3*R3CC+B2*R3CE)*
     ^PBOR*C3*WPB*3.0/CMC
      IF (KOUNT3.GT.1)GO TO 510
      OBJ(1)=BC2
      GUESS(1)=CE
      CE=CE*0.95
      GO TO 210
 510  OBJ(2)=BC2
      GUESS(2)=CE
      IF(ABS(OBJ(2)).LT.TOLER2)GO TO 410
      IF(ABS(OBJ(2)-OBJ(1)).LT.1.E-9)GO TO 999
      CE=(OBJ(1)*GUESS(2)-GUESS(1)*OBJ(2))/(OBJ(1)-OBJ(2))
      IF(CE.LT.0.) CE=0.
      OBJ(1)=OBJ(2)
      GUESS(1)=GUESS(2)
      GO TO 210
 899  WRITE(IOUT,8999)
 999  WRITE(IOUT,9999)
 410  CONTINUE
      CBB = (CCH*UB*EB*FW*EMF+CBH*UB*EB+UGE*CE)/U0
C
C-----------------------------------------------------------------------
C
C     DETERMINATION OF OXYGEN CONSUMPTION RATE.
      QOUT=Q0+VMOIST
      COUT=CBB
```

```
      COSTP = (CBB*(T+273.))/(298.*P)*2240.
      O2RATE=COIN*QIN-COUT*QOUT
      POWER = O2RATE*23700.*100./5.5951
      O2RM2 = O2RATE/A
      WRITE(IOUT,9103) POWER,O2RM2
 9103 FORMAT(' THERMAL POWER = ',G11.4,' KW',/
     +,' O2 CONSUMPTION RATE/M2 ',G11.4,' KMOL/M2')
 1110 FORMAT(' ELUTRIATED COAL KG/S = ',2E15.7)
C     WRITE(IOUT,1100)CBH,CCH,CE,HT,UB,UGE,EB,FC,CMR
 1100 FORMAT(' CBH,CCH,CE,HT,UB,UGE,EB,FC,CMR',/,9(1X,G12.4))
C     WRITE(IOUT,9100) CBB
 9100 FORMAT(' EXIT O2 CONC KGMOL/M3 = ',G15.4)
 9999 FORMAT(16H KOUNT1 EXCEEDED)
 8999 FORMAT(16H KOUNT1 EXCEEDED)
 6100 FORMAT(F30.10,I3)
C
C-----------------------------------------------------------------------
C
C---------- DECREASE INTEGRATION TOLERANCE FOR LAST ITERATION
      IF(TOL.EQ.TOL2) GO TO 1490
      TOL = TOL2
      TOLER = TOLER3
      GO TO 100
C
C-----------------------------------------------------------------------
C
C---------- CALCULATE SIZE DISTRIBUTION OF COAL IN BED & ELUTRIATED
 1490 DR = (ZMAX-ZMIN)/30.
      WRITE(IOUT,3100)KOUNT3,CE,OBJ(2)
      WRITE(IOUT,5100)KOUNT1,EB,OBJ1(2)
      WRITE(IOUT,9253) WPB
      WRITE(IOUT,1357) F0,F1,F3,PBOR,CMR
      WRITE(IOUT,3101)UMF,RHOC,CMG,U0
      WRITE(IOUT,4100)CKY,R3CE,R3CC,R4,WPB,CMR,F0,F0D
      WRITE(IOUT,7100)USE,UB,UGB,EEB
      WRITE(IOUT,2100)F2,CE,CCH,HT,UB,UGC,EB,FC,CMR
      WRITE(IOUT,8100)U0,U0D,CB0,C0,CCH,CBH
      WRITE(IOUT,1100)CBH,CCH,CE,HT,UB,UGE,EB,FC,CMR
      WRITE(IOUT,9100) CBB
      WRITE(IOUT,9101) O2RATE
      WRITE(IOUT,9102) COSTP
 9102 FORMAT(' PERCENT O2 @STP = ',F6.2)
 9101 FORMAT(' OXYGEN CONSUMPTION RATE =',E15.7)
      WRITE(6,1) HT,QR1,QR2
      WRITE(6,9895)A11,A12,A21,A22
 9895 FORMAT('    A11,A12,A21,A22 = ',4E15.7)
 1    FORMAT(' HT,QR1,QR2 = ',3E15.7)
      WRITE(6,9995) CHQCC0,CHQCB0
 9995 FORMAT(' CHQCC0,CHQCB0 = ',2E15.7)
      DO 1500 I=1,31
      RR(I) = (I-1)*DR + ZMIN
      PBR(I) = -F0*FUNC2(RR(I))/(WPB*R4)
      P1R(I) = U0*WPB*PBR(I)/(C1*F3*RR(I))
 1500 CONTINUE
      CALL GSPN(31,RR,P1R,RS,2,0.,0.,0.,0.,0.,1.,0.,0.,TEMP)
 3111 CONTINUE
      Q=Q+0.01
 3112 CONTINUE
      NCALL=1
      STOP
```

```
      SUBROUTINE CCHCBH
C       THIS SUBROUTINE CALCULATES THE OXYGEN CONCENTRATION FOR THE
C       CLOUD-WAKE AND BUBBLE PHASE AT THE EXIT POINT FROM THE FB
      DIMENSION OBJ(2),GUESS(2),TEMP(31),PBR(51)
      COMMON TOL,HMIN,ZMIN,ZMAX,B1,B2,B3,C1,C2,C3,R4,HT,T,C0,CKY,
     +CCH,CE,F0,WPB,PBOR,CMR,A11,A12,A21,A22,A23,CC0,CB0,CBH,U0,
     1ISTAGE
      COMMON /COMM1/ WB,Q,F1,CBB,F0D,U0D,SBM,GBM,QR1,QR2,CHQCC0,CHQCB0,
     1NSKRYF,NB,NH,NCALL
      COMMON /DISTRB/ SIZE(9),FRACT(9),SPLINE(9),RR(31),P1R(31),RS(31)
C----------BUBBLE PHASE OXYGEN CONCENTRATION
      QR1=((A11+A22)+SQRT((A11+A22)**2-4.0*(A11*A22-A21*A12)))/2.0
      QR2=((A11+A22)-SQRT((A11+A22)**2-4.0*(A11*A22-A21*A12)))/2.0
       A8=QR1*HT
       A9=QR2*HT
         IF(ABS(A8).GT. 1.0E+02) A8=-1.0E+02
         IF(ABS(A9).GT. 1.0E+02) A9=-1.0E+02
      A4=A12*A23/(QR1*QR2)
        A5=(CB0*QR1*(QR1-A22)+A12*CC0*QR1+A12*A23)/(QR1*(QR1-QR2))
      A6=(CB0*QR2*(QR2-A22)+A12*CC0*QR2+A12*A23)/(QR2*(QR2-QR1))
      CBH=A5*EXP(A8)+A6*EXP(A9)+A4
C----------THE CLOUD PHASE OXYGEN CONCENTRATION
      S1=-A11*A23/(QR1*QR2)
      S2=(CC0*QR1*(QR1-A11)+A21*QR1*CB0+A23*(QR1-A11))/(QR1*(QR1-
     ^QR2))
      S3=(CC0*QR2*(QR2-A11)+A21*CB0*QR2+A23*(QR2-A11))/(QR2*(QR2-
     ^QR1))
      CCH=S2*EXP(A8)+S3*EXP(A9)+S1
      CHQCC0=S2+S3+S1
      CHQCB0=A5+A6+A4
      IF(CCH.LT. 0.0E+00)CCH=0.0E+00
      IF(CBH.LT. 0.0E+00) CBH=0.0E+00
      RETURN
      END
```

```
      SUBROUTINE CALWPB
C       THIS SUBROUTINE CALCULATES THE COAL RESIDENT IN THE FB
      EXTERNAL FUNC2
      COMMON TOL,HMIN,ZMIN,ZMAX,B1,B2,B3,C1,C2,C3,R4,HT,T,C0,CKY,
     +CCH,CE,F0,WPB,PBOR,CMR,A11,A12,A21,A22,A23,CC0,CB0,CBH,U0
      ZA = 0.5*(ZMIN+ZMAX)
      CALL INTEG2(ZA,ZMIN,FUNC2,ANSW,TOL)
      CALL INTEG2(ZA,ZMAX,FUNC2,ANS,TOL)
      WPB=-(ANS-ANSW)*F0/R4
```

```
459.            END
460.            FUNCTION FUNC2 (Z)
461.            EXTERNAL FUNC3
462.            DIMENSION TIME(7)
463.            COMMON TOL,HMIN,ZMIN,ZMAX,B1,B2,B3,C1,C2,C3,R4,HT,T,C0,CKY,
464.           +CCH,CE,F0,WPB,PBOR,CMR,A11,A12,A21,A22,A23,CC0,CB0,CBH,U0
465.            COMMON/VAR/ZZ,ZZZ
466.            ZZZ = Z
467.            ZZ=Z
468.            CALL INTEG3(Z,ZMAX,FUNC3,ANSW,TOL)
469.            FUNC2=ANSW
470.        6   FORMAT(5(2X,G10.3))
471.            RETURN
472.            END
473.            FUNCTION FUNC3(SIG)
474.            DIMENSION TIME(7)
475.            COMMON TOL,HMIN,ZMIN,ZMAX,B1,B2,B3,C1,C2,C3,R4,HT,T,C0,CKY,
476.           +CCH,CE,F0,WPB,PBOR,CMR,A11,A12,A21,A22,A23,CC0,CB0,CBH,U0,
477.           1ISTAGE
478.            COMMON/VAR/Z,ZZZ
479.            COMMON /DISTRB/ SIZE(9),FRACT(9),SPLINE(9),RR(31),P1R(31),RS(31)
480.            IF(ISTAGE.EQ. 1) P0Z = SPNDER(9,SIZE,FRACT,SPLINE,SIG)
481.            IF(ISTAGE.EQ. 2) P0Z=ESPN(31,RR,P1R,RS,SIG)
482.            FUNC3 = P0Z*(SIG/Z)**(C2-3.)
483.        2   FORMAT(9(2X,G10.3))
484.            RETURN
485.            END
486.            SUBROUTINE CAPBOR
487.        C     THIS SUBROUTINE CALCULATES THE INTEGRAL OF PBOR DIVIDED BY THE
488.        C     PARTICLE RADIUS R
489.            EXTERNAL FUNC4
490.            COMMON TOL,HMIN,ZMIN,ZMAX,B1,B2,B3,C1,C2,C3,R4,HT,T,C0,CKY,
491.           +CCH,CE,F0,WPB,PBOR,CMR,A11,A12,A21,A22,A23,CC0,CB0,CBH,U0
492.            CALL INTEG4(ZMIN,ZMAX,FUNC4,ANSW,TOL)
493.            PBOR=-ANSW*F0/(R4*WPB)
```

```
      FUNCTION FUNC4(Z)
      FUNC4 = FUNC2(Z)/Z
      RETURN
      END
C      SUBROUTINES INTEG2,INTEG3,INTEG4 ARE USED TO INTEGRATE THE
C      MASS BALANCE EQUATIONS ACROSS THE HEIGHT OF THE FB



      SUBROUTINE INTEG2(A,B,SUB,ANSWER,EPS)
      DIMENSION W(20,20)
      CC = B
      H = B-A
      ANSWER=0.
      IF(H.EQ.0.)RETURN
      K = 0
      EN = SUB(A)
      F = SUB(B)
      IF(EPS.LE.0.) STOP 1111
      TOLL = 0.18*EPS
      TOLU = 0.22*EPS
      IF(ABS(F/EN).GT.EPS) GO TO 130
      AA = A
      BB = B
  110 CC = 0.5*(AA+BB)
      G = CC- A
      FF = SUB(CC)
      RATIO = ABS((H-G)*(F+FF)/(G*(F+EN)))
      IF(RATIO.GE.TOLL) GO TO 120
      BB = CC
      GO TO 110
  120 IF(RATIO.LE.TOLU) GO TO 130
      AA = CC
      GO TO 110
  130 CONTINUE
      H = CC - A
      ANSWER = 0.
      IF(H.EQ.0.) RETURN
      F = FF
      W(1,1) =  (F+EN)*H*0.5
    4 K = K+1
      IF(K.GE.20) GO TO 6
      H = 0.5*H
      SIG = 0.
      M = 2**(K-1)
```

```
      J1 = 2*J-1
      XX = A+J1*H
      F = SUB(XX)
    1 SIG = SIG+F
      W(K+1,1) = W(K,1)*0.5 + H*SIG
      DO 2 L=1,K
      IU = K+1-L
      IV = L+1
    2 W(IU,IV) = (4.**(IV-1)*W(IU+1,IV-1)-W(IU,IV-1))/(4.**(IV-1)-1.)
      WP = ABS(W(IU,IV))
      WQ = ABS(W(IU,IV-1))
      IF(WP.LT.1.E-12.AND.WQ.LT.1.E-12) GO TO 3
      WW = (W(IU,IV)-W(IU,IV-1))/W(IU,IV)
      IF(ABS(WW)-EPS)3,3,4
    3 ANSWER = W(1,IV)
      ROMINT = W(1,IV)
      RETURN
    6 WRITE(6,5)
    5 FORMAT(' INTEG2 - NO CONVERGENCE AFTER 20 ITERATIONS')
      GO TO 3
      END
```

```
      SUBROUTINE INTEG3(A,B,SUB,ANSWER,EPS)
      DIMENSION W(20,20)
      CC = B
      H = B-A
      ANSWER=0.
      IF(H.EQ.0.)RETURN
      K = 0
      EN = SUB(A)
      F = SUB(B)
      IF(EPS.LE.0.) STOP 1111
      TOLL = 0.18*EPS
      TOLU = 0.22*EPS
      IF(ABS(F/EN).GT.EPS) GO TO 130
      AA = A
      BB = B
  110 CC = 0.5*(AA+BB)
      G = CC- A
      FF = SUB(CC)
      RATIO = ABS((H-G)*(F+FF)/(G*(F+EN)))
      IF(RATIO.GE.TOLL) GO TO 120
      BB = CC
      GO TO 110
  120 IF(RATIO.LE.TOLU) GO TO 130
      AA = CC
      GO TO 110
  130 CONTINUE
      H = CC - A
      ANSWER = 0.
      IF(H.EQ.0.) RETURN
      F = FF
```

```
      IF(K.GE.20) GO TO 6
      H = 0.5*H
      SIG = 0.
      M = 2**(K-1)
      DO 1 J=1,M
      J1 = 2*J-1
      XX = A+J1*H
      F = SUB(XX)
    1 SIG = SIG+F
      W(K+1,1) = W(K,1)*0.5 + H*SIG
      DO 2 L=1,K
      IU = K+1-L
      IV = L+1
    2 W(IU,IV) = (4.**(IV-1)*W(IU+1,IV-1)-W(IU,IV-1))/(4.**(IV-1)-1.)
      WP = ABS(W(IU,IV))
      WQ = ABS(W(IU,IV-1))
      IF(WP.LT.1.E-12.AND.WQ.LT.1.E-12) GO TO 3
      WW = (W(IU,IV)-W(IU,IV-1))/W(IU,IV)
      IF(ABS(WW)-EPS)3,3,4
    3 ANSWER = W(1,IV)
      ROMINT = W(1,IV)
      RETURN
    6 WRITE(6,5)
    5 FORMAT(' INTEG3 - NO CONVERGENCE AFTER 20 ITERATIONS')
      GO TO 3
      END
```

```
      SUBROUTINE INTEG4(A,B,SUB,ANSWER,EPS)
      DIMENSION W(20,20)
      CC = B
      H = B-A
      ANSWER=0.
      IF(H.EQ.0.)RETURN
      K = 0
      EN = SUB(A)
      F = SUB(B)
      IF(EPS.LE.0.) STOP 1111
      TOLL = 0.18*EPS
      TOLU = 0.22*EPS
      IF(ABS(F/EN).GT.EPS) GO TO 130
      AA = A
      BB = B
  110 CC = 0.5*(AA+BB)
      G = CC- A
      FF = SUB(CC)
      RATIO = ABS((H-G)*(F+FF)/(G*(F+EN)))
      IF(RATIO.GE.TOLL) GO TO 120
      BB = CC
      GO TO 110
  120 IF(RATIO.LE.TOLU) GO TO 130
      AA = CC
```

```
      130   CONTINUE
            H = CC - A
            ANSWER = 0.
            IF(H.EQ.0.) RETURN
            F = FF
            W(1,1) =  (F+EN)*H*0.5
      4     K = K+1
            IF(K.GE.20) GO TO 6
            H = 0.5*H
            SIC = 0.
            M = 2**(K-1)
            DO 1 J=1,M
            J1 = 2*J-1
            XX = A+J1*H
            F = SUB(XX)
      1     SIC = SIC+F
            W(K+1,1) = W(K,1)*0.5 + H*SIC
            DO 2 L=1,K
            IU = K+1-L
            IV = L+1
      2     W(IU,IV) = (4.**(IV-1)*W(IU+1,IV-1)-W(IU,IV-1))/(4.**(IV-1)-1.)
            WP = ABS(W(IU,IV))
            WQ = ABS(W(IU,IV-1))
            IF(WP.LT.1.E-12.AND.WQ.LT.1.E-12) GO TO 3
            WW = (W(IU,IV)-W(IU,IV-1))/W(IU,IV)
            IF(ABS(WW)-EPS)3,3,4
      3     ANSWER = W(1,IV)
            ROMINT = W(1,IV)
            RETURN
      6     WRITE(6,5)
      5     FORMAT(' INTEG4 - NO CONVERGENCE AFTER 20 ITERATIONS')
            GO TO 3
            END
```

```
            SUBROUTINE CSPN(N,X,Y,S,IFLG,AB,BB,CB,DB,AE,BE,CE,DE,C)
            DIMENSION X(1),Y(1),C(1),S(1)
C-----------------------------------------------------------------------
C
C     ---- PURPOSE ----
C
C     TO FIT A CUBIC SPLINE INTERPOLATION FUNCTION TO A SET OF POINTS.TW . O TYPES
C     OF END CONDITION ARE PROVIDED FOR ; A - THE SPLINE BECOMES A PARAB . OLA OVER
C     THE END INTERVAL ; B - THE SPLINE OBEYS THE RELATIONSHIP
C                          A*(D2Y/DX2) + B*(DY/DX) + C*Y = D
C     AT THE END POINT.
C
C     ---- ARGUMENTS ----
C
C     N              - NUMBER OF POINTS IN X AND Y ARRAYS.
C     X              - ARRAY CONTAINING THE VALUES OF THE INDEPENDENT VARIA . BLE AT
C                      THE N POINTS. THESE MUST BE IN ORDER OF INCREASING V . ALUE.
```

```
C                 PONDING TO THE VALUES IN THE X ARRAY.
C       S         - ARRAY IN WHICH THE N SPLINE COEFFICIENTS ARE RETURNE . D.
C       IFLG      - A FLAG WORD WHICH INDICATES WHICH END CONDITIONS WIL . L BE
C                 USED ACCORDING TO THE FOLLOWING TABLE -
C                   0 - PARABOLIC CONDITION AT BOTH ENDS
C                   1 - SPECIFIED RELATIONSHIP AT LOWER END, PARABOLA AT .  UPPER.
C                   2 - PARABOLA AT LOWER END, SPECIFIED RELATIONSHIP AT .  UPPER.
C                   3 - SPECIFIED RELATIONSHIP AT BOTH ENDS.
C       AB,BB,CB,DB - COEFFICIENTS FOR THE LOWER END CONDITION (NOT USED F . OR
C                 IFLG = 0 OR 2)
C       AE,BE,CE,DE - COEFFICIENTS FOR THE UPPER END CONDITION (NOT USED F . OR
C                 IFLG = 0 OR 1)
C       C         - A WORKING ARRAY USED FOR STORAGE OF INTERMEDIATE RES . ULTS.
C
C       ---- NB ----  THE ARRAYS X,Y,S AND C MUST BE DIMENSIONED AT LEAST  . N IN THE
C                 CALLING PROGRAM.
C
C-------------------------------------------------------------- . -------
C
      DATA IO/3/
      IF(N.GT.2) GO TO 2
      WRITE(IO,1)
 1    FORMAT(34HSPLINE MUST HAVE AT LEAST 3 POINTS)
      STOP
C---------- FIRST POINT
 2    AI = X(2)-X(1)
      PI = (Y(2)-Y(1))/AI
      NM1 = N-1
      IB = 1
      IF(IFLG.EQ.1.OR.IFLG.EQ.3) GO TO 3
C---------- PARABOLA
      S(1) = -1.
      C(1) = 0.
      DI = -AI
      CI = 0.
      GO TO 4
C----------SPECIFIED RELATIONSHIP
 3    WO = AB-BB*AI/3.
      S(1) = -BB*AI/(6.*WO)
      C(1) = (DB-CB*Y(1)-BB*PI)/WO
      DI = AI*S(1)
      CI = AI*C(1)
C----------- INTERIOR POINTS
 4    DO 10 I=2,NM1
      AI1 = X(I+1)-X(I)
      Z = 2.*(AI1+AI)-DI
      PI1 = (Y(I+1)-Y(I))/AI1
      C(I) = (6.*(PI1-PI)-CI)/Z
      CI = C(I)*AI1
      PI = PI1
      S(I) = AI1/Z
      DI = S(I)*AI1
 10   AI = AI1
C---------- LAST POINT
      IF(IFLG.LT.2) GO TO 11
C---------- SPECIFIED RELATIONSHIP
      DI = DE-CE*Y(N)-BE*(Y(N)-Y(N-1))/AI
      DI = 6.*DI/AI - BE*C(N-1)
      Z = 6.*AE/AI + 2.*BE - BE*S(N-1)
```

```
      GO TO 12
C---------- PARABOLA
 11   S(N) = C(N-1)/(1.+S(N-1))
C---------- BACK SUBSTITUTION OF THOMAS ALGORITHM
 12   J = N
      DO 20 I = IB,NM1
      J = J-1
 20   S(J) = C(J)-S(J)*S(J+1)
      RETURN
      END
```

```
      FUNCTION SPNDER(N,X,Y,S,XX)
      DIMENSION X(1),Y(1),S(1)
C
C-----------------------------------------------------------------------
C
C     A SUB-PROGRAM TO CALCULATE THE DERIVATIVE OF A SPLINE INTERPOLATIO . N
C      FUNTION. THE SPLINE INTERPOLATES BETWEEN THE POINTS CONTAINED IN
C     THE FIRST N PLACES OF THE X AND Y ARRAYS. THERE ARE N SPLINE COEFF . -
C     ICIENTS IN THE S ARRAY.THE DERIVATIVE IS EVALUATED AT XX.
C
C-----------------------------------------------------------------------
C
C--------- FIND INTERVAL CONTAINING XX
C
      IF(XX.LT.X(1)) GO TO 30
      IF(XX.GT.X(N)) GO TO 50
      I = 1
      IU = N
 10   II = I+(IU-I)/2
      IF(II.EQ.I) GO TO 40
      IF(XX.LT.X(II)) GO TO 20
      I = II
      GO TO 10
 20   IU = II
      GO TO 10
C
C--------- XX IS BEFORE X(1)
C
 30   T = X(1)-X(2)
      SPNDER = (Y(1)-Y(2))/T+T*(S(2)+2.*S(1))/6.+2.*S(1)*(XX-X(1))
      RETURN
C
C--------- XX IS BETWEEN X(I) AND X(I+1)
C
 40   T = X(I+1)-X(I)
      T1 = XX-X(I)
      T2 = X(I+1)-XX
      SPNDER = 0.5*(S(I+1)*T1*T1-S(I)*T2*T2)/T + (Y(I+1)-Y(I))/T
      SPNDER = SPNDER - 0.166667*(S(I+1)-S(I))*T
      RETURN
C
```

```
C---------- XX IS AFTER X(N)
C
 50     T = X(N)-X(N-1)
        SPNDER = (Y(N)-Y(N-1))/T+T*(2.*S(N)+S(N-1))/6.+2.*S(N)*(XX-X(N))
        RETURN
        END



        BLOCK DATA
        COMMON /DISTRB/ SIZE(9),FRACT(9),SPLINE(9),RR(31),P1R(31),RS(31)
        DATA SIZE/1.E-8,.00015,.0003,.0006,.00118,.00236,.00475,.0063,.01/
        DATA FRACT/0.,.1209,.2106,.3418,.5706,.682,.8452,.8981,1./
        END
```

APPENDIX 10

MATHEMATICAL MODEL FOR THE TRANSFER OF HEAT FROM SOLIDS IN AN FB TO IMMERSED COOLING COILS. LISTING OF COMPUTER PROGRAM

1. DERIVATION OF MATHEMATICAL MODEL

The heat and mass balance equation for an element (dl) of the cooling coil shown below can be written as follows

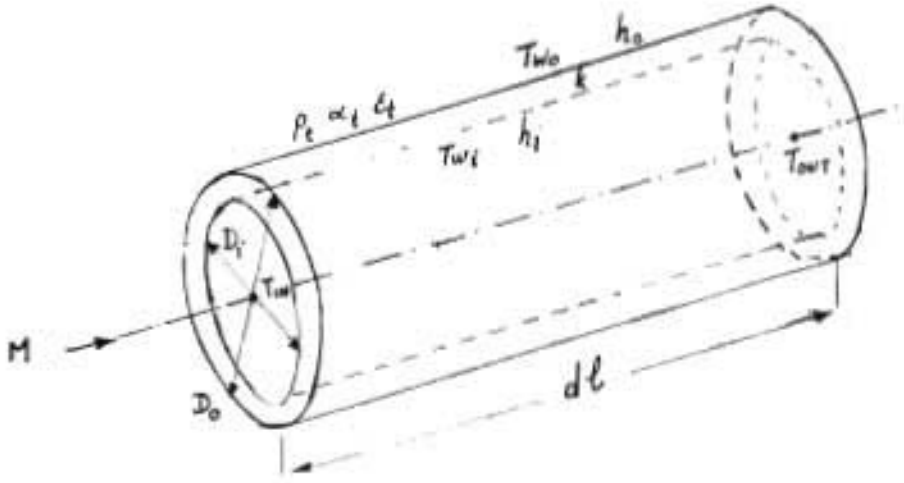

$$dQ = h_o \pi dl D_o (T_B - T_{w_o}) + \pi dl D_o \sigma [(\epsilon_s \alpha_t T_B^4 + \rho_t \epsilon_t T_B^4 \rho_s \alpha_t + \epsilon_s T_B^4 \rho_s^2 \rho_t^2 \alpha_t^2 + \ldots) - (\epsilon_t \alpha_s T_{w_o}^4 + \rho_s \epsilon_t T_{w_o}^4 \rho_t \alpha_s + \epsilon_t T_{w_o}^4 \rho_s^2 \rho_t^2 \alpha_s^2 + \ldots) \quad \text{E.A.10.1.}$$

$$= \frac{2\pi k dl (T_{w_o} - T_{w_i})}{\ln(D_o/D_i)} \quad \text{E.A.10.2.}$$

$$= h_i \pi dl D_i (T_{w_i} - (\frac{T_{in} + T_{out}}{2})) \quad \text{E.A.10.3.}$$

$$= MCp(T_{out} - T_{in}) \quad \text{E.A.10.4.}$$

where dQ (w) is the heat transferred to the element due to radiation and convection and M is the coolant flowrate (m^3/s for air, kg/s for steam and water)

Since the sand and coil are opaque, $\alpha + \rho = 1$. If the surfaces are assumed to be grey then $\alpha = \varepsilon$ even when the system is not at thermal equilibrium.

E.A.10.1 thus simplifies to

$$dQ = h_o \pi d l D_o (T_B - T_{w_o}) + \pi D_o dl [\varepsilon_s \varepsilon_t T_B^4 (1+(1-\varepsilon_t)(1-\varepsilon_s) + (1-\varepsilon_t)^2(1-\varepsilon_s)^2 \varepsilon_t + \ldots) - \varepsilon_s \varepsilon_t T_{w_o}^4 (1+(1-\varepsilon_t)(1-\varepsilon_s) + (1-\varepsilon_t)^2(1-\varepsilon_s)^2 \varepsilon_s + \ldots)]$$

$$= h_o \pi d l D_o (T_B - T_{w_o}) + \pi d l D_o [\varepsilon_s \varepsilon_t T_B^4 (1+\sum_{n=1}^{\infty}(1-\varepsilon_t)^n(1-\varepsilon_s)^n \varepsilon_t^{n-1}) - \varepsilon_s \varepsilon_t T_{w_o}^4 (1+\sum_{n=1}^{\infty}(1-\varepsilon_t)^n(1-\varepsilon_s)^n \varepsilon_s^{n-1}] \quad \text{E.A.10.5.}$$

E.A.10.5 can be further simplified since

$$\sum_{n=1}^{\infty}(1-\varepsilon_t)^n(1-\varepsilon_s)^n \varepsilon_t^{n-1} = \frac{(1-\varepsilon_t)(1-\varepsilon_s)}{1-(1-\varepsilon_t)(1-\varepsilon_s)\varepsilon_t}$$

and

$$\sum_{n=1}^{\infty}(1-\varepsilon_t)^n(1-\varepsilon_s)^n \varepsilon_s^{n-1} = \frac{(1-\varepsilon_t)(1-\varepsilon_s)}{1-(1-\varepsilon_t)(1-\varepsilon_s)\varepsilon_s}$$

Thus

$$dQ = h_o \pi d l D_o (T_B - T_{w_o}) + \sigma \pi d l D_o (\varepsilon\varepsilon_s T_B^4 - \varepsilon\varepsilon_t T_{w_c}^4) \quad \text{E.A.10.6.}$$

where $\varepsilon\varepsilon_s$ and $\varepsilon\varepsilon_t$ are the effective emissivity of sand and the stainless-steel coil tube respectively, after taking multi-reflection into account.

$$cc_s = \epsilon_s\epsilon_t\left(\frac{1+(1-\epsilon_t)(1-\epsilon_s) - (1-\epsilon_s)(1-\epsilon_t)\epsilon_t}{1-(1-\epsilon_t)(1-\epsilon_s)\epsilon_t}\right) \qquad \text{E.A.10.7.}$$

$$cc_t = \epsilon_s\epsilon_t\left(\frac{1+(1-\epsilon_t)(1-\epsilon_s) - (1-\epsilon_s)(1-\epsilon_t)\epsilon_s}{1-(1-\epsilon_t)(1-\epsilon_s)\epsilon_s}\right) \qquad \text{E.A.10.8.}$$

The total heat removed by the cooling coils is obtained by integrating E.A.10.6 along the length of the coil using a stepwise integration method.

2. EXECUTION OF THE COMPUTER PROGRAM

To execute the computer program, code named FBHEAT, on the departmental computer (CDC 1700), batch disc 2 must be placed on the disc drive and the following data cards must be submitted.

Card	
1	*
2	* FBHEAT
3	TB, TIN, DT, H, ES, ET, HI, K 8 F 10.6
4	DI, DO, L, DL, TOL, M, FTOL, CNTREF 8 F 10.6
5	RUN F 12.6
6	* Z

The computer then requests the values of these variables where

TB	bed temperature (K)
TIN	coolant inlet temperature (K)
DT	use of 1.0 is adequate (K)
H	outside film coefficient - Wender and Cooper correlation $(w/m^2.K)$[60]

ES emissivity of sand[61]

ET emissivity of tubes[61]

HI inside film coefficient ($w/m^2.K$)[62]. If water is used as coolant an internal correlation is used so any real value may be put on the data card. The use of 1.0 is recommended to remind the user that value printed in the programme headings under 'Input data' has not been used

K thermal conductivity of the tube wall ($w/m.K$)[63]. (Although K is a function of temperature the dependence is not strong and an average value may normally be used)

DI tube inside diameter (m)

DO tube outside diameter (m)

L tube length (m)

DL step length along tube (m)

TOL iteration tolerance to which successive estimates of the outlet temperature from a particular element of length must agree in order for the calculation to be considered as having converged. Normally 0.1 is adequate but convergence is still rapid with a value of TOL equal to 0,01

M coolant flowrate, Nm^3/min for air, kg/s for water or steam

FTOL minimum flux below which heat transfer is regarded as insignificant (w/m^2)

CONTREF coolant reference number

1.0 for air

2.0 for water

3.0 for steam

RUN run identification number

3. FLOWCHART OF PROGRAM FBHEAT

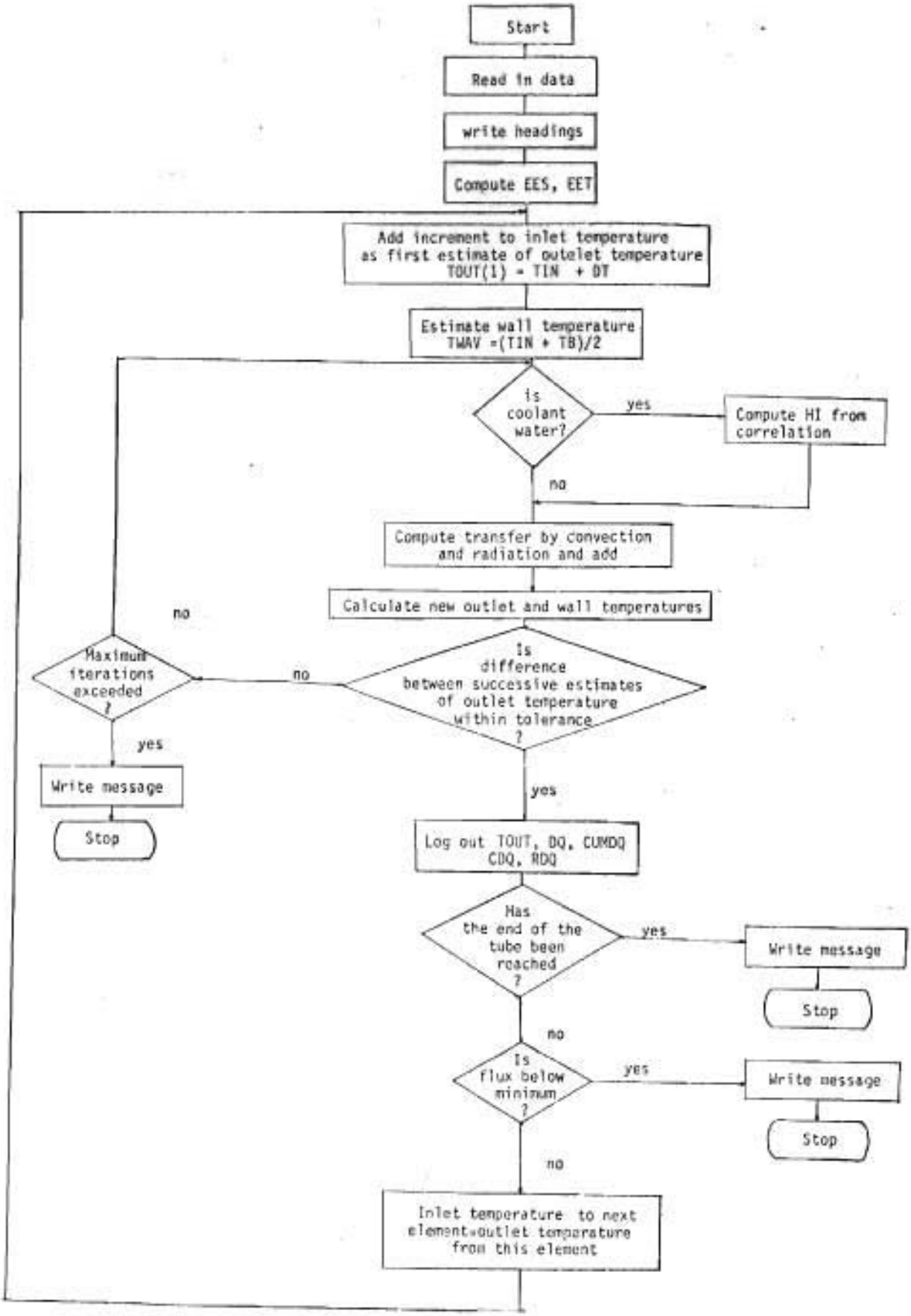

4. COMPLETE LISTING OF PROGRAM FBHEAT AS STORED ON BATCH DISK 2 ON THE CDC 1700 SC COMPUTER IN THE DEPARTMENT OF CHEMICAL ENGINEERING, UNIVERSITY OF NATAL

16 JANUARY 1980.

```
      PROGRAM FBHEAT
C----------THIS PROGRAM COMPUTES HEAT TRANSFER TO A TUBE IMMERSED IN A
C          FLUIDISED BED.  BOTH CONVECTION AND RADIATION ARE CONSIDERED
C          THE SAND AND TUBES ARE ASSUMED TO BE GRAY BODIES I.E.EMISS=
C          IVITY=ABSORBTIVITY EVEN WHEN NOT AT THERMAL EQUILIBRIUM.

C----------SIGNIFICANCE OF SYMBOLS
C----------INPUT AND OUTPUT VARIABLES
C          CNTREF  COOLANT REFERENCE NUMBER.  AIR   1.0
C                                             WATER 2.0
C                                             STEAM 3.0
C          CUMDL  CUMULATIVE LENGTH M
C          CUMDQ  CUMULATIVE HEAT TRANSFERRED W
C          CUMCDQ  CUMULATIVE HEAT TRANSFERRED DUE TO CONVECTION W
C          CUMRDQ  CUMULATIVE HEAT TRANSFERRED DUE TO RADIATION  W
C          DI  TUBE INTERNAL DIAMETER M
C          DL  LENGTH INCREMENT ALONG TUBE M
C          DO  TUBE EXTERNAL DIAMETER M
C          DQ  HEAT TRANSFERRED TO ELEMENT OF TUBE W
C          DT  ESTIMATED TEMP RISE ON FIRST ITERATION ON A PARTICULAR
C              ELEMENT K
C          ES  EMISSIVITY OF SAND
C          ET  EMISSIVITY OF TUBE
C          FTOL  MIN FLUX BELOW WHICH HEAT TRANSFER IS REGARDED AS
C                INSIGNIFICANT
C          H  FILM COEFFICIENT BETWEEN BED AND OUTER TUBE WALL-WENDER
C             AND COOPER CORRELATION. W/M**2.K
C          HI  FILM COEFFICIENT BETWEEN  COOLANT  AND TUBE INNER WALL
C              W/M**2.K
C          K  THERMAL CONDUCTIVITY OF TUBE WALL W/M.K
C          L  TUBE LENGTH M
C          M  COOLANT FLOW;AIR  M**3/MIN@STP;WATER KG/S;STEAM KG/S
C          RUN  RUN IDENTIFICATION
C          TB  BED TEMP K
C          TIN  INLET TEMP K
C          TOL  ITERATION TOLERANCE K
C----------VARIABLES INTERNAL TO THE PROGRAM
C          CDQ  HEAT TRANSFERRED TO ELEMENT BY CONVECTION W
C          CP  SPECIFIC HEAT OF COOLANT;AIR  J/M**3.C
C                                      WATER J/KG.C
C                                      STEAM J/KG.C
C          DITER  DIFFERENCE BETWEEN CONSECUTIVE ESTIMATES OF TOUT(I) K
C          EES  EFFECTIVE EMISSIVITY OF SAND TAKING RE-REFLECTION INTO
C               ACCOUNT.
C          EET  EFFECTIVE EMISSIVITY OF TUBE TAKING RE-REFLECTION INTO
C               ACCOUNT.
C          FLUX  LOCAL HEAT FLUX W/M**2
C          I  ITERATION NUMBER
C          IPR  PRINTER UNIT IDENTIFICATION
C          RDQ  HEAT TRANSFERRED TO ELEMENT BY RADIATION W
C          T  AVERAGE AIR TEMP IN ELEMENT DL K
C          TOUT(I)  OUTLET TEMP FROM ELEMENT DL AT ITERATION I K
C          TWAV  AVERAGE OUTER TUBE WALL TEMP K

      REAL K,L,M
      DIMENSION TOUT(50)

C----------READ IN THE DATA
```

```
      READ(5,100)TB,TIN,DT,H,ES,ET,HI,K,DI,DO,L,DL,TOL,M ,FTOL,CNTREF
      READ(5,101)RUN

C----------WRITE HEADINGS
      IPR=3
      CUMCDQ=0.0
      CUMRDQ=0.0
      CUMDQ=0.0
      CUMDL=0.0
      CDQ=0.0
      RDQ=0.0
      DQ=0.0
      WRITE(IPR,102)RUN
      WRITE(IPR,112)TB,TIN,DT,H,ES,ET,HI,K,DI,DO,L,DL,TOL,M,FTOL
      IF(CNTREF.EQ.1.0)WRITE(IPR,197)M
      IF(CNTREF.EQ.2.0)WRITE(IPR,198)M
      IF(CNTREF.EQ.3.0)WRITE(IPR,199)M
      WRITE(IPR,200)TB,  TIN,DO   ,CUMDQ,CUMDL,CDQ,RDQ

C----------COMPUTE HEAT TRANSFER
      EES=ES*ET*(1.+(1.-ET)*(1.-ES)-(1.-ET)*(1.-ES)*ET)/
     $(1.-(1.-ET)*(1.-ES)*ET)
      EET=ES*ET*(1.+(1.-ET)*(1.-ES)-(1.-ET)*(1.-ES)*ES)/
     $(1.-(1.-ET)*(1.-ES)*ES)
 1    I=1
      TOUT(I)=TIN+DT
      TWAV=(TB+TIN)/2.0
 2    T=(TIN+TOUT(I))/2.0
      IF(CNTREF.EQ.2.0)HI=1063.0*(1.0+0.00293*T)*
     $((M/(785.4*(DI**2.0)))**0.8)/DI**0.2
      CDQ=3.14159*H*DL*DO*(TB-TWAV)/2.0
      RDQ=5.6703E-08*3.14159*DL*DO*(EES*(TB**4.)-EET*(TWAV**4.))
      DQ=CDQ+RDQ

C----------CALCULATE OUTLET TEMP FROM ELEMENT AND WALL TEMP
      T=(TIN+TOUT(I))/2.0
      IF(CNTREF.EQ.1.0)CP=3.114*(6.557+0.1477E-2*T-0.02148E-5*(T**2.))
      IF(CNTREF.EQ.2.0)CP=4186.
      IF(CNTREF.EQ.3.0)CP=2500.
      TWAV=(TIN+TOUT(I))/2.0+DO*(1.0/(3.14159*HI*DI)
     $+(1.0/(2.0*3.14159*K))*ALOG(DO/DI))
      TOUT(I+1)=TIN+DQ/(M*CP)

C----------CHECK IF ITERATIONS HAVE CONVERGED OR MAX NO OF ITERATIONS
C           EXCEEDED
      DITER=ABS(TOUT(I+1)-TOUT(I))
      IF(DITER.LE.TOL)GO TO 5
      IF(I.GE.49)GO TO 8
      I=I+1
      GO TO 2
 5    CUMDQ=CUMDQ+DQ
      CUMDL=CUMDL+DL
      CUMCDQ=CUMCDQ+CDQ
      CUMRDQ=CUMRDQ+RDQ

C----------HAS THE END OF THE TUBE BEEN REACHED BEFORE COOLANT TEMP
C           REACHED BED TEMP
      IF(CUMDL.GE.L)GO TO 7
      WRITE(IPR,500)TOUT(I+1),DO   ,CUMDQ,CUMDL,CDQ,RDQ
```

```
C----------CHECK IF HEAT FLUX HAS DROPPED BELOW MINIMUM
      FLUX=DO    /(3.1416**DO**DL)
      IF(FLUX.LE.FTOL)GO TO 6
      TIN=TOUT(I+1)
      GO TO 1

C----------STOP OPTIONS
 6    WRITE(IPR,600)FLUX,CUMDL
      WRITE(IPR,700)CUMDO,CUMCDO,CUMRDO
      STOP
 7    WRITE(IPR,500)TOUT(I+1),DO,CUMDO,CUMDL
      WRITE(IPR,400)TOUT(I+1)
      WRITE(IPR,700)CUMDO,CUMCDO,CUMRDO
      STOP
 8    WRITE(IPR,300)
      WRITE(IPR,300)
      STOP

C----------FORMATS
 100  FORMAT(8F10.6)
 101  FORMAT(F12.6)
 102  FORMAT(//40X,10HRUN NUMBER,F12.6/)
 112  FORMAT(10H1INPUT DATA/3HTB=,F7.2,4X,4HTIN=,F6.2,4X,3HDT=,F4.2,4X,
     $2HH=,F7.2,4X,3HES=,F4.3,4X,3HET=,F4.3,4X,3HHI=,F7.2/2HK=,F5.2,4X,
     $3HDI=,F6.5,4X,3HDO=,F6.5,4X,2HL=,F6.3,4X,3HDL=,F4.3,4X,4HTOL=,F4.3
     $,4X,2HM=,F5.3,4X,5HFTOL=,F7.3//)
 197  FORMAT(15HCOOLANT IS AIR./28HCOOLING AIR FLOW (NM**3/MIN),F10.6)
 198  FORMAT(17HCOOLANT IS WATER./25HCOOLING WATER FLOW (KG/S),F10.6)
 199  FORMAT(17HCOOLANT IS STEAM./17HSTEAM RATE (KG/S),F10.6)
 200  FORMAT(12HBED TEMP (K),F9.1/
     $/38X,21HCONDITIONS ALONG TUBE//97HTEMPERATURE    HEAT TRANSFERRED
     $TO    CUMULATIVE HEAT    LENGTH    TRANSFER BY    TRANSFER BY/
     $4X,3H(K),10X,16HTHIS ELEMENT (W),5X,15HTRANSFERRED (W),5X,3H(M),6X
     $,14HCONVECTION (W),4X,13HRADIATION (W)/
     $1X,F7.2,12X,F7.3,12X,F9.3,7X,F6.3,5X,F9.3,8X,F8.3)
 300  FORMAT(/31X,34H**********ITERATIONS NOT CONVERGED**********)
 400  FORMAT(6X,56HREACHED END OF TUBE BEFORE COOLANT TEMP REACHED BED T
     $EMP/24X,12HOUTLET TEMP=,F7.2)
 500  FORMAT(1X,F7.2,12X,F7.3,12X,F9.3,7X,F6.3,5X,F9.3,8X,F8.3)
 600  FORMAT(/30HLOCAL HEAT FLUX HAS DROPPED TO,F8.3,30HW/M**2. OPTIMUM
     $TUBE LENGTH IS,F6.2,1HM)
 700  FORMAT(/23HTOTAL HEAT TRANSFERRED=,F9.3,5HWATTS/12X,
     $11HCONVECTION=,F9.3,5HWATTS/13X,10HRADIATION=,F9.3,5HWATTS)
      END
```

REFERENCES

1. NAUDE, D.P. The potential of fluidized bed combustion for industrial steam raising in South Africa. *S.Afr. Mech. Engng* vol. 29, July 1979. pp 243-250.

2. JUDD, M.R., DAWSON, M.F., and ELEFTHERIADES, C.M. Fluidized combustion of high ash coal. SOUTH AFRICAN INSTITUTION OF CHEMICAL ENGINEERS, THIRD NATIONAL MEETING, STELLENBOSCH, SOUTH AFRICA. April 1980. pp 4G1-4G15.

3. DE KOCK, J.W. The South African coal industry. DEPARTMENT OF CHEMICAL AND METALLURGICAL ENGINEERING, UNIVERSITY OF STELLENBOSCH, SOUTH AFRICA, July 1978.

4. EHRLICH, S. History of the development of the fluidized bed boiler. PROCEEDINGS OF THE FOURTH INTERNATIONAL CONFERENCE ON FLUIDIZED BED COMBUSTION MITRE CORP., Virginia, U.S.A. Dec. 1975.

5. GAMBLE, R.L., and WARSHANY, F.R. Commercial development of atmospheric fluidized bed utility steam generators. *ASME and IEEE*. JOINT POWER GENERATION CONFERENCE PORTLAND OREGON, U.S.A. Sep. 1975.

6. BERMAN, I.M. Fluidized bed combustion systems: Progress and outlook. *Power Engng Series 83*, Issue II, Nov. 1979. pp 46-56.

7. DAVIDSON, J.F., HARRISON, D. Fluidization. Academic Press, London, 1971.

8. LEVENSPIEL, O. Chemical reaction engineering, J. Wiley and Sons, N.Y. 1972.

9. SKINNER, D.G. The fluidized combustion of coal M&B Monograph CE/3 Mills and Boon Ltd, London 1971.

10. McLAREN, J., and WILLIAMS, D.F. Combustion efficiency, sulphur retention and heat transfer in pilot plant fluidized-bed combustors. *J. Inst. Fuel*, vol. 42, Aug. 1969. pp 303-308.

11. BOWLING, K. McG., and WATERS, P.L. Fuel processing in fluidized beds. *Br. chem. Engng*, vol. 13, no. 8, 1968. pp 1127-1138.

12. BISHOP, J.W., EHRLICH, S., ROBINSON, E.B., and CHEN, P.S. Status of the direct contact heat transferring fluidized bed boiler ASME WINTER ANNUAL MEETING, paper 68-WA/FU-4, Dec. 1968, pp 1-10.

13. HIGHLEY, M.G., KAYE, W.G., CHIBA, T., NIENOW, A.W., and ROWE, P.N. The application of fluidized combustion to industrial boilers and furnaces. FLUIDIZED COMBUSTION CONFERENCE, SYMPOSIUM SERIES no. 1, vol. 1. London, Sep. 1975, pp B3-1-B3-9.

14. KHARCHENKO, N.V., and MAKHORIN, K.E. The rate of heat transfer between a fluifized bed and an immersed body at high temperatures. *Int. Chem. Engng*, vol. 4, no. 4. Oct. 1964, pp 650-654.

15. HALL, A.M., VAUGHAM, D.A., KRAUSE Jr, H.H., CARLTON, H.F., STICKFORD Jr, G.H., BOARSKI, A.A., and LUCE, R.G. Final Report. U.S. Department of Energy, Contract no. E(49-18)-2325, Dec. 1977.

16. ZELLARS, G.R., ROWE, A.P., and LOWELL, C.E. Erosion/Corrosion of turbine airfoil materials in the high velocity effluent of a pressurized fluidized coal combustor. NASA TECHNICAL PAPER 1274, Jul. 1978.

17. Pressurized fluidized bed combustion. RES. & DEV. Report - United States office of coal research no. 85, Washington D.C., 1973.

18. WRIGHT, S.J., KETLEY, H.C., and HICKMAN, R.G. Heat transfer in fluidized beds of wide size spectrum at elevated temperatures. *J. Inst. Fuel*, vol. 42, Jun. 1969, pp 235-240.

19. ZENZ, F.A. Bubble formation and grid design. TRIPARTITE CHEMICAL ENGINEERING CONFERENCE SYMPOSIUM SERIES NO. 30, Montreal, Canada, Sep. 1968. pp 136-139.

20. BEHIE, L.A., VOEGELIN, B.E., BERGOUGNOU, M.A. The design of fluid bed grids using the orifice equation. *Can. J.Chem. Engng*, vol.

56, Jun. 1978. pp 404-405.

21. WHITEHEAD, A.B., GARTSIDE, G., DENT, D.C. Flow and pressure multidistribution at the distributor level of a gas-solid fluidized bed. *Chem. Engng J.* vol. 1, 1970. pp 175-185.

22. WHITEHEAD, A.B., and DENT, D.C. Behaviour of multiple tuyere assemblies in large fluidized beds. INTERNATIONAL SYMPOSIUM ON FLUIDIZATION ENDHAVEN CONFERENCE. Jun. 1967. pp 802-820.

23. FAKHIMI, S., and HARRISON, D. Multiorifice distributors in fluidized beds: a guide to design Chemeca 70 Butterworths of Australia, 29, 1970.

24. SKF Steel Engineering AB, Hofors. SKF Plasmamelt. Plasma Technology for smelt reduction in crude iron production. Hofors, The Company, 1980.

25. JOHNSON, J.W., and DAVIDSON, J. Reduction of iron ore by the flame smelting process. *J. Iron Steel Inst.* vol. 202, 1964. p 406.

26. BASKAKOV, A.P., and MAKHORIN, K.E. Combustion of natural gas in fluidized beds. FLUIDIZED COMBUSTION CONFERENCE, SYMPOSIUM SERIES NO. 1, vol. 1 London Sep. 1975. pp C3-1-C3-9.

27. BROUGHTON, J. Combustion in shallow fluidized beds. *Applied Energy*, Applied Science Publishers Ltd, England, vol. 1, 1975, pp 61-78.

28. PILLAI, K.K. Premixed gas combustion in shallow fluidized beds. *J. Inst. Fuel*, vol. 49, Dec. 1976. pp 200-205.

29. KNOWLTON, T., and HIRSAN, L. Solids flow control using a non-mechanical L valve. NINTH SYNTHETIC PIPELINE GAS SYMPOSIUM, CHICAGO, ILLINOIS. Chicago, Institute of Gas Technology, Oct/Nov. 1977, 36 pp.

30. KNOWLTON, T., LEUNG, L.S., and HIRSAN, I. The effect of aeration tap location on the performance of a J-valve. FLUIDIZATION

PROCEEDINGS OF THE SECOND ENGINEERING FOUNDATION CONFERENCE, CAMBRIDGE, *Davidson, J.F., and Keairns, D.L. (eds)*. April 1978.

31. JUDD, M.R., DIXON, P.D. The flow of fine dense solids down a vertical standpipe. *AICHE ANNUAL CONFERENCE*, Nov. 1976.

32. KOJABASHIAN, C. The properties of fluidized solids in vertical downflow. M.Sc. Thesis, Cambridge Mass, 1954.

33. LEUNG, L.S. Design of fluidized gas-solids flow in standpipes *Powder Technol.*, 1977, vol. 16, pp 1-6.

34. LEUNG, L.S. Concurrent downflow suspensions in standpipes. PROCEEDINGS OF THE INTERNATIONAL FLUIDIZATION CONFERENCE, PACIFIC GROVE, CALIFORNIA, vol. II, *Keairns D.L. (ed)*, Jun. 1975.

35. MATSEN, J.M. Flow of fluidized solids and bubbles in standpipes and risers. *Powder Technol.* vol. 7, 1973. pp 93-96.

36. ERGUN, S. Fluid flow through packed columns. *Chem. Engng Prog.* vol. 48, no. 2. 1952. pp 89-94.

37. YOON, S.M., KUNII, D. Gas flow and pressure drop through moving beds. *Ind. Engng Chem. Prod. Res. Dev.* vol. 9, no. 4, 1970. pp 559-565.

38. ELEFTHERIADES, C.M., and JUDD, M.R. The design of downcomers joining gas fluidized beds in multistage systems. *Powder Technol.* vol. 21, no. 21, 1978. pp 217-225.

39. JONES, D.R.M., DAVIDSON, J.F. The flow of particles from a fluidized bed through an orifice. *Rheologica Acta*, vol. 4, no. 3, 1965. pp 180-192.

40. BURKETT, R.J., CHALMERS-DIXON, P., MORRIS, P.J., and PYLE, D.L. On the flow of fluidized solids through orifices. *Chem. Engng Sci.*, vol. 26. 1971, p. 405.

41. DE JONG, J.A.H., and HOELEN, Q.E.J.J.M. Concurrent gas and particle flow during pneumatic discharge from a bunker through

an orifice. *Powder Technol.*, 1975, vol. 12, pp 201-208.

42. WALTERS, J.K. A theoretical analysis of stresses in silos with vertical walls. *Chem. Engng Sci.*, 1973, vol. 28, pp 13-21.

43. SPINK, C.D., and NEDDERMAN, R.M. Gravity discharge rate of particles from hoppers. *Powder Technol.* 1978, vol, 21, pp 245-261.

44. MASSIMILLA, L., BETTA, V., and DELLA ROCCA, C. A study of streams of solids flowing from solids-gas fluidized beds. *AIChE J.*, 1961, vol. 7, no. 3, 1961. pp 502-508.

45. STOCKEL, I.H. High speed flow of fluidized solids in changing area. *Chem. Engng Prog., Symp. Ser.*, vol. 58, no. 38, 1962. pp 106-120.

46. DAVIDSON, J.F., and HARRISON, D. Fluidized particles. Cambridge University Press, 1963.

47. FRYER, C., and POTTER, O.E. Countercurrent backmixing model for fluidized bed catalytic reactors. Applicability of simplified solutions. *Ind. Engng Chem. Fundam.* vol. II, no. 3, 1972. pp 338-344.

48. AVEDESIAN, M.M., and DAVIDSON, J.F. Combustion carbon particles in a fluidized bed. *Trans Instn Chem Engng*, vol. 51, 1973. pp 121-131.

49. LEVENSPIEL, O., KUNII, D., and FITZGERAL, T. The processing of solids of changing size in bubbling fluidized beds. *Powder Technol.* no. 2, 1968/69. pp 87-96.

50. CHEN, T.P., SAXENA, S.C. Mathematical modelling of non catalytic solid-gas reactions in fluidized beds. Department of Energy Engineering. University of Illinois 60680. U.S.A. Manuscript, Aug. 1976.

51. SAXENA, S.C., and REHMAT, A. A mathematical model for the continuous combustion of char particles in a fluidized bed. PROCEEDINGS OF THE 15th INTERSOCIETY ENERGY CONVERSION ENGINEERING CONFERENCE, Seatle, U.S.A. vol. 1, Aug. 1980. pp 50-56.

52. DONSI, G., MASSIMILLA, L., MICCIO, M., RUSSO, G., and STECCONI, P. The calculation of carbon load and axial profiles of oxygen concentration in the bed of a fluidized combustor. *Combust. Science and Techol.*, vol. 21, 1979. pp 25-33.

53. GIBBS, B.M., HEDLEY, A.B. A pilot study of large coal combustion in a fluidized bed. 17th INTERNATIONAL SYMPOSIUM ON COMBUSTION, LEEDS, U.K. vol. 17, 1978. pp 211-220.

54. YAGI, S., and KUNII, D. 5th SYMPOSIUM ON COMBUSTION. Reinhold, New York, 1955, pp. 231.

55. ELEFTHERIADES, C.M. Drawings nos GW-241077 (1 & 2) JG 230178. Dept of Chem. Engng, Univ. of Natal, Durban. South Africa, 1978.

56. ELEFTHERIADES, C.M. Drawings nos CH2-9, CH2-10. Dept of Chem. Engng. University of Natal, Durban. South Africa, 1979.

57. SGS Engineering Inspection Company, Durban, South Africa. Pressure test certificates:

(a) Main Combustor. Serial no. 71703-A. Inspection no. EN1480, 1978/03/13.

(b) Coal Hopper. Serial no. 71703-B, Inspection no. EN1481, 1978/03/15.

(c) Coal Hopper, Serial no. 1084, Inspection no. EN96, 1979/05/28.

(d) CYCLONE, Serial no. 1085, Inspection no. EN94, 1975/05/28.

58. JUDD, M.R., ELEFTHERIADES, C.M., and DAWSON, M.F. Combustion of coalin a multistage pressurized fluidized bed. INSTITUTE OF ENERGY, FLUIDIZED SYSTEMS: SYSTEMS AND APPLICATIONS CONFERENCE, LONDON, Nov. 1980, p. III-4-1, III-4-7.

59. STANMORE, B.R., and JUNG, K. The burnout rates of brown coal char particles in fluidized bed combustors. *Trans. I. Chem. E.*, vol. 58, 1980. pp. 66-68.

60. WENDER, L., and COPPER, G.T. Heat transfer between Fluidized solids Beds and boundary surfaces - Correlation of data. *AIChE Journal*, vol. 4, no. 1, pp 15-23.

61. HOTTEL, H.C., and SAROFIM, A.F. Radiative transfer. New York, McGraw Hill, 1967.

62. COULSON,J.M., and RICHARDSON, J.F. Chemical Engineering, 3rd edition. Pergamon Press, London, vol. 1. Fluid Flow Heat Transfer and Mass Transfer, 1964.

63. PERRY, H.R., CHILTON, C.H., and KIRKPATRICK, S.D. Chemical Engineers Handbook. Fourth Ed. McGraw Hill, N.Y., 1950.

64. CAMMAROTA, A., DI MURO, N., DONSI, G., MASSIMILLA, L., RUSSO, G., SIECCONI, P., and TARANTINO, A. Variabile di un Impianto pre-pilota per la combustione in letto fluido. CONGRESSO DELLA SOCIETÀ, CHIMICA ITALIANA, MERANO, 1978.